



NTNU – Trondheim
Norwegian University of
Science and Technology

Kinetic study of oxychlorination process

Reza Abdollahi

Chemical Engineering

Submission date: June 2014

Supervisor: De Chen, IKP

Norwegian University of Science and Technology
Department of Chemical Engineering

NTNU
Norwegian University of Science
Engineering and Technology

Faculty of Natural Sciences and Technology
Department of Chemical



MASTER THESIS 2012

Title: Kinetic Study of Oxychlorination Process	Subject (3-4 words): Effects of CeO ₂ as a promoter
Author: Reza Abdollahi	Carried out through:
Advisor: De Chen	Number of pages Main report: 62 Appendix: 69
ABSTRACT	
<p>Goal of work (key words): Previous studies demonstrate that oxidation of Cu^+ is a rate determining step in oxychlorination reaction which leads to a high concentration of Cu^+ as an intermediate which can deactivate the catalyst (Due to sintering). In this study, effects of CeO₂ additions (As a promoter) on the kinetic behavior of three steps involved in oxychlorination reaction is investigated.</p>	
<p>Conclusions and recommendations (key words): CeO₂ is proved to be a good promoter due to the ability to accelerate oxidation of Cu^+ to Cu^{+2} in oxychlorination reaction. However it should be taken into account that high concentrations of ceria deactivate the catalyst by forming an inert phase on the catalyst.</p>	
I declare that this is an independent work according to the exam regulations of the Norwegian University of Science and Technology	

ABSTRACT

Doped $\text{CuCl}_2/\text{Alumina}$ is the catalyst for ethylene dichloride ($\text{C}_2\text{H}_4\text{Cl}_2$) production. Ethylene dichloride is the intermediate for generating polyvinyl chloride (PVC) and is produced as result of catalytic oxy-chlorination of ethylene (C_2H_4). The process of ethylene oxy-chlorination can be split at three steps on gamma-alumina support. The first step is reduction of cupric chloride which is actually ethylene chlorination step where the second and third steps are re-oxidation and Chlorination of cuprous chloride respectively, using O_2 and HCL . Results obtained from oxychlorination of ethylene on $\text{CuCl}_2/\text{G}-\text{Al}_2\text{O}_3$ catalyst, Showed a lower reaction rate on the second step than the first step[1] which leads to deactivation of catalyst due to the excess amount of intermediate (CuCl). Therefore, CeO_2 is used as promoter to enhance the catalytic performance of the reaction by reducing the reaction rate at first step in one hand and increasing the oxidation rate on the other hand. Various weight percentages of Ceria (1, 3 and 5 wt%) doped with $\text{CuCl}_2/\text{G}-\text{Al}_2\text{O}_3$ is been used in several cycles. UV/VIS and Mass Spectroscopies, Combined with laboratory techniques, made it possible to have a good understanding in kinetic behavior of the active phase and effects of CeO_2 as promoter for the catalyst. Results show that even low concentrations of ceria in $\text{CuCl}_2/\text{G}-\text{Al}_2\text{O}_3$ can highly enhance catalytic performance of the catalyst however high concentration of CeO_2 has negative impacts on activity of the catalyst.

Acknowledgements

I would like to thank Professor De Chen for giving me the opportunity to work at this project. I would like to express my appreciation for his guidance, assistance and encouragement during the study.

In addition, I wish to thank Fina mart, the PhD student at the project for her ideas, assistance and guidance.

My special thanks to employees of Chemical Engineering Department, especially Lisbeth Reel, Harry Brun, Arne Fossum and Karin Dragsten for their support and attention. They were so helpful and supportive during the carrier.

To my family

And

*Whoever existed, exists, or will exist in my life
who has had, has, or will have a great influence on my thinking...*

Reza Abdollahi

20.06.2014

*Norwegian University Of
Science and Technology*

و تقدیم به او و حرآن کس که او در اوست...
که دهنده او، دهنده او،
نگرنده او و نگارنده اوست.
یا حق، یا هو، یا او...

Abbreviate

Symbol	Meaning
PVC	Polyvinyl chloride
VCM	Vinylchloride Monomer
EDC	Ethylene dichloride
C ₂ H ₄ (Eth)	Ethylene
Cu	Copper
Reactant	Corresponding reactants : C ₂ H ₄ ,O ₂ and HCl
Inert	Corresponding inert gases: Ar or He
He	Helium
Ar	Argon
HCl	Hydrogen Chloride
MPa	Mega pascal
UV/VIS	Ultraviolet/Visible
R_{∞}	Diffuse reflection
MS	Mass Spectrometer
MFC	Mass flow controller
EXP	Experiment, Cycle

Table1: Abbreviate

Contents

1. INTRODUCTION	1
1.1. Vinyl chloride monomer(VCM)	1
1.2. Oxychlorination	2
1.2.1. Direct chlorination of ethylene	2
1.2.2. Oxy-chlorination of ethylene	2
1.3 The oxychlorination catalyst	3
2. Experimental	5
2.1 Ultraviolet-visible spectroscopy (UV-VIS)	5
2.2 Mass spectrometry	6
2.3 Set up	7
2.4 Mass flow controllers (MFC)	9
2.5 Method of catalyst synthesis	9
2.5.1 Impregnation of CuCl_2 on $\gamma - \text{Al}_2\text{O}_3$	9
2.5.2 Impregnation of $\text{CuCl}_2 \cdot \text{CeO}_2$ on $\gamma - \text{Al}_2\text{O}_3$	10
2.5.3 Calculations	11
2.6 UV/VIS spectrometer	12
2.7 UV/VIS Blank	13
2.8 Procedure of UV/VIS spectroscopy	14
2.9 Procedure of MS	15
2.10 MS Data processing	18
2.11 Methodology	19
2.12 Experiments	20
3. RESULTS AND DISCUSSION	21
3.1 Catalyst properties	21
3.1.1 BET Analysis	21
3.1.2 X-Ray diffraction	22
3.1.3 Effect of Ceria additions on the peaks	27
3.2 Activation of catalysts	28

3.2.1 Effects of ceria additions on reflectance spectra.....	31
3.3 Reduction of CuCl ₂ By C ₂ H ₄	32
3.3.1 Ethylene flow over time.....	32
3.3.2.Etylene conversion.....	33
3.3.3Ethylene and chlorine uptake	34
3.3.4.Reaction rate versus removable chlorine	35
3.3.5. Removable chlorine	36
3.3.6.Reflectance versus wave length.....	36
3.4 Effects of Ceria on reduction step.....	38
3.4.1 Effects on Chlorine uptake.....	39
3.4.2 Effects on reaction rate.....	42
3.5 Overall view of effect of ceria additions on chlorine uptake and reaction rate	45
3.6 Effects of Ceria on Oxidation step.....	47
3.7 Correlation of MS and UV/VIS Data	49
4. CONCLUSION	52
References	53
Appendix A: Mass spectrometer	55
Appendix B: UV/VIS Spectrometer.....	93
Appendix C: Correlation of MS and UV/VIS Data.....	112
Appendix D: Calibration of Mass Flow Controlers	119

Table of figures

Figure 1: Examples of PVC products in everyday life[6]	1
Figure 2: UV/VIS Spectrometer.....	5
Figure 3: Mass Spectrometer.....	6
Figure 4: Schematic Design of Setup.....	8
Figure 5: XRD analysis of G-Al ₂ O ₃ before and after impregnation of CuCl ₂	23
Figure 6: XRD analysis of G-Al ₂ O ₃ , CeO ₂ /G-Alumina (1wt%Ce) and CuCl ₂ /G-Alumina. CeO ₂ (5wt%Cu, 1wt%Ce)	24
Figure 7: XRD analysis of G-Al ₂ O ₃ , CeO ₂ / G-Al ₂ O ₃ (3wt%Ce) and CuCl ₂ / G-Al ₂ O ₃ . CeO ₂ (5wt%Cu, 3wt%Ce)	25
Figure 8: XRD analysis of G-Al ₂ O ₃ and CuCl ₂ / G-Al ₂ O ₃ . CeO ₂ (5wt%Cu, 5wt%Ce).....	26
Figure 9: XRD analysis of G-Al ₂ O ₃ and CuCl ₂ / G-Al ₂ O ₃ ,CeO ₂ . Cerium loading is increased from 1 to 5wt% at the same Cu concentration (5wt%)	27
Figure 10: Activation of $CuCl_2/\gamma - Al_2O_3$ (Cu 5wt%).....	28
Figure 11: Activation of $CuCl_2.CeO_2/\gamma - Al_2O_3$ (5wt%Cu,1wt%Ce)	29
Figure 12: Activation of $CuCl_2.CeO_2/\gamma - Al_2O_3$ (5wt%Cu,3wt%Ce)	30
Figure 13: Activation of $CuCl_2.CeO_2/\gamma - Al_2O_3$ (5wt%Cu, 5wt%Ce)	31
Figure 14 Ethylene flow versus time. First cycle. Catalyst: $CuCl_2.CeO_2/\gamma - Al_2O_3$ (5wt%Cu,3wt%Ce)Reaction First Cycle conditions: T=503K, Peth=0.1 bar, Ptot=1 bar	32
Figure 15: Ethylene Conversion First cycle. Catalyst: $CuCl_2.CeO_2/\gamma - Al_2O_3$ (5wt%Cu,3wt%Ce)Reaction First Cycle conditions: T=503K, Peth=0.1 bar, Ptot=1 bar	33
Figure 16: Uptake versus Time First cycle. Catalyst: $CuCl_2.CeO_2/\gamma - Al_2O_3$ (5wt%Cu,3wt%Ce)Reaction First Cycle conditions: T=503K, Peth=0.1 bar, Ptot=1 bar	34
Figure 17: Reaction rate versus Removable chlorine. First cycle. Catalyst: $CuCl_2.CeO_2/\gamma - Al_2O_3$ (5wt%Cu,3wt%Ce)Reaction First Cycle conditions: T=503K, Peth=0.1 bar, Ptot=1 bar.....	35
Figure 18: Removable chlorine versus Time First cycle. Catalyst: $CuCl_2.CeO_2/\gamma - Al_2O_3$ (5wt%Cu,3wt%Ce)Reaction First Cycle conditions: T=503K, Peth=0.1 bar, Ptot=1 bar.....	36
Figure 19: Reflectance versus Wave length. Peak height at 792.64. First cycle. Catalyst: $CuCl_2.CeO_2/\gamma - Al_2O_3$ (5wt%Cu,3wt%Ce)Reaction First Cycle conditions: T=503K, Peth=0.1 bar, Ptot=1 bar.....	37
Figure 20: Reflectance versus Wave length. Peak height at 792.64. First cycle .Catalyst: $CuCl_2.CeO_2/\gamma - Al_2O_3$ (5wt%Cu,3wt%Ce)Reaction First Cycle conditions: T=503K, PO ₂ =0.1 bar, Ptot=1 bar	38
Figure 21: Chlorine uptake versus time in first cycles of all four catalysts at the same conditions:	39
Figure 22: Chlorine uptake versus time in second cycles of all four catalysts at the same conditions:	40
Figure 23: Chlorine uptake versus time in third cycles of all four catalysts at the same conditions:.....	41
Figure 24: Reaction rate versus Chlorine Uptake in first cycles of all four catalysts at the same conditions:	42

Figure 25: Reaction rate versus Chlorine Uptake in second cycles of all four catalysts at the same conditions:	43
Figure 26: Reaction rate versus Chlorine Uptake in third cycles of all four catalysts at the same conditions:	44
Figure 27: Chlorine uptake as a function of Cerium wt%.	45
Figure 28: Reaction rate as a function of Cerium wt%.	46
Figure 29: Relative Kubelka-Munk function as a function of time. Oxidation Step. first cycles of all four catalysts at the same conditions: T=503K PTotal=1 bar PO ₂ =0.1 (5wt% Cu, variable C _{ewt} %).	47
Figure 30: Relative Kubelka-Munk function as a function of time. Oxidation Step. second cycles of all four catalysts at the same conditions: T=503K PTotal=1 bar PO ₂ =0.1 (5wt% Cu, variable C _{ewt} %)	48
Figure 31: Relative Kubelka-Munk function as a function of time. Oxidation Step. third cycles of all four catalysts at the same conditions: T=503K PTotal=1 bar PO ₂ =0.1 (5wt% Cu, variable C _{ewt} %)	49
Figure 32: Correlation of UV/VIS data (Relative Kubelka-Munk function) and MS data (Ethylene conversion) obtained from second cycle on CuCl ₂ /G-Al ₂ O ₃ .CeO ₂ (5wt% Cu, 3wt% Ceria) Conditions: conditions:T=503K PTotal=1 bar PEth=0.1.....	50
Figure 33: Correlation of UV/VIS data (Relative Kubelka-Munk function) and MS data (Ethylene conversion) obtained from First cycle on CuCl ₂ /G-Al ₂ O ₃ (4.8wt% Cu). Conditions: conditions:T=503K PTotal=1 bar PEth=0.1.....	51
Figure 34: schematic illustration of ethylene chlorination	51

1. INTRODUCTION

1.1. Vinyl chloride monomer(VCM)

Polyvinyl chloride (PVC) is a semi-crystalline polymer with a relatively high tensile modulus of 2400 to 4140 mega Pascal (MPa). PVC can be made by polymerization of vinyl chloride monomers (VCM or C_2H_3Cl). PVC is known as one of the most commercially important plastic materials. According to ECVI (1988) more than 70% of all PVC products have long lives of more than ten years. Nowadays PVC is widely used in chemical industries as well as in everyday life. [2-5]



Figure 1: Examples of PVC products in everyday life[6]

Vinyl chloride monomer (VCM) is formed by cracking 1, 2-dichloroethane to vinyl chloride and hydrogen chloride (HCl). The major proportion of formed EDC (85%) is dehydrochlorinated to produce VCM [7-9]



1.2. Oxychlorination

1.2.1. Direct chlorination of ethylene

In this mechanism, Cl_2 is directly added to C_2H_4 to make Ethylene dichloride (EDC). In this mechanism, Fe is used as catalyst and the selectivity to produce EDC approaches to 99%. Direct Ethylene chlorination is done in a relatively lower and globally simpler process than oxy-chlorination of ethylene.



1.2.2. Oxy-chlorination of ethylene

Oxy-chlorination of ethylene has been applied to the industrial process to produce vinyl chloride, where the intermediate product is 1,2-dichloroethane formed by using ethylene, hydrogen chloride, and oxygen. The overall reaction is:



The overall reaction is exothermic ($\Delta H = -239$ KJ/mol) and the desired temperature and pressure to approach the selectivity of higher than 99% are at 475-525 C and 1.4-3Mpa.

The overall reaction can be separated to three steps shown as below:

Step 1: Chlorination of ethylene using CuCl₂ as chlorinating agent



Step 2: Oxidation of CuCl to form Oxy-chloride



it is also possible to use air instead of oxygen in the second step but then air should be exposed with a more intensity as its been calculated to fulfill hydrocarbons conversion.

Step 3: Re-chlorination of oxy-chloride to form CuCl₂ and H₂O



First step is considered as main step while the other two steps are actually steps to regenerate the catalyst. It has also been approved that the rate determining step is oxidation of Cu⁺ which leads to a high concentration of Cu⁺ as an intermediate. Deactivation of catalyst due to sintering can be a consequence of high amount of Cu⁺. Hence Oxychlorination reaction requires more studies to improve the catalytic activity of the catalyst. [10-14]

1.3 The oxychlorination catalyst

A copper (Cu) based catalyst is normally used in oxychlorination process. Copper chloride (CuCl₂) is used as catalyst in oxychlorination reaction of hydrocarbons since the discovery of the fact that it can catalyze the conversion of hydrogen chloride to chlorine in Deacon process. *γ - Alumina* is used as the support due to its high surface area (Which enhance dispersion) and high thermal stability.[15]

Investigations show two different groups of copper species on alumina. The first group is formed at low concentrations of copper on alumina. In fact they are the product of an interaction between copper and alumina which leads to a highly dispersed copper species. Other group is chlorine clusters which are formed at higher copper concentration. These clusters doesn't interact with the carrier.[9]

Alkali or alkaline earth metals such as potassium chloride (KCl) and lanthanum chloride (LaCl_3) are often used as promoter making catalyst more suitable for industrial reactors. Commercial catalysts are synthesized by impregnation of CuCl_2 on γ -*Alumina* .[11, 16-19] .

Copper in CuCl_2 is the catalyst and chlorine plays the role of the adsorbate on the surface. During the first step, Chlorine is directly removed from the surface and then during the chlorination step is reloaded to the catalyst.

In this study, cerium oxide is used as the additive to the catalyst. Some of advantages of ceria addition are:

- Ceria can stabilize the dispersion of active phase
- Cooper oxide/Ceria interactions effects catalytic properties
- Ceria can be assumed as an oxygen storage material which increases the concentration of the superficial oxygen on the catalyst. Hence the reaction rate will be increased.[20, 21]

2. Experimental

2.1 Ultraviolet-visible spectroscopy (UV-VIS)

Spectroscopy in the ultraviolet (UV), visible (Vis) and near infrared (NIR) region of the electromagnetic spectrum is called electronic spectroscopy. Electrons transfer from low-energy to high-energy atomic orbital due to irradiation with light. This electron transfer may occur in transition metal ions (d-d transitions and metal-to-ligand or ligand-to-metal charge transfer transitions) and also both organic and inorganic molecules.



Figure 2: UV/VIS Spectrometer

Since catalyst is of the heterogeneous kind, then the radiation transfer theory can be used which is capable to solve the radiation transfer equation:

$$\frac{-dI}{k \cdot \rho \cdot ds} = I - \frac{j}{k} \quad (2-1)$$

Where:

I , is the incident light intensity of a given wavelength

dI/ds , is the change of the intensity with the path length ds

ρ , is the density of the medium

k , is an attenuation coefficient corresponding with the total radiation loss due to absorption and scattering

j , is the scattering coefficient

2.2 Mass spectrometry

Mass spectrometry (MS) is an analytical method for determining the mass of charged species by measuring the mass to charge ratio of them. The hint is, Chemical components are ionized first to achieve charged molecules then, different species are able to be distinguished by their mass-to-charge ratio.[22]



Figure 3: Mass Spectrometer

Since MS shows ion intensity versus time, then the first step for MS calculation is to convert ion flow to molar flow as:

$$n_i = \frac{I_i - I_{min}}{I_{max} - I_{min}} \cdot n_{max} \quad (2-2)$$

Where:

n_i , is the molar flow of specie i

I_i , is ion intensity of specie i (Obtained from MS)

I_{min} , is the minimum ion intensity of specie i during the measurement

I_{max} , is the maximum ion intensity of specie i during the measurement

And n_{max} is the maximum molar flow of specie i

Maximum molar flow of species can be calculated, using ideal gas equation as:

$$n = \frac{P.V}{R.T} \quad (2-3)$$

2.3 Set up

Regarding to Figure 4, Gases can be exposed to the reactor either as individual stream or a mixture of different streams. The intensity of exposed gas is controlled using mass flow controller (MFC). Ar and He are used as diluting gas and inert gas respectively. The aim for diluting the reactants with argon is to avoid the probable explosion due to mixing of explosive gases and He is used to avoid the pressure drop inside the reactor due to the gap between steps. He is flowing as same volume as both reactant and diluting gas(Ethylene/Oxygen and argon).

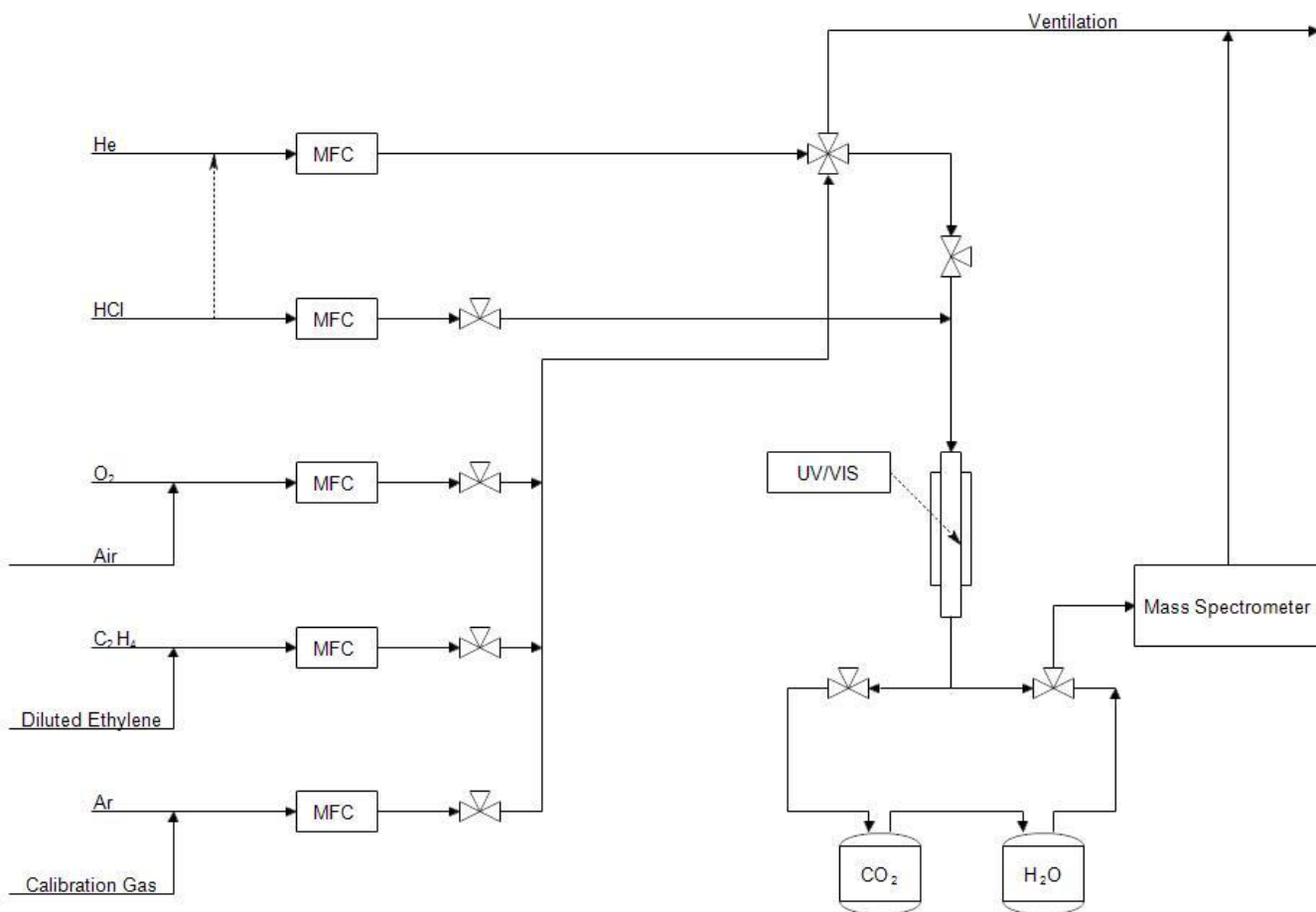


Figure 4: Schematic Design of Setup

In Figure 4 there are some valves namely 4-way valve and 3-way valve.

4-way valve is used to change the stream either from reactor to ventilation or vice versa. Therefore, as it is shown in the setup, during the experiment there is always one stream to the reactor (either reactant gas or inert gas) and the other one to the ventilation. Some 3-way valves are also which their responsibility is to change the direction of gas from one bottle to the other one. Reactor is located inside an oven, hence reaction can be done at high temperatures but it should be taken into account that if temperature exceeds a certain amount, Deactivation of the catalyst occurs.

2.4 Mass flow controllers (MFC)

There are several Mass flow controllers in the setup, making it possible to control flow of gases heading to the reactor. The procedure how to run automated valves is described below:

- Launch the “Flowdde2.exe” program locating on either desktop or start menu.
- Click on the “Communications” in the menu bar of the program and then choose “Open communications”. After a moment a notification will be shown up as “ready for client”.
- After receiving the notification now it’s the time to launch the “Flowview.exe” program which makes it possible to control the flow of each individual gas.

Mass flow controllers are only controllable by setting the percentages which valve could be open, Hence they need to be calibrated before running the experiments. Bubble flow meter mechanism is used for calibration of all mass flow controllers.

2.5 Method of catalyst synthesis

Incipient wetness impregnation mechanism is used to synthesis the catalyst. Precursor ($\text{CuCl}_2 \cdot 2\text{H}_2\text{O}$ or $\text{Ce}(\text{NO}_3)_3 \cdot 6\text{H}_2\text{O}$) is dissolved in the water. Amount of water (Solvent) is the same as pore volume of the support. Impregnation is followed by drying (2.5.1), Calcinations (2.5.2) and activation of the catalyst (3.2). [9, 18, 23]

2.5.1 Impregnation of CuCl_2 on $\gamma\text{-Al}_2\text{O}_3$

The start point in order to prepare the catalyst, Is to know the copper loading in the catalyst. The next step is to predict the total amount of the catalyst. Since the catalyst is supposed to go through several tests like BET, XRD and also the experiment, then the amount of catalyst should be enough to fulfill the needs.

By having both, the total amount of the catalyst and the amount of copper loading, the weight of CuCl_2 can be calculated. Since CuCl_2 is available as $\text{CuCl}_2 \cdot 2\text{H}_2\text{O}$ then mass of $2\text{H}_2\text{O}$ should be also taken into account during calculations. Total amount of water as solvent can be calculated as is described in 2.5.3.

After impregnating the support, it's time to dry the catalyst. Catalyst should be heated up with a rate of $5^\circ\text{C}/\text{min}$ to 120°C using a programmable furnace. Sample should be kept inside the oven whole the night at this temperature to remove the Excess water from the catalyst. Obtained catalyst should be kept in a bottle with cap to remain dry.[23]

2.5.2 Impregnation of $\text{CuCl}_2 \cdot \text{CeO}_2$ on $\gamma\text{-Al}_2\text{O}_3$

The procedure is mostly the same as 2.5.1 but includes two stepwise impregnation step. Ceria is firstly impregnated to the support and then CuCl_2 is impregnated to the support(Which already includes Ceria). The reason for stepwise addition of CeO_2 and CuCl_2 is the relatively high calcinations temperature of Ceria which makes it impossible to load both CuCl_2 and CeO_2 at the same time since

300°C deactivates the CuCl_2 . The rate of heating for both impregnation steps is $5^\circ\text{C}/\text{min}$ and catalyst should undergoes calcinations for at least 6 hours in the oven before second impregnation step.[23]

2.5.3 Calculations

In order to prepare the catalyst some calculations need to be done. First thing which should be clear is the concentration of active phase (Copper), which is identified as the ratio between the mass of the individual Copper to the total mass of the catalyst.

$$w_{cu} = \frac{m_{cu}}{m_{support} + m_{cucl_2}} \quad (2-4)$$

Where:

w_{cu} is the weight fraction of cu

m_{cu} is weight of cu

$m_{support}$ is weight of support

m_{cucl_2} is weight of $cucl_2$

The amount of water is needed to use as solvent should be the same as the total pore volume of the support. Total pore volume can be obtained by multiplying the amount of the support in pore volume of the support (pore volume is calculated using BJH).

$$V = M_{SUPPORT} * V_{P,\delta-alumina} \quad (2-5)$$

Where:

$V_{P,\delta-alumina}$ is pore volume of $\delta - alumina$. Pore volume of $\delta - Alumina$ is shown in the part'' characterization of the catalyst/BET analysis''.

it is necessary to take into account also the water crystals which already exist in precursor ($CUCL_2 \cdot 2H_2O$).

Volume of water crystals can be calculated as:

$$V_{water,crystals} = \frac{m_{water,crystals}}{\rho_{water}} = \frac{M_{H_2O} \cdot n_{water,crystals}}{\rho_{water}} \quad (2-6)$$

Where $n_{water,crystals}$ is mole of water-crystals which easily can be calculated by multiplying moles of $CuCl_2$ by two (Stoichiometry of H_2O in $CuCl_2 \cdot 2H_2O$ is twice as much as $CuCl_2$)

So the desired volume of water should be used as solvent is calculated as:

$$V_{H_2O} = V - V_{water,crystals} \quad (2-7)$$

2.6 UV/VIS spectrometer

The UV/VIS detector should be placed close to the reactor during the experiment, pointing the reactor catalyst. The right place of detector can be obtained by looking at the beam reflected on the catalyst bed. Practically we set it at place in which the height of absorbance trend (before activation of catalyst) is showing an amount in range of 45-55(Out of 100). The reason is, Due to activation of catalyst in a high temperature the attached crystal waters are vaporized, leading to a significant decrease in the absorbance height. Hence the initial height of absorbance trend should be high enough to fulfill.

It should be also taken into account that incident light can be affected by light coming from outside of the reactor. Hence, the lights should be off as well as both top and bottom of the reactor should be covered with wool fiber to enhance the accuracy of results.

The diffuse reflection (R_∞) of sample is related to an apparent scattering coefficient (S) and apparent absorption (K), expressed by the Schuster-Kubelka-Munk (S-K-M) or Kubelka-Munk (K-M) function[24] :

$$F(R_\infty) = \frac{(1 - R_\infty)^2}{2R_\infty} = \frac{K}{S} \quad (2-8)$$

Where :

$$R_\infty = \frac{R_{Sample}}{R_{BaSO_4}} \quad (2-9)$$

Equation (2-9) is valid under following conditions:

- Diffuse monochromatic irradiation of the powdered sample;
- An infinite layer thickness;
- A low concentration of absorbing centers;
- The absence of fluorescence.

Apparent absorption (K) for semiconductors in the region near absorption edge is given as:

$$K = \frac{(hv - E_0)^n}{hv} \quad (2-10)$$

Where:

hv is photon energy and E_0 is the optical absorption edge energy.[25, 26]

$$hv = \frac{h.c.10^9}{\lambda} \quad (2-11)$$

2.7 UV/VIS Blank

Before loading the main catalyst into the reactor, a blank test should be done, using $BaSO_4$. The reasons are the white color of $BaSO_4$ as well as its low UV-Radiation absorption. Wool fiber is used as bed in reactor cell (The advanced reactor has a quartz bed). The amount of $BaSO_4$ should be enough such it can cover UV/VIS beam. Then the program ‘‘Avasoft 7.5’’ is used to save the reference. The procedure is as below:

- Run ‘‘Ava soft 7.5’’ and switch on ‘‘TTL-On’’ and ‘‘Halogen’’
- Selecting Scope mode
- Save the reference

- Turn off ‘‘TTL-On’’
- Save dark reference

2.8 Procedure of UV/VIS spectroscopy

Since UV/VIS lamp takes about 40 minutes to be ready, then the first action at start up of the set up would be turning on the UV/VIS lamp and it should remain turned on all along the experiment.

The next step would be addressing the place in which we want results to save on. In order to do that follow the procedure below:

- Click on ‘‘Ava soft 7.5 USB2’’ Icon in desktop in order to run the program.
- If new catalyst is going to be used, then the reference and dark should be saved as is been described in UV/VIS blank part, otherwise load both references. So it is no need to do the blank every time before the new experiment.
- Switch to Reflectance mode.
- Next step is to record the data by the path ‘‘file/start new experiment ‘‘. Then the software wants you to address the place in which you want results to be saved on.
- Naming the recorded files is better to be done with respect to the date and name of the experiment
- Then click on ‘‘Setup/option/Auto spectra periodically’’
- Now it is time to set the time gap between the recorded cycles. A suggestion could be like table below:

Start up	Ethylation	Oxydation	Chlorination
Preparation	Eth	Oxy	Chl
30s	30	5	No need to record

Table2: Suggested time gap between cycles for various steps

- Note that before starting to record UV/VIS data, MS has to be ready to record the data. Both UV/VIS and Mass spectrometer start to record the data at the same time however 4way valve should be switched on after two minutes to record the data. The reason for exposing reactants after two minutes recording is to do calibration for both MS and UV/VIS spectrometer.

After finishing the experiment, then it's time to process the data following steps below:

- Run "Avasoft 7.5"
- Use path" File/convert graph/to excel"
- Choose the recorded UV data. Since only 250 cycles can be transferred to excel sheet each time, then in case if the number of cycles exceed, the conversion can be done several times and then they can be merged to one excel sheet.

To turn off the UV/VIS spectrometer, it is need to just switch off the UV/VIS lump and close the program.

2.9 Procedure of Mass Spectrometer

2.9.1 Mass Spectrometer Calibration

Mass spectrometer should be calibrated each time before starting to record. Once the four-way valve switches to introduce reactants to the reactor, it takes a time for the flow to reach steady state (reaction time). It's also the same when we switch the four-way valve to Inert gas. Hence, it is need to wait enough among cycles to reach steady state and then expose the second or third reactant to the catalyst bed. Since the initial value of each component which is screened on is going to be used as the criteria for MS calculations, then a blank per experiment is required.

The procedure of blank is done by switching 4-way valve to introduce helium to the reactor. This step last until all the trends approach steady state.

The blank of each reactant can also be used as the total amount of that reactant so the reacted amount of the reactant can be calculated at any time within the reaction.

2.9.2 Procedure of operation

Although starting up the Ms is not so time consuming, but all the steps should be handled so carefully.

The procedure is as:

- Switch on the MS spectrometer by pushing the button I/O which located on the back side of the MS.
- After some seconds, first and third buttons (Heater and pump) located at front of MS should be pressed. Then it takes about 15 minutes for MS warming up to 200 °C.
- Once the MS is warmed up, then open the folder ‘‘Pfeiffer vacuum quadstar 32-bit’’ and run the program ‘‘measure.exe’’.
- Go to menu and follow the path ‘‘Manual/Di/DO’’. A new window appears. Mark on non-lighted squares by double-clicking on them.
- Wait for 10 minutes.
- Then follow the path ‘‘Setup/Sem/emission control’’. A new window appears. Mark on Emission square

Now MS is ready to record the data. The procedure, how to start and then save the data is described below:

- Run ‘‘measure.exe’’
- Follow ‘‘MID/versus time’’. A new window appears in which available programs are shown in it. The one should be chosen which contains all the components.

Then the ion intensity of each component versus time is shown. In order to save the data follow:

- Go to save cycle data
- Name the file and determine the place where to save the data.
- Ensure that the maximum number of cycles is selected
- Before clicking on ok, ensure that UV/VIS is ready to record the data.

In this step as it is discussed in "MS Calibration" part, MS spectrometer should be already calibrated. Then Start recording the MS data by Clicking on Ok.

- Switch the 4-way valve to introduce the main reactants to MS exactly two minutes after you started to save the data by MS.

Note:

Do not forget to start recording UV/VIS data (As is described in 2.8) at the same time as MS recording since at initial time of recording UV/VIS data there would be a sudden increase in the absorbance trend and after some seconds it approach it's actual amount.

Stopping the MS recording can be done by closing the graph window.

The data are obtained from MS are in "mdc" format. They need to be converted to "ASCII" format so they can be easily converted to excel afterward. The procedure is as below:

- Open the folder "Pfeiffer vacuum quadstar 32-bit" and run "dispsav.exe".
- Follow the path "Process/Cycles" and select the file.
- Once the file is open follow the path "File/convert to ASCII"
- Then address the file with ASCII format
- Next step is to convert the ASCII to excel format. It can be done by opening the ASCII file and Copy all the contents and paste them all in an excel file.

The procedure for turning off the MS is described as below:

- First switch off the filament by following the path "Setup/Sem/emission control". A new window appears. Mark off Emission square.

- Wait for 10 minutes. The reason is to prevent filament to get oxidized due to reaction with the oxygen available in the air since the filament is incandescent and oxidized so fast.
- Then switch off both diodes by following the path “Manual/Di/DO” and marking off both squares by double-clicking on them.
- Press both heat and pump buttons at front of the MS to turn the both off.
- Wait for some minutes to hear the noise generating from interrupting the vacuum.
- Switch off the MS by pressing I/O button on the back side of the MS.

2.10 MS Data processing

In order to calculate the amount of products, a blank is done after the reaction. In this way the reactants are re-injected after the reaction in which no reactant would react within the reactor, then obtained shape and intensity versus time from the blank can be compared with the intensity and shape versus time of reaction period. The difference shows consumed reactant.

$$n_{reacted} = n_{blank} - n_{reactant} \quad (2-12)$$

$$n_{blank} = Eth_{cat} * \frac{Inert_{steadystate}}{Eth_{steadystate}} \quad (2-13)$$

Then the reaction rate and conversion can be calculated following steps below:

$$X_i = \frac{n_{reacted}}{n_{blank}} \quad (2-14)$$

$$r_{rate} = \frac{X_i * n_{blank}}{mol_{Cu}} \quad (2-15)$$

Subtracted ethylene can be then calculated as below:

$$Eth_{subtracted} = \frac{n_{reacted}}{mol_{Cu}} \quad (2-16)$$

Ethylene uptake at any time is obtained using equation below:

$$IU_{Eth,i} = (Eth_{subtracted,i} \cdot \Delta T) + IU_{Eth,i-1} \quad (2-17)$$

Since each mole of ethylene reacts with 2 moles of chlorine then chlorine uptake would be twice as much as ethylene uptake

$$IU_{cl,i} = 2 \cdot (IU_{Eth,i}) \quad (2-18)$$

2.11 Methodology

Each step is run separately in the reactor. Therefore, the kinetic information (total volume and partial pressure of reactants) for each individual step should be available.

In this study, it has been tried to get the kinetic information of reduction and oxidation steps in oxychlorination of ethylene on $CuCl_2.CeO_2/\gamma-Al_2O_3$ catalyst with three different cerium loading of 1,3 and 5 wt% and then compare it to the obtained information from $CuCl_2/\gamma-Al_2O_3$ (Without ceria). In fact, it's been tried to see if CeO_2 additions can enhance the rate in oxidation step so that to reduce the probability of sintering.

Same conditions (Temperature, pressure), are applied to all the cycles on all four samples and the data are recorded by MS and UV/VIS spectrometers within the reaction.

2.12 Experiments

A total of 12 experiments were done. 3 experiments on $CuCl_2/\gamma - Al_2O_3$ and the rest 9 experiments on $CuCl_2.CeO_2/\gamma - Al_2O_3$ catalyst with 3 different ceria loading of 1,3 and 5 wt%. All the data obtained from both MS and UV/VIS is processed.

Reaction temperature, total pressure and also partial pressure of reactants are the same for all the experiments as is shown in table 3.

Catalyst	C ₂ H ₄ flow(ml/min)	P _{C₂H₄} (bar)	O ₂ flow(ml/min)	P _{O₂} (bar)	T(K)	Sample(gr)	Cooper%	Cerium%
CuCl ₂ /G-Alumina	90.72	0.1	139.912	0.1	503	0.7379	4.81	0
CuCl ₂ /CeO ₂ /G-Alumina	90.72	0.1	139.912	0.1	503	1.5001	5	1
CuCl ₂ /CeO ₂ /G-Alumina	90.72	0.1	139.912	0.1	503	1.5383	5	3
CuCl ₂ /CeO ₂ /G-Alumina	90.72	0.1	139.912	0.1	503	0.7345	4.73	5

Table3: Catalysts and conditions in which catalysts are tested in.

3. RESULTS AND DISCUSSION

3.1 Catalyst properties

3.1.1 BET Analysis

Physical properties of the catalyst are investigated using Brunauer-Emmet-Teller (BET) and Barrett-Joyner-Halenda (BJH) method. Surface area, pore volume and pore sizes of support is measured for pure $\gamma\text{-Al}_2\text{O}_3$, $\text{CeO}_2/\gamma\text{-Al}_2\text{O}_3$, $\text{CuCl}_2/\gamma\text{-Al}_2\text{O}_3$ and $\text{CuCl}_2.\text{CeO}_2/\gamma\text{-Al}_2\text{O}_3$ [27]

	Surface Area(m^2/gr)	Pore Volume(cm^3/gr)	Pore Size(\AA)
Pure $\gamma\text{-Al}_2\text{O}_3$	165.9193	0.467572	109.1198
<i>4.7% Cu loading</i>			
$\text{CuCl}_2/\gamma\text{-Al}_2\text{O}_3$	142.8957	0.385178	103.4612
<i>5%Cu, 1wt% Ce</i>			
$\text{CeO}_2/\gamma\text{-Al}_2\text{O}_3$	163.5028	0.450105	106.1671
$\text{CuCl}_2/\text{CeO}_2, \gamma\text{-Al}_2\text{O}_3$	146.0815	0.389277	102.0221
<i>5%Cu, 3wt% Ce</i>			
$\text{CeO}_2/\gamma\text{-Al}_2\text{O}_3$	156.6606	0.420312	103.1417
$\text{CuCl}_2/\text{CeO}_2, \gamma\text{-Al}_2\text{O}_3$	144.0013	0.371662	98.8866
<i>4.8wt%Cu, 5wt% Ce</i>			

$\text{CeO}_2 / \gamma - \text{Al}_2\text{O}_3$	155.1428	0.434507	107.8538
$\text{CuCl}_2/\text{CeO}_2, \gamma - \text{Al}_2\text{O}_3$	144.3502	0.369752	98.3500

Table4: Physical properties of support and catalyst

3.1.2 X-Ray diffraction

X-Ray Diffraction (XRD) is a method used for determining the atomic and molecular structure of a crystal. In this method, crystalline atoms cause a beam of X-rays to diffract into many specific directions. XRD can do a qualitative and quantitative analysis of a crystalline material with an amount greater than 1%. [28]

XRD analysis of $\gamma - \text{Al}_2\text{O}_3$ and stepwise impregnation of 5wt% copper Chloride (CuCl_2) and different concentrations of Cerium(Ce) is shown in Fig5, Fig6, Fig7, Fig8 and Fig9.

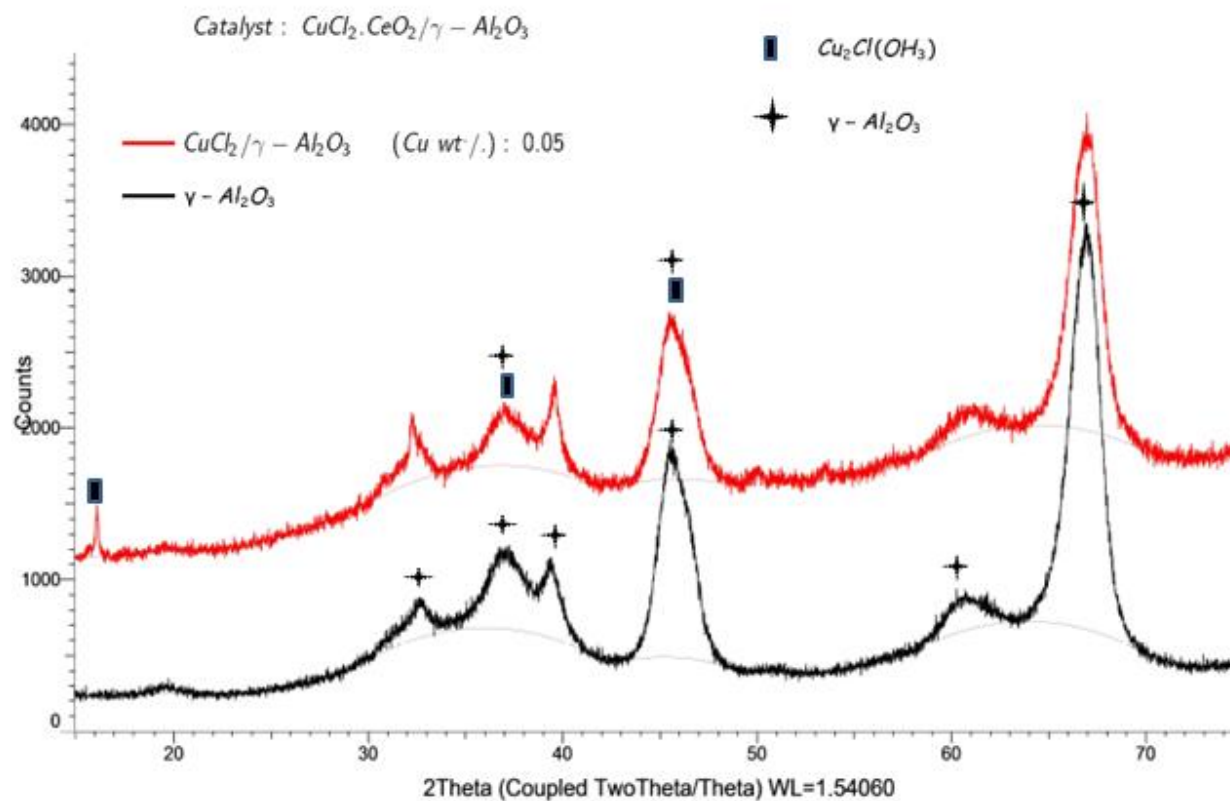


Figure 5: XRD analysis of $\gamma\text{-Al}_2\text{O}_3$ before and after impregnation of CuCl_2

The black trend in Fig5 belongs to pure $\gamma - \text{Al}_2\text{O}_3$ and peaks are shown via black stars. The red trend shows the peaks after impregnation of 5wt% CuCl_2 . As it is shown in the figure, Impregnation of CuCl_2 results in an excess peak on the structure ($\text{Cu}_2\text{Cl}(\text{OH}_3)$) as well as two changes in peak heights of $\gamma - \text{Al}_2\text{O}_3$ due to peak overlaps between $\gamma - \text{Al}_2\text{O}_3$ and CuCl_2 .

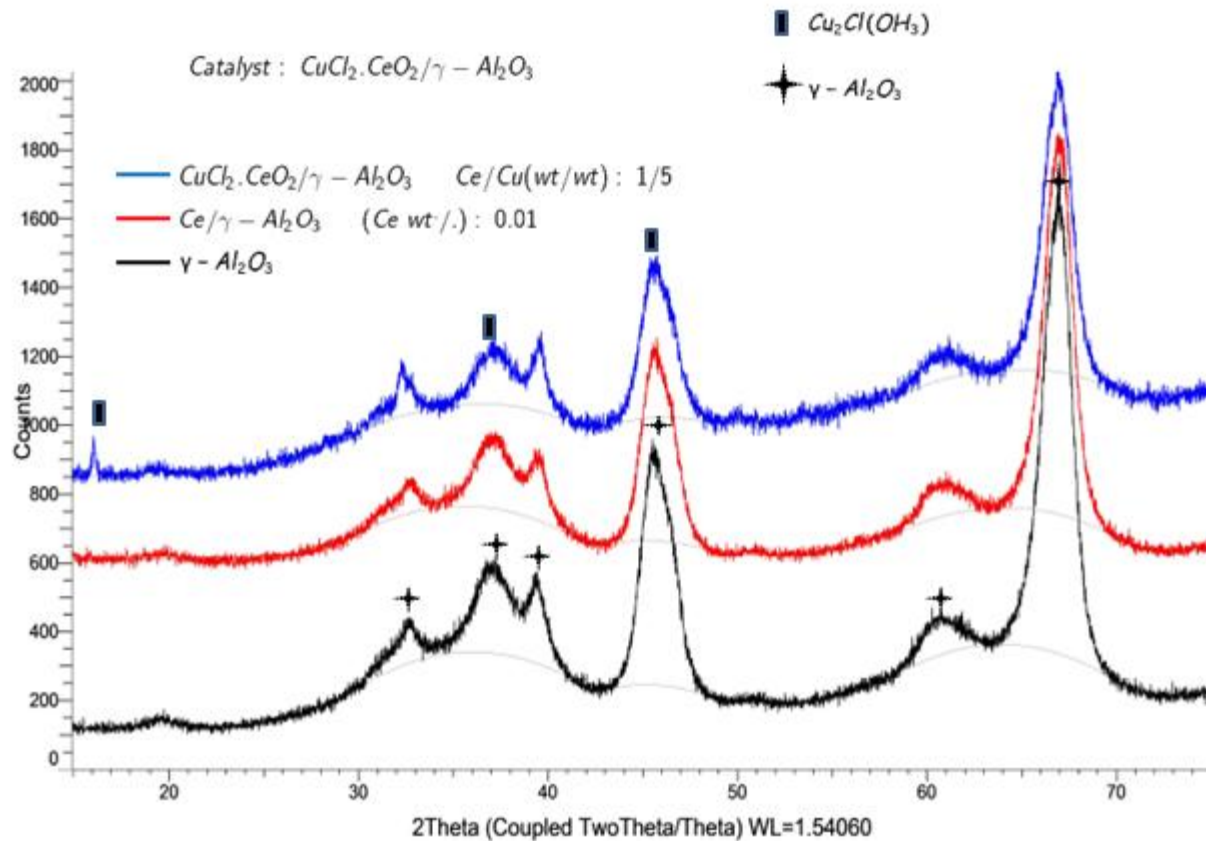


Figure 6: XRD analysis of γ - Al_2O_3 , CeO_2/γ -Alumina (1wt%Ce) and $CuCl_2/\gamma$ -Alumina, CeO_2 (5wt%Cu, 1wt%Ce)

Black, red and blue trends indicate the structures of γ - Al_2O_3 before impregnation, After impregnation with 1wt% Ceria and after impregnation of 5wt% $CuCl_2$ Into CeO_2/γ -Alumina respectively.

The red trend which belongs to 1wt% Ceria impregnated γ - Al_2O_3 shows that addition of 1wt% Ceria is not observable in XRD analysis. The reason is the low concentration of CeO_2 which leads to formation of a very thin layer which is not observable by XRD. The blue trend however shows Crystals of $Cu_2Cl(OH)_3$ on the structure due to deposition of 5wt%Cu on γ -Alumina, CeO_2 .

Figure 7 shows the trends in which Ceria concentration is increased to 3wt%.

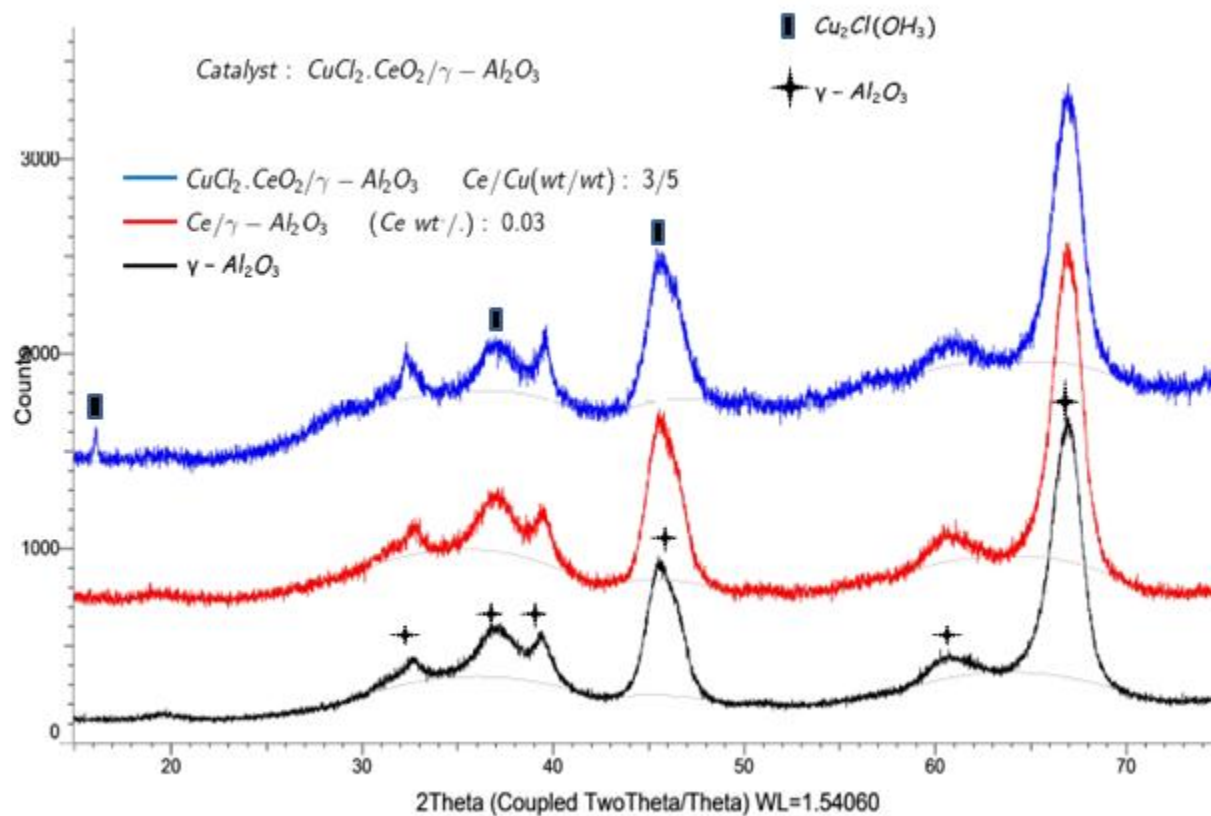


Figure 7: XRD analysis of $\gamma\text{-Al}_2\text{O}_3$, $\text{CeO}_2 / \gamma\text{-Al}_2\text{O}_3$ (3wt%Ce) and $\text{CuCl}_2 / \gamma\text{-Al}_2\text{O}_3 \cdot \text{CeO}_2$ (5wt%Cu, 3wt%Ce)

Black, red and blue trends in Figure 7 are showing $\gamma\text{-Al}_2\text{O}_3$, $\text{CeO}_2 / \gamma\text{-Al}_2\text{O}_3$ (3wt%Ce) and $\text{CuCl}_2 \cdot \text{CeO}_2 / \gamma\text{-Al}_2\text{O}_3$ (5wt% Cu, 3wt%Ce).

The red trend which belongs to the 3wt% Ceria impregnated $\gamma\text{-Al}_2\text{O}_3$ shows no change in the structure by ceria impregnation however addition of 5wt% Cu causes same changes as is shown in Figure 7.

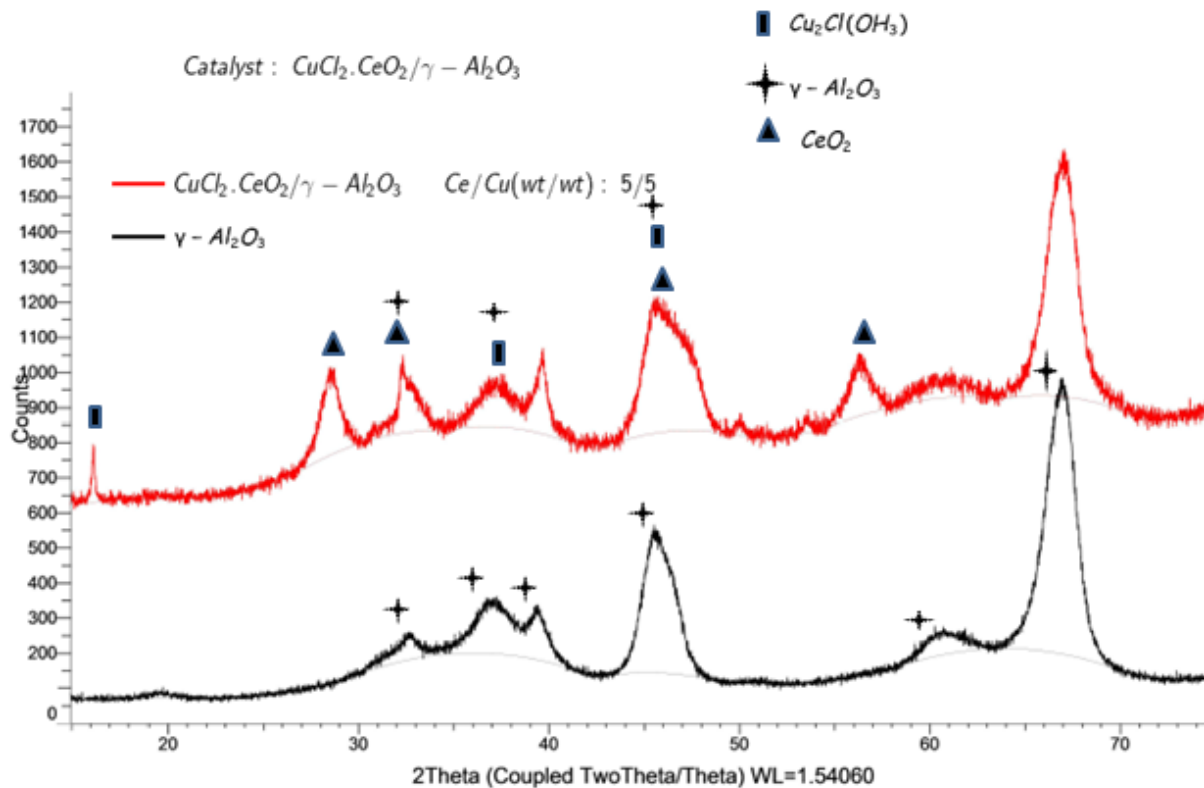


Figure 8: XRD analysis of $\gamma\text{-Al}_2\text{O}_3$ and $\text{CuCl}_2 / \gamma\text{-Al}_2\text{O}_3 \cdot \text{CeO}_2$ (5wt%Cu, 5wt%Ce)

As is shown in the figure8, Crystals of CeO_2 and $\text{Cu}_2\text{Cl}(\text{OH}_3)$ exist on the surface of $\text{CuCl}_2 / \text{CeO}_2 / \gamma - \text{Alumina}$.

Figure 9 shows the differences in structure of $\text{CuCl}_2 / \gamma\text{-Al}_2\text{O}_3 \cdot \text{CeO}_2$ with different Ceria loading of 1, 3 and 5wt% Ce while the concentration of Cu is almost the same (4.8-5wt%) for all the three catalyst.

3.1.3 Effect of Ceria additions on the peaks

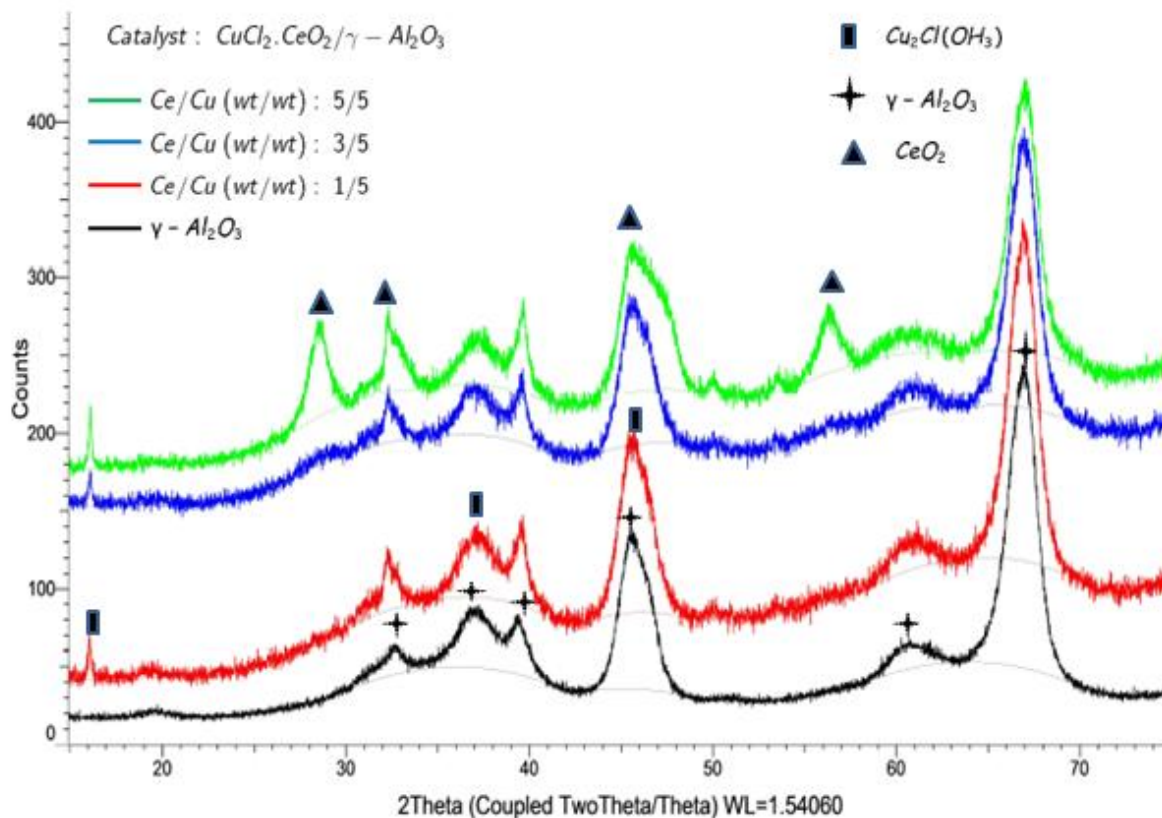


Figure 9: XRD analysis of G- Al_2O_3 and $\text{CuCl}_2/ \text{G-}\text{Al}_2\text{O}_3, \text{CeO}_2$. Cerium loading is increased from 1 to 5wt% at the same Cu concentration (5wt%)

As it can be seen in Fig 9, the formed films on the surface, made up of 1 and 3wt% Ceria additions to the catalyst is such thin which XRD cannot display it. An increase in concentration of ceria from 3 to 5wt% results in a significant change in the structure of catalyst so that two more peaks are formed on the surface and two other peaks are also affected. Beside $\gamma - \text{Al}_2\text{O}_3$ (Support) peaks, Which are shown in the trends, $\text{Cu}_2\text{Cl}(\text{OH}_3)$ crystals are also present on the surface however this crystals are such small that the effects of their presence can be neglected.

3.2 Activation of catalysts

Fresh catalyst contains water crystals. These Crystals can influence MS and UV/VIS spectrometer data. To prevent this error, the water crystals should be removed before running and recording the data. Activation is done by flowing he to the reactor while the temperature is increasing to 220 C. Figures below show the reflectance versus wave length during removing water crystals. As a result it could be said that removing water from catalyst reduces the reflectance height, hence it is necessary to remove water in order to have accurate results.

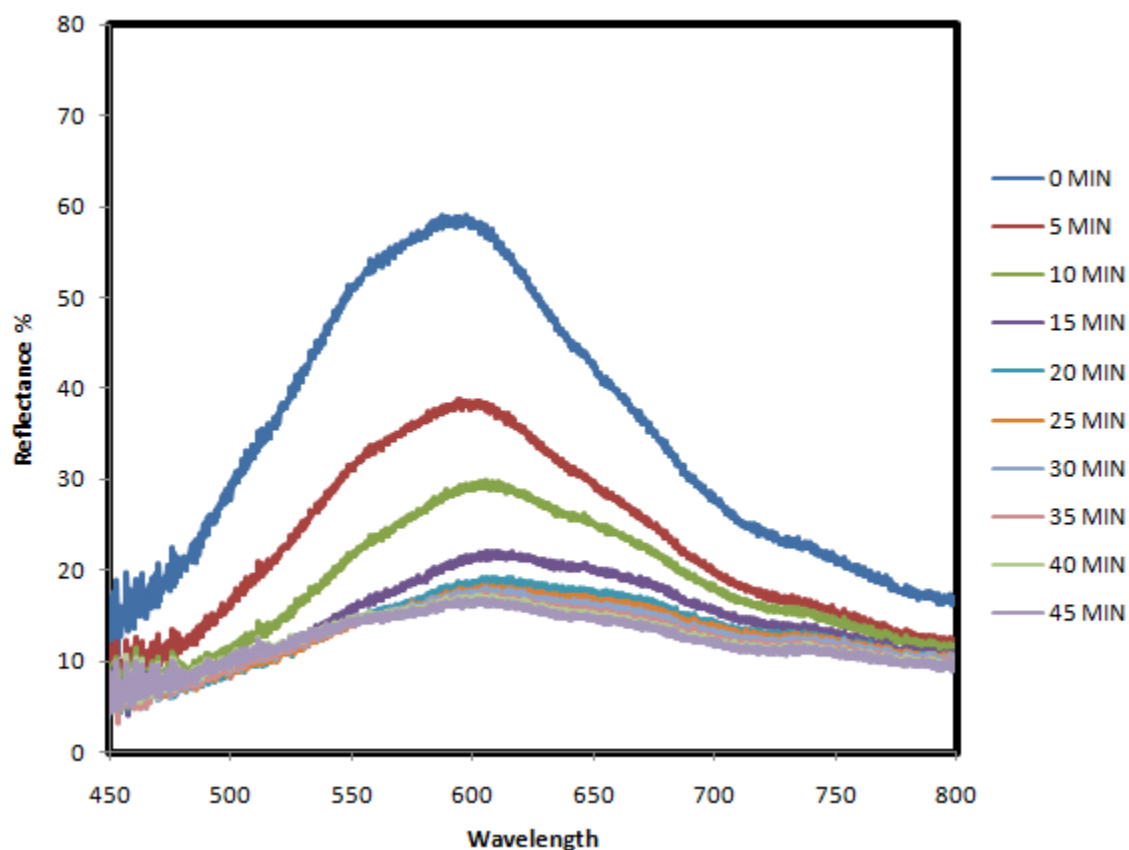


Figure 10: Activation of $\text{CuCl}_2/\gamma\text{-Al}_2\text{O}_3$ (Cu 5wt%)

Figure 10 shows the changes in reflectance versus time at increasing temperature (Maximum 220) for $\text{CuCl}_2/\gamma\text{-Al}_2\text{O}_3$ (5 wt% Cu). Reflectance decreases dramatically at the beginning due to high water vaporization rate in catalyst bed. After 15 minutes, most of the water is removed and it takes long another 25 minutes for rest of the water crystals to be removed.

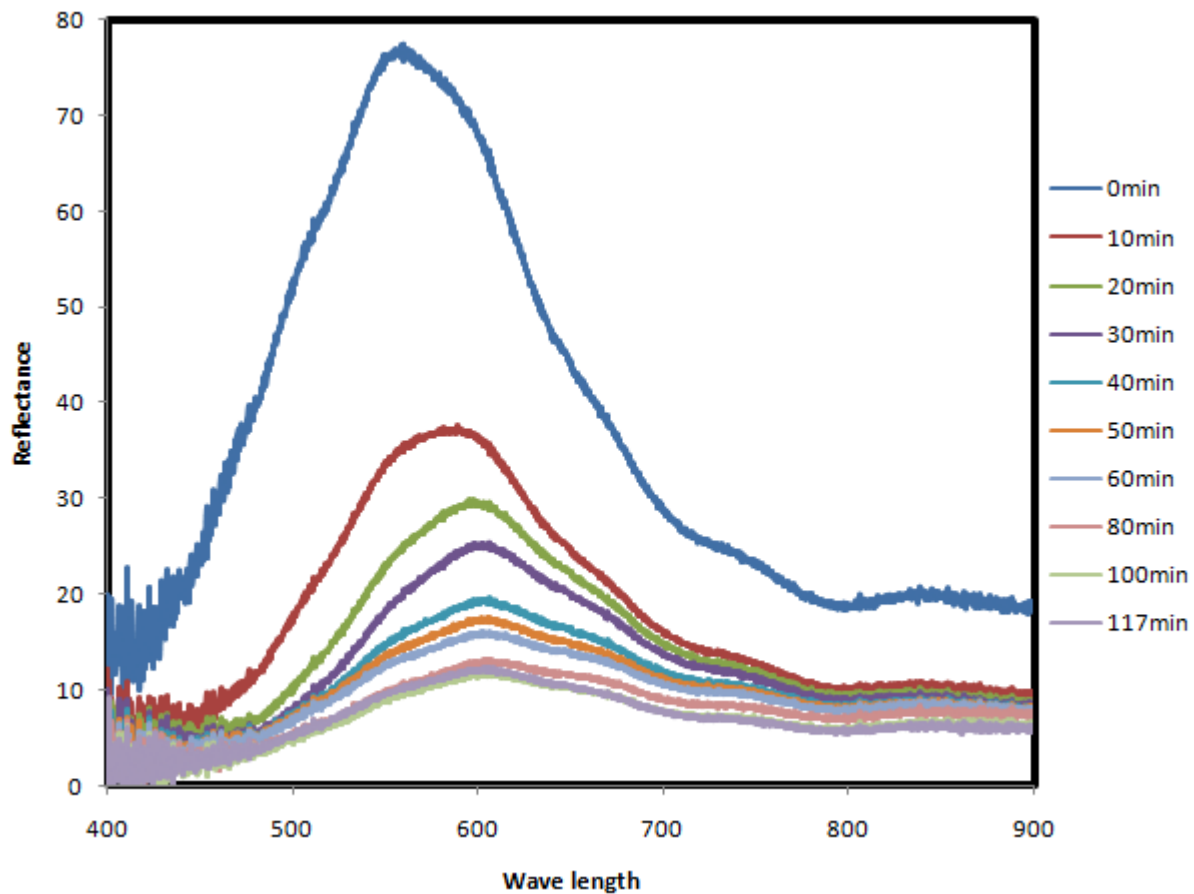


Figure 11: Activation of $\text{CuCl}_2.\text{CeO}_2/\gamma\text{-Al}_2\text{O}_3$ (5wt%Cu,1wt%Ce)

Figure 11 shows how water crystals are removed by helium flow at increasing temperature to 220C. Sample is dried after about two hours when the highest drying rate is at the first 10 minutes of the procedure (Regarding to spectra changes) and then rate is decreased due to the less availability of water crystals.

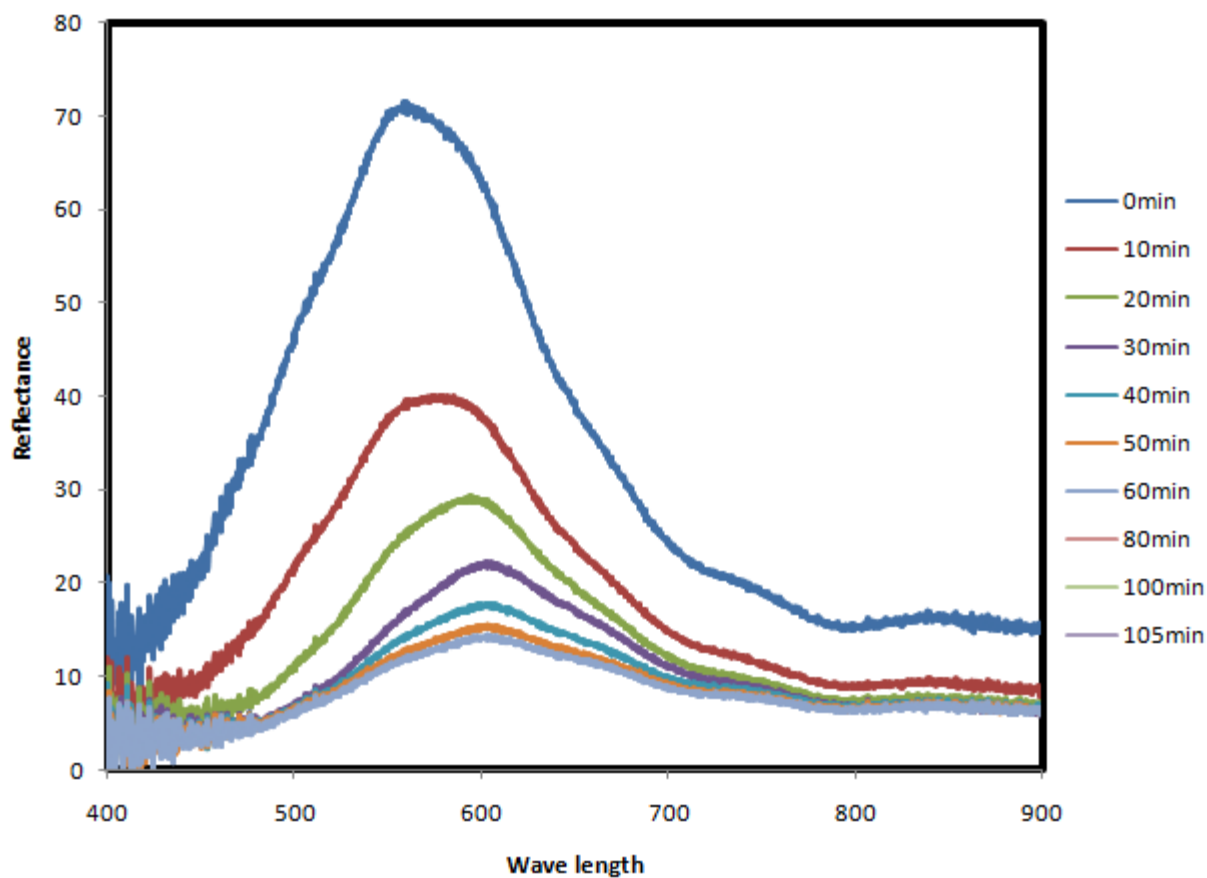


Figure 12: Activation of $CuCl_2.CeO_2/\gamma - Al_2O_3$ (5wt%Cu,3wt%Ce)

Figure 12 shows the changes in reflectance of $CuCl_2.CeO_2/\gamma - Al_2O_3$ (5wt%Cu, 3wt% Ce) within activation of catalyst. Total drying duration is 105 minutes and most of the water crystals are removed within 40 minutes since starting heating up the sample.

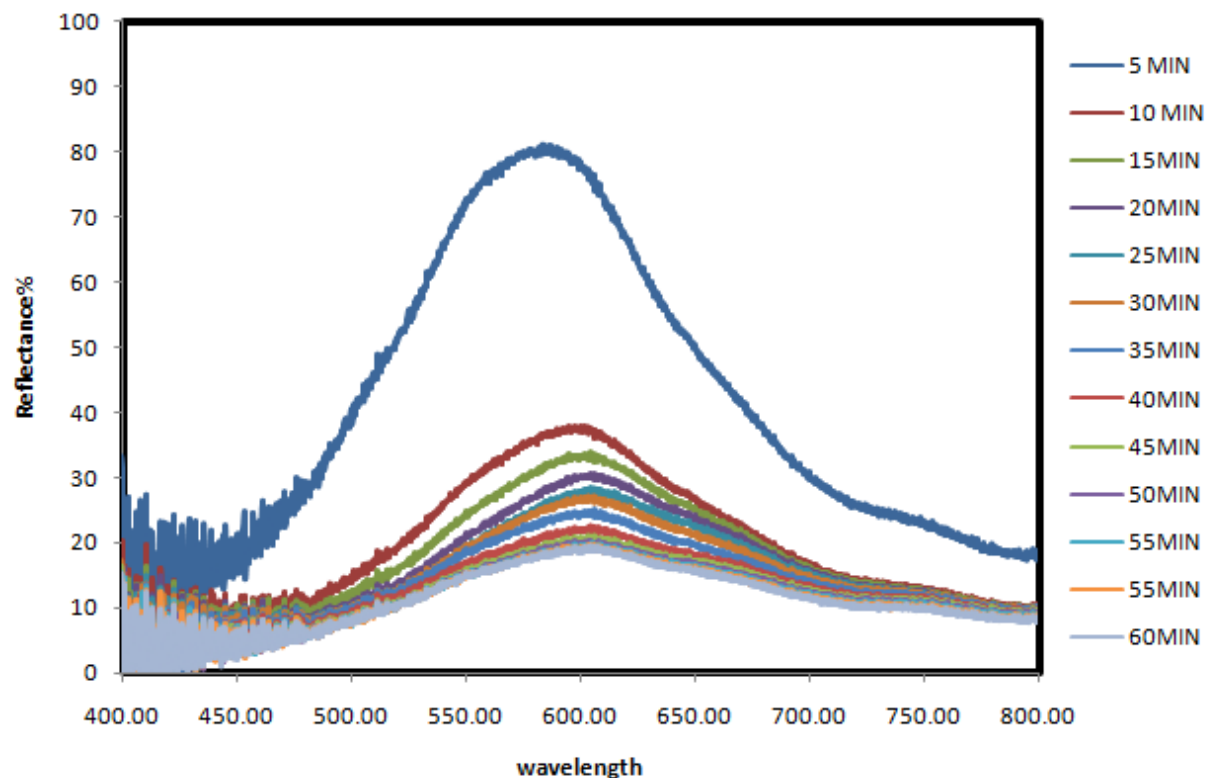


Figure 13: Activation of $\text{CuCl}_2 \cdot \text{CeO}_2 / \gamma - \text{Al}_2\text{O}_3$ (5wt%Cu, 5wt%Ce)

Water crystals desorb from catalyst within heating the catalyst inside the furnace. Once all the water crystals are removed, there would be no more change in the reflectance trends. As is shown in figure 13, the changes in reflectance trends between initial trends is significant which is due to high amount of water exist on the catalyst while the changes in last trends are negligible.

3.2.1 Effects of ceria additions on reflectance spectra

Comparing the reflectance versus wave length obtained from the cycles on $\text{CuCl}_2 / \gamma - \text{Al}_2\text{O}_3$ and $\text{CuCl}_2 \cdot \text{CeO}_2 / \gamma - \text{Al}_2\text{O}_3$ gives information below:

Ceria additions to $\text{CuCl}_2 / \gamma - \text{Al}_2\text{O}_3$ leads to a reduction in number of peaks from 2 to 1 however, there is no study available at moment discussing the reason. It also can be seen that the drying duration for $\text{CuCl}_2 \cdot \text{CeO}_2 / \gamma - \text{Al}_2\text{O}_3$ is shown to be more than of $\text{CuCl}_2 / \gamma - \text{Al}_2\text{O}_3$.

In addition, the peaks in the spectra of all four samples undergo a shift to the right as result of evaporation of the water crystals from the samples.

3.3 Reduction of CuCl_2 By C_2H_4

Oxychlorination of ethylene has three steps but only the data obtained from the first two steps are used to investigate the kinetics.

Data are recorded since start of reaction to end of the reaction. End of reaction is defined as the time in which trends in MS reach steady state and there would be no more change in absorbance wave in UV/VIS.

3.3.1 Ethylene flow over time

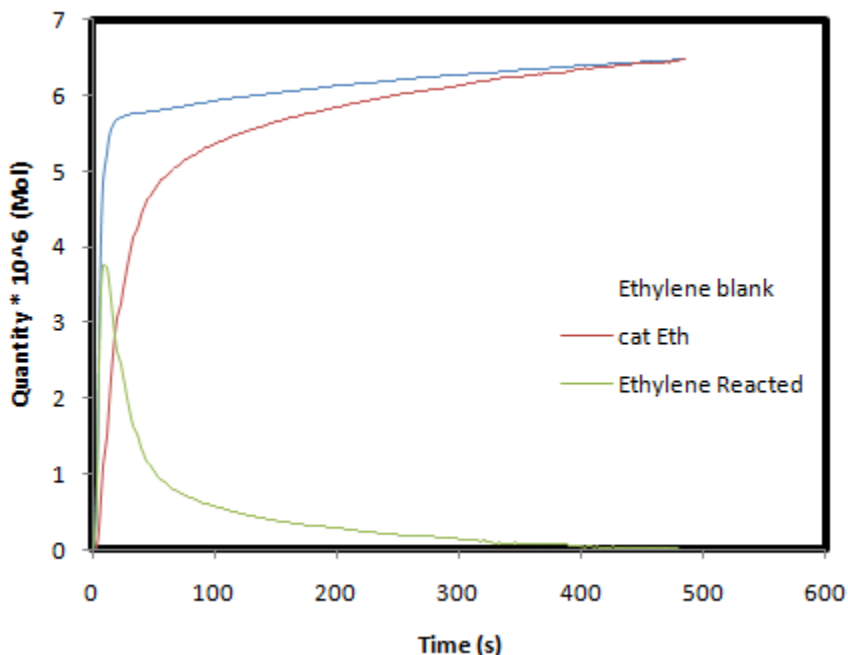


Figure 14 Ethylene flow versus time. First cycle. Catalyst: $\text{CuCl}_2 \cdot \text{CeO}_2 / \gamma - \text{Al}_2\text{O}_3$ (5wt%Cu,3wt%Ce) Reaction First Cycle conditions: $T=503\text{K}$, $P_{\text{eth}}=0.1$ bar, $P_{\text{tot}}=1$ bar

Once ethylene is introduced to the catalyst bed during first step of oxychlorination process, ethylene starts to react within the catalyst bed. During reaction, Cu^{2+} is reduced to Cu^+ . As is shown in the Figure 14, ethylene conversion to ethylene dichloride has the highest intensity at start of reaction once the highest concentration of Cu^{2+} is available. Catalyzed ethylene increases by time as reacted ethylene decrease. Once catalyzed ethylene reaches ethylene blank curve, then as result it can be said that no more ethylene is reacting within the catalyst.

3.3.2 Ethylene conversion

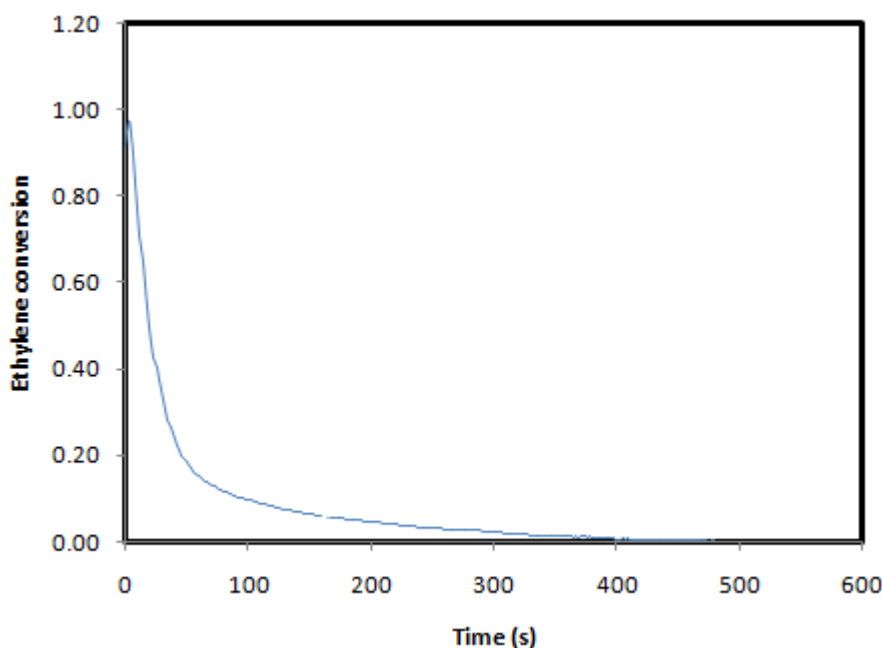


Figure 15: Ethylene Conversion First cycle. Catalyst: $CuCl_2.CeO_2/\gamma-Al_2O_3$ (5wt%Cu, 3wt%Ce) Reaction First Cycle conditions: T=503K, Peth=0.1 bar, Ptot=1 bar

As is shown in the figure15, Ethylene conversion decreases by time from around 95% at start of the reaction to 0 after 420 seconds from the beginning. This behavior is due to maximum amount of Cu^{2+} at start of the reaction and lowest amount (Zero) of Cu^{2+} after 420 seconds. As a result it could be said that availability of cupric chloride within the catalyst bed determines the magnitude of ethylene conversion.

3.3.3 Ethylene and chlorine uptake

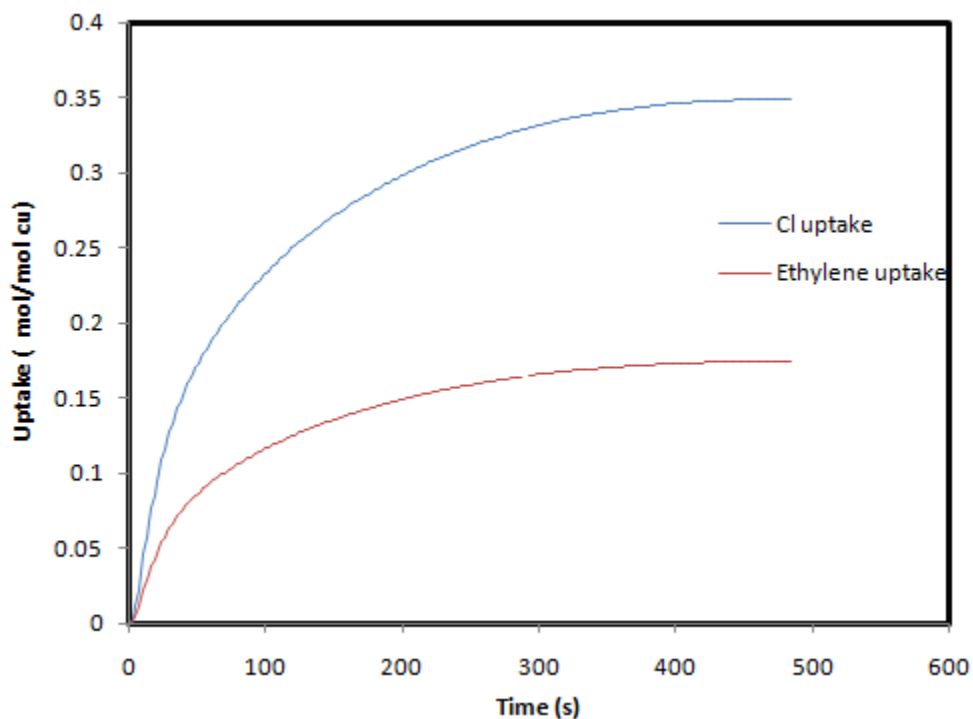


Figure 16: Uptake versus Time First cycle. Catalyst: $CuCl_2.CeO_2/\gamma-Al_2O_3$ (5wt%Cu,3wt%Ce) Reaction First Cycle conditions: T=503K, Peth=0.1 bar, Ptot=1 bar

Figure 16 shows uptake of ethylene and chlorine as a function of time within the reaction. As it can be seen, the slope ethylene Uptake versus time, due to availability of Cu^{2+} (as is discussed in "Ethylene conversion" part) is the highest at start of the reaction and then slope decreases as result of consumption of Cu^{2+} . Ethylene uptake however is not measured directly but due to the stoichiometry between chlorine and ethylene in the reaction (1-5), is considered to be twice as much as ethylene uptake.

3.3.4. Reaction rate versus removable chlorine

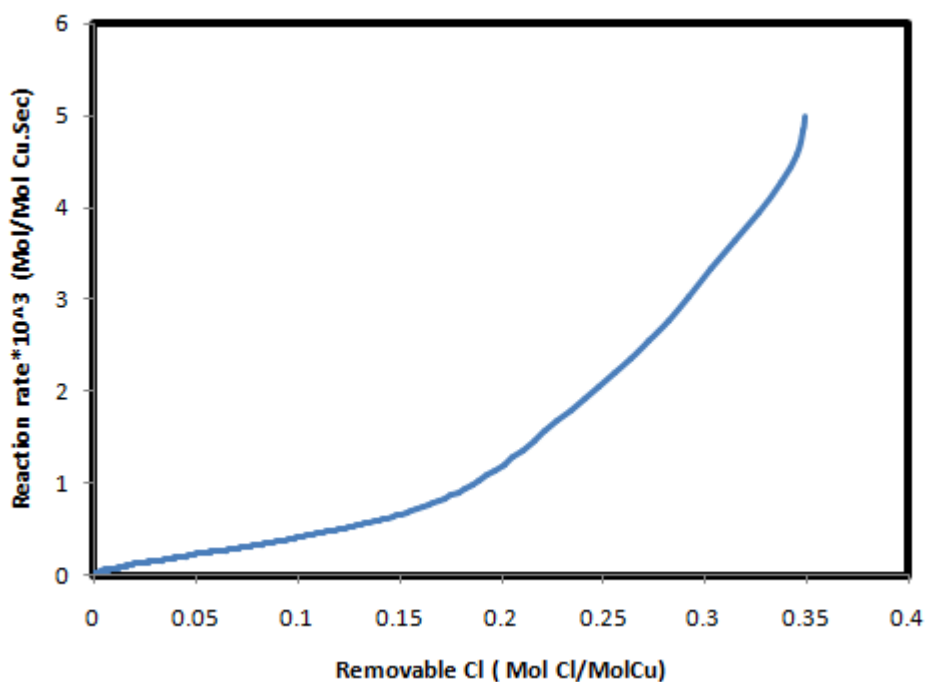


Figure 17: Reaction rate versus Removable chlorine. First cycle. Catalyst: $CuCl_2.CeO_2/\gamma-Al_2O_3$ (5wt%Cu,3wt%Ce) Reaction First Cycle conditions: T=503K, Peth=0.1 bar, Ptot=1 bar

As it can be seen reaction rate is almost linearly proportion to removable chlorine. Highest reaction rate belongs to start point of reaction (When all removable chlorine is present at the catalyst) and reaction rate approaches to zero when there is no removable chlorine left within the catalyst bed.

3.3.5. Removable chlorine

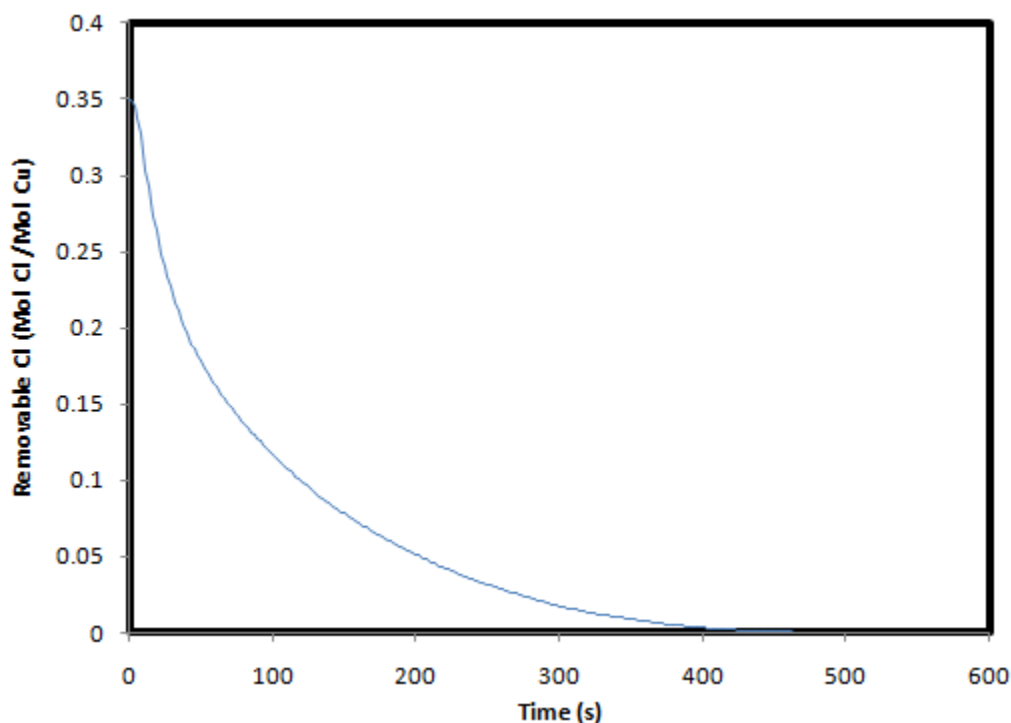


Figure 18: Removable chlorine versus Time First cycle. Catalyst: $CuCl_2.CeO_2/\gamma-Al_2O_3$ (5wt%Cu,3wt%Ce) Reaction First Cycle conditions: T=503K, Peth=0.1 bar, Ptot=1 bar

Figure 18 shows the reduction of removable chlorine over time due to consumption by exposed ethylene within the reaction. Removable chlorine is identified as that proportion of chlorine that can be absorbed by ethylene during the reaction. It should be taken into account that removable chlorine cannot exceed 1mol/mol cu.

3.3.6 Reflectance versus wave length

Figures below show the Kubelka-Munk function versus wave length. Peak height is considered to be at wave length of 792.64. Results obtained from first step (Reduction step) and second step (Oxidation) are shown in Figure19 and 20 respectively.

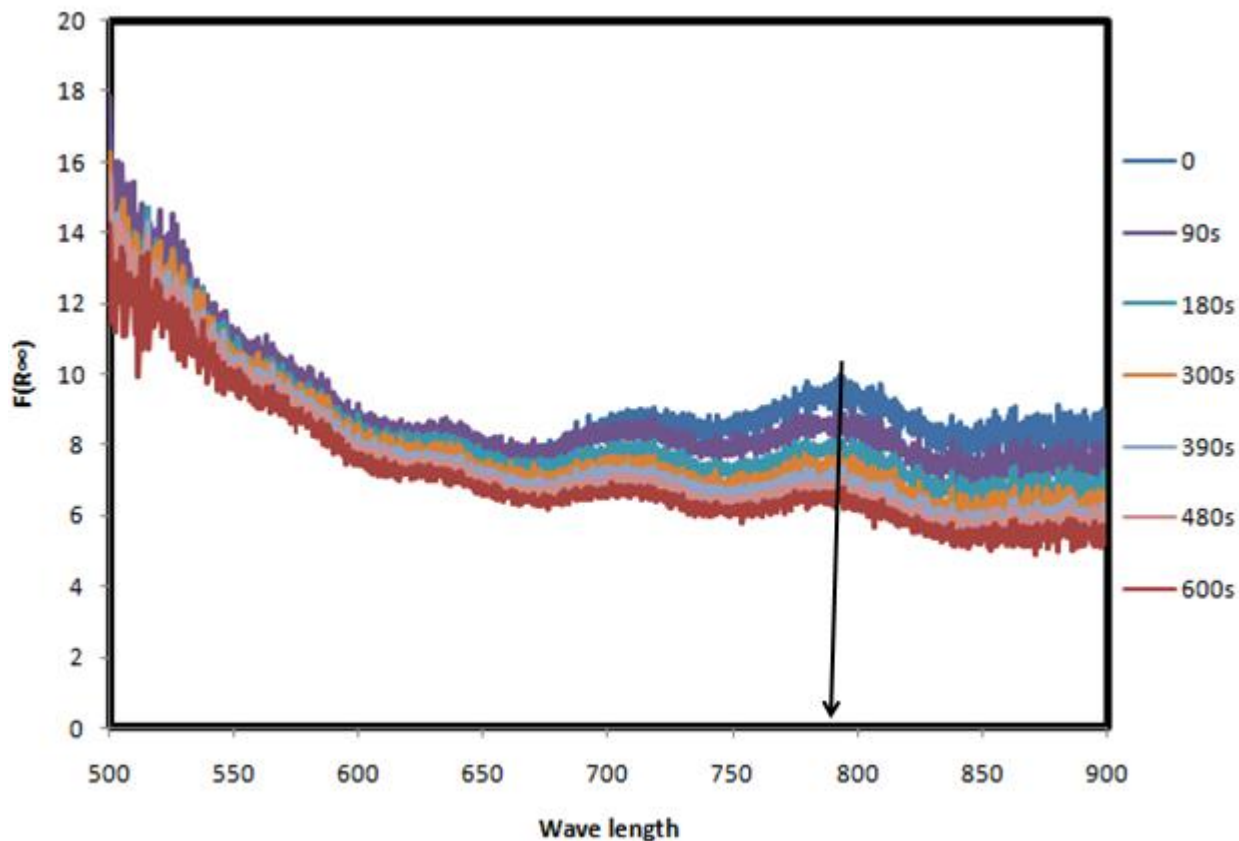


Figure 19: Reflectance versus Wave length. Peak height at 792.64. First cycle. Catalyst: $\text{CuCl}_2 \cdot \text{CeO}_2 / \gamma - \text{Al}_2\text{O}_3$ (5wt%Cu,3wt%Ce) Reaction First Cycle conditions: $T=503\text{K}$, $P_{\text{eth}}=0.1 \text{ bar}$, $P_{\text{tot}}=1 \text{ bar}$

As it can be seen in Figure19, Kubelka-Munk function decreases from 10 to 6 due to conversion of Cu^{2+} to Cu^+ . Although total time for the reaction as is shown in the figure is 600 seconds but the changes between first trends seem to be bigger than the last ones, indicating a higher rate of conversion at beginning of the reaction.

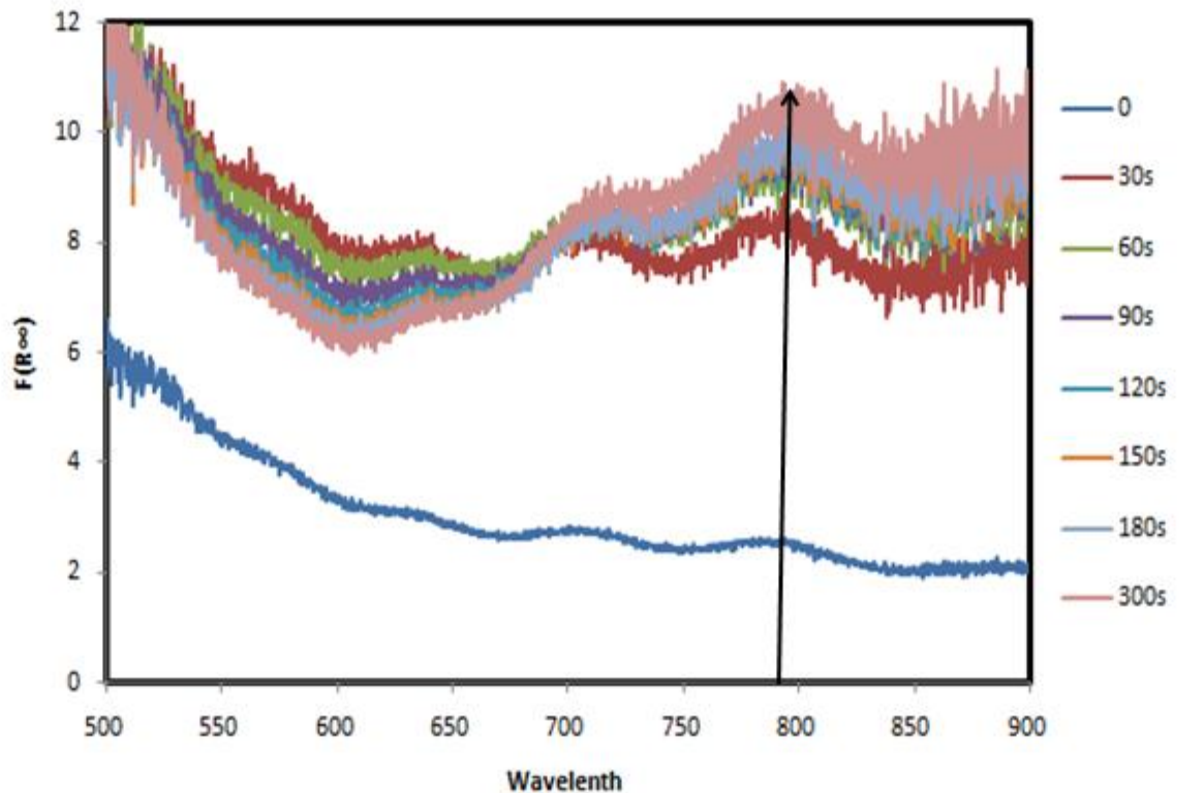


Figure 20: Reflectance versus Wave length. Peak height at 792.64. First cycle .Catalyst: $CuCl_2.CeO_2/\gamma - Al_2O_3$ (5wt%Cu,3wt%Ce)Reaction First Cycle conditions: T=503K, PO₂=0.1 bar, P_{tot}=1 bar

Figure 20 shows how reduced catalyst oxidizes to its initial value (10) within a short time by oxidation. The criteria to know if the catalyst is completely oxidized, is the change in kubelka-Munk function trend. Once there is no more change in the trend, catalyst is completely oxidized.

3.4 Effects of Ceria on reduction step

In order to investigate the effects of Ceria on first and second step in Oxychlorination of ethylene, chlorine uptake versus time and reaction rates versus chlorine uptake for the first step and reaction rate for the second steps on $CuCl_2/-Alumina$ and $CuCl_2/G-Alumina$, CeO_2 are used as criteria.

3.4.1 Effects on Chlorine uptake

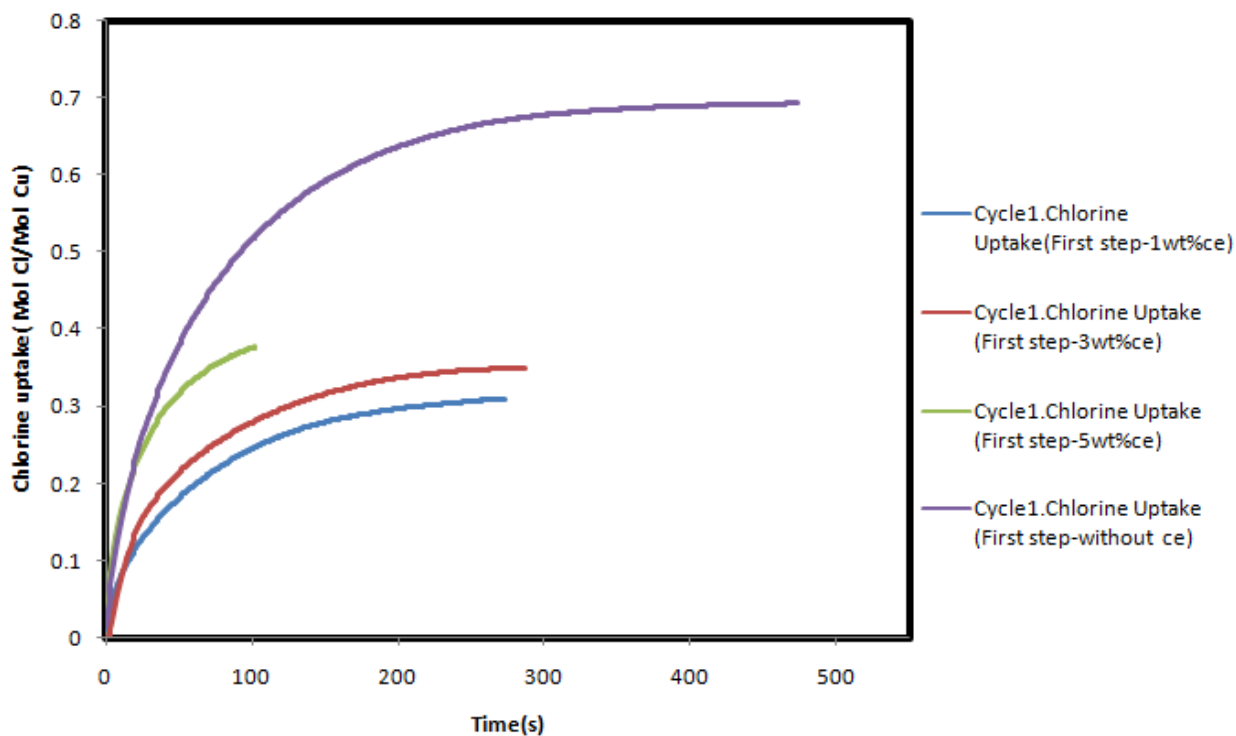


Figure 21: Chlorine uptake versus time in first cycles of all four catalysts at the same conditions:

T=503K P_{Total}=1 bar P_{Eth}=0.1 (5wt% Cu, variable Ce wt%)

Figure 21 shows a remarkable difference in chlorine uptakes between CuCl₂/G-Al₂O₃ and Ceria doped CuCl₂ on G-Al₂O₃. The catalyst without ceria has an uptake of almost twice as much as those with ceria and for those catalysts with ceria, ones with 5wt% ceria and 1wt% ceria have the highest and lowest chlorine uptake respectively.

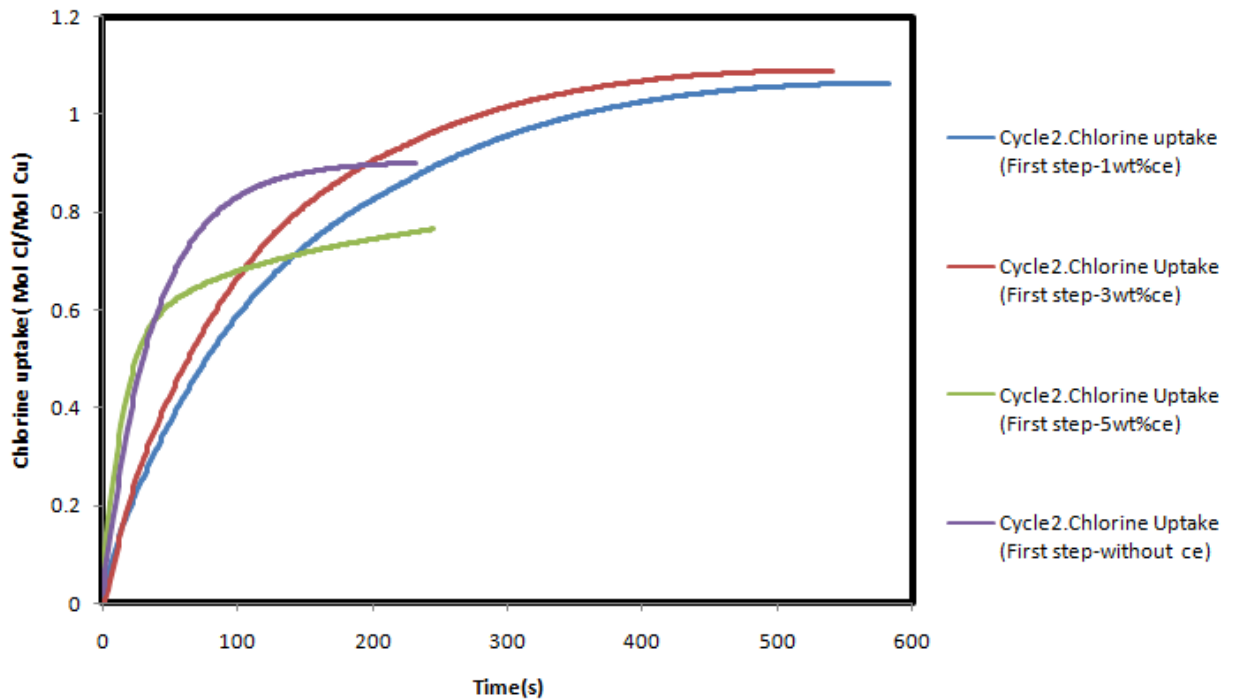


Figure 22: Chlorine uptake versus time in second cycles of all four catalysts at the same conditions:

T=503K P_{Total}=1 bar P_{Eth}=0.1 (5wt% Cu, variable C_{ewt}%)

As it can be seen in Figure 22, chlorine uptakes in second cycles for all catalysts except the one with 5wt% ceria, is much more than uptakes at the first cycles, showing more activity than first cycle. The reason is removing all the impurities in the catalyst bed during running the first cycle. In order to have accurate results, all the impurities should be removed from the catalyst. The most probable impurity is water crystals which can be removed within heating up the catalyst.

On the other hand, the high loading of ceria in $CuCl_2/CeO_2/\delta - Alumina$ (5wt%Cu, 5wt% Ce) leads to either Ceria-Alumina or Ceria-Copper bonds which result in partial deactivation of the catalyst in second cycle.[29]

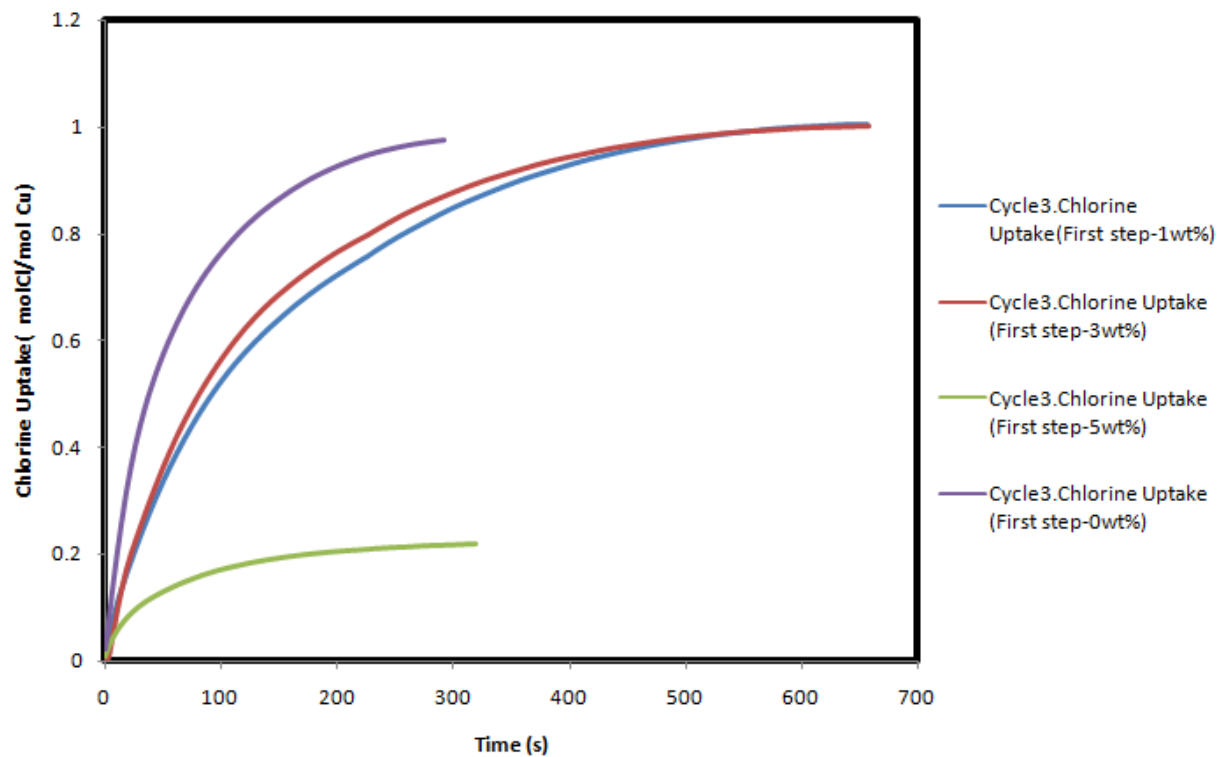


Figure 23: Chlorine uptake versus time in third cycles of all four catalysts at the same conditions:

$T=503K$ $P_{Total}=1$ bar $P_{Eth}=0.1$ (5wt% Cu, variable Cewt%)

Figure above shows almost the same Chlorine uptakes for non doped $CuCl_2/\delta - Alumina$ and Ceria doped $CuCl_2/\delta - Alumina$ with 1 and 3 wt% Ceria loading. However the reaction duration for catalysts with 1 and 3 wt% Ceria is twice as much as the time for $CuCl_2/\delta - Alumina$ (5wt% Cu). Green trend which belong to $CuCl_2/CeO_2/\delta - Alumina$ (5wt%Cu, 5wt% Ce) shows that this catalyst is mostly deactivated.

3.4.2 Effects on reaction rate

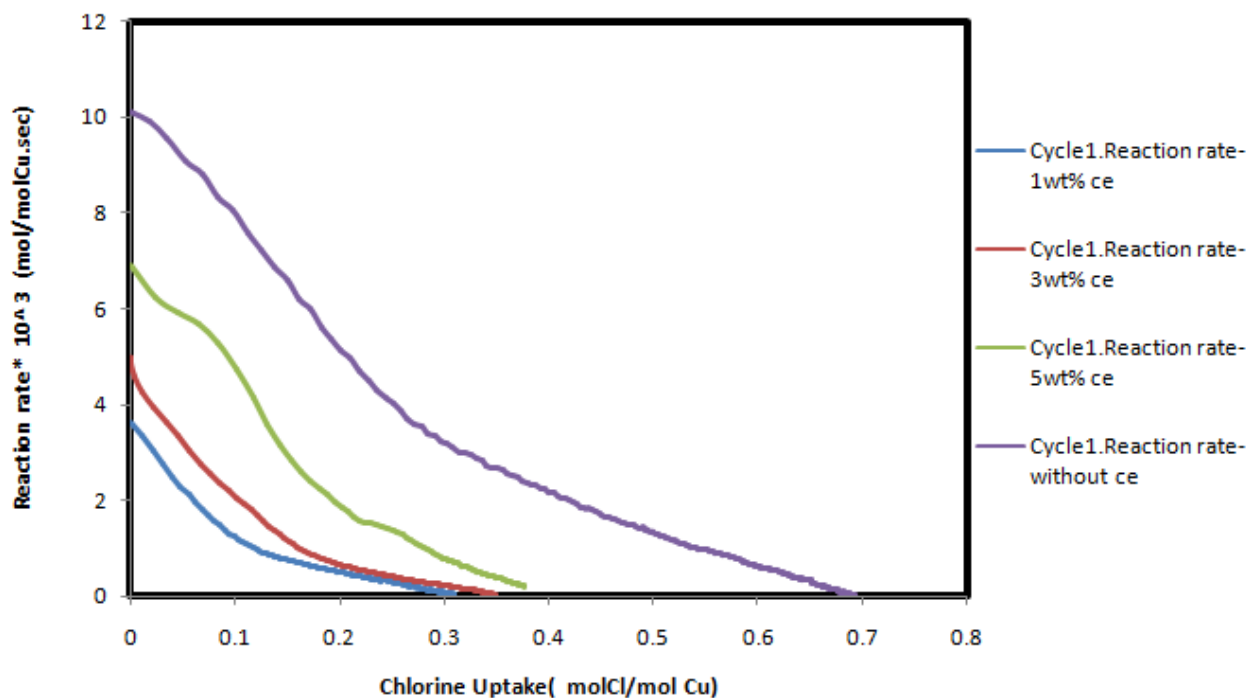


Figure 24: Reaction rate versus Chlorine Uptake in first cycles of all four catalysts at the same conditions:

T=503K P_{Total}=1 bar P_{Eth}=0.1 (5wt% Cu, variable Ce wt%)

In Figure 24, Reaction rate (mol/mol Cu. Sec) of all four catalysts in the first cycle is shown as a function of chlorine uptake (mol Cl/mol Cu). As is shown in the figure, Ceria additions can significantly decrease the reaction rate in reduction step such as addition of 1wt% ceria can reduce the reaction rate to one third. The reason is reaction of cerium with the carrier to form an inert phase.[20]

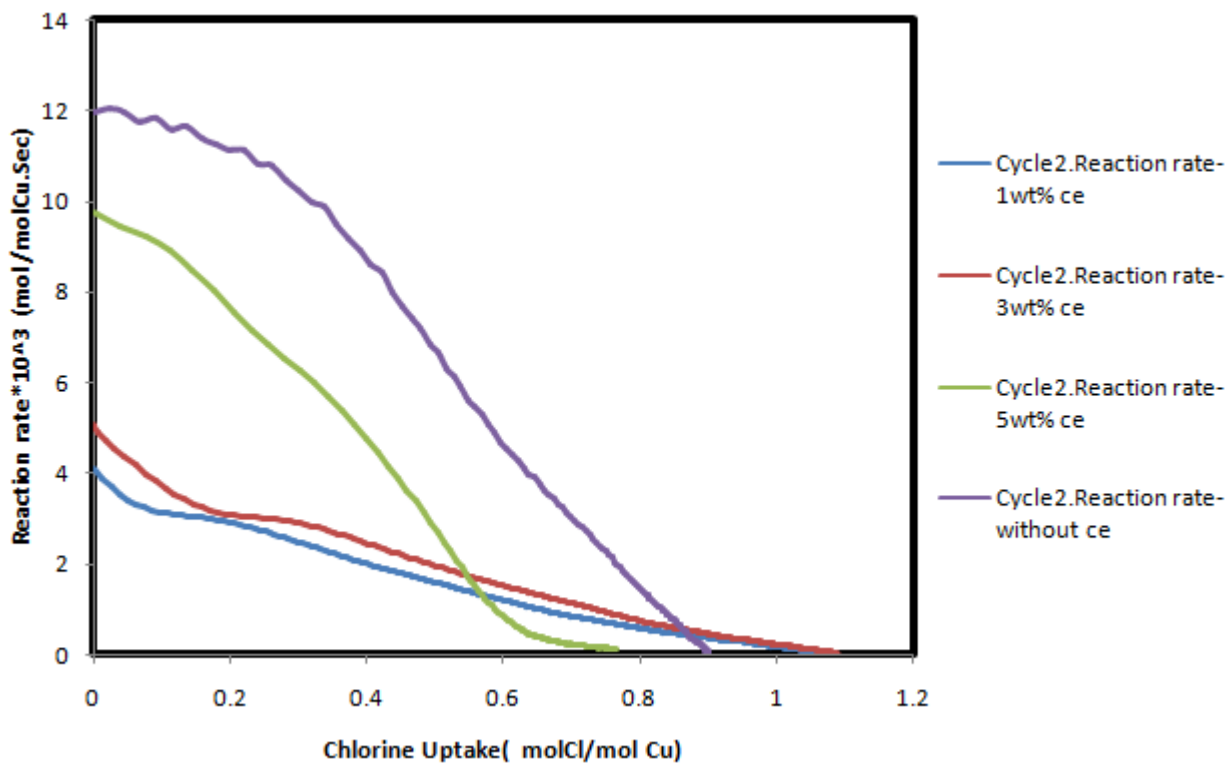


Figure 25: Reaction rate versus Chlorine Uptake in second cycles of all four catalysts at the same conditions:

T=503K PTotal=1 bar PEth=0.1 (5wt% Cu, variable Cewt%)

Although the reaction rates in the second cycle for almost all the catalyst is increased but, still the highest reaction rate belongs to the catalyst without Ceria. $\text{CuCl}_2 \cdot \text{CeO}_2 / \gamma - \text{Al}_2\text{O}_3$ with 5 and 1wt% ceria have the highest and lowest reaction rate among cerium doped catalysts respectively. In this experiment, chlorine uptake of $\text{CuCl}_2 \cdot \text{CeO}_2 / \gamma - \text{Al}_2\text{O}_3$ with 1 and 3 wt% are more than $\text{CuCl}_2 / \delta - \text{Alumina}$ however the reaction rates are less.

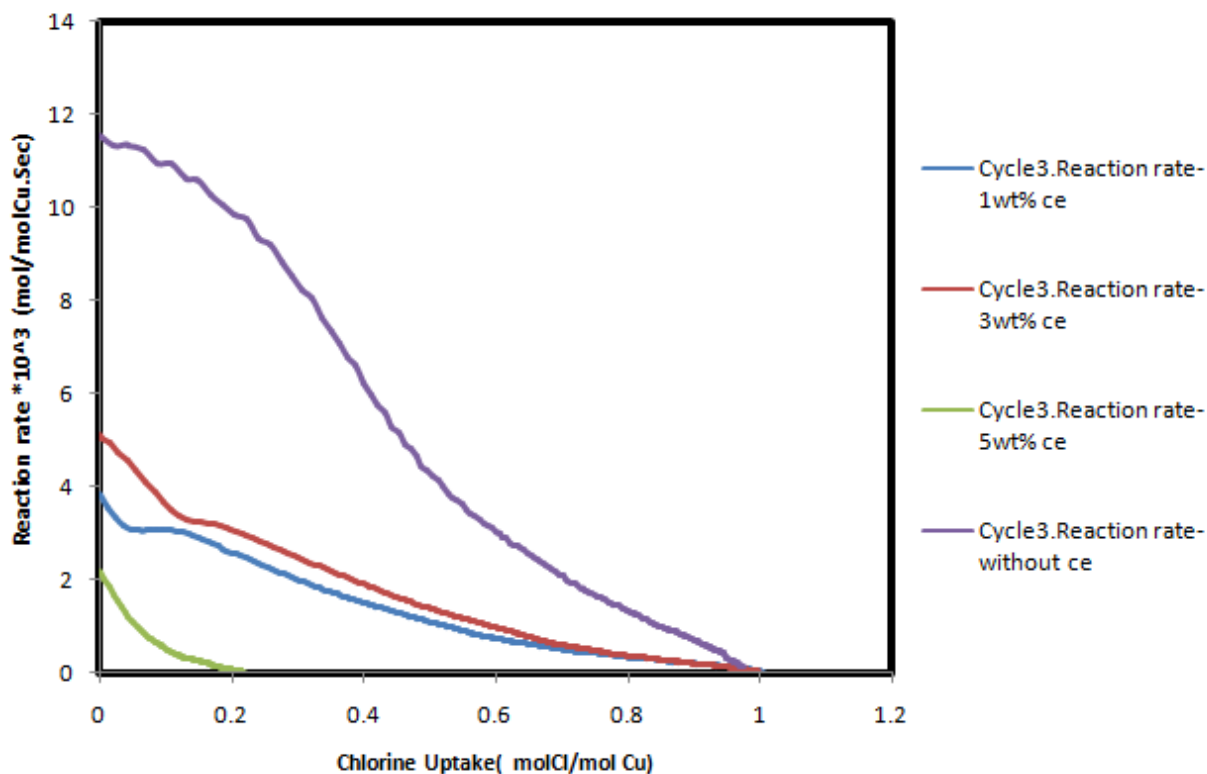


Figure 26: Reaction rate versus Chlorine Uptake in third cycles of all four catalysts at the same conditions:

T=503K PTotal=1 bar PEth=0.1 (5wt% Cu, variable Cewt%)

Figure 26 demonstrate that addition of 5wt% ceria to $CuCl_2.CeO_2/\gamma-Al_2O_3$ almost deactivates the catalyst after two experiments while for less concentration reduction in catalyst activity is negligible. Growth and reaction of CeO_2 crystals with carrier during the reaction are reported as the main reasons for deactivation of Copper-based oxychlorination catalyst.[20, 30, 31]

3.5 Overall view of effect of ceria additions on chlorine uptake and reaction rate

Figures 27 and 28 show how chlorine uptake and reaction rate in 3 cycles change as a function of concentration of Ceria in $\text{CuCl}_2 \cdot \text{CeO}_2 / \gamma - \text{Al}_2\text{O}_3$. Data are obtained from

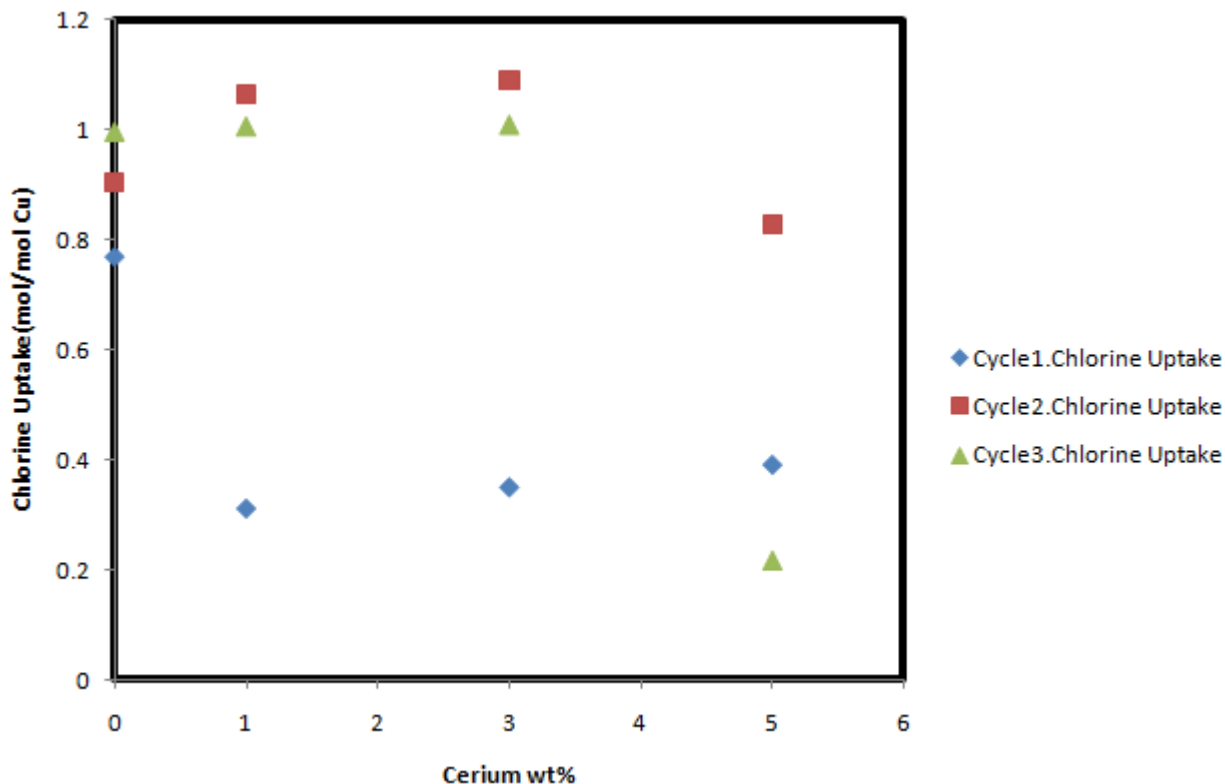


Figure 27: Chlorine uptake as a function of Cerium wt%.

conditions: $T=503\text{K}$ $P_{\text{Total}}=1$ bar $P_{\text{Eth}}=0.1$ (5wt% Cu, variable Cewt%)

Figure 27 shows chlorine uptake in the oxychlorination reaction as a function of cerium wt%. At the first cycle (Shown as Exp1) chlorine uptake of $\text{CuCl}_2 / \gamma - \text{Al}_2\text{O}_3$ is shown to be twice as much as $\text{CuCl}_2 \cdot \text{CeO}_2 / \gamma - \text{Al}_2\text{O}_3$ however total uptake of chlorine in first cycle is less than chlorine uptake in the second and third cycle. The reason is presence of impurities (which are bonded to active phase) in the catalyst at the first cycle. Impurities are removed within the first cycle such that the removable chlorine in the second cycle is almost doubled. In third cycle, the chlorine uptake for all the catalysts with ceria are decreased which is due to formation of CeOCl or CeAlO_3 on the surface.[32] The higher concentration of

ceria the faster deactivation of the catalyst however $CuCl_2/\delta - Alumina$ doesn't follow $CuCl_2.CeO_2/\gamma - Al_2O_3$ and it has a higher amount of chlorine uptake in third cycle than second cycle.

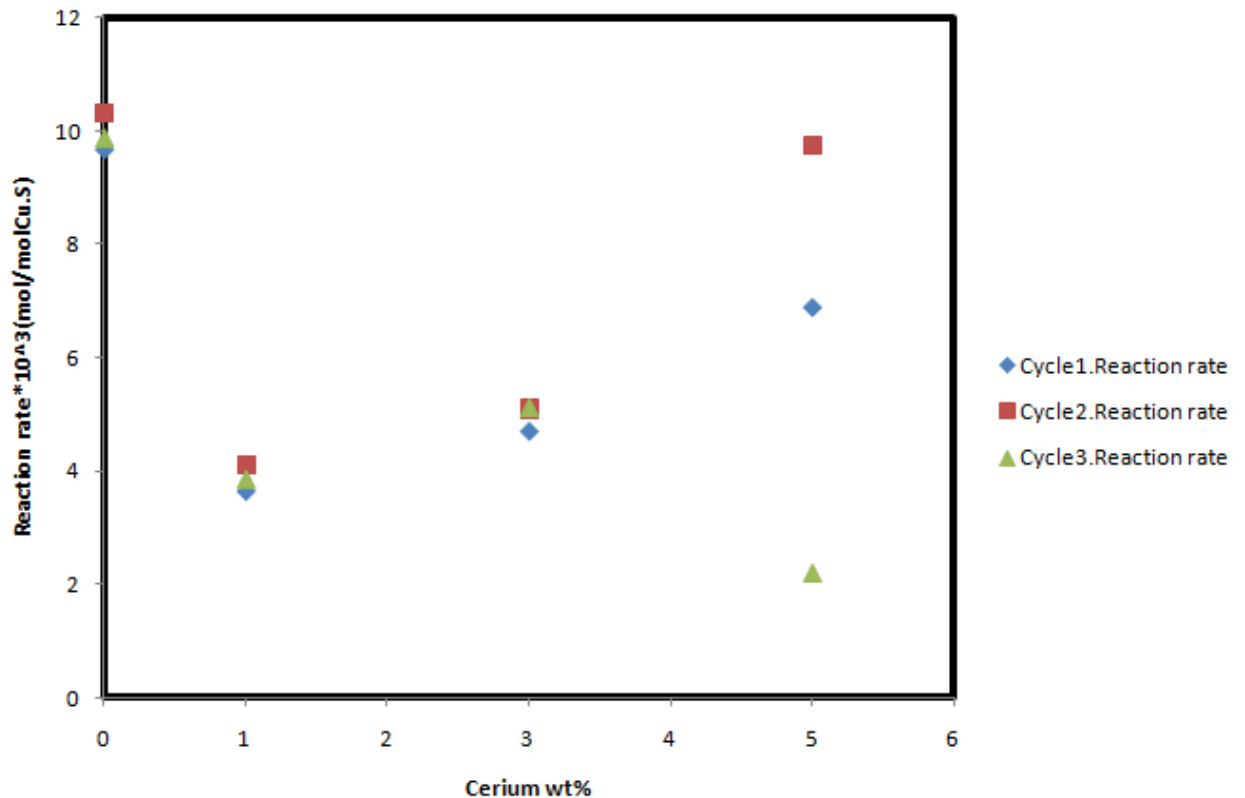


Figure 28: Reaction rate as a function of Cerium wt%. conditions: T=503K PTotal=1 bar PEth=0.1 (5wt% Cu, variable Cewt%)

As it can be seen in Figure 28, Ceria additions to $CuCl_2/\gamma - Al_2O_3$, significantly decreases the reaction rate in reduction step however the reaction rate at second cycle on $CuCl_2.CeO_2/\gamma - Al_2O_3$ with 5 wt% ceria shows almost a same reaction rate as $CuCl_2/\gamma - Al_2O_3$.

The reason for the reduction in the reaction rate due to ceria additions can be justified by formation of CeOCl or CeAlO₃ at the surface which leads to a less amount of removable chlorine.[32]

3.6 Effects of Ceria on Oxidation step

Relative Kubeka-Munk function versus time is used as a criteria to see the effects of ceria additions to $CuCl_2/\delta - Alumina$ in oxidation step. Relative Kubelka-Munk function changes from 0 (At beginning of the reaction) to 1(End of the reaction) in oxidation step.

$$\frac{F_t - F_0}{F_\infty - F_0} \quad (2-1)$$

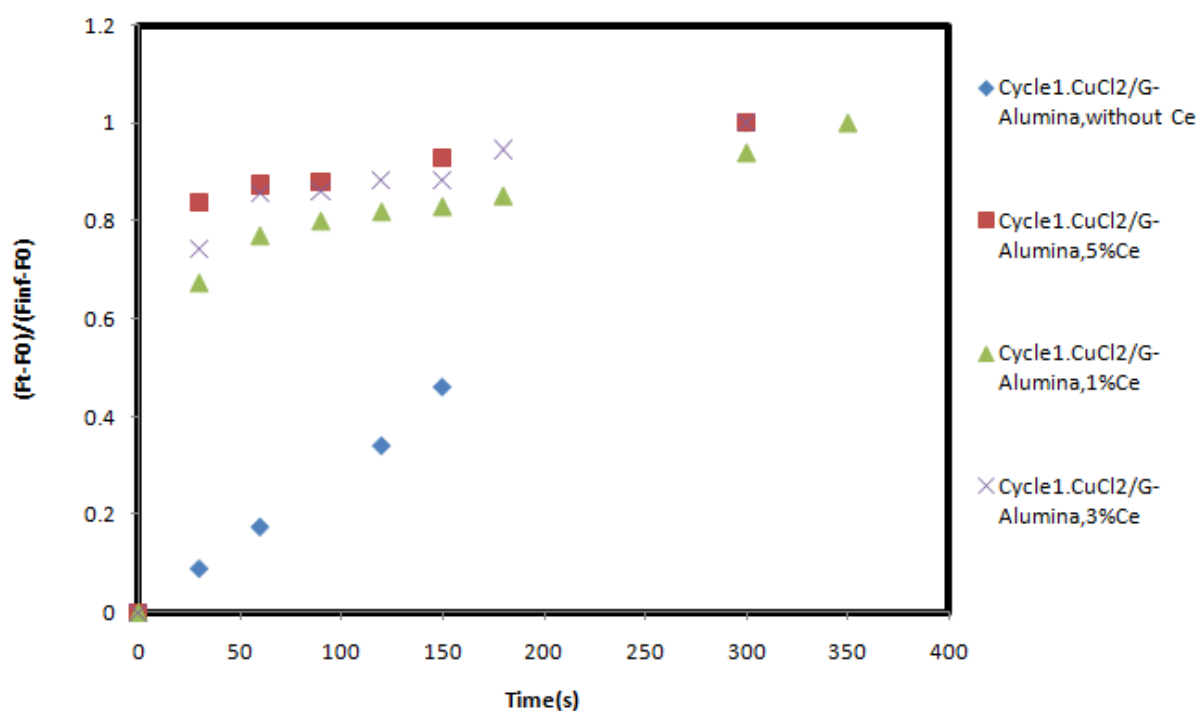


Figure 29: Relative Kubelka-Munk function as a function of time. Oxidation Step. first cycles of all four catalysts at the same conditions: $T=503K$ $P_{Total}=1$ bar $PO_2=0.1$ (5wt% Cu, variable Ce wt%).

Figure 29 shows relative Kubelka-Munk function versus time within the reaction in first cycles. At a certain time, the higher amount the more oxidation state. $CuCl_2/CeO_2/\delta - Alumina$ with 5 wt% ceria is fastest following by the catalyst with 3wt% Ce, 1wt% Ce and the catalyst without Ceria.

As it can be seen presence of CeO_2 in the catalyst plays a major role in oxidation rate of catalyst when even for the catalyst with 1wt% Ceria mostly 70 percentage of the oxidation reaction is done within the

first 30 seconds. The reason is functionality of CeO_2 which works as oxygen storage on the surface leading to acceleration in the oxidation step, which was the rate limiting step of this reaction.[20, 30, 32]

The other two cycles also show the same behavior as the first one.

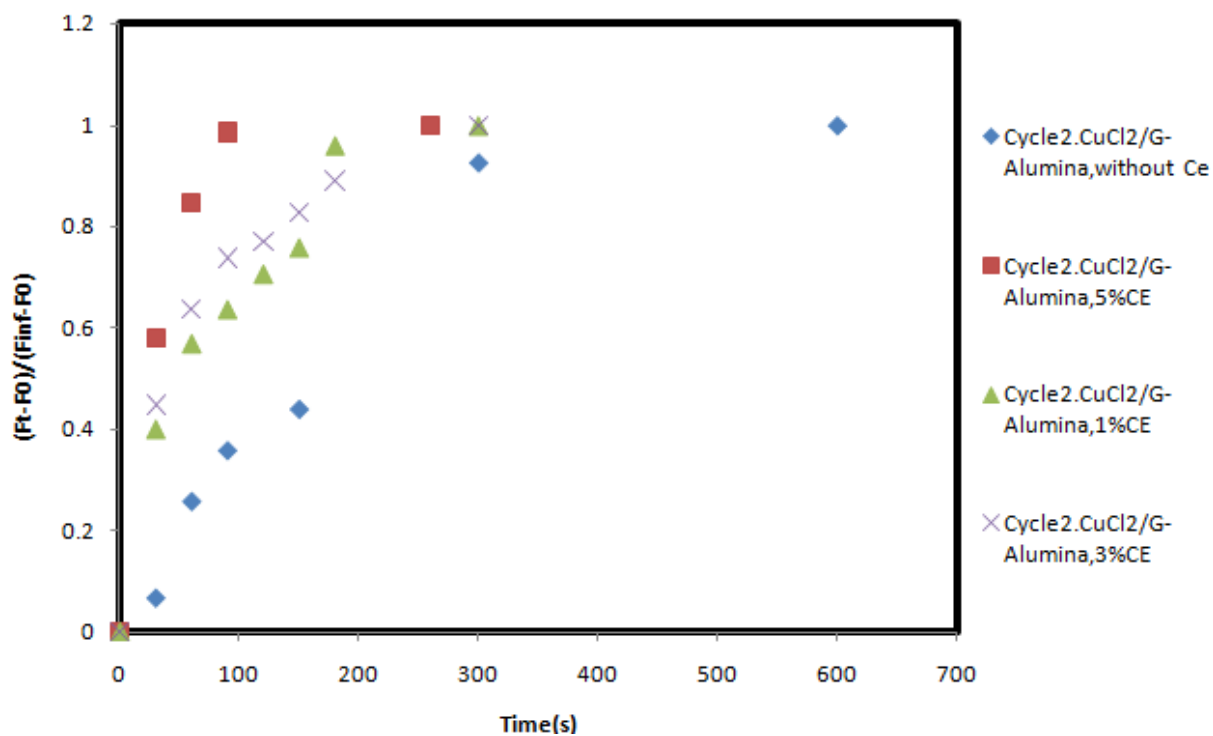


Figure 30: Relative Kubelka-Munk function as a function of time. Oxidation Step. second cycles of all four catalysts at the same conditions: $T=503\text{K}$ $P_{\text{Total}}=1$ bar $P_{\text{O}_2}=0.1$ (5wt% Cu, variable Ce wt%)

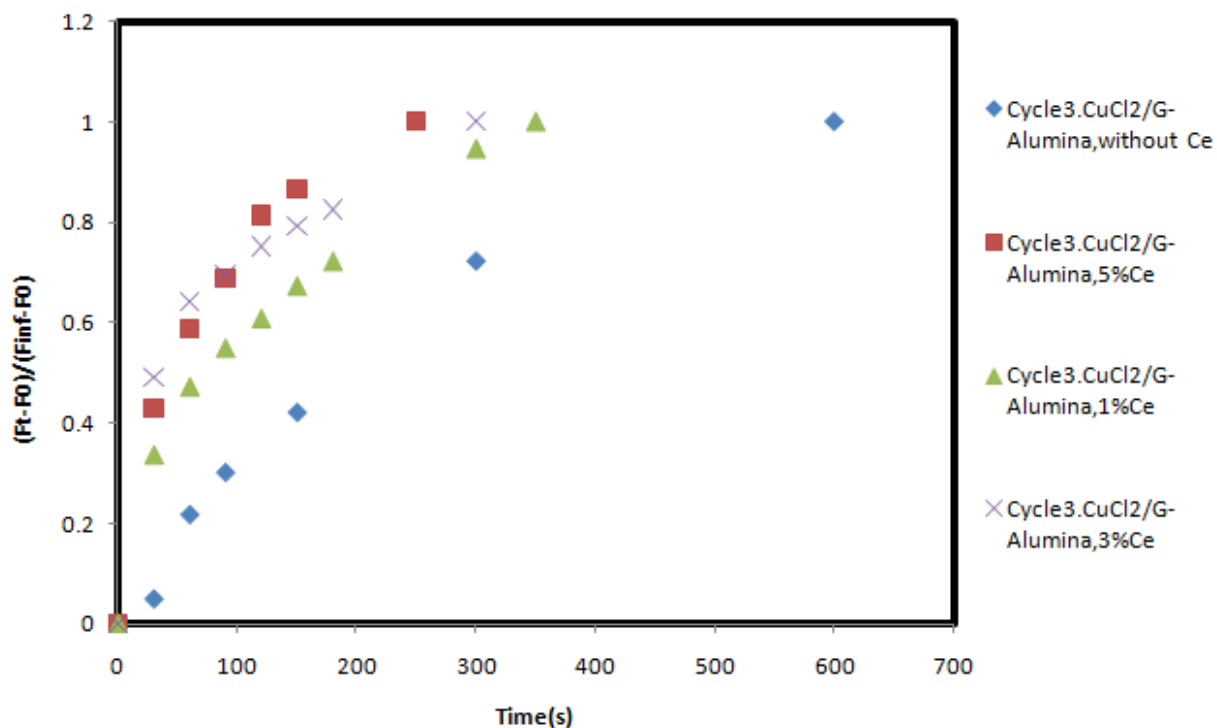


Figure 31: Relative Kubelka-Munk function as a function of time. Oxidation Step. third cycles of all four catalysts at the same conditions: $T=503K$ $P_{Total}=1$ bar $PO_2=0.1$ (5wt% Cu, variable Ce wt%)

3.7 Correlation of MS and UV/VIS Data

Figure below shows how the data obtained from mass spectrometer are related to the data obtained from UV/VIS spectrometer.

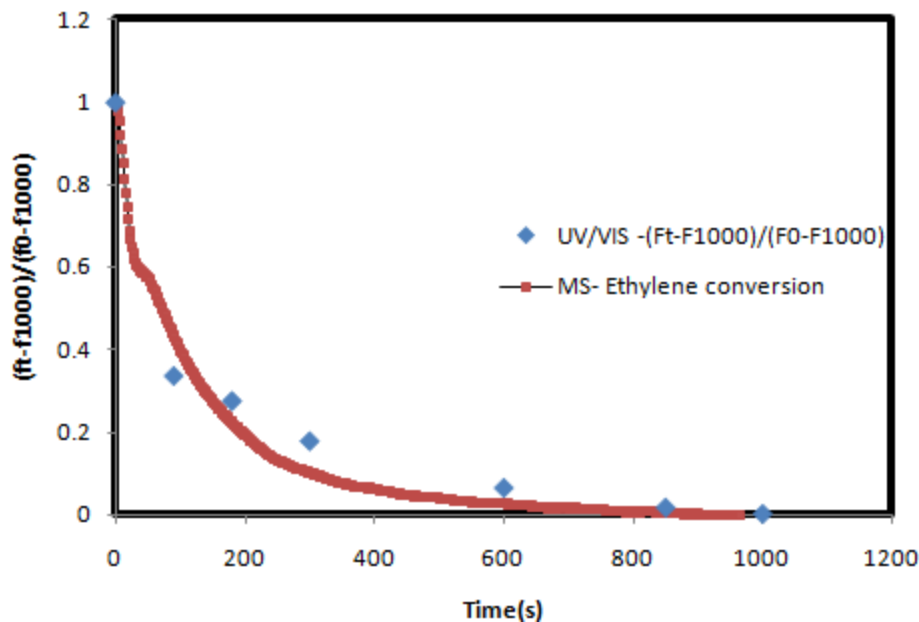


Figure 32: Correlation of UV/VIS data (Relative Kubelka-Munk function) and MS data (Ethylene conversion) obtained from second cycle on $\text{CuCl}_2/\text{G-Al}_2\text{O}_3.\text{CeO}_2$ (5wt% Cu, 3wt% Ceria) Conditions: conditions: $T=503\text{K}$ $P_{\text{Total}}=1$ bar $P_{\text{Eth}}=0.1$

As is shown in figure 32, ethylene conversion obtained from mass spectrometer shows a good fitness with relative Kubelka-Munk function obtained from UV/VIS at second cycle on $\text{CuCl}_2/\text{CeO}_2/\delta$ - Alumina (5wt% Cu, 3wt% Ceria).

During recording the data by Mass Spectrometer at a certain point the spectra doesn't show anymore change, meaning the reaction time is over. Nevertheless the spectra in UV/VIS undergoes more changes. A possible reason for this behavior could be the extraction of remained chlorine within catalyst bed which influence the spectra in UV/VIS spectrometer. Hence as it can be seen in Figure 32, the overall reaction time for UV/VIS is a bit more than of Mass Spectrometer.

As is can be seen in Figure 33, In some experiments due to the high intensity of exposing gas to the surface, diffusion limitation occurs which prevent a good fitness between MS data and UV/VIS data.

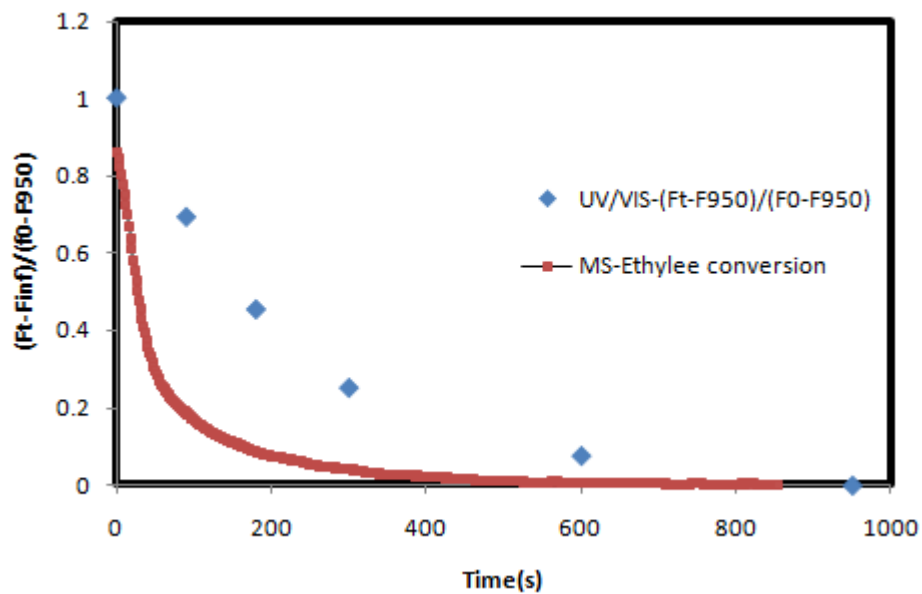


Figure 33: Correlation of UV/VIS data (Relative Kubelka-Munk function) and MS data (Ethylene conversion) obtained from First cycle on $\text{CuCl}_2/\text{G-Al}_2\text{O}_3$ (4.8wt% Cu). Conditions: conditions: $T=503\text{K}$ $P_{\text{Total}}=1$ bar $P_{\text{Eth}}=0.1$

Diffusion limitation occurs when the rate on the surface (R_{Surface}) is less than diffusion rate. Figure 33 shows a good demonstration of this process.

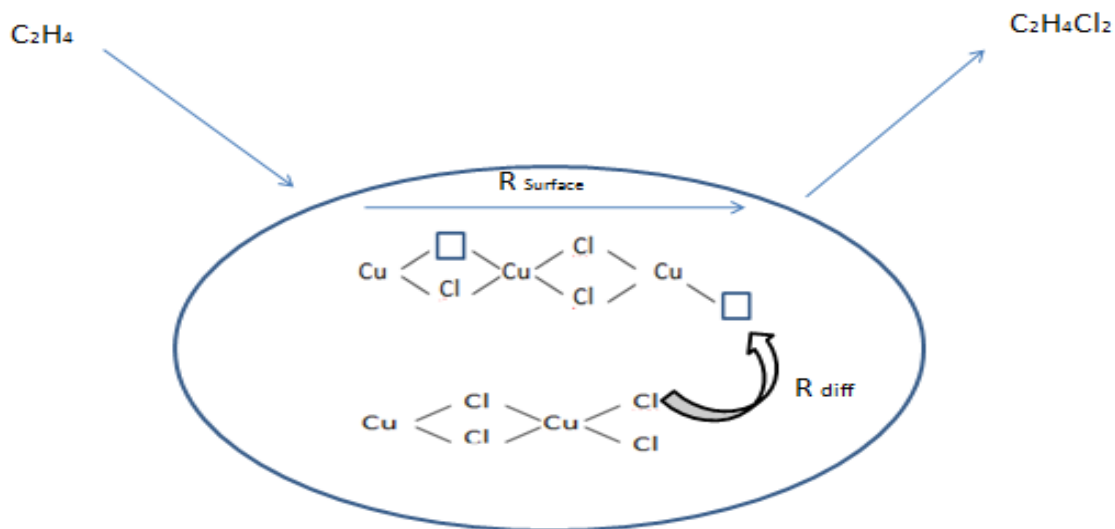


Figure 34: schematic illustration of ethylene chlorination

4. CONCLUSION

Based on the results of ethylene oxychlorination on $CuCl_2/\delta - Alumina$ (5wt%Cu) and $CuCl_2/CeO_2/\delta - Alumina$ (5wt%Cu, 1,3 and 5wt% Ceria), following conclusions are given:

Ceria concentration plays a decisive role in catalytic behavior of $CuCl_2/CeO_2/\delta - Alumina$ used for production of chloroethylene.

Low amount of ceria additions can highly reduce the reduction rate while it has no negative impacts on total chlorine uptake.

High concentration of ceria leads to the interaction between ceria and carrier to form $CeAlO_3$ or ceria and active phase to form $CeOCl$ which results in faster deactivation of catalyst.

Ceria additions to $CuCl_2/\delta - Alumina$ as a promoter can enhance the oxidation rate. CeO_2 increases the concentration of superficial oxygen on the catalyst (Due to presence of mixed oxidation states (3+/4+) of cerium) and accelerate the reaction rate.

References

1. Arganbright, R.P.Y., W. F., *chlorination with cupric chloride*. *J. Org. Chem*, 1962: p. 1205-1208.
2. Mersiowsky, I., M. Weller, and J. Ejlertsson, *Fate of Plasticised PVC Products under Landfill Conditions: A Laboratory-Scale Landfill Simulation Reactor Study*. *Water Research*, 2001. **35**(13): p. 3063-3070.
3. Mersiowsky, I., *Long-term fate of PVC products and their additives in landfills*. *Progress in Polymer Science*, 2002. **27**(10): p. 2227-2277.
4. Charles E. Wilkes, J.W.S., Chales Anthony Daniels, Mark T. , *PVC handbook*. p. 29-35.
5. Seok Go, K.K., Y. ; Real Son, S. ; Done Kim , S. , *1,2-dichloroethane production by two step oxychlorination reactions in fluidized bed reactor*, *chemical Engineering science*. 2010: p. 499-503.
6. Trade note company <http://www.tradenote.net>. 16/05/2014.
7. Ali zahrani, S.M.A., A. M. ; Wagialla, K. M . *Modelling and simulation of 1,2-dichloroethane production by ethylene oxychlorination in fluidized-bed reactor*. *chemical engineering science* 2001: p. 621-626.
8. Nawroski, j.S.V., E. S., *Oxychlorination of ethylene*. 1983: p. 239-273.
9. Finocchio, E., et al., *Characterization and Catalytic Activity of CuCl₂-Al₂O₃Ethylene Oxychlorination Catalysts*. *Journal of Catalysis*, 1998. **179**(2): p. 606-618.
10. Wachi, S.A., Y. , *Kinetics of 1,2-dichloroethane formation from ethylene and cupric chloride*. *Chem*, 1994(Ind. Eng): p. 259-264.
11. leofanti, G.P., M.; Carmello, D. ; Zecchina, A. ; spoto, G. : Bordita, S. : Turnes Palomino, G. ; Lamberte, C. , *Alumina supported copper chloride*. *journal of catalyst*, 2000: p. 91-104.
12. Al-Hajri, R. and D. Chadwick, *Single-stage oxychlorination of ethanol to ethylene dichloride using a dual-catalyst bed*. *Applied Catalysis A: General*, 2010. **388**(1-2): p. 96-101.
13. Potharaju S. Sai Prasad, K.B.S.P.a.M.S.A., Ind. Eng., *Parameter estimation in fixed-bed reactor operating under unsteady state; Oxy chlorination of ethylene*. 2001: p. 5487-5495.
14. Sjovoll, M., *The chemistry of oxychlorination catalysts - Aliterature survey*. *Research Centre Prsgrum*. 2006: p. 1-40.
15. Xueju, L.J.e.a., *Ethylene oxychlorination over gamma-alumina supported CuCl₂ - KCl-LaCl₃*. *Catalysis letters Vol 100Nos. 3-4*, , April 2005: p. 153-159.
16. L. Xueju, L.J., Z. Guangdong, Z. Kaiji, L. Wenxing, and C. Tiexin*, *Ethane oxychlorination over c-Al₂O₃ supported CuCl₂-KCl-LaCl₃*. 2005.
17. Lamberti, C., et al., *The Chemistry of the Oxychlorination Catalyst: an In Situ, Time-Resolved XANES Study*. *Angewandte Chemie International Edition*, 2002. **41**(13): p. 2341-2344.
18. Gianolio, D., et al., *Doped-CuCl₂/Al₂O₃ catalysts for ethylene oxychlorination: Influence of additives on the nature of active phase and reducibility*. *Nuclear Instruments and Methods in Physics Research Section B: Beam Interactions with Materials and Atoms*, 2012. **284**(0): p. 53-57.
19. Li, C., et al., *Effect of impregnation procedure of La₂O₃ precursor on copper-based catalysts for ethane oxychlorination*. *Catalysis Communications*, 2011. **13**(1): p. 22-25.
20. Zhitao, C., et al., *Influence of Cerium on the Stability of Copper-Based Oxychlorination Catalyst*. *Chinese Journal of Catalysis*, 2008. **29**(10): p. 951-953.
21. Menon, U., et al., *Nature of the active sites for the total oxidation of toluene by CuOCeO₂/Al₂O₃*. *Journal of Catalysis*, 2012. **295**(0): p. 91-103.

22. Batey, J.H., *The physics and technology of quadrupole mass spectrometers*. Vacuum, 2014. **101**(0): p. 410-415.
23. Baiker, A. and W.L. Holstein, *Impregnation of alumina with copper chloride-modeling of impregnation kinetics and internal copper profiles*. Journal of Catalysis, 1983. **84**(1): p. 178-188.
24. Abouliatim, Y., et al., *Optical characterization of stereolithography alumina suspensions using the Kubelka–Munk model*. Journal of the European Ceramic Society, 2009. **29**(5): p. 919-924.
25. Rodger, A. and K. Sanders, *Biomacromolecular Applications of UV-Visible Absorption Spectroscopy*, in *Encyclopedia of Spectroscopy and Spectrometry (Second Edition)*, J.C. Lindon, Editor. 1999, Academic Press: Oxford. p. 166-173.
26. Weckhuysen, B.M., *Ultraviolet-Visible Spectroscopy*. 2004(Department of Inorganic Chemistry and Catalysis, Debye Institute, Utrecht University, Sorbonnelaan 16, 3584 CA Utrecht, The Netherlands).
27. Ladavos, A.K., et al., *The BET equation, the inflection points of N₂ adsorption isotherms and the estimation of specific surface area of porous solids*. Microporous and Mesoporous Materials, 2012. **151**(0): p. 126-133.
28. Ryland, A.L., *X-ray diffraction*. Journal of Chemical Education, 1958. **35**(2): p. 80.
29. Fortini, E.M., C.L. García, and D.E. Resasco, *Stabilization of the active phase by interaction with the support in CuCl₂ oxychlorination catalysts*. Journal of Catalysis, 1986. **99**(1): p. 12-18.
30. Nunan, J.G., et al., *Physicochemical properties of Ce-containing three-way catalysts and the effect of Ce on catalyst activity*. Journal of Catalysis, 1992. **133**(2): p. 309-324.
31. Leofanti, G., et al., *Alumina-Supported Copper Chloride: 2. Effect of Aging and Thermal Treatments*. Journal of Catalysis, 2000. **189**(1): p. 105-116.
32. Li, C., et al., *Effect of ceria on the MgO- γ -Al₂O₃ supported CeO₂/CuCl₂/KCl catalysts for ethane oxychlorination*. Applied Catalysis A: General, 2011. **400**(1–2): p. 104-110.

Appendix A: Mass spectrometer

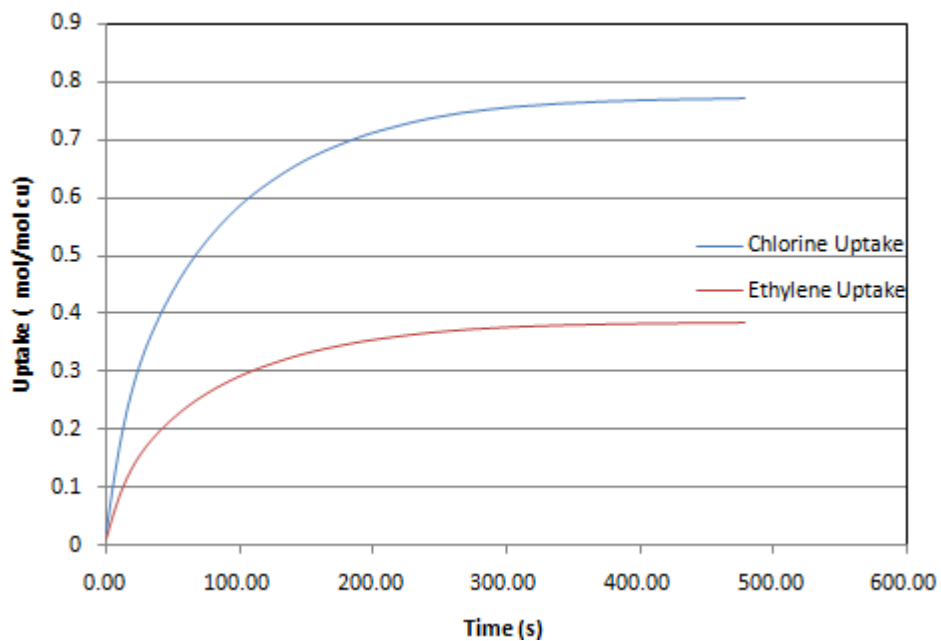


Figure 35: Uptake versus time. First cycle Reaction conditions: $T=503\text{K}$ $P_{\text{Total}}=1$ bar $P_{\text{Eth}}=0.1$ $\text{CuCl}_2/\gamma - \text{Al}_2\text{O}_3$ (4.81wt% Cu, 0wt% Ceria)

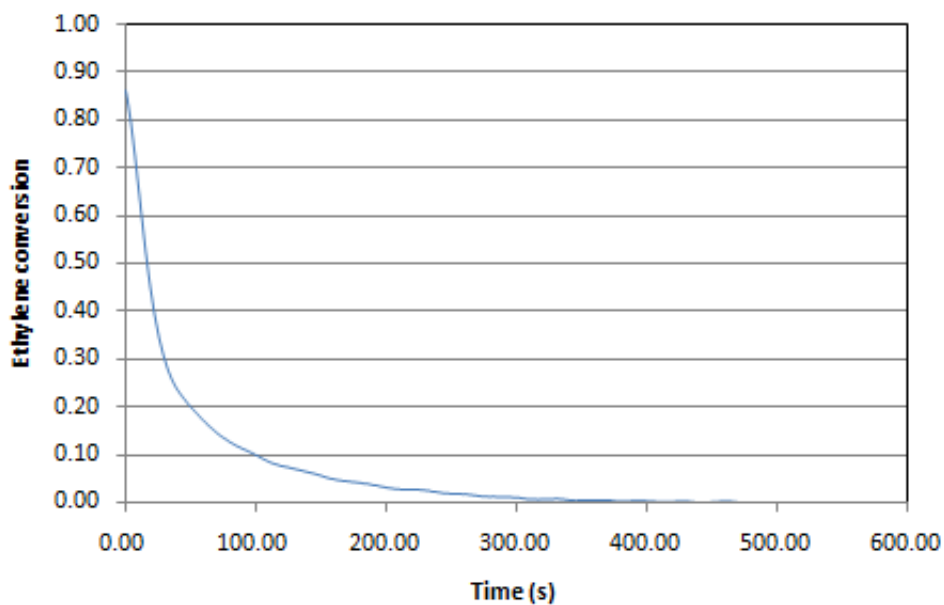


Figure 36: Ethylene conversion versus time. First cycle, Reaction conditions: $T=503\text{K}$ $P_{\text{Total}}=1$ bar $P_{\text{Eth}}=0.1$ $\text{CuCl}_2/\gamma - \text{Al}_2\text{O}_3$ (4.81wt% Cu, 0wt% Ceria)

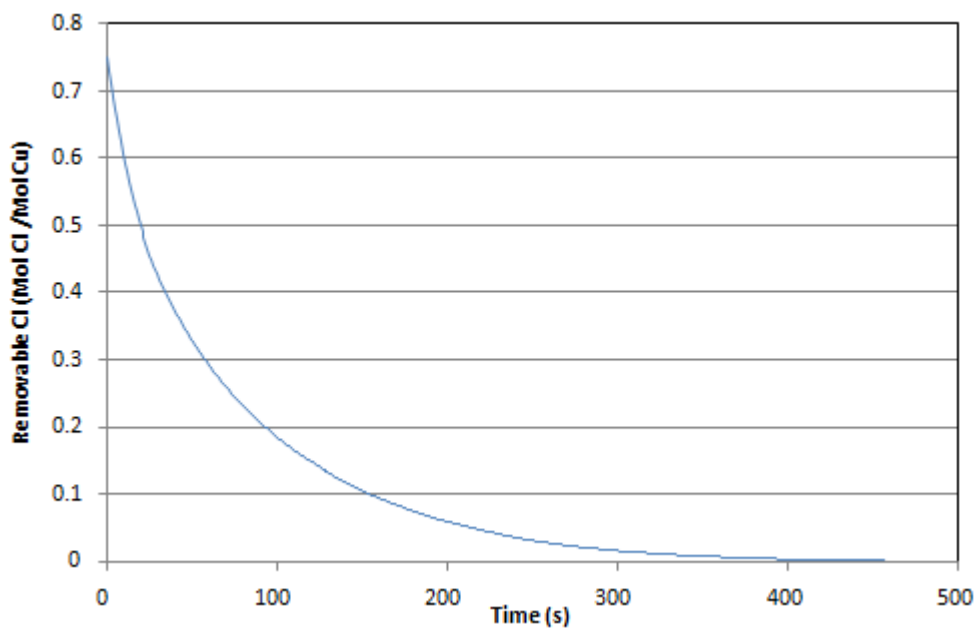


Figure 37: Removable chlorine versus time. First cycle, Reaction conditions: T=503K PTotal=1 bar PEth=0.1 $CuCl_2/\gamma - Al_2O_3$ (4.81wt% Cu, 0wt% Ceria)

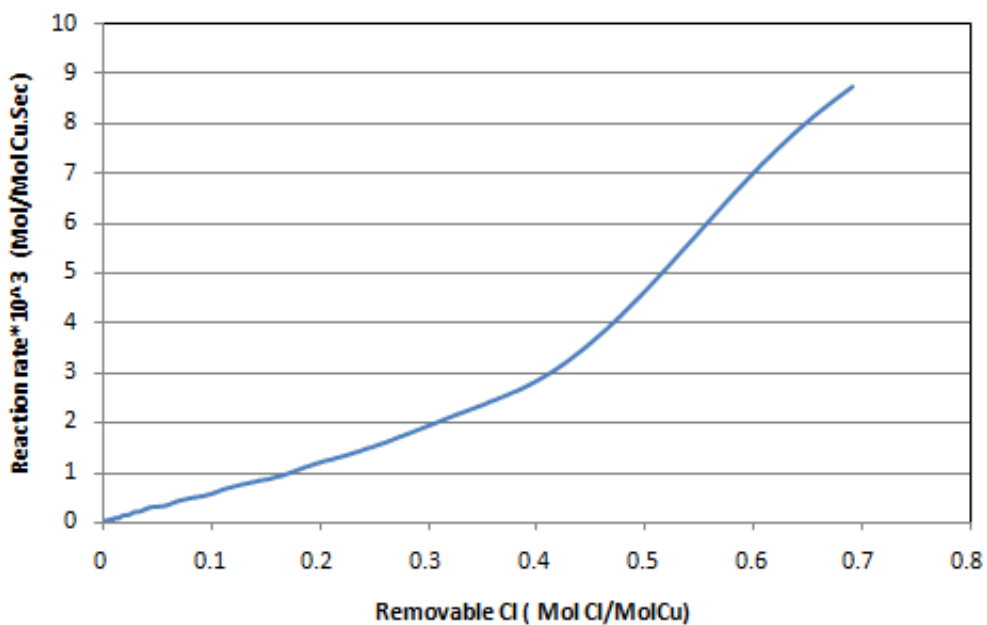


Figure 38: Reaction rate versus Removable Chlorine. First cycle, Reaction conditions: T=503K PTotal=1 bar PEth=0.1 $CuCl_2/\gamma - Al_2O_3$ (4.81wt% Cu, 0wt% Ceria)

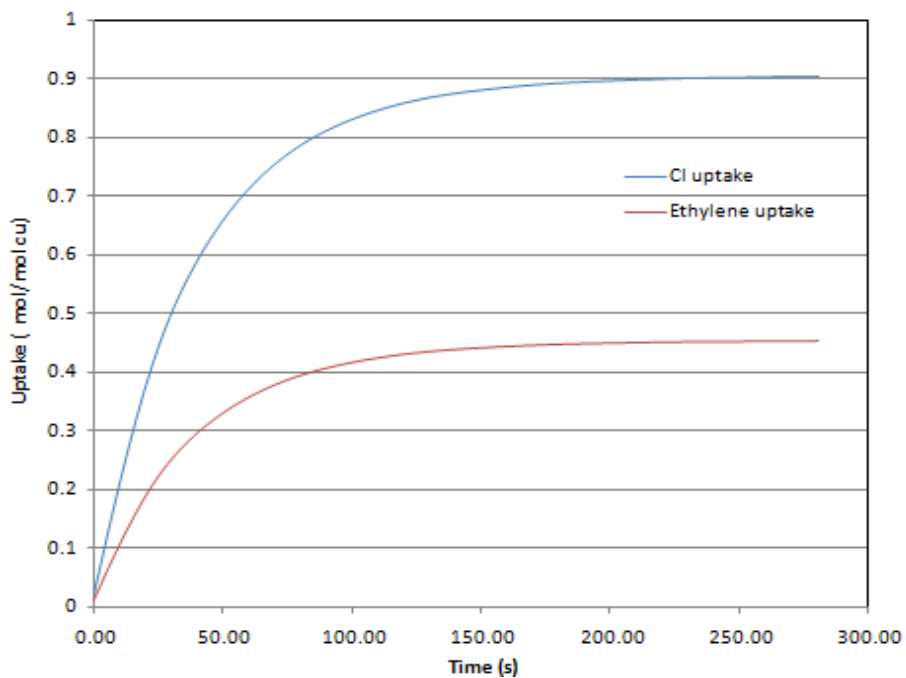


Figure 39: Uptake versus time. Second cycle, Reaction conditions: $T=503\text{K}$ $P_{\text{Total}}=1$ bar $P_{\text{Eth}}=0.1$ $\text{CuCl}_2/\gamma - \text{Al}_2\text{O}_3$ (4.81wt% Cu, 0wt% Ceria)

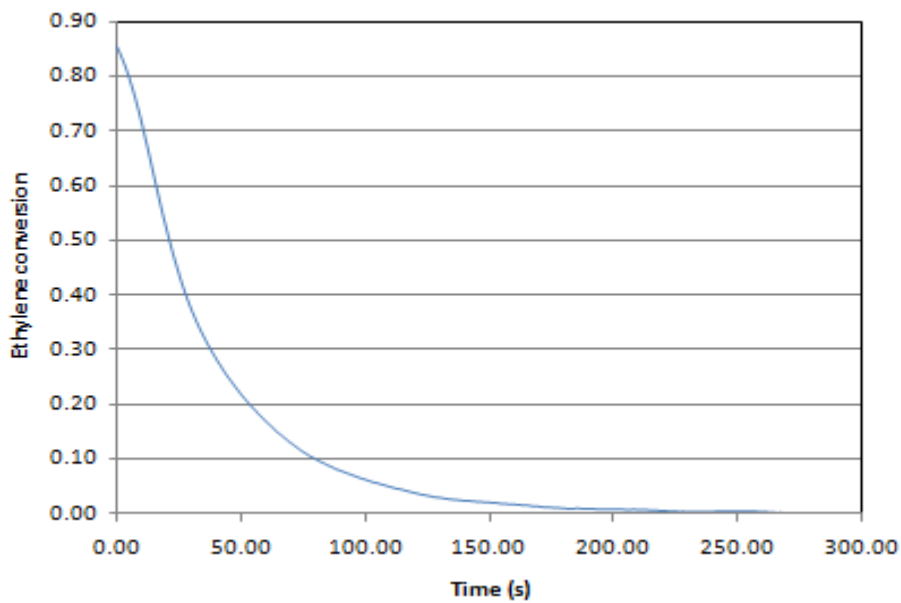


Figure 40: Ethylene conversion versus time. Second cycle, Reaction conditions: $T=503\text{K}$ $P_{\text{Total}}=1$ bar $P_{\text{Eth}}=0.1$ $\text{CuCl}_2/\gamma - \text{Al}_2\text{O}_3$ (4.81wt% Cu, 0wt% Ceria)

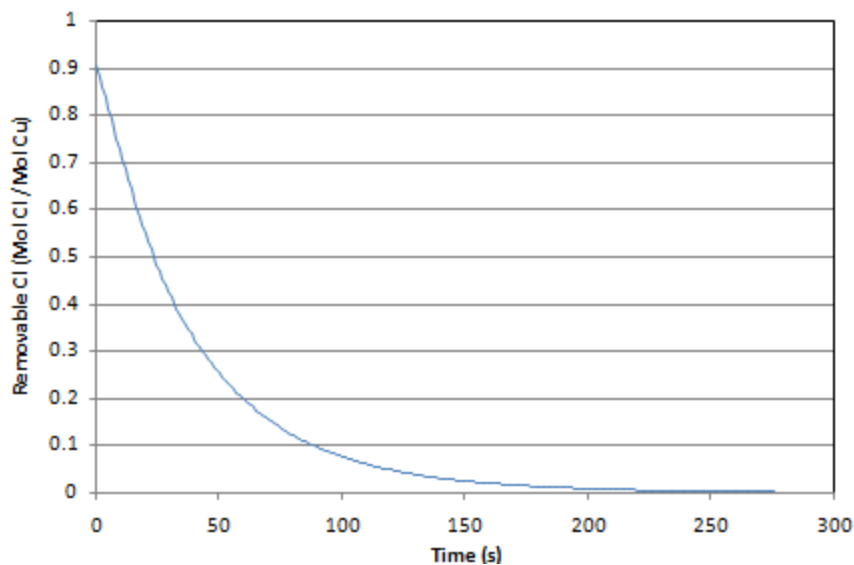


Figure 41: Removable chlorine versus time. Second cycle, Reaction conditions: T=503K PTotal=1 bar PEth=0.1 $CuCl_2/\gamma - Al_2O_3$ (4.81wt% Cu, 0wt% Ceria)

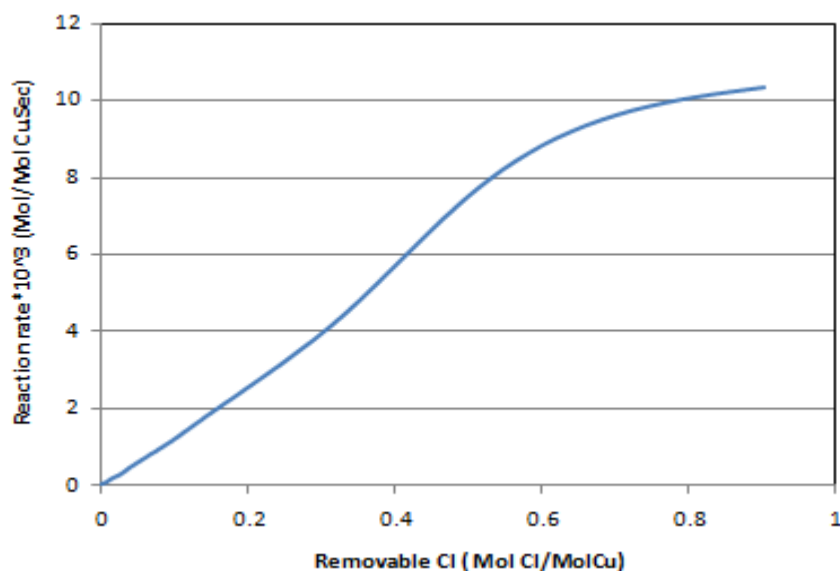


Figure 42: Reaction rate versus Removable Chlorine. Second cycle, Reaction conditions: T=503K PTotal=1 bar PEth=0.1 $CuCl_2/\gamma - Al_2O_3$ (4.81wt% Cu, 0wt% Ceria)

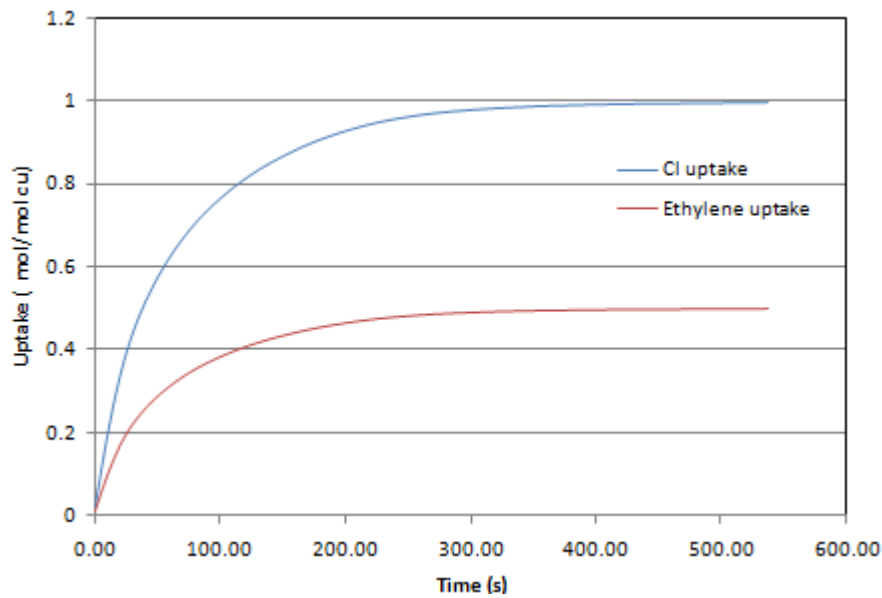


Figure 43: Uptake versus time. Third cycle, Reaction conditions: T=503K PTotal=1 bar PEth=0.1 $\text{CuCl}_2/\gamma - \text{Al}_2\text{O}_3$ (4.81wt% Cu, 0wt% Ceria)

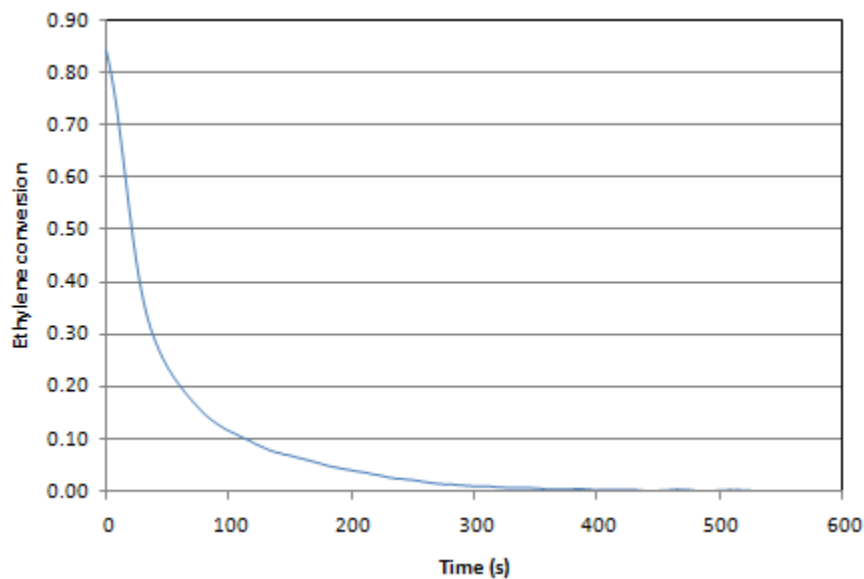


Figure 44: Ethylene conversion versus time. Third cycle, Reaction conditions: T=503K PTotal=1 bar PEth=0.1 $\text{CuCl}_2/\gamma - \text{Al}_2\text{O}_3$ (4.81wt% Cu, 0wt% Ceria)

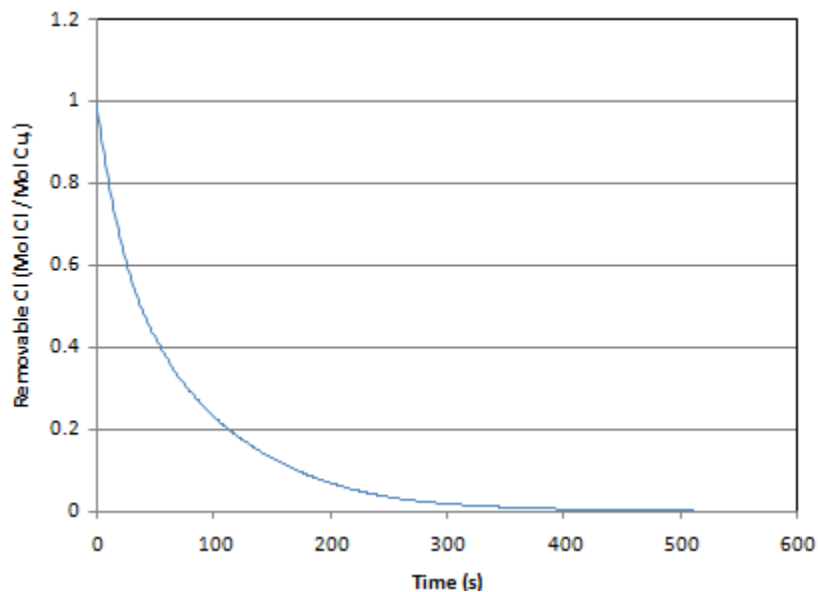


Figure 45: Removable chlorine versus time. Third cycle, Reaction conditions: $T=503\text{K}$ $P_{\text{Total}}=1$ bar $P_{\text{Eth}}=0.1$ $\text{CuCl}_2/\gamma - \text{Al}_2\text{O}_3$ (4.81wt% Cu, 0wt% Ceria)

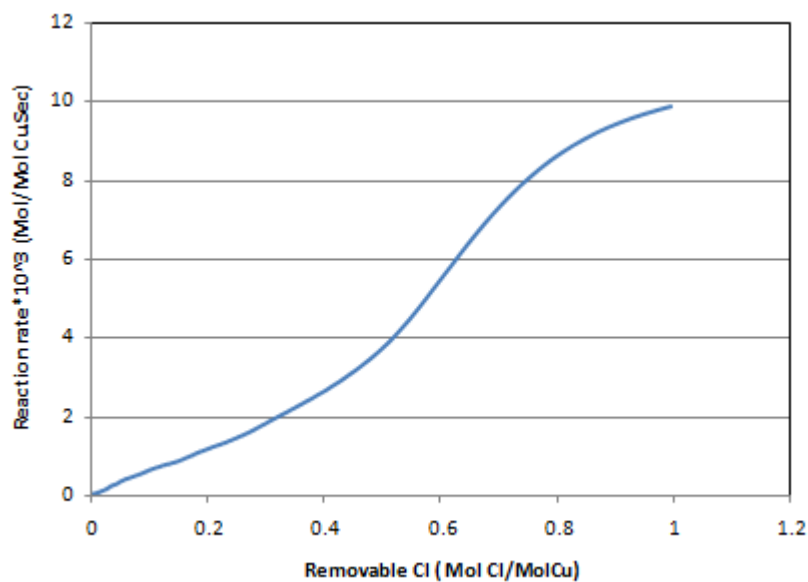


Figure 46: Reaction rate versus Removable Chlorine. Third cycle, Reaction conditions: $T=503\text{K}$ $P_{\text{Total}}=1$ bar $P_{\text{Eth}}=0.1$ $\text{CuCl}_2/\gamma - \text{Al}_2\text{O}_3$ (4.81wt% Cu, 0wt% Ceria)

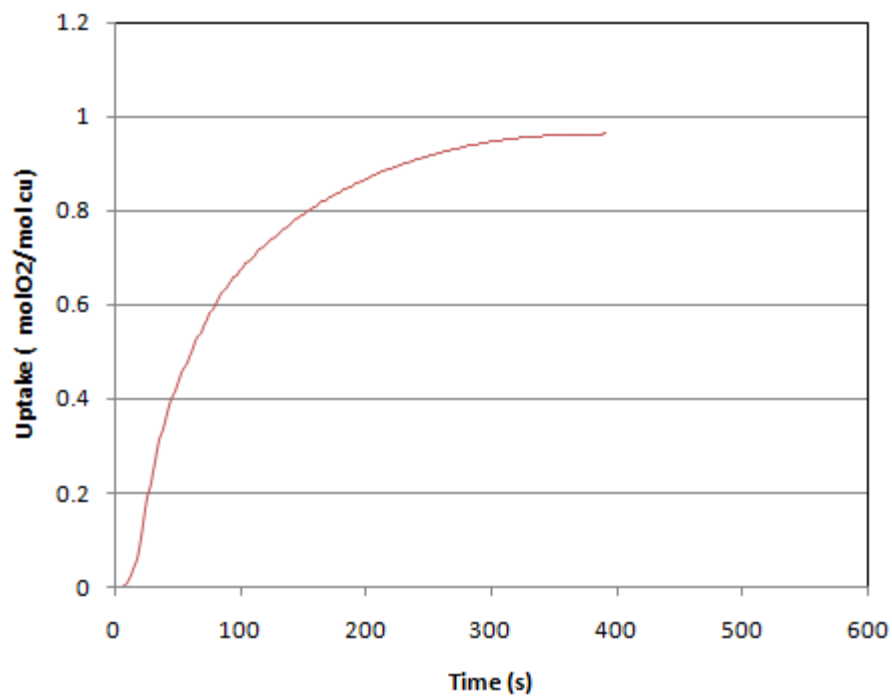


Figure 47: Uptake versus time. First cycle, Reaction conditions: T=503K P_{Total}=1 bar P_{O2}=0.1 $CuCl_2/\gamma - Al_2O_3$ (4.81wt% Cu, 0wt% Ceria)

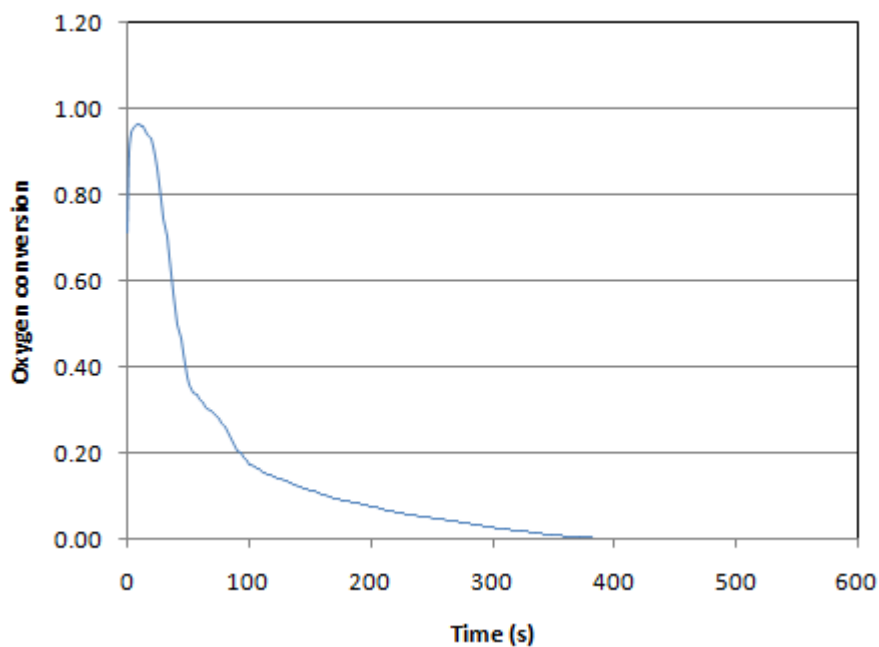


Figure 48: Oxygen conversion versus time. First cycle, Reaction conditions: T=503K P_{Total}=1 bar P_{O2}=0.1 $CuCl_2/\gamma - Al_2O_3$ (4.81wt% Cu, 0wt% Ceria)

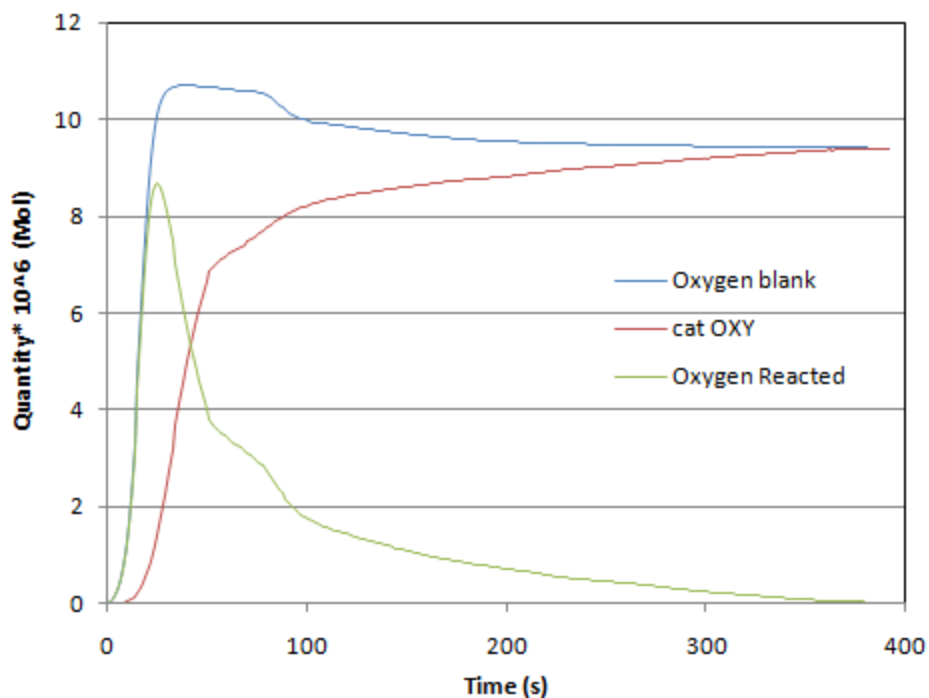


Figure 49: Oxygen profile within the reaction time. First cycle, Reaction conditions: T=503K PTotal=1 bar PO2=0.1 $CuCl_2/\gamma - Al_2O_3$ (4.81wt% Cu, 0wt% Ceria)

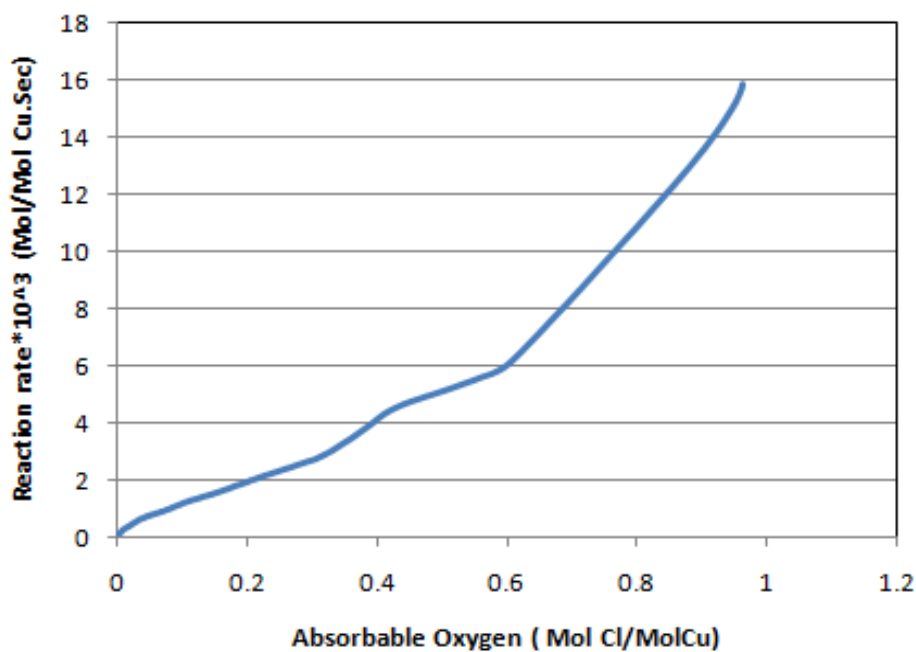


Figure 50: Reaction rate versus Absorbable Oxygen. First cycle, Reaction conditions: T=503K PTotal=1 bar PO2=0.1 $CuCl_2/\gamma - Al_2O_3$ (4.81wt% Cu, 0wt% Ceria)

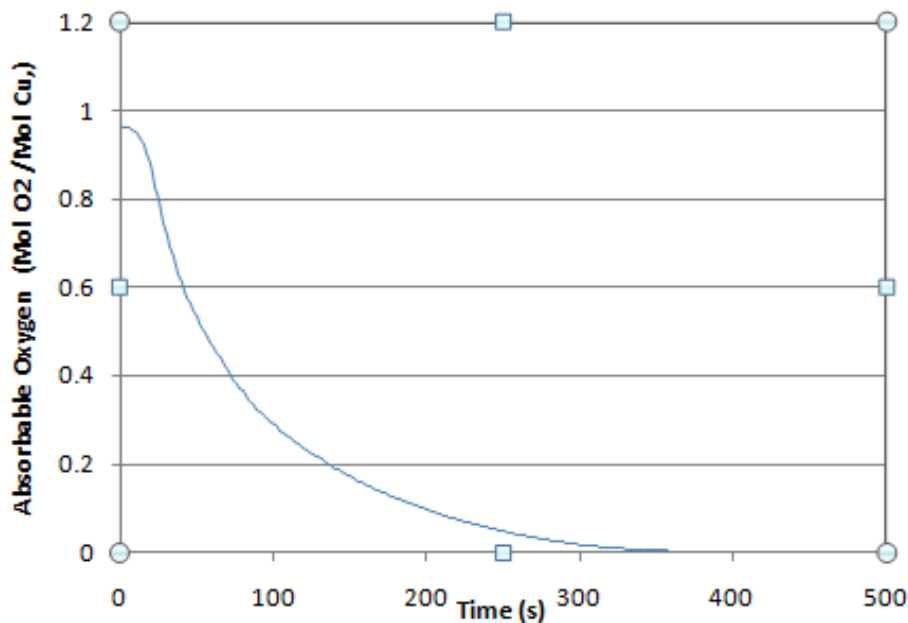


Figure 51: Absorbable Oxygen versus time. First cycle, Reaction conditions: T=503K PTotal=1 bar PO₂=0.1 CuCl₂/γ - Al₂O₃ (4.81wt% Cu, 0wt% Ceria)

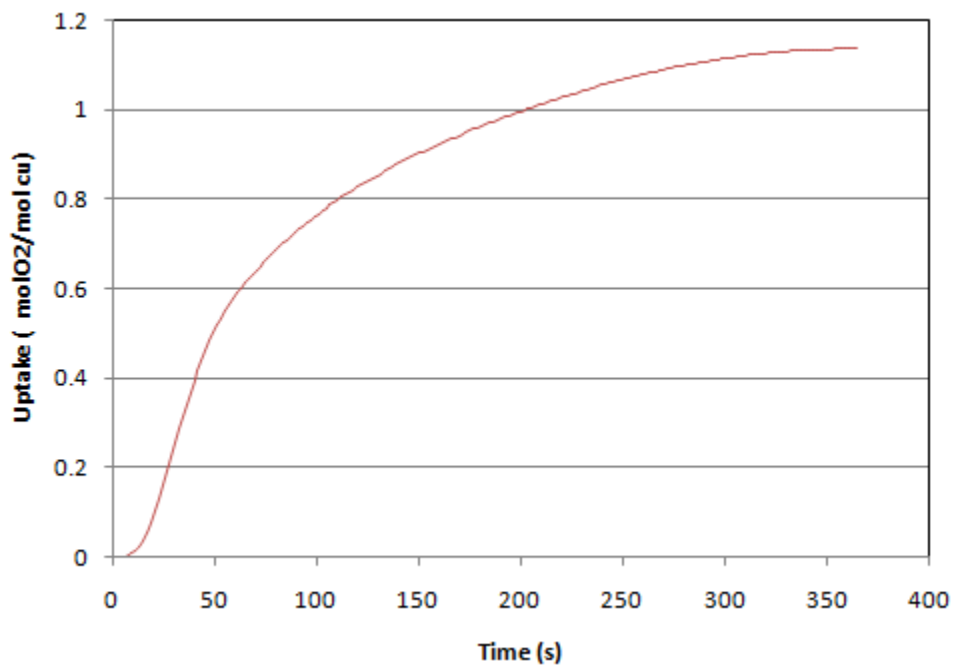


Figure 52: Uptake versus time. Second cycle, Reaction conditions: T=503K PTotal=1 bar PO₂=0.1 CuCl₂/γ - Al₂O₃ (4.81wt% Cu, 0wt% Ceria)

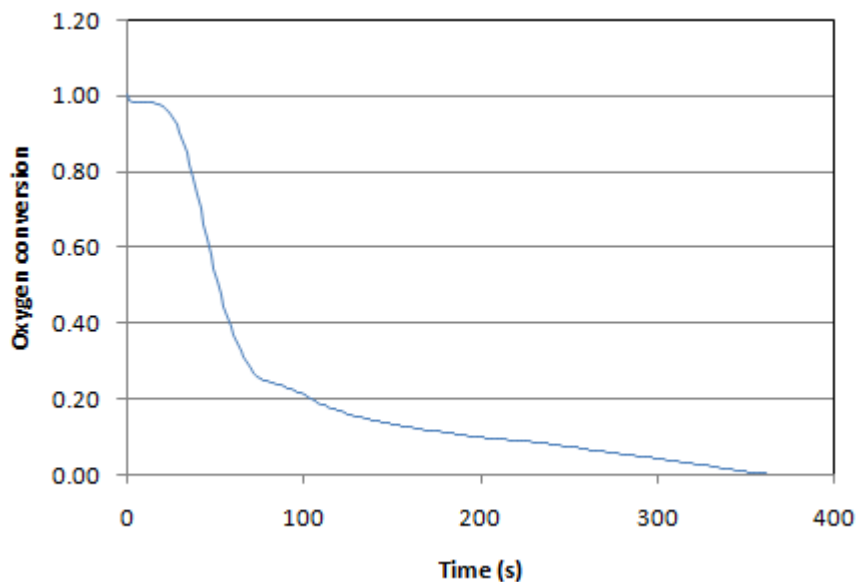


Figure 53: Oxygen conversion versus time. Second cycle, Reaction conditions: T=503K PTotal=1 bar PO₂=0.1 CuCl₂/γ - Al₂O₃ (4.81wt% Cu, 0wt% Ceria)

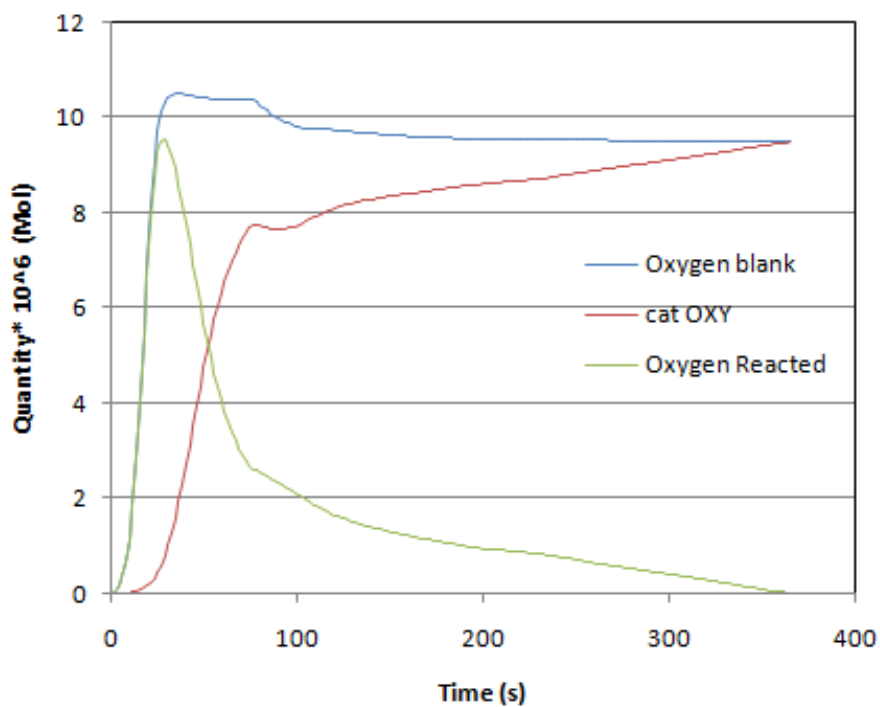


Figure 54: Oxygen profile within the reaction time. Second cycle, Reaction conditions: T=503K PTotal=1 bar PO₂=0.1 CuCl₂/γ - Al₂O₃ (4.81wt% Cu, 0wt% Ceria)

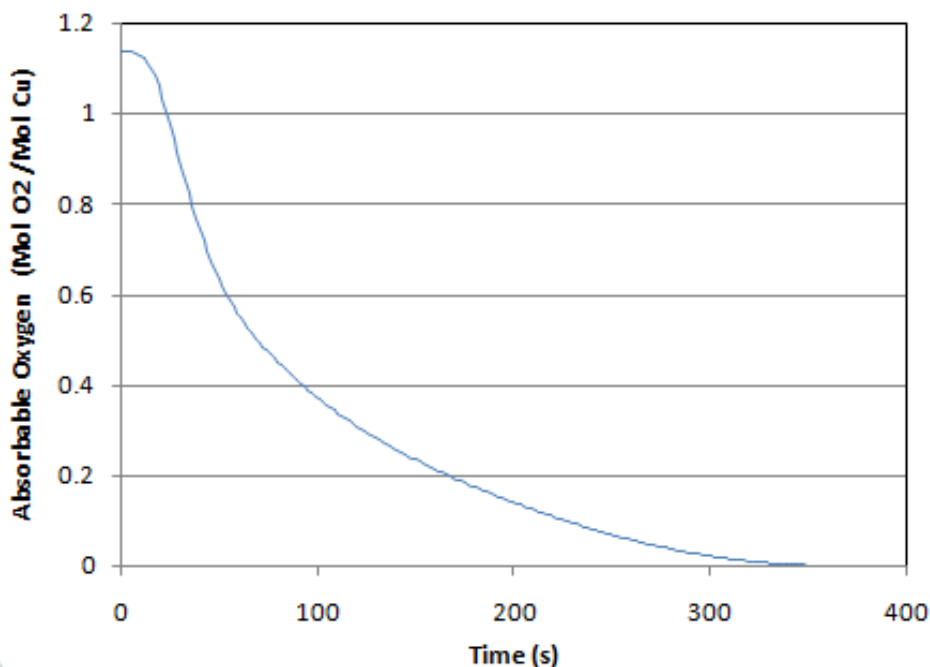


Figure 55: Absorbable Oxygen versus time. Second cycle, Reaction conditions: T=503K PTotal=1 bar PO₂=0.1 $\text{CuCl}_2/\gamma - \text{Al}_2\text{O}_3$ (4.81wt% Cu, 0wt% Ceria)

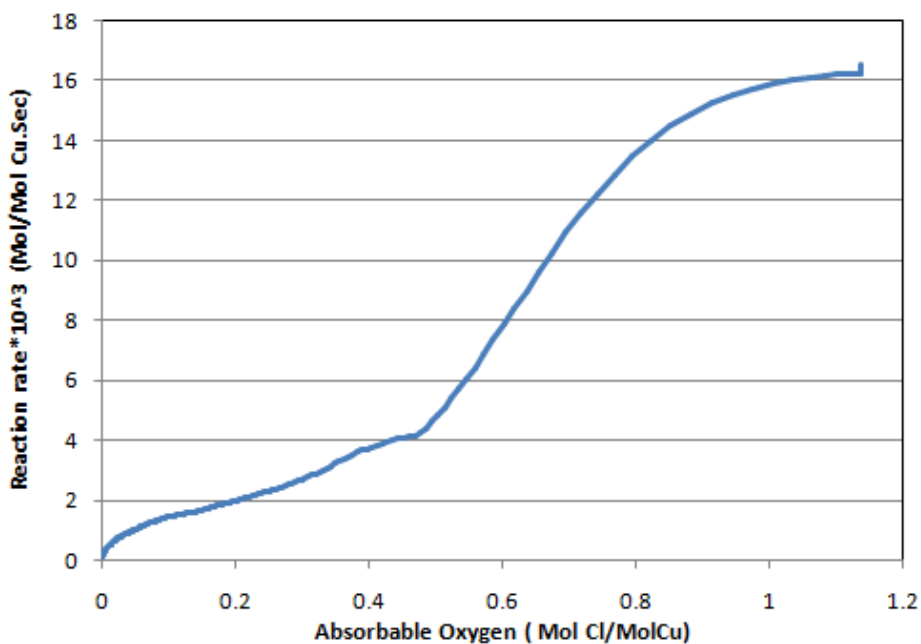


Figure 56: Reaction rate versus Absorbable Oxygen. Second cycle, Reaction conditions: T=503K PTotal=1 bar PO₂=0.1 $\text{CuCl}_2/\gamma - \text{Al}_2\text{O}_3$ (4.81wt% Cu, 0wt% Ceria)

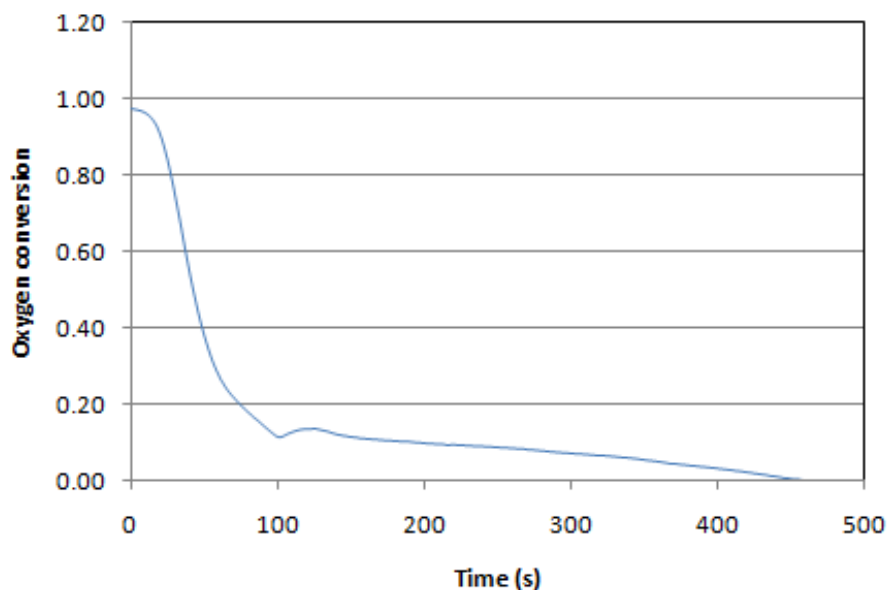


Figure 57 : Oxygen conversion versus time. Third cycle, Reaction conditions: T=503K PTotal=1 bar PO₂=0.1 $CuCl_2/\gamma - Al_2O_3$ (4.81wt% Cu, 0wt% Ceria)

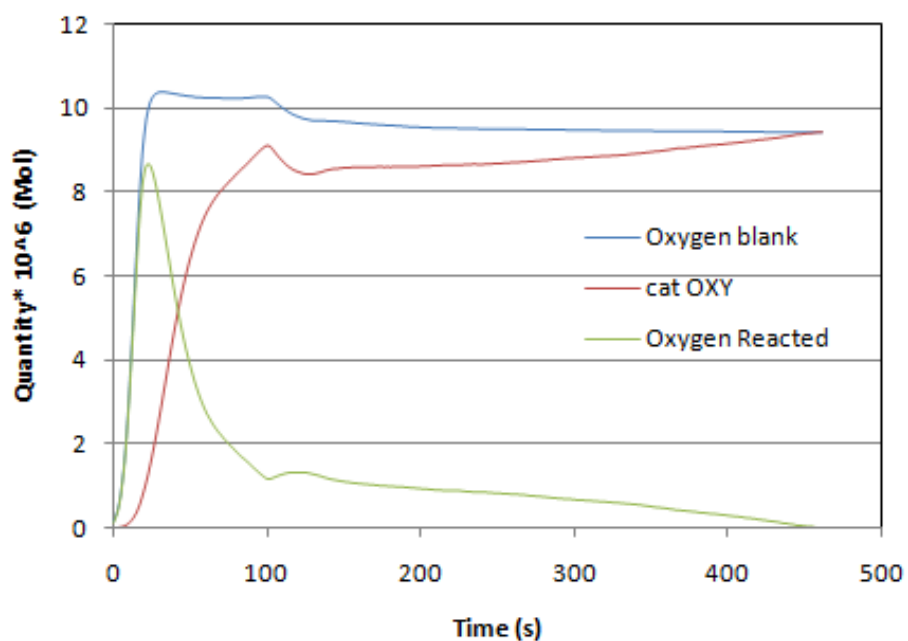


Figure 58: Oxygen profile within the reaction time. Third cycle, Reaction conditions: T=503K PTotal=1 bar PO₂=0.1 $CuCl_2/\gamma - Al_2O_3$ (4.81wt% Cu, 0wt% Ceria)

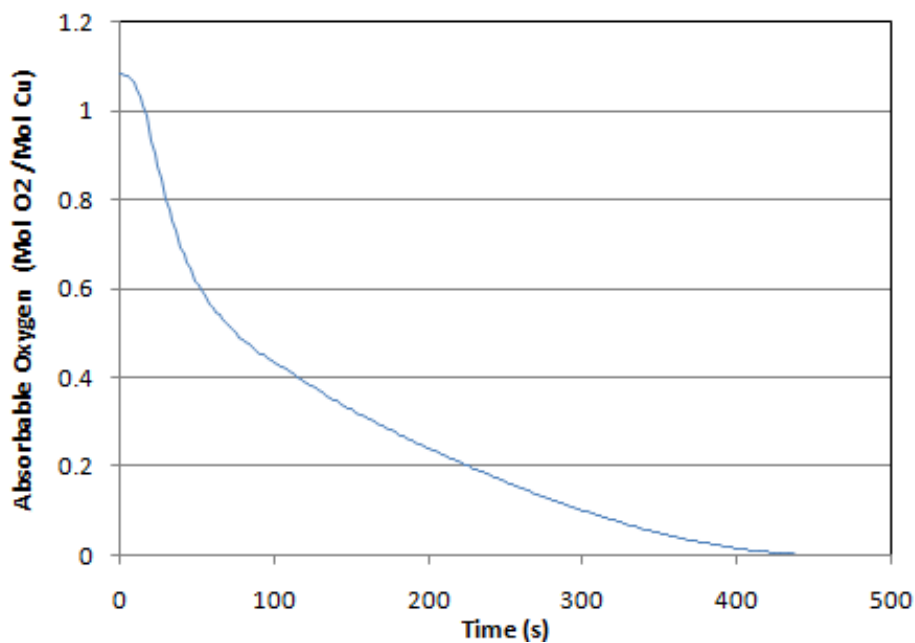


Figure 59: Absorbable Oxygen versus time. Third cycle, Reaction conditions: T=503K P_{Total}=1 bar P_{O2}=0.1
 $CuCl_2/\gamma - Al_2O_3$ (4.81wt% Cu, 0wt% Ceria)

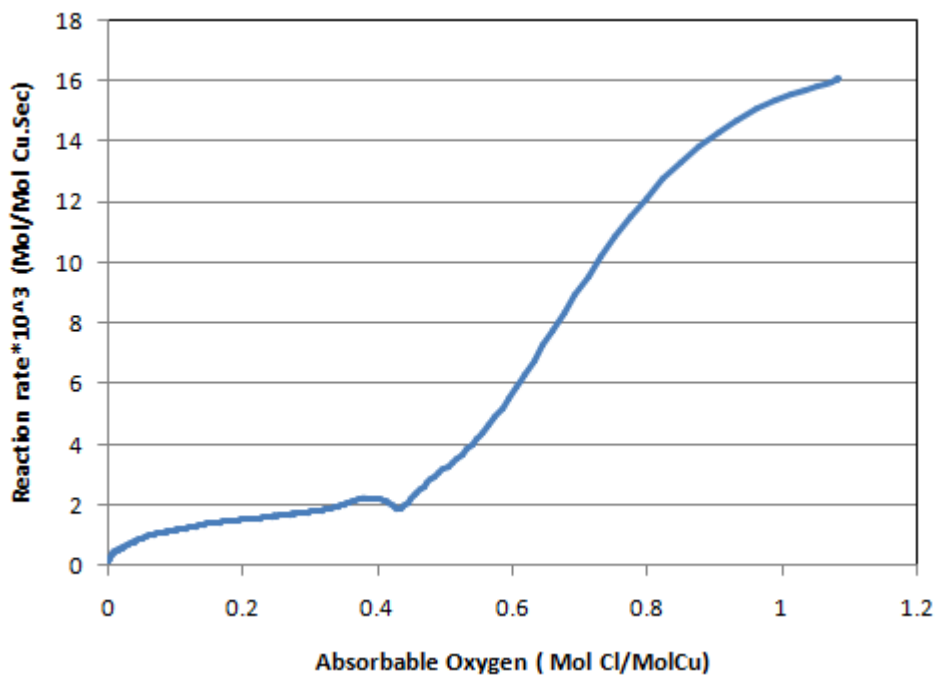


Figure 60: Reaction rate versus Absorbable Oxygen. Third cycle, Reaction conditions: T=503K P_{Total}=1 bar P_{O2}=0.1
 $CuCl_2/\gamma - Al_2O_3$ (4.81wt% Cu, 0wt% Ceria)

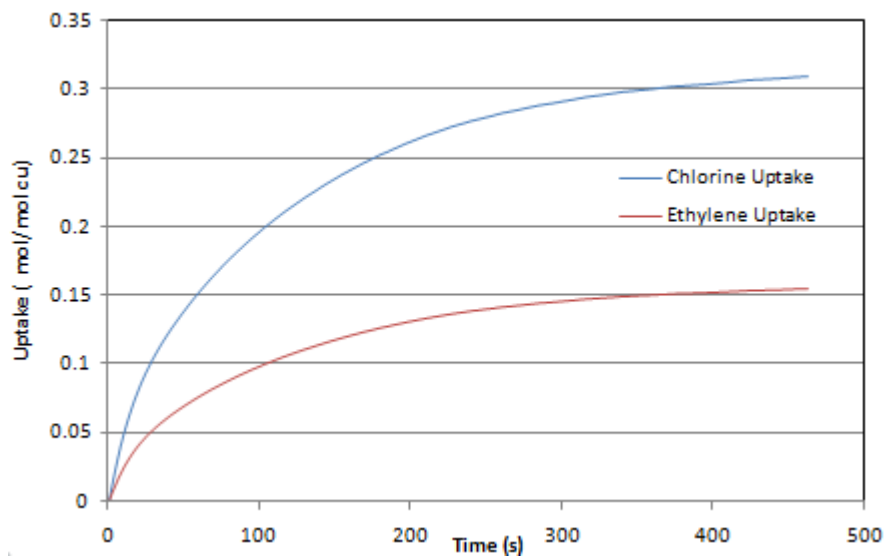


Figure 61: Uptake versus time. First cycle, Reaction conditions: $T=503\text{K}$ $P_{\text{Total}}=1$ bar $P_{\text{Eth}}=0.1$ $\text{CuCl}_2 \cdot \text{CeO}_2/\gamma - \text{Al}_2\text{O}_3$ (5wt% Cu, 1wt% Ceria)

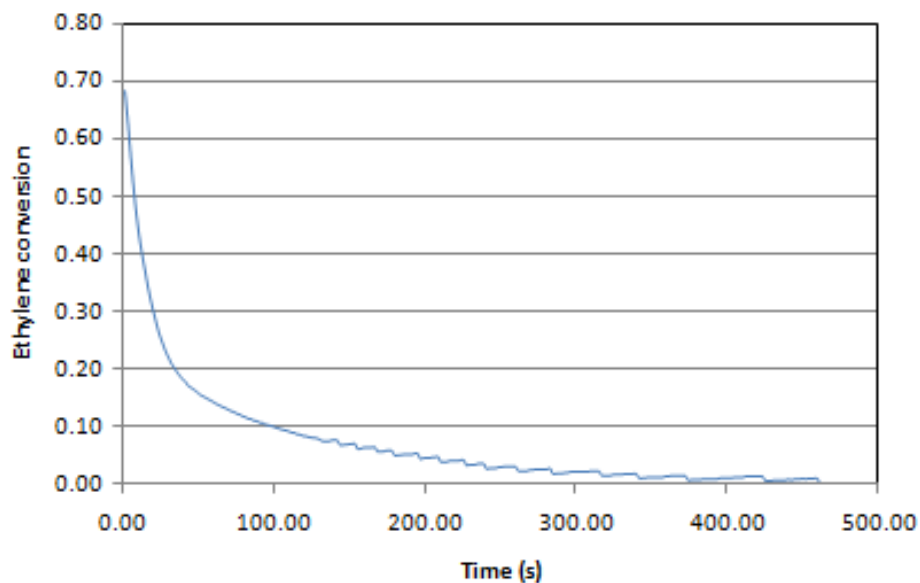


Figure 62: Ethylene conversion versus time. First cycle, Reaction conditions: $T=503\text{K}$ $P_{\text{Total}}=1$ bar $P_{\text{Eth}}=0.1$ $\text{CuCl}_2 \cdot \text{CeO}_2/\gamma - \text{Al}_2\text{O}_3$ (5wt% Cu, 1wt% Ceria)

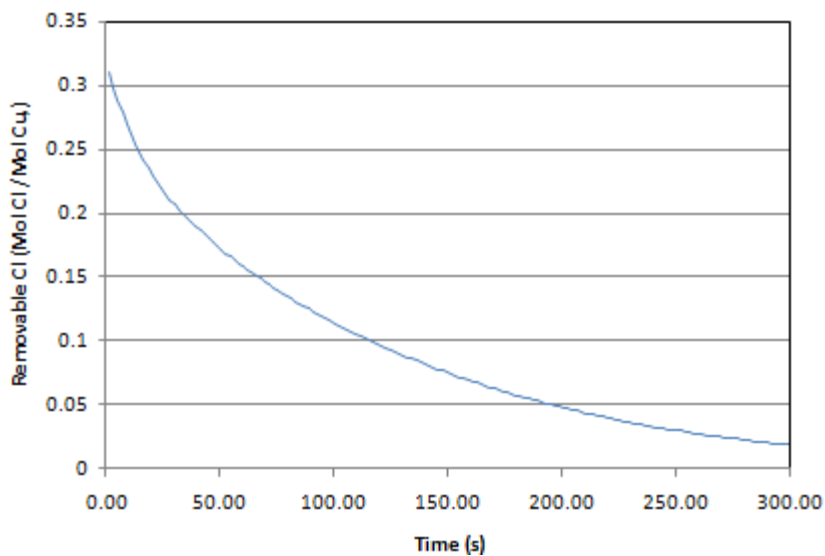


Figure 63: Removable chlorine versus time. First cycle, Reaction conditions: T=503K PTotal=1 bar PEth=0.1 $CuCl_2.CeO_2/\gamma-Al_2O_3$ (5wt% Cu, 1wt% Ceria)

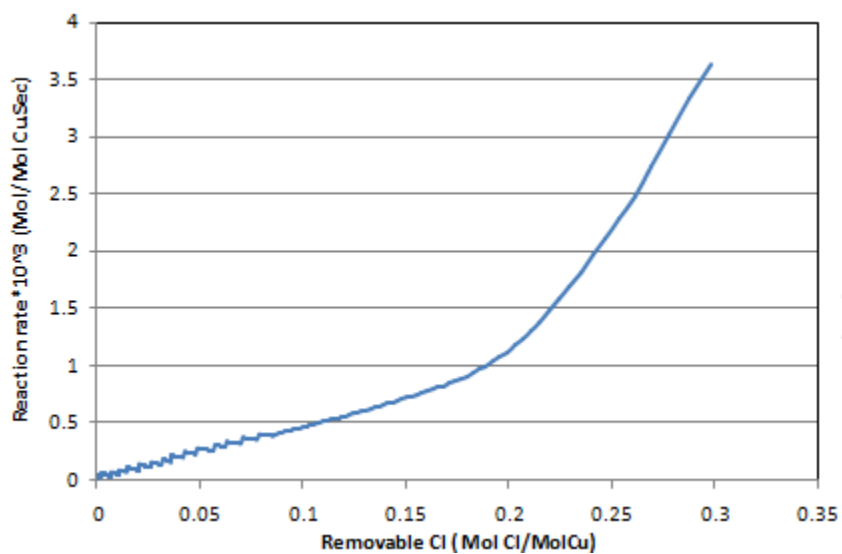


Figure 64: Reaction rate versus Removable Chlorine. First cycle, Reaction conditions: T=503K PTotal=1 bar PEth=0.1 $CuCl_2.CeO_2/\gamma-Al_2O_3$ (5wt% Cu, 1wt% Ceria)

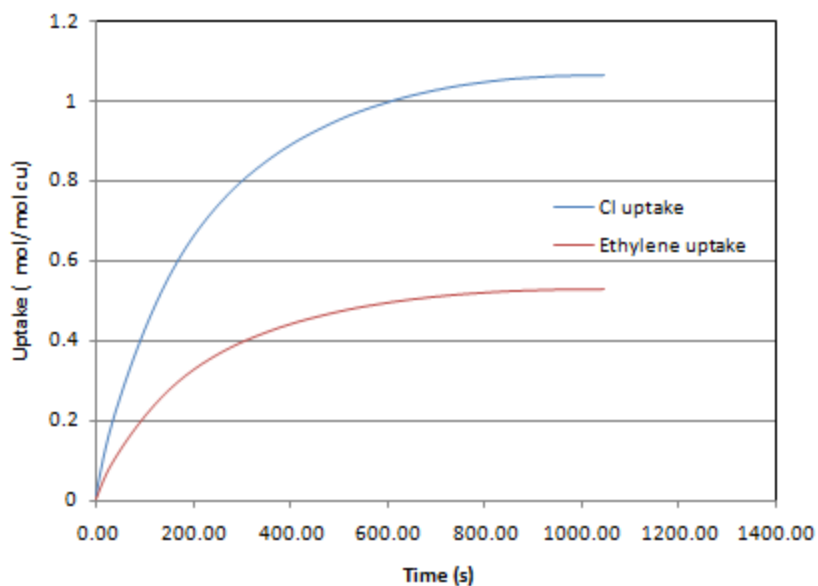


Figure 65: Uptake versus time. Second cycle, Reaction conditions: T=503K PTotal=1 bar PEth=0.1 $\text{CuCl}_2 \cdot \text{CeO}_2 / \gamma - \text{Al}_2\text{O}_3$ (5wt% Cu, 1wt% Ceria)

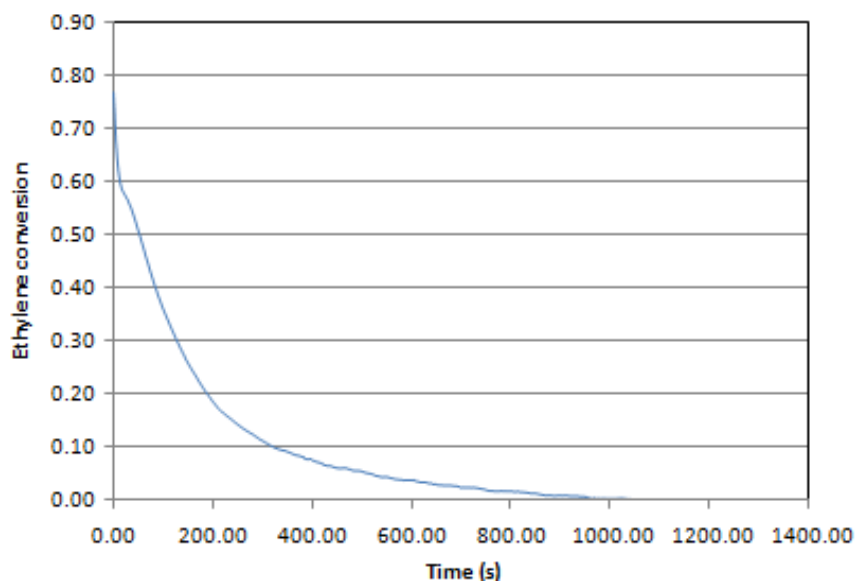


Figure 66: Ethylene conversion versus time. Second cycle, Reaction conditions: T=503K PTotal=1 bar PEth=0.1 $\text{CuCl}_2 \cdot \text{CeO}_2 / \gamma - \text{Al}_2\text{O}_3$ (5wt% Cu, 1wt% Ceria)

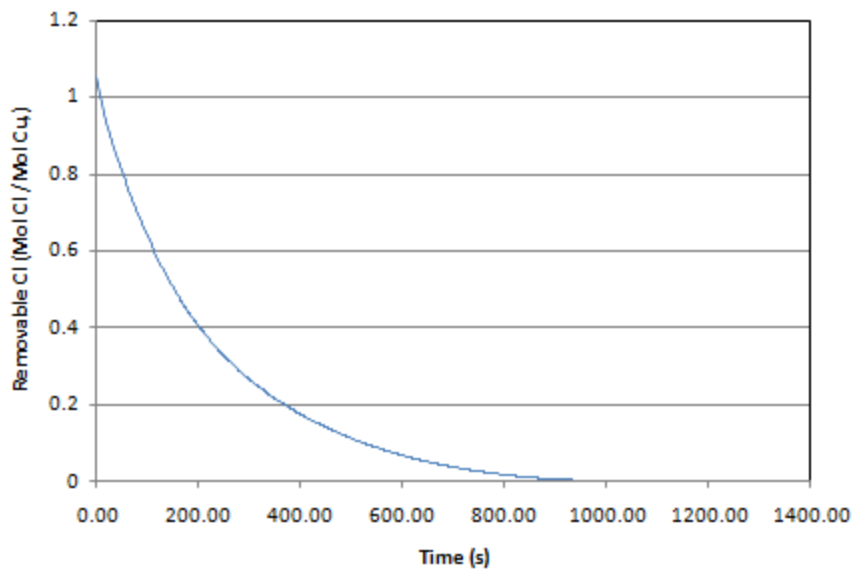


Figure 67: Removable chlorine versus time. Second cycle, Reaction conditions: T=503K PTotal=1 bar PEth=0.1 $CuCl_2.CeO_2/\gamma-Al_2O_3$ (5wt% Cu, 1wt% Ceria)

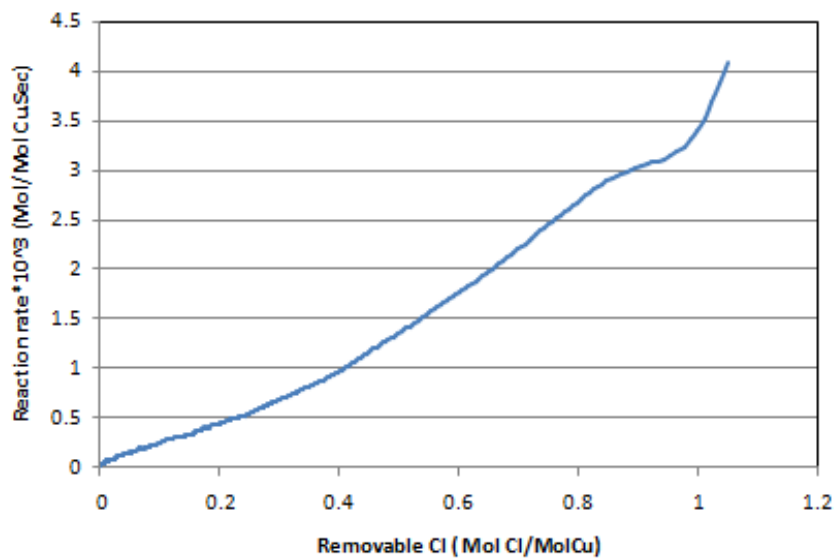


Figure 68: Reaction rate versus Removable Chlorine. Second cycle, Reaction conditions: T=503K PTotal=1 bar PEth=0.1 $CuCl_2.CeO_2/\gamma-Al_2O_3$ (5wt% Cu, 1wt% Ceria)

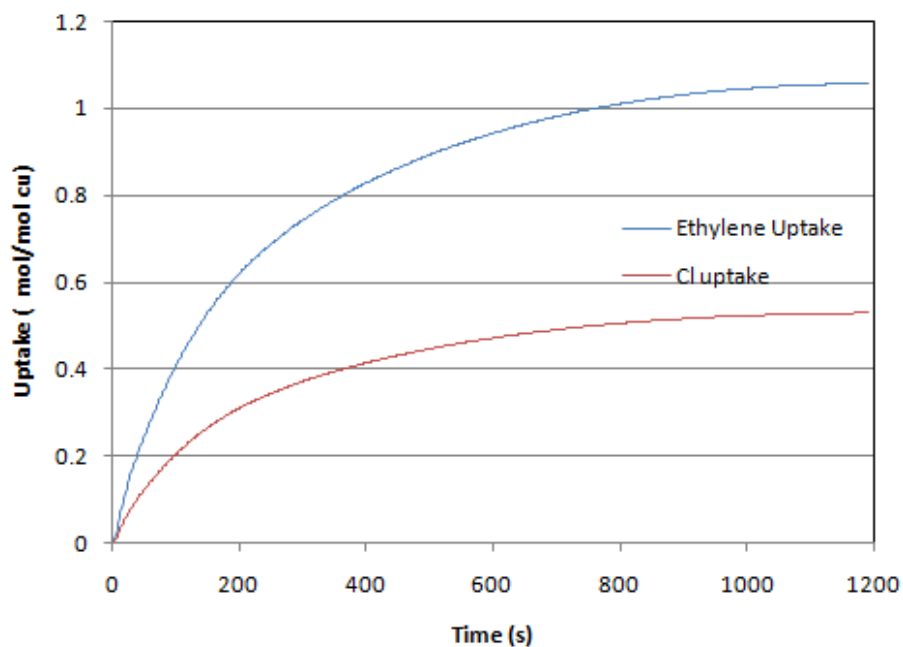


Figure 69: Uptake versus time. Third cycle, Reaction conditions: T=503K PTotal=1 bar PEth=0.1 $CuCl_2.CeO_2/\gamma-Al_2O_3$ (5wt% Cu, 1wt% Ceria)

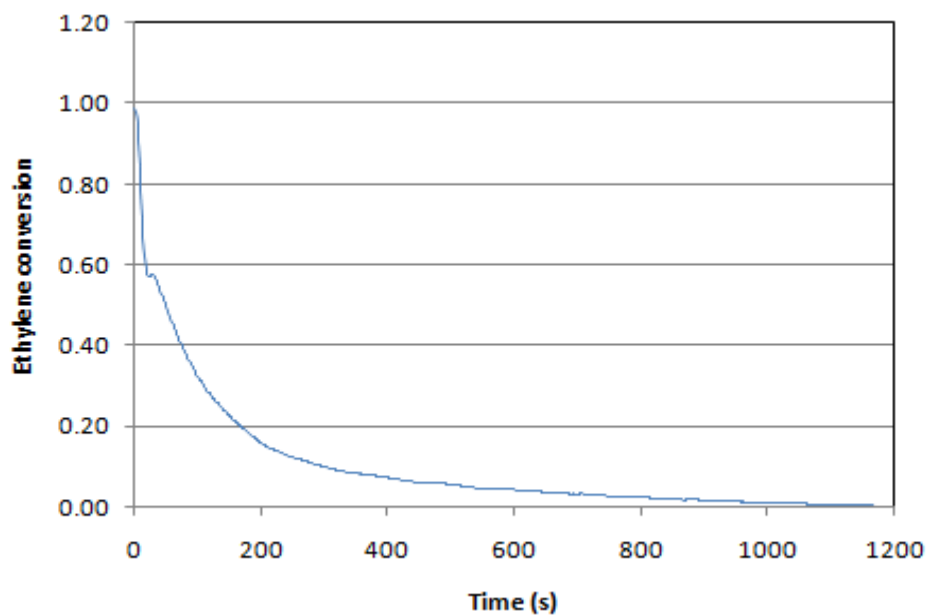


Figure 70: Ethylene conversion versus time. Third cycle, Reaction conditions: T=503K PTotal=1 bar PEth=0.1 $CuCl_2.CeO_2/\gamma-Al_2O_3$ (5wt% Cu, 1wt% Ceria)

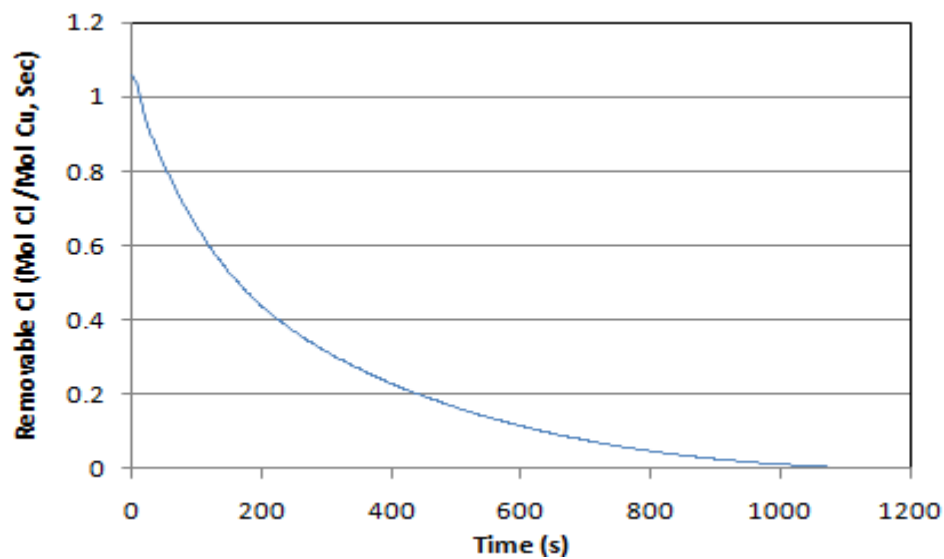


Figure 71: Removable chlorine versus time. Third cycle, Reaction conditions: $T=503\text{K}$ $P_{\text{Total}}=1$ bar $P_{\text{Eth}}=0.1$ $\text{CuCl}_2 \cdot \text{CeO}_2/\gamma - \text{Al}_2\text{O}_3$ (5wt% Cu, 1wt% Ceria)

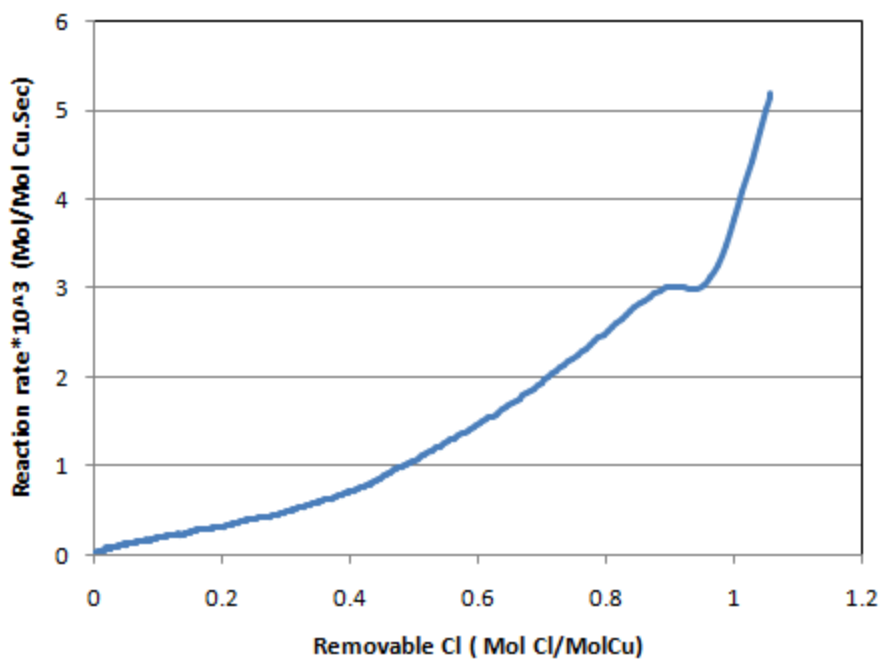


Figure 72: Reaction rate versus Removable Chlorine. Third cycle, Reaction conditions: $T=503\text{K}$ $P_{\text{Total}}=1$ bar $P_{\text{Eth}}=0.1$ $\text{CuCl}_2 \cdot \text{CeO}_2/\gamma - \text{Al}_2\text{O}_3$ (5wt% Cu, 1wt% Ceria)

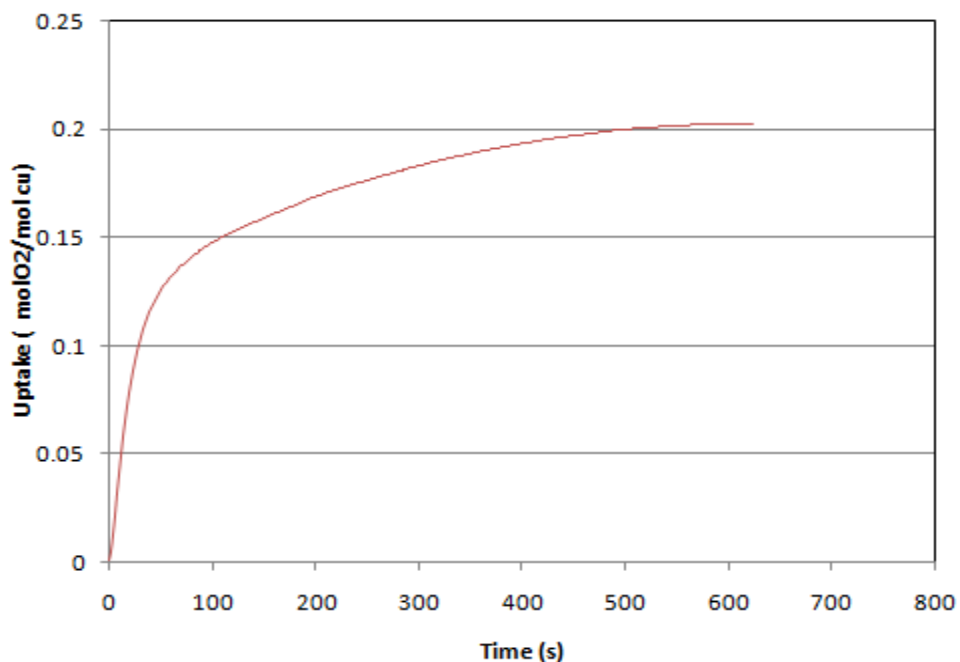


Figure 73: Uptake versus time. First cycle, Reaction conditions: T=503K PTotal=1 bar PO₂=0.1 $CuCl_2.CeO_2/\gamma - Al_2O_3$ (5wt% Cu, 1wt% Ceria)

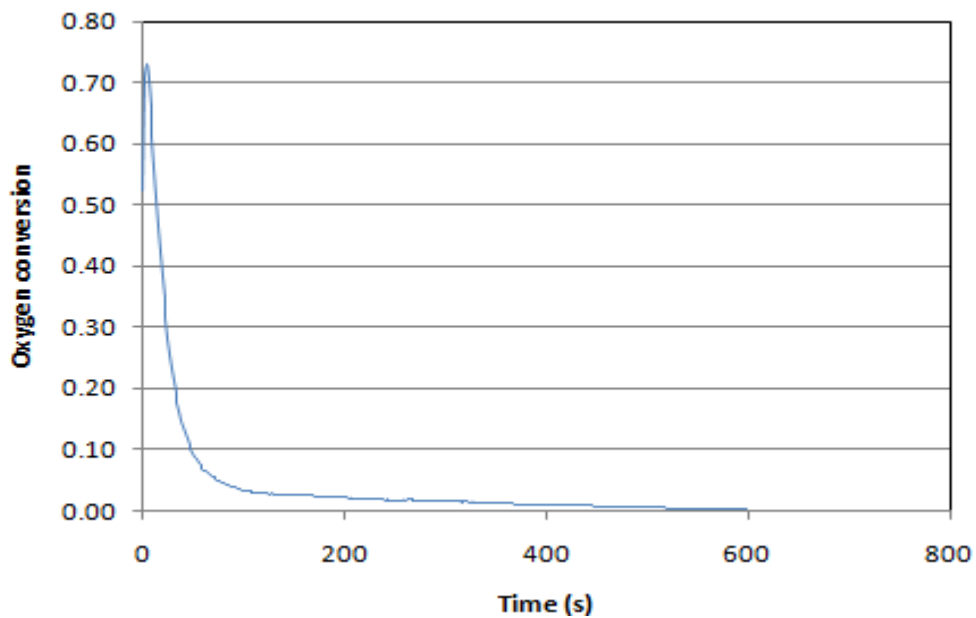


Figure 74: Oxygen conversion versus time. First cycle, Reaction conditions: T=503K PTotal=1 bar PO₂=0.1 $CuCl_2.CeO_2/\gamma - Al_2O_3$ (5wt% Cu, 1wt% Ceria)

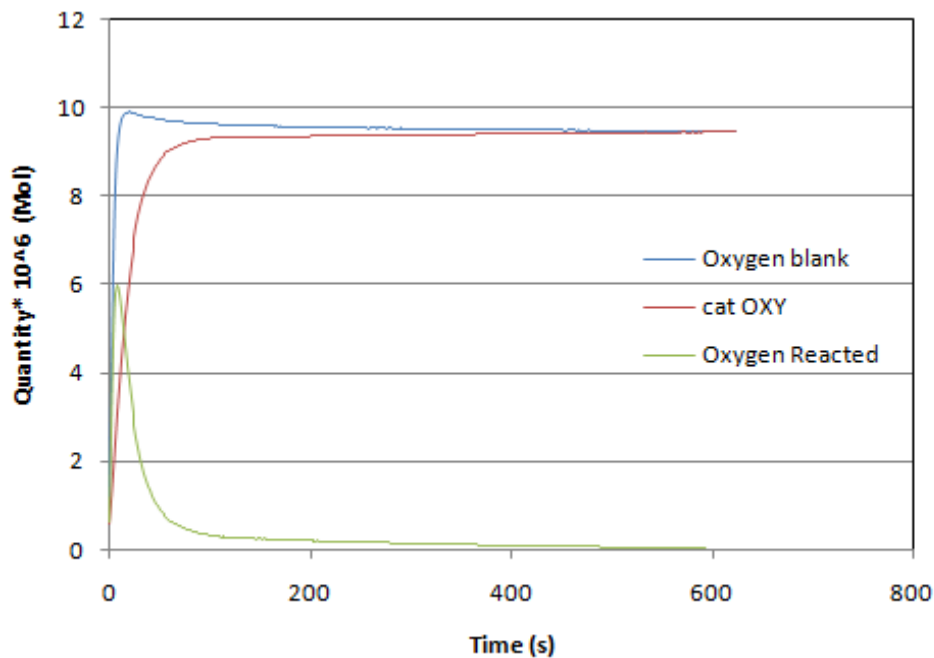


Figure 75: Oxygen profile within the reaction time. First cycle, Reaction conditions: T=503K PTotal=1 bar PO2=0.1 $CuCl_2.CeO_2/\gamma-Al_2O_3$ (5wt% Cu, 1wt% Ceria)

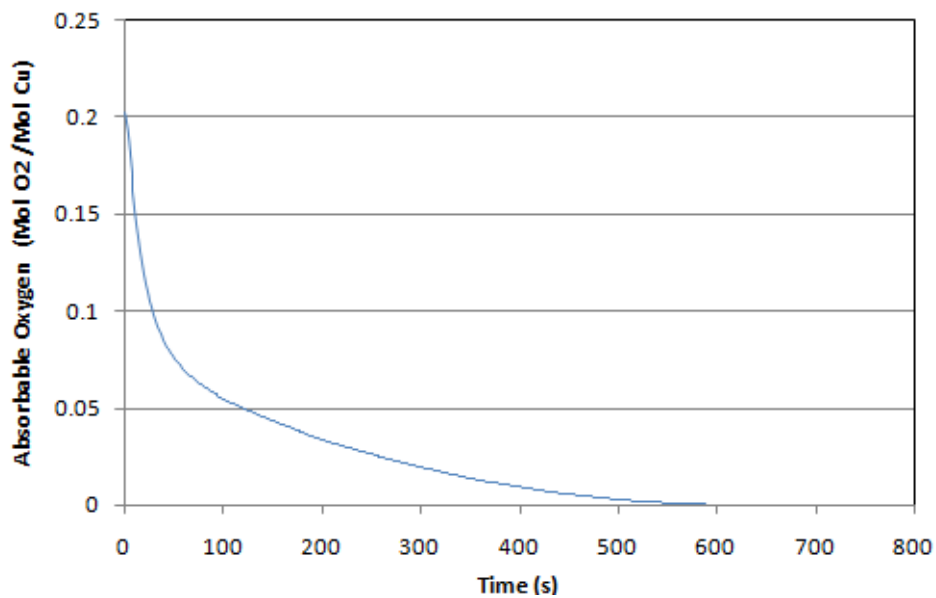


Figure 76: Absorbable Oxygen versus time. First cycle, Reaction conditions: T=503K PTotal=1 bar PO2=0.1 $CuCl_2.CeO_2/\gamma-Al_2O_3$ (5wt% Cu, 1wt% Ceria)

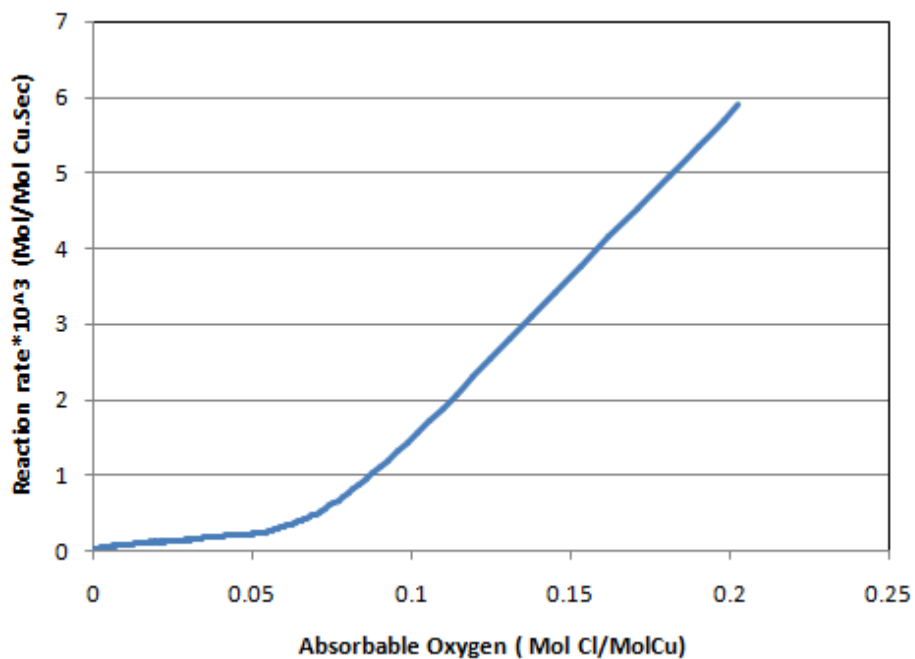


Figure 77: Reaction rate versus Absorbable Oxygen. First cycle, Reaction conditions: T=503K PTotal=1 bar PO₂=0.1 CuCl₂.CeO₂/γ-Al₂O₃ (5wt% Cu, 1wt% Ceria)

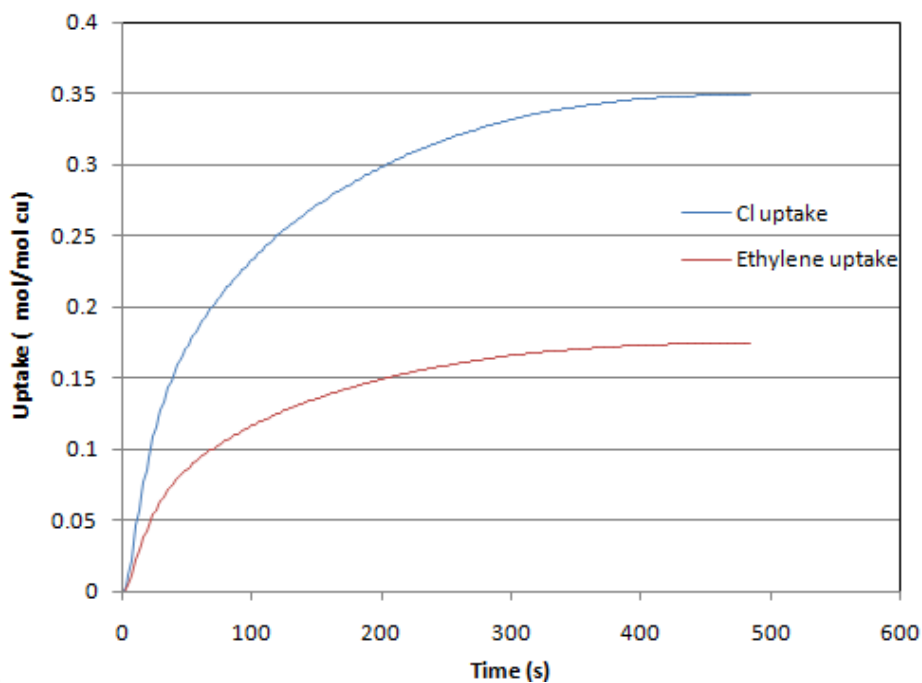


Figure 78: Uptake versus time. First cycle, Reaction conditions: T=503K PTotal=1 bar PEth=0.1 CuCl₂.CeO₂/γ-Al₂O₃ (5wt% Cu, 3wt% Ceria)

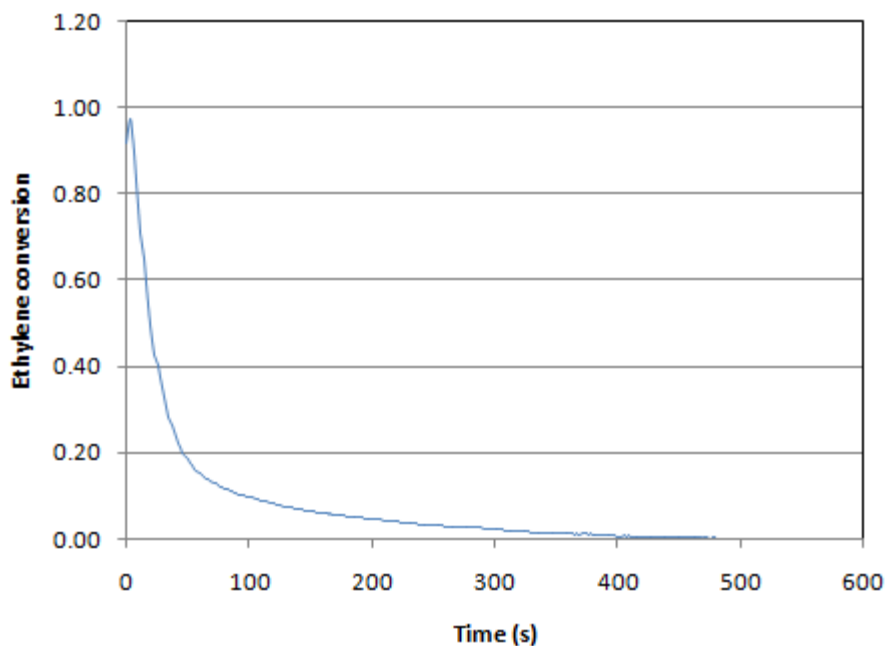


Figure 79: Ethylene conversion versus time. First cycle, Reaction conditions: T=503K PTotal=1 bar PEth=0.1 $CuCl_2.CeO_2/\gamma-Al_2O_3$ (5wt% Cu, 3wt% Ceria)

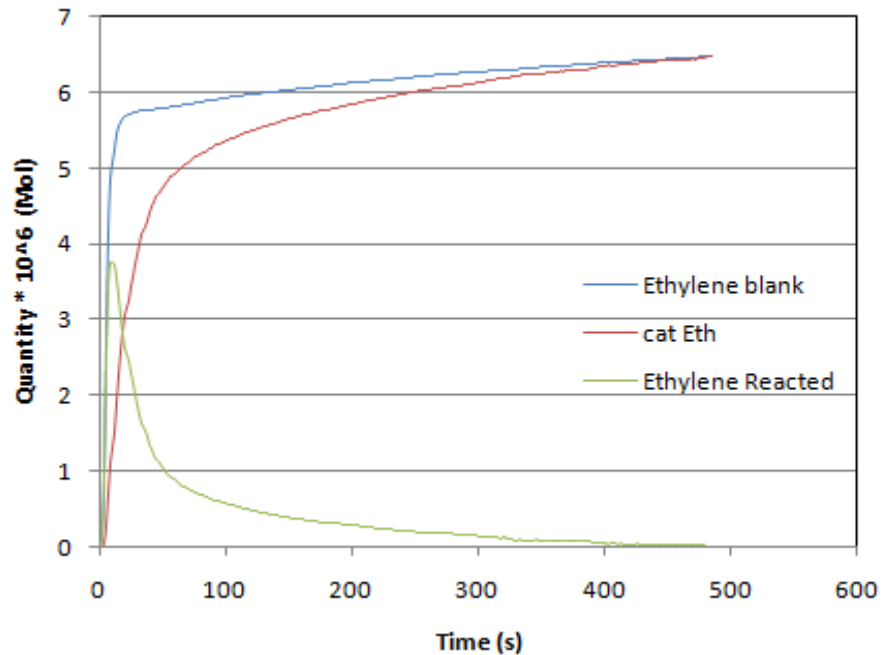


Figure 80: Ethylene profile within the reaction time. First cycle, Reaction conditions: T=503K PTotal=1 bar PEth=0.1 $CuCl_2.CeO_2/\gamma-Al_2O_3$ (5wt% Cu, 3wt% Ceria)

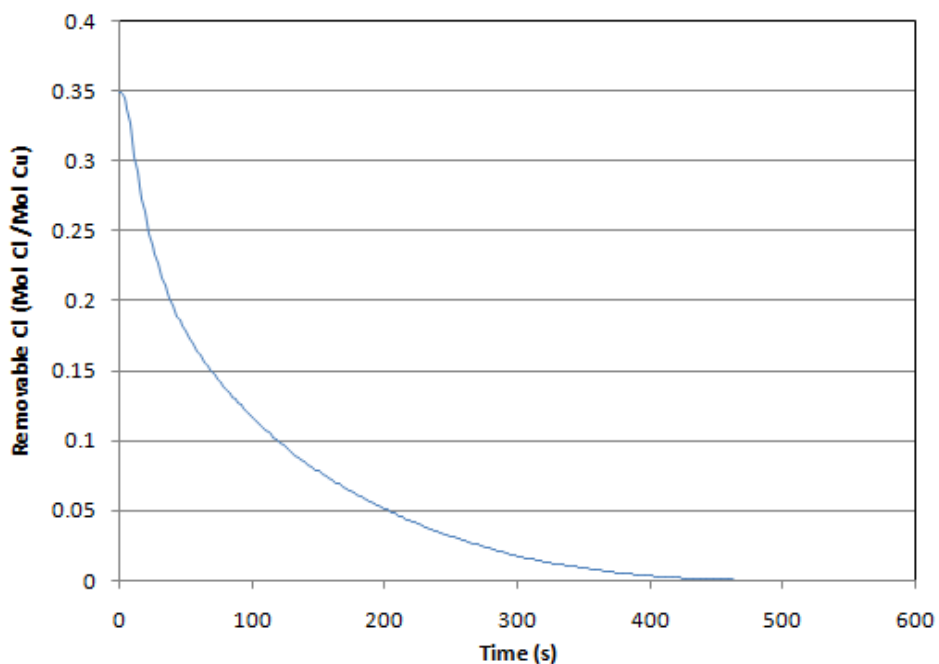


Figure 81: Removable chlorine versus time. First cycle, Reaction conditions: T=503K PTotal=1 bar PEth=0.1 $CuCl_2 \cdot CeO_2 / \gamma - Al_2O_3$ (5wt% Cu, 3wt% Ceria)

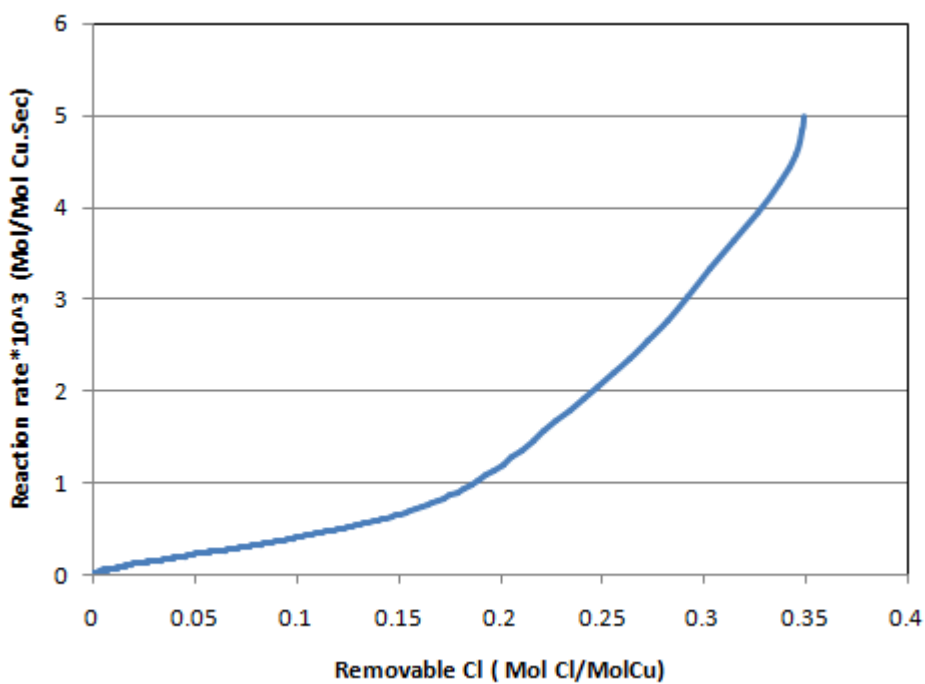


Figure 82: Reaction rate versus Removable Chlorine. First cycle, Reaction conditions: T=503K PTotal=1 bar PEth=0.1 $CuCl_2 \cdot CeO_2 / \gamma - Al_2O_3$ (5wt% Cu, 3wt% Ceria)

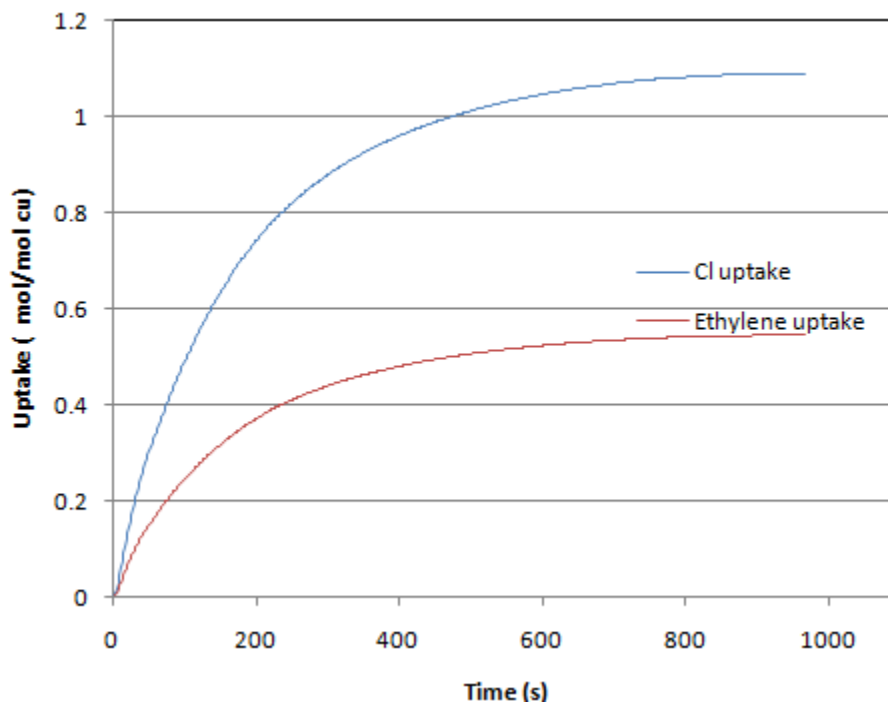


Figure 83: Uptake versus time. Second cycle, Reaction conditions: T=503K PTotal=1 bar PEth=0.1 $\text{CuCl}_2 \cdot \text{CeO}_2 / \gamma - \text{Al}_2\text{O}_3$ (5wt% Cu, 3wt% Ceria)

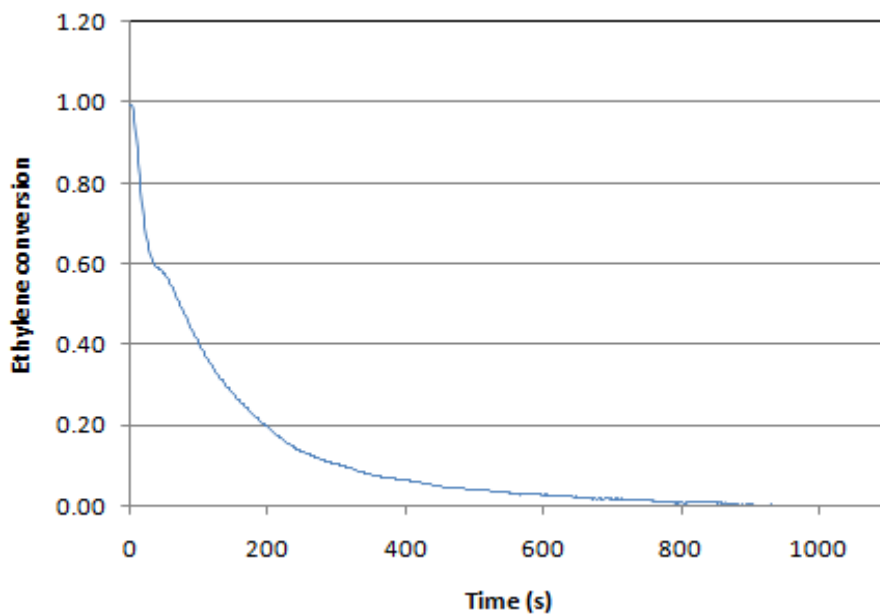


Figure 84: Ethylene conversion versus time. Second cycle, Reaction conditions: T=503K PTotal=1 bar PEth=0.1 $\text{CuCl}_2 \cdot \text{CeO}_2 / \gamma - \text{Al}_2\text{O}_3$ (5wt% Cu, 3wt% Ceria)

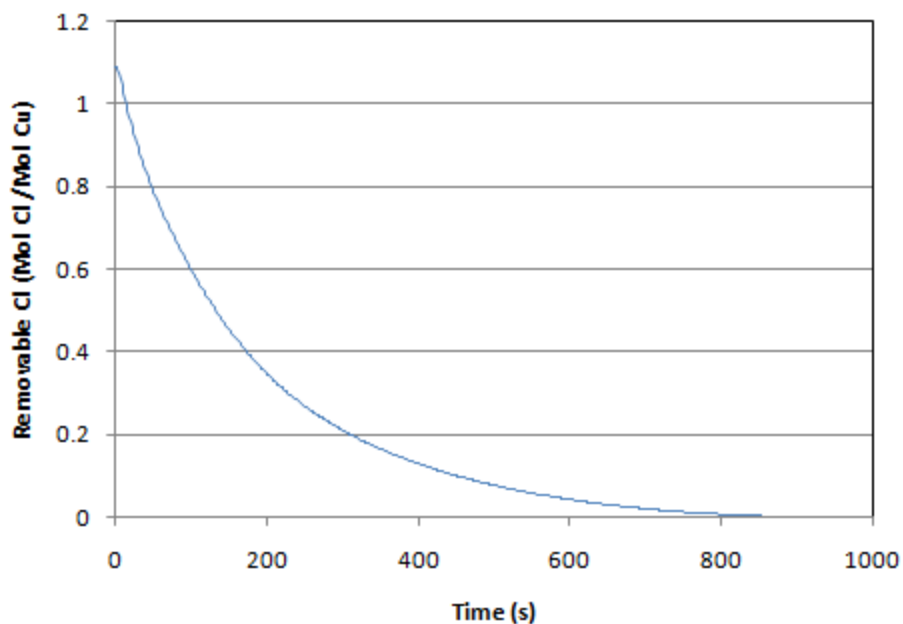


Figure 85: Removable chlorine versus time. Second cycle, Reaction conditions: T=503K PTotal=1 bar PEth=0.1 $CuCl_2.CeO_2/\gamma - Al_2O_3$ (5wt% Cu, 3wt% Ceria)

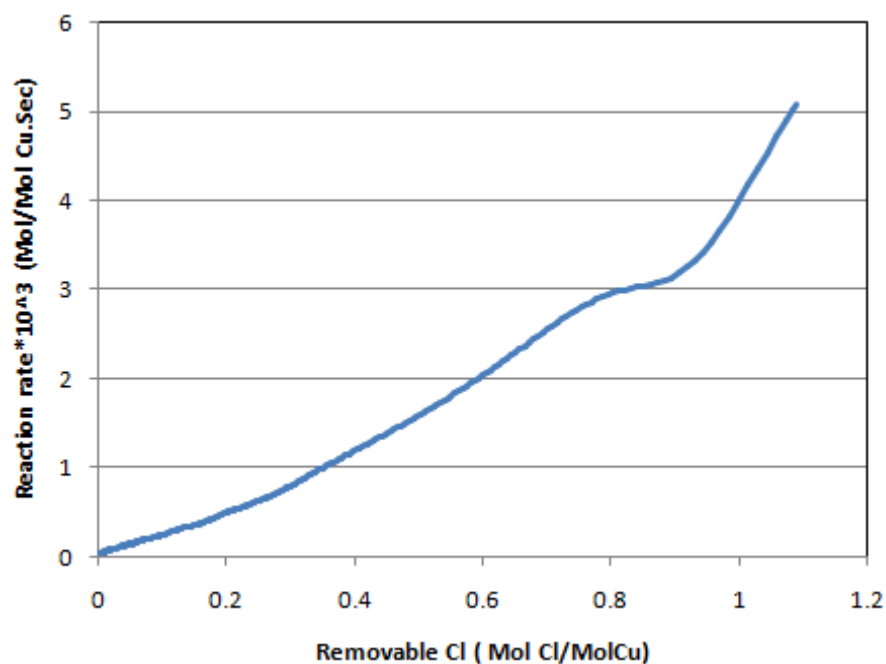


Figure 86: Reaction rate versus Removable Chlorine. Second cycle, Reaction conditions: T=503K PTotal=1 bar PEth=0.1 $CuCl_2.CeO_2/\gamma - Al_2O_3$ (5wt% Cu, 3wt% Ceria)

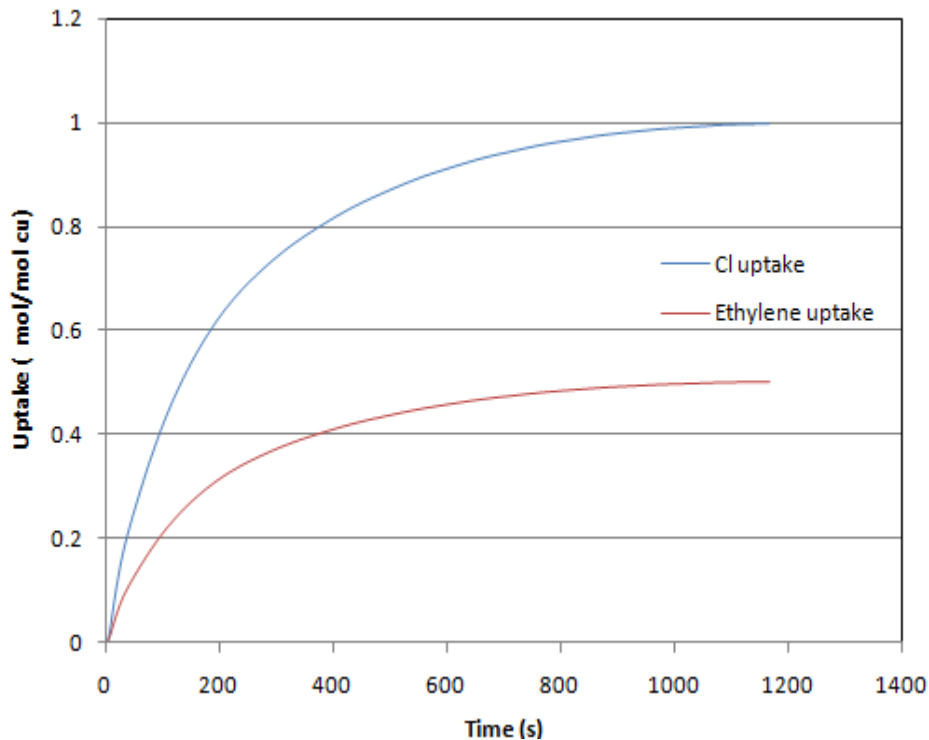


Figure 87: Uptake versus time. Third cycle, Reaction conditions: T=503K PTotal=1 bar PEth=0.1 $CuCl_2.CeO_2/\gamma-Al_2O_3$ (5wt% Cu, 3wt% Ceria)

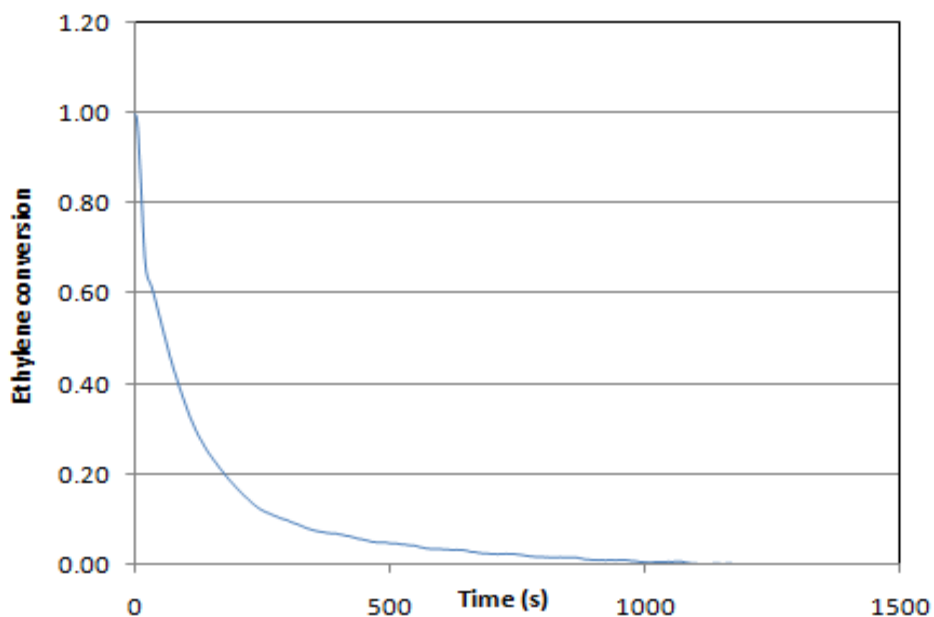


Figure 88: Ethylene conversion versus time. Third cycle, Reaction conditions: T=503K PTotal=1 bar PEth=0.1 $CuCl_2.CeO_2/\gamma-Al_2O_3$ (5wt% Cu, 3wt% Ceria)

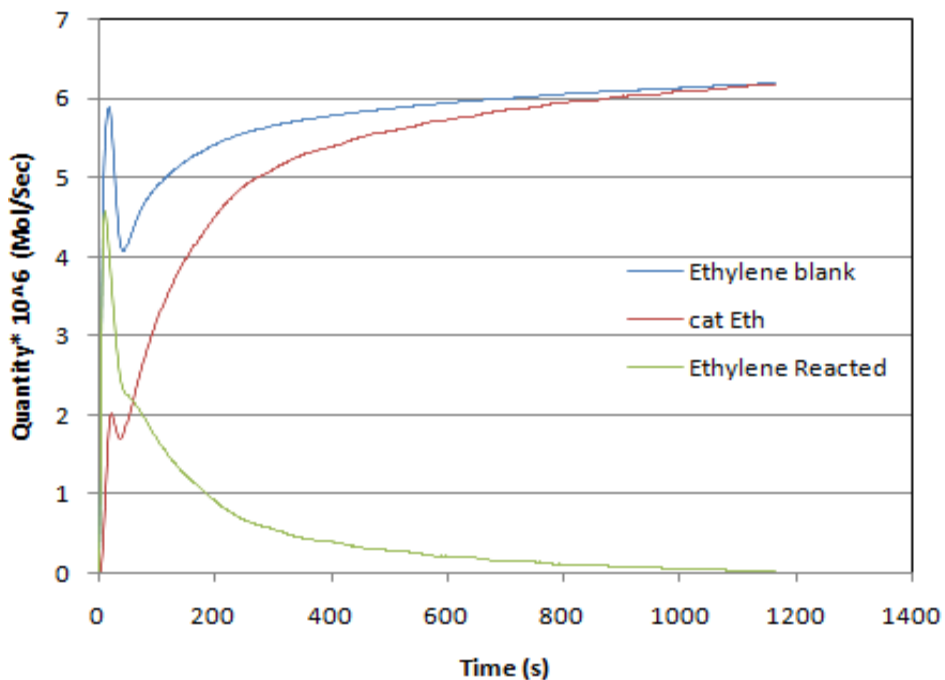


Figure 89: Ethylene profile within the reaction time. Third cycle, Reaction conditions: T=503K PTotal=1 bar PEth=0.1 $CuCl_2.CeO_2/\gamma-Al_2O_3$ (5wt% Cu, 3wt% Ceria)

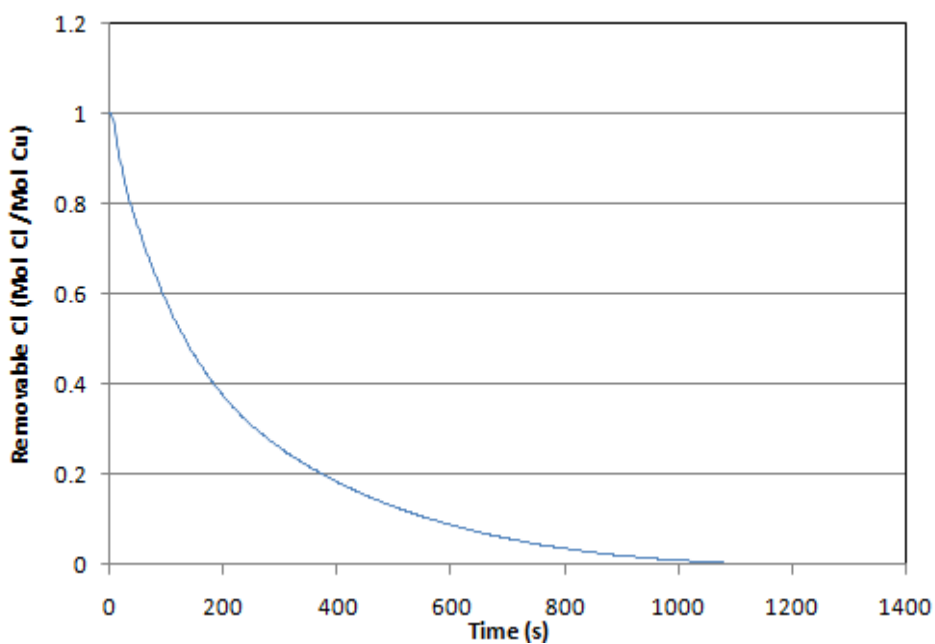


Figure 90: Removable chlorine versus time. Third cycle, Reaction conditions: T=503K PTotal=1 bar PEth=0.1 $CuCl_2.CeO_2/\gamma-Al_2O_3$ (5wt% Cu, 3wt% Ceria)

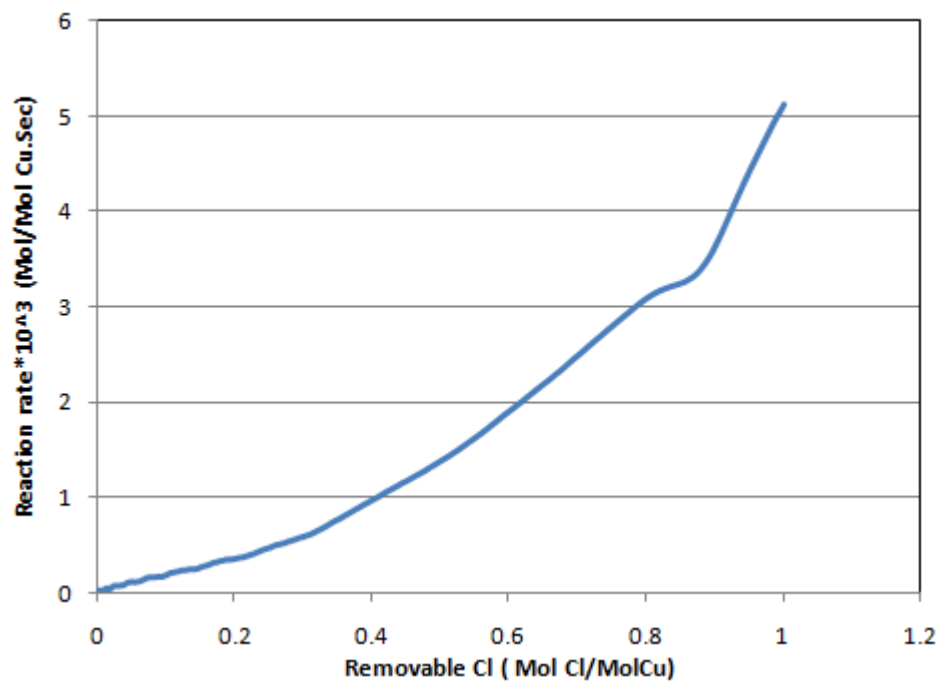


Figure 91: Reaction rate versus Removable Chlorine. Third cycle, Reaction conditions: T=503K PTotal=1 bar PEth=0.1 $CuCl_2.CeO_2/\gamma - Al_2O_3$ (5wt% Cu, 3wt% Ceria)

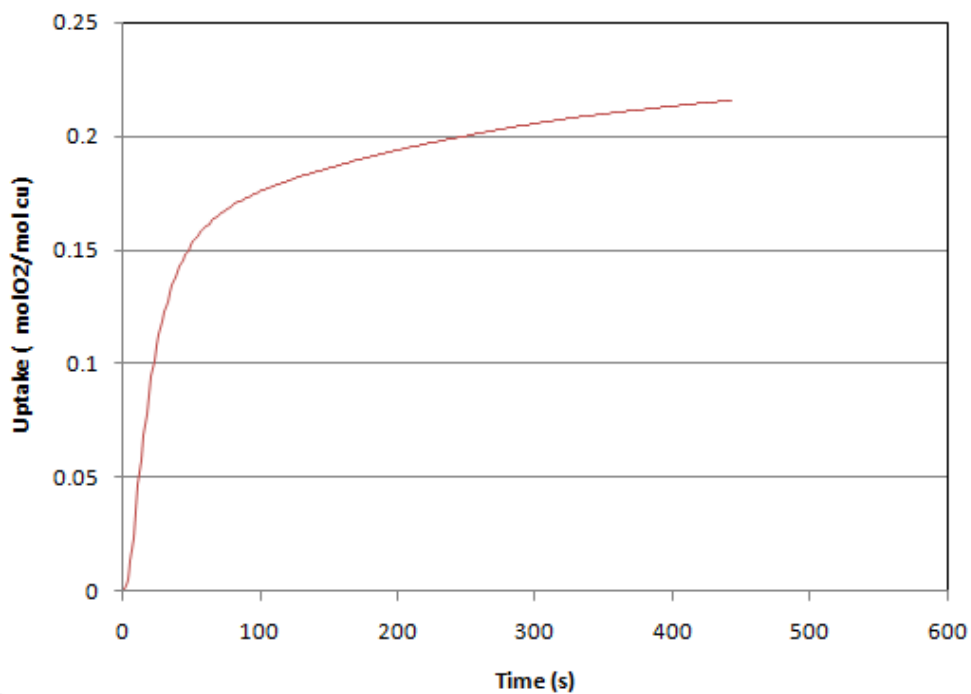


Figure 92: Uptake versus time. First cycle, Reaction conditions: T=503K PTotal=1 bar PO2=0.1 $CuCl_2.CeO_2/\gamma - Al_2O_3$ (5wt% Cu, 3wt% Ceria)

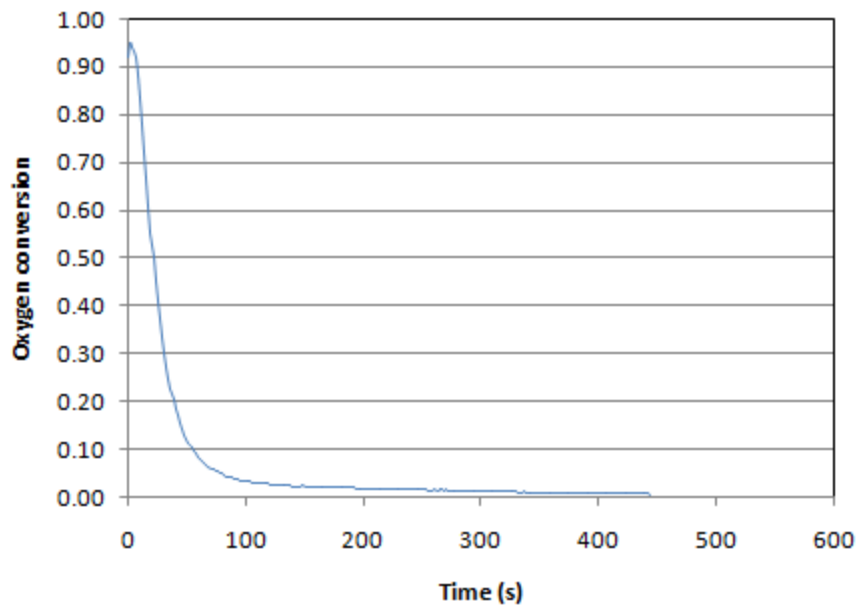


Figure 93: Oxygen conversion versus time. First cycle, Reaction conditions: T=503K PTotal=1 bar PO₂=0.1 CuCl₂.CeO₂/γ-Al₂O₃ (5wt% Cu, 3wt% Ceria)

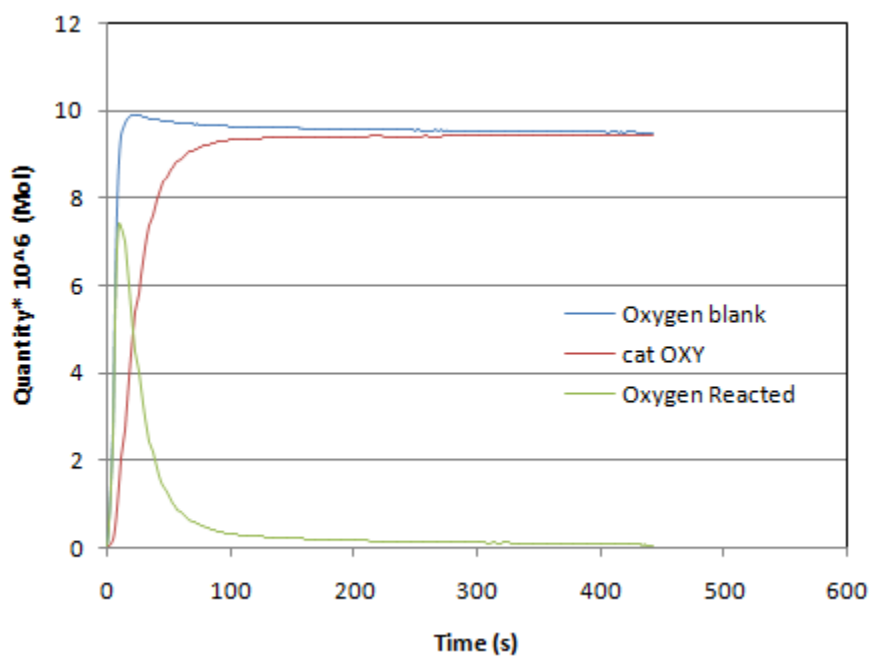


Figure 94: Oxygen profile within the reaction time. First cycle, Reaction conditions: T=503K PTotal=1 bar PO₂=0.1 CuCl₂.CeO₂/γ-Al₂O₃ (5wt% Cu, 3wt% Ceria)

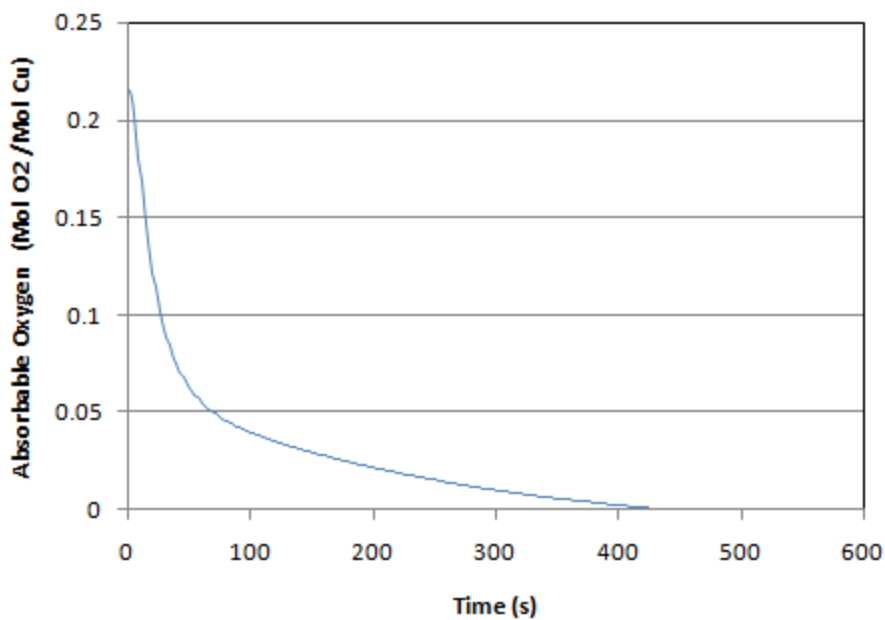


Figure 95: Absorbable Oxygen versus time. First cycle, Reaction conditions: T=503K PTotal=1 bar PO₂=0.1 CuCl₂.CeO₂/γ-Al₂O₃ (5wt% Cu, 3wt% Ceria)

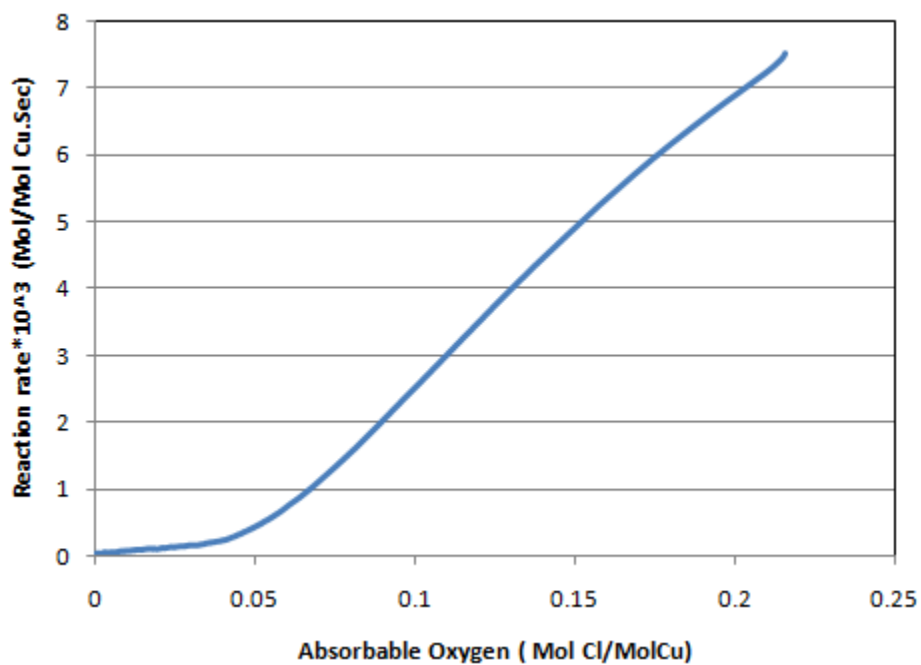


Figure 96: Reaction rate versus Absorbable Oxygen. First cycle, Reaction conditions: T=503K PTotal=1 bar PO₂=0.1 (5wt% Cu, 3wt% Ceria)

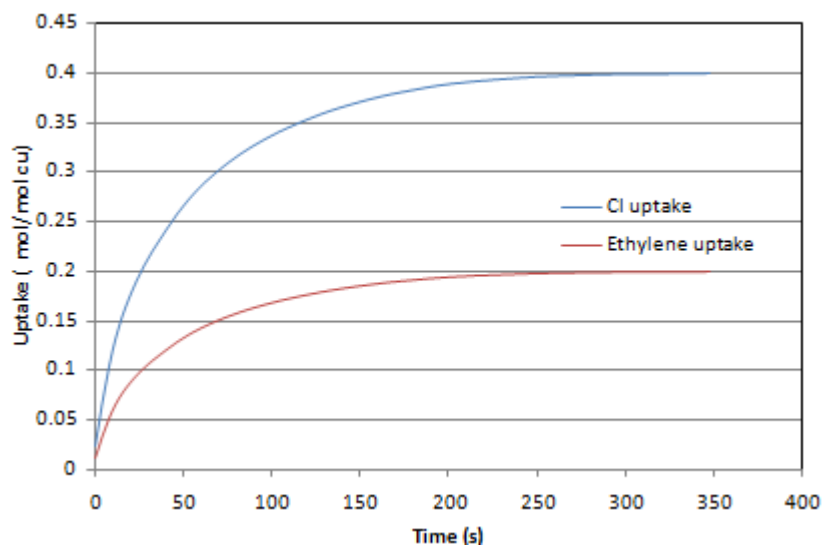


Figure 97: Uptake versus time. First cycle, Reaction conditions: $T=503\text{K}$ $P_{\text{Total}}=1$ bar $P_{\text{Eth}}=0.1$ $\text{CuCl}_2 \cdot \text{CeO}_2 / \gamma - \text{Al}_2\text{O}_3$ (4.73wt% Cu, 5wt% Ceria)

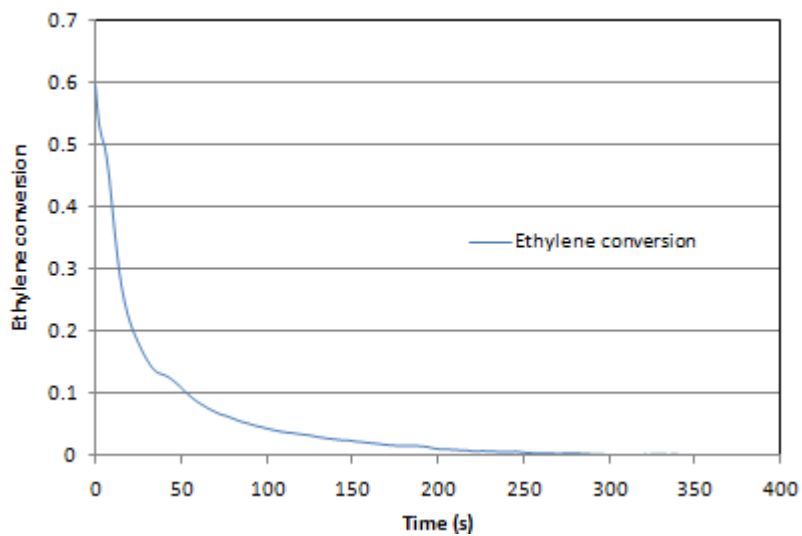


Figure 98: Ethylene conversion versus time. First cycle, Reaction conditions: $T=503\text{K}$ $P_{\text{Total}}=1$ bar $P_{\text{Eth}}=0.1$ (4.73wt% Cu, 5wt% Ceria)

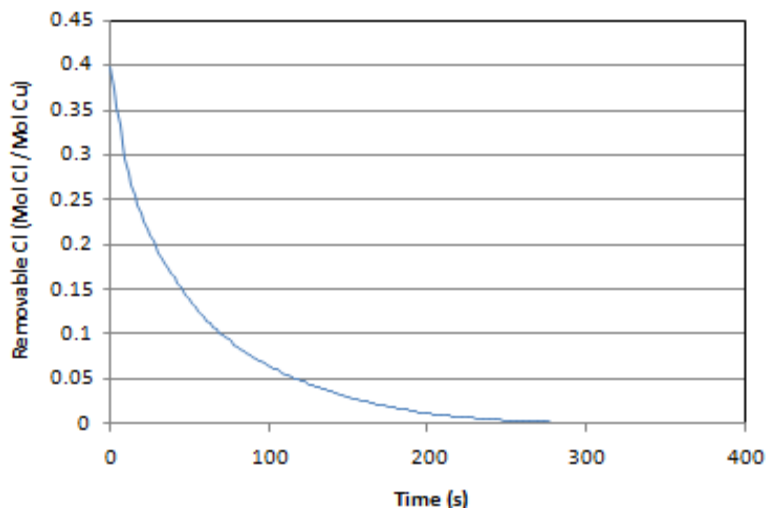


Figure 99: Removable chlorine versus time. First cycle, Reaction conditions: T=503K PTotal=1 bar PEth=0.1 (4.73wt% Cu, 5wt% Ceria)

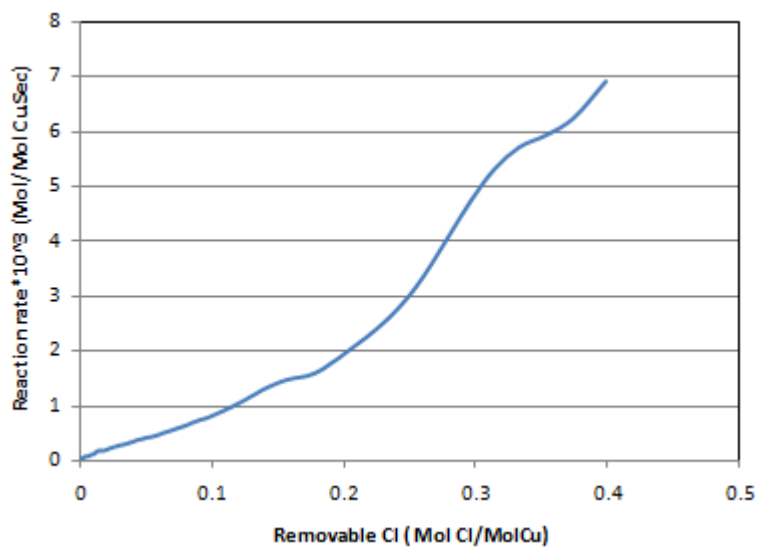


Figure 100: Reaction rate versus Removable Chlorine. First cycle, Reaction conditions: T=503K PTotal=1 bar PEth=0.1 (4.73wt% Cu, 5wt% Ceria)

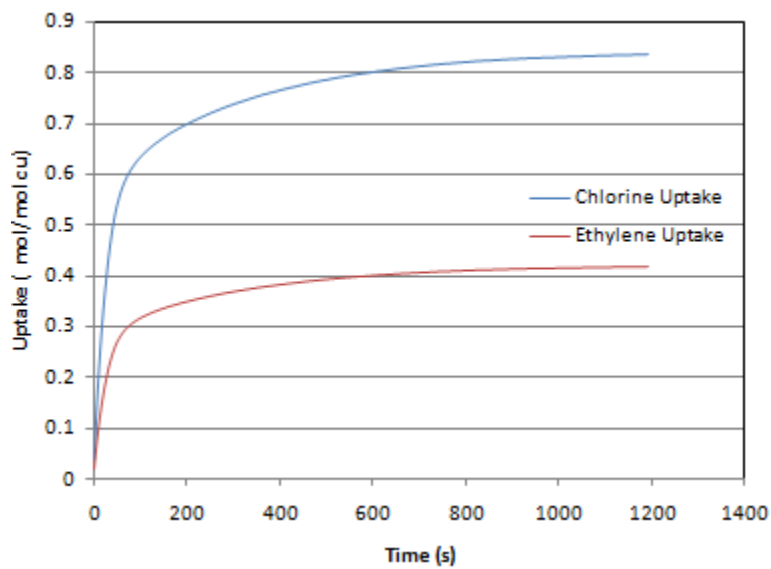


Figure 101: Uptake versus time. Second cycle, Reaction conditions: T=503K PTotal=1 bar PEth=0.1 (4.73wt% Cu, 5wt% Ceria)

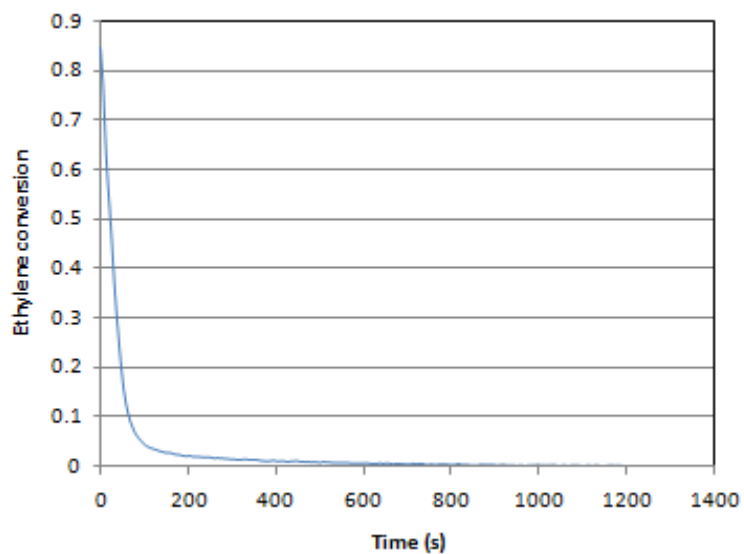


Figure 102: Ethylene conversion versus time. Second cycle, Reaction conditions: T=503K PTotal=1 bar PEth=0.1 (4.73wt% Cu, 5wt% Ceria)

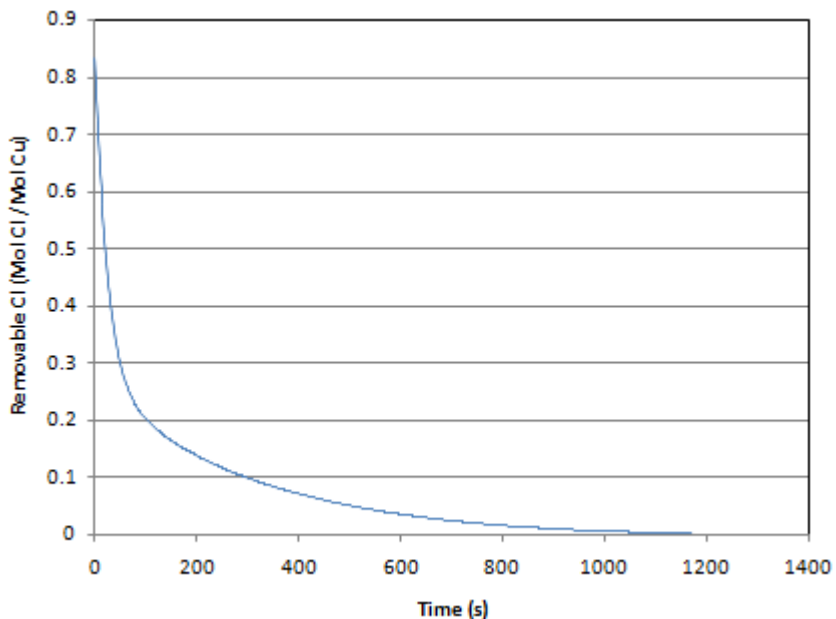


Figure 103: Removable chlorine versus time. Second cycle, Reaction conditions: T=503K PTotal=1 bar PEth=0.1 (4.73wt% Cu, 5wt% Ceria)

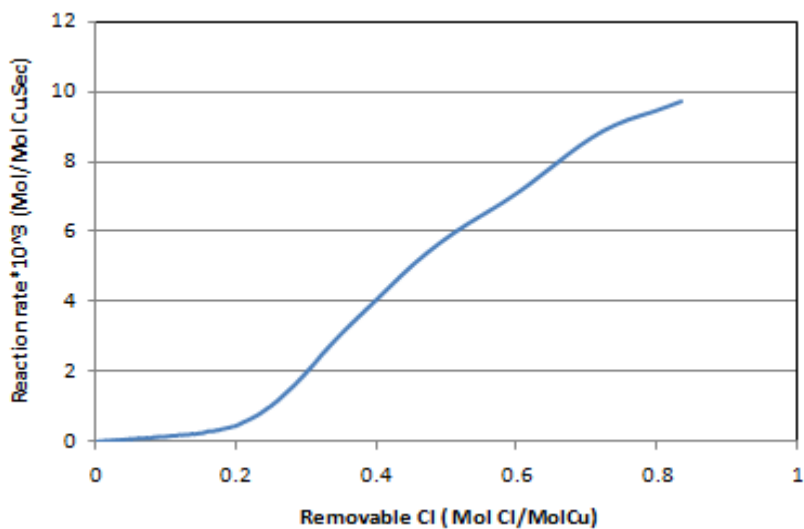


Figure 104: Reaction rate versus Removable Chlorine. Second cycle, Reaction conditions: T=503K PTotal=1 bar PEth=0.1 $CuCl_2.CeO_2/\gamma-Al_2O_3$ (4.73wt% Cu, 5wt% Ceria)

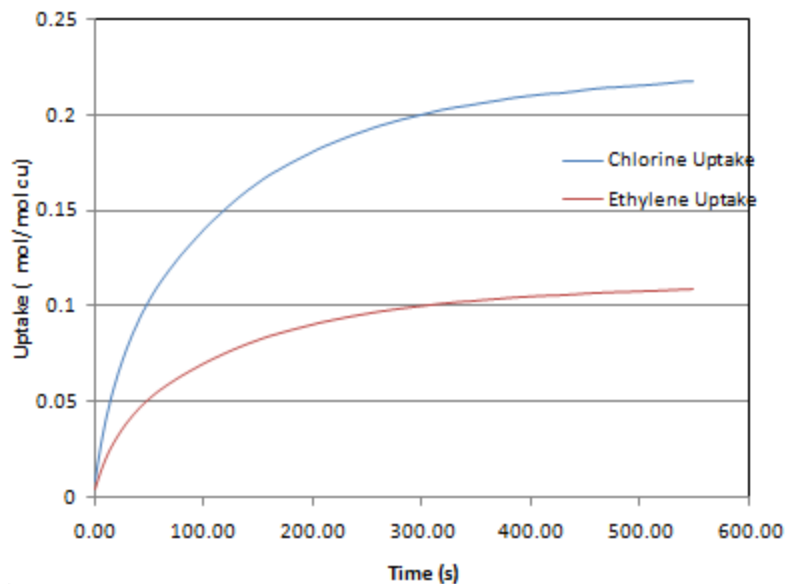


Figure 105: Uptake versus Time. Third cycle, Reaction conditions: T=503K PTotal=1 bar PEth=0.1 $\text{CuCl}_2 \cdot \text{CeO}_2 / \gamma - \text{Al}_2\text{O}_3$ (4.73wt% Cu, 5wt% Ceria)

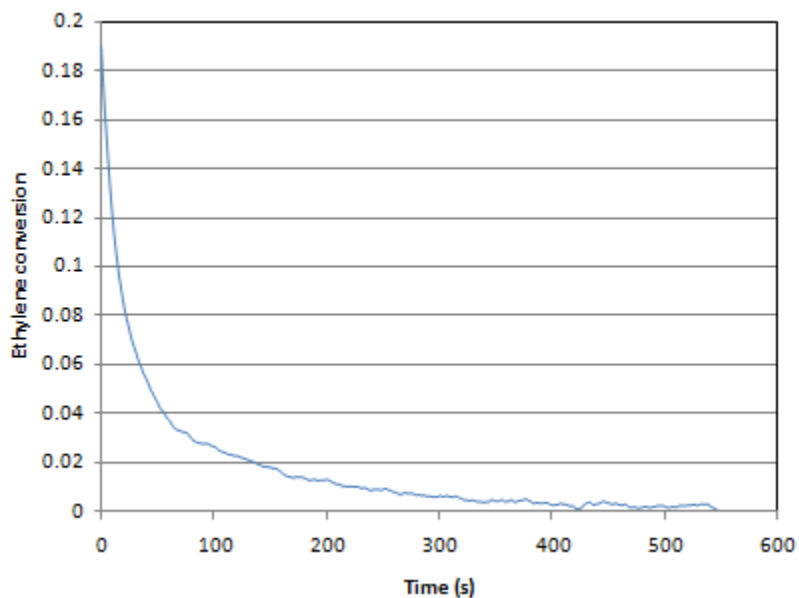


Figure 106: Ethylene conversion versus time. Third cycle, Reaction conditions: T=503K PTotal=1 bar PEth=0.1 $\text{CuCl}_2 \cdot \text{CeO}_2 / \gamma - \text{Al}_2\text{O}_3$ (4.73wt% Cu, 5wt% Ceria)

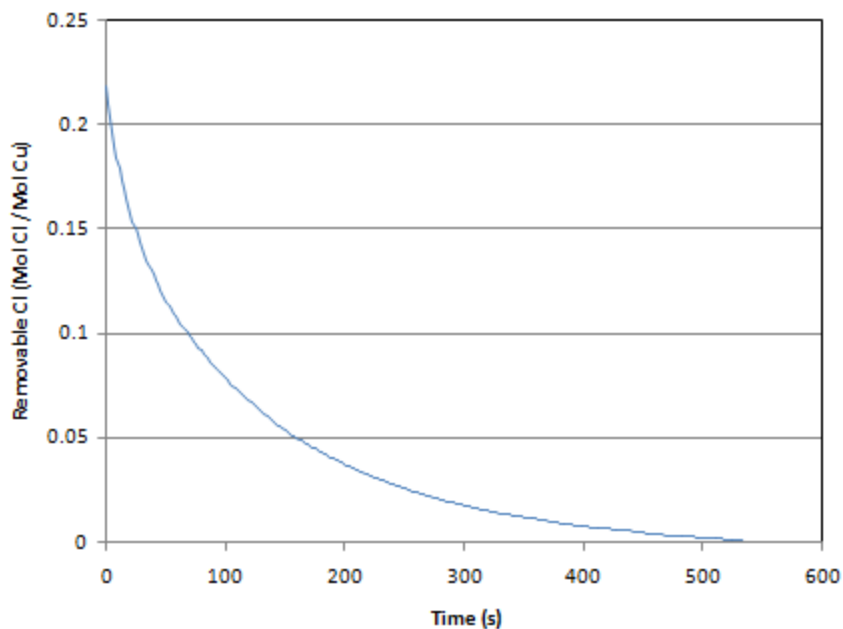


Figure 107: Removable chlorine versus time. Third cycle, Reaction conditions: T=503K PTotal=1 bar PEth=0.1 $CuCl_2 \cdot CeO_2 / \gamma - Al_2O_3$ (4.73wt% Cu, 5wt% Ceria)

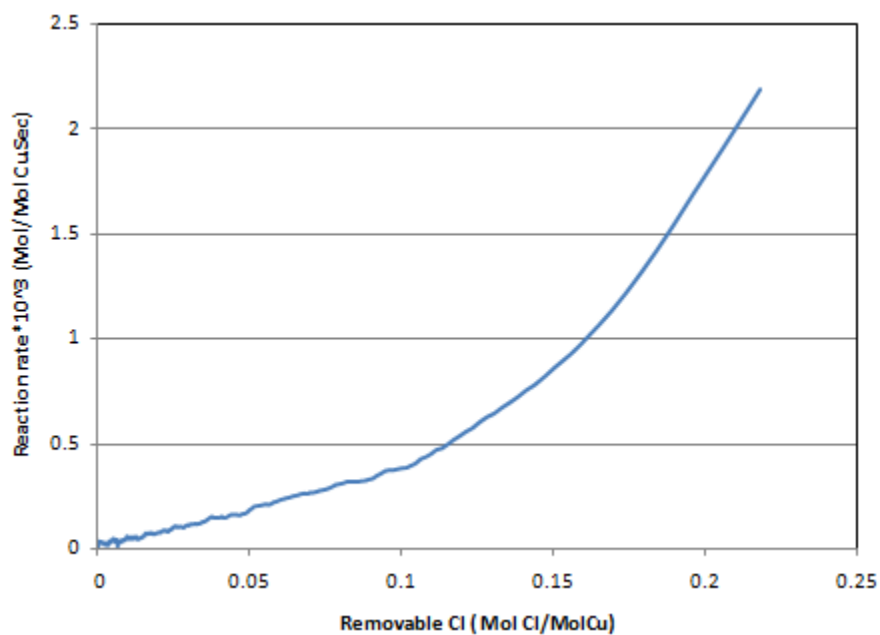


Figure 108: Reaction rate versus Removable Chlorine. Third cycle, Reaction conditions: T=503K PTotal=1 bar PEth=0.1 $CuCl_2 \cdot CeO_2 / \gamma - Al_2O_3$ (4.73wt% Cu, 5wt% Ceria)

Appendix B: UV/VIS Spectrometer

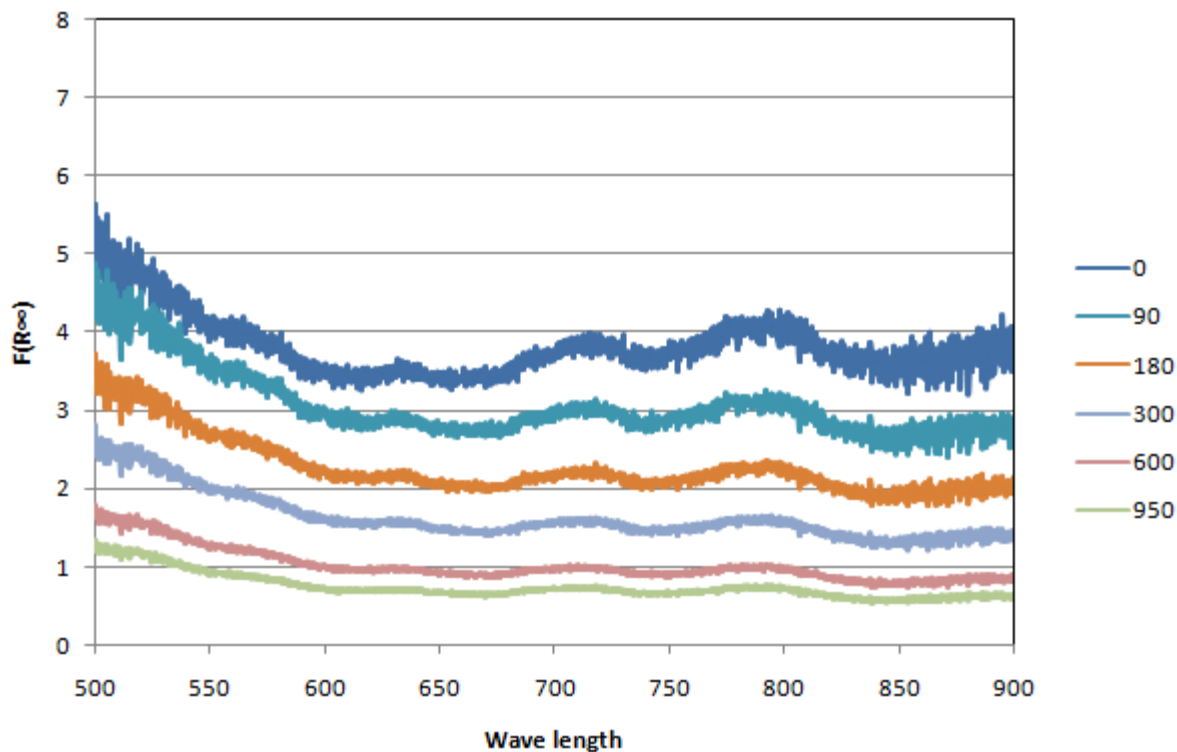


Figure 109: Kubelka-Munk function versus Wave length. First cycle, Reaction conditions: T=503K PTotal=1 bar PEth=0.1 $CuCl_2/\gamma - Al_2O_3$ (4.81wt% Cu, 0wt% Ceria)

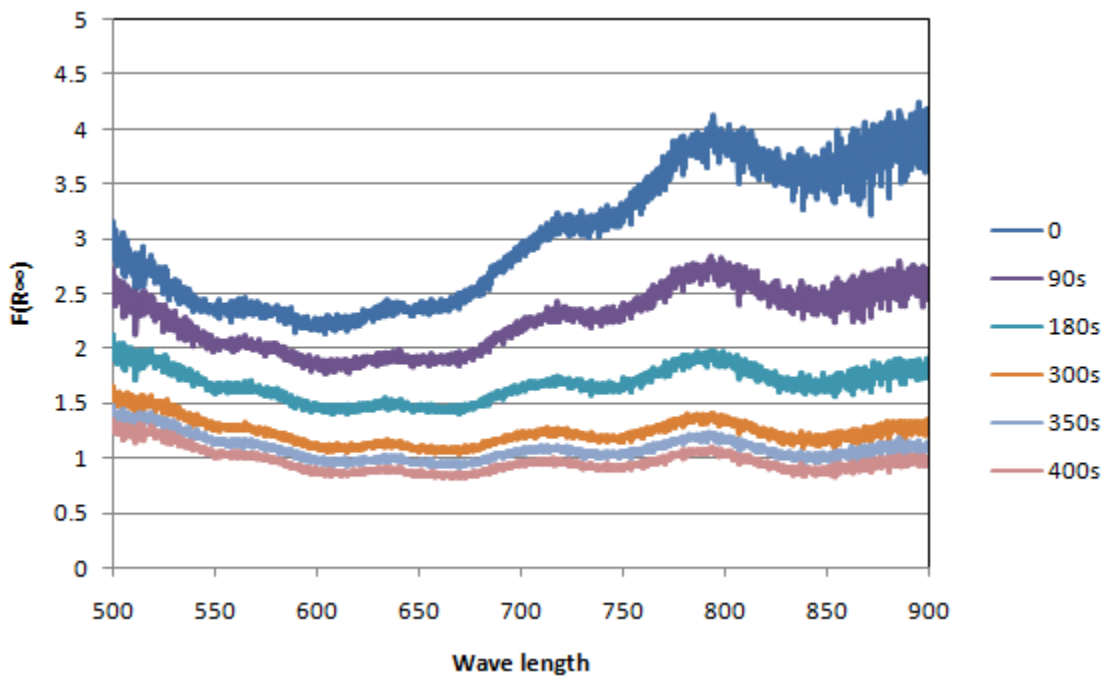


Figure 110: Kubelka-Munk function versus Wave length. Second cycle, Reaction conditions: T=503K PTotal=1 bar PEth=0.1 $CuCl_2/\gamma - Al_2O_3$ (4.81wt% Cu, 0wt% Ceria)

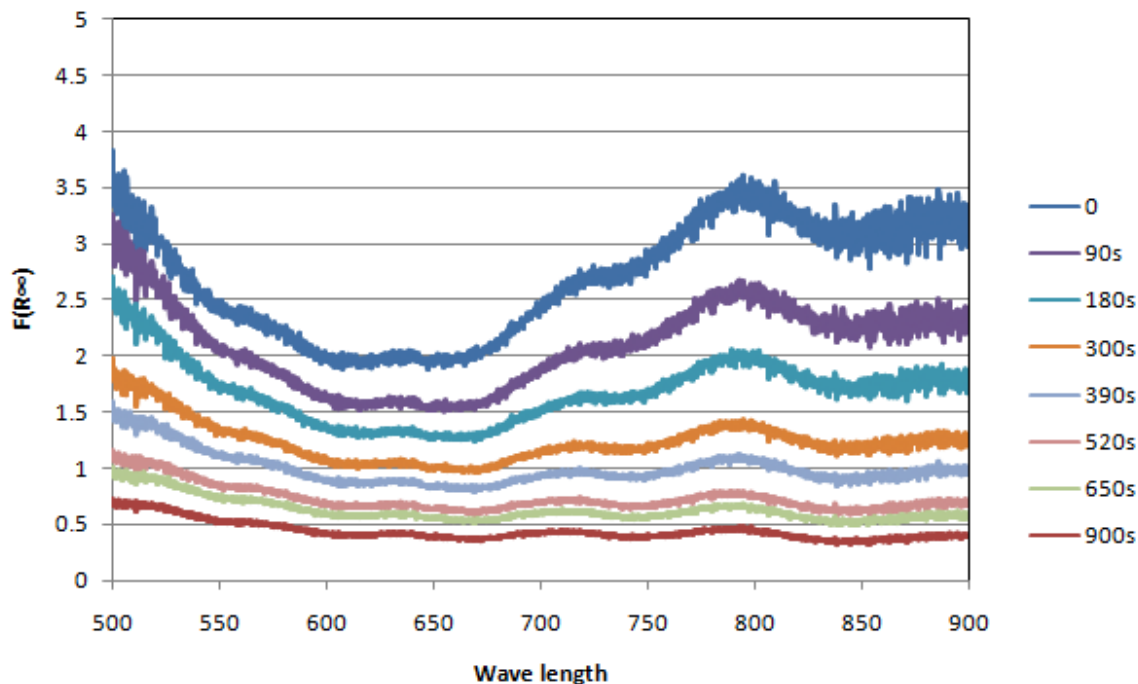


Figure 111: Kubelka-Munk function versus Wave length. Third cycle, Reaction conditions: T=503K PTotal=1 bar PEth=0.1 $CuCl_2/\gamma - Al_2O_3$ (4.81wt% Cu, 0wt% Ceria)

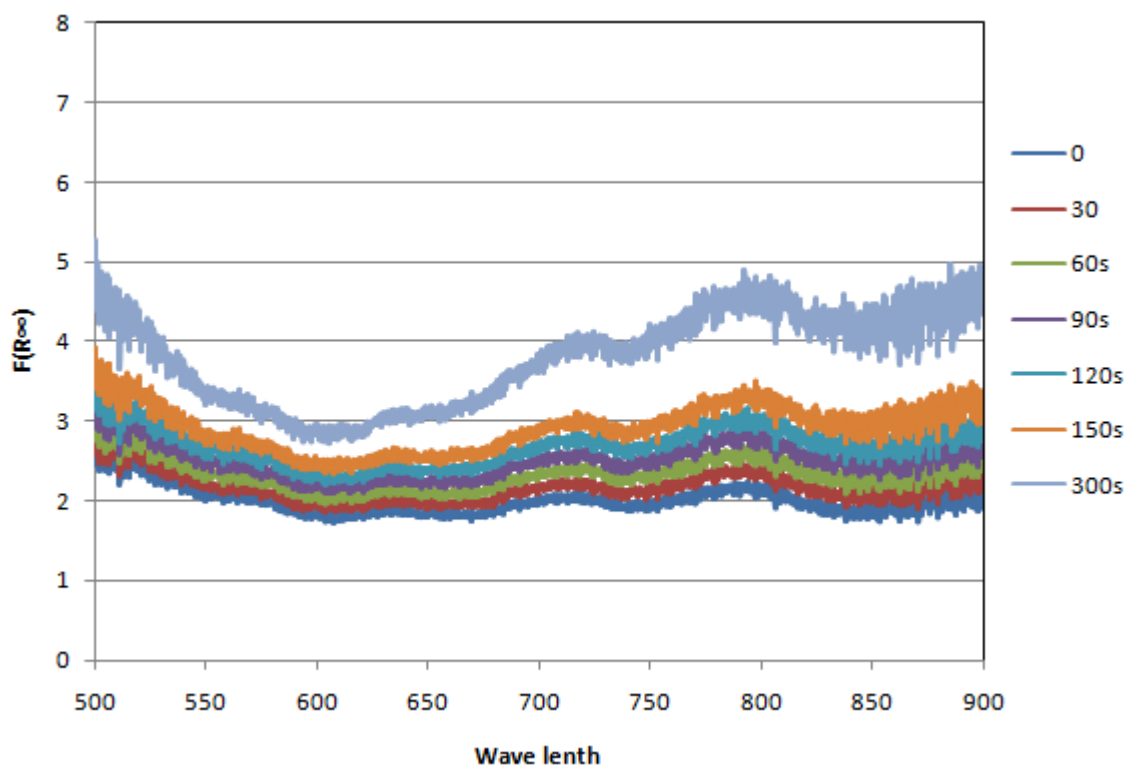


Figure 112: Kubelka-Munk function versus Wave length. First cycle, Reaction conditions: T=503K PTotal=1 bar PO2=0.1 $CuCl_2/\gamma - Al_2O_3$ (4.81wt% Cu, 0wt% Ceria)

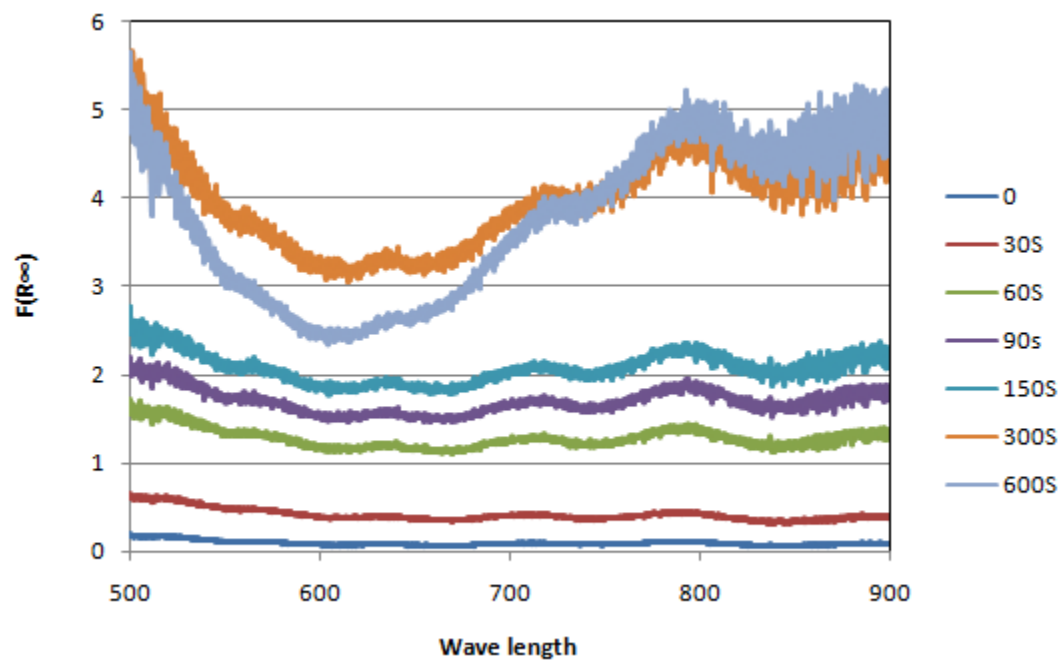


Figure 113: Kubelka-Munk function versus Wave length. Second cycle, Reaction conditions: T=503K PTotal=1 bar PO₂=0.1 CuCl₂/γ-Al₂O₃ (4.81wt% Cu, 0wt% Ceria)

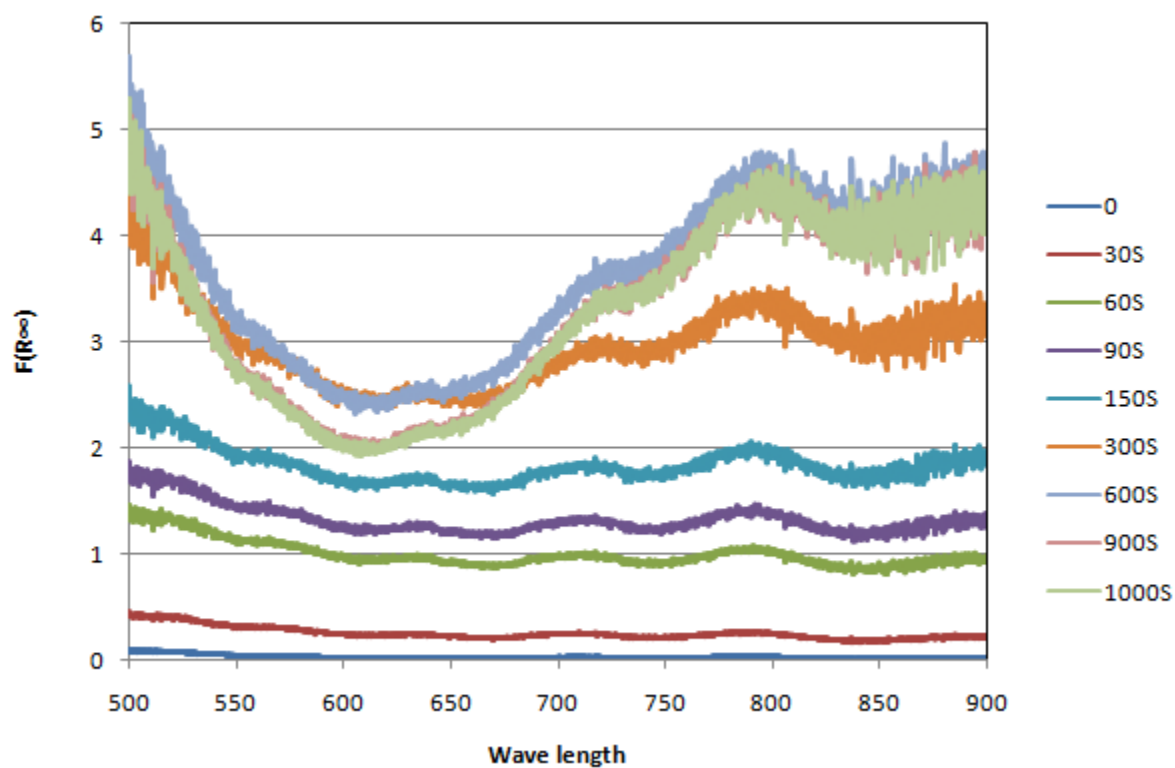


Figure 114: Kubelka-Munk function versus Wave length. Third cycle, Reaction conditions: T=503K PTotal=1 bar PO₂=0.1 CuCl₂/γ-Al₂O₃ (4.81wt% Cu, 0wt% Ceria)

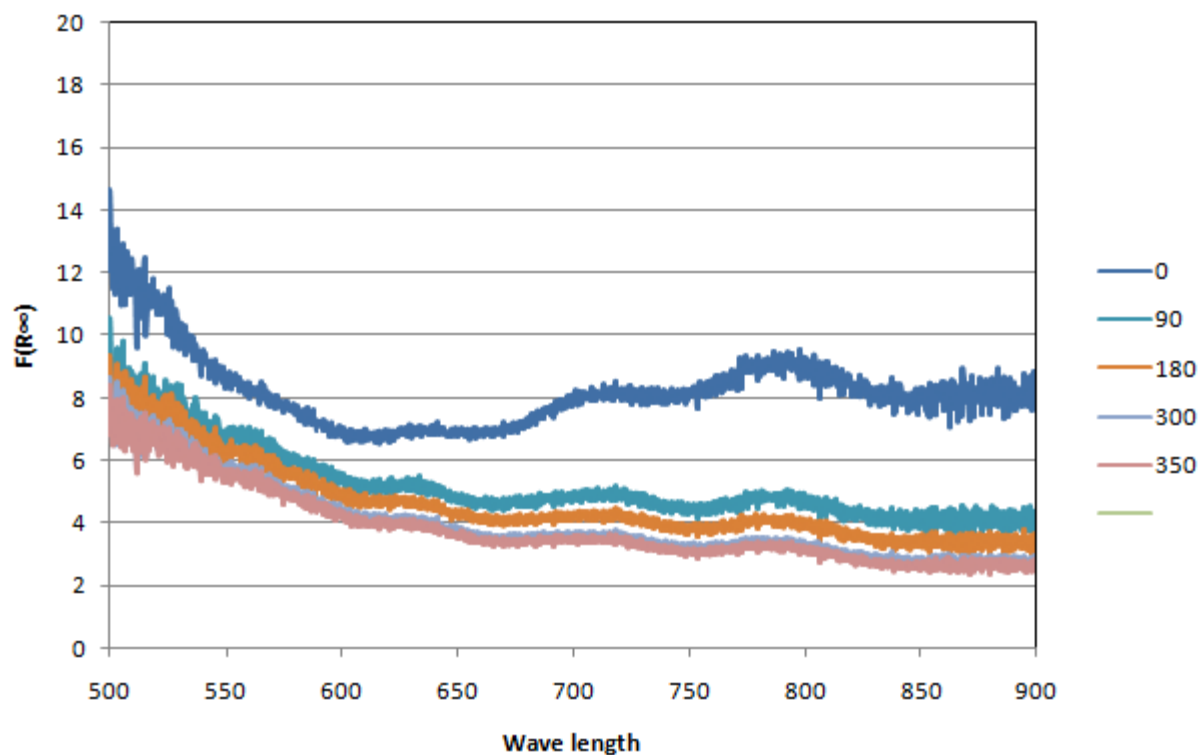


Figure 115: Kubelka-Munk function versus Wave length. First cycle, Reaction conditions: T=503K PTotal=1 bar PEth=0.1 $CuCl_2.CeO_2/\gamma-Al_2O_3$ (5wt% Cu, 1wt% Ceria)

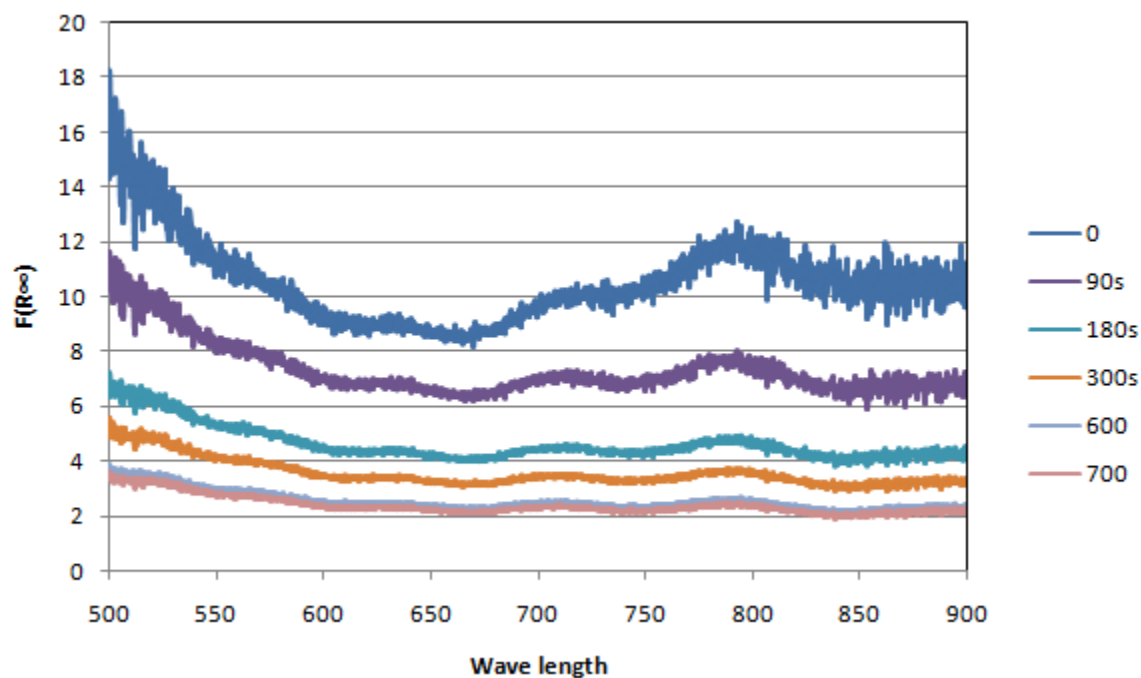


Figure 116: Kubelka-Munk function versus Wave length. Second cycle, Reaction conditions: T=503K PTotal=1 bar PEth=0.1 $CuCl_2.CeO_2/\gamma-Al_2O_3$ (5wt% Cu, 1wt% Ceria)

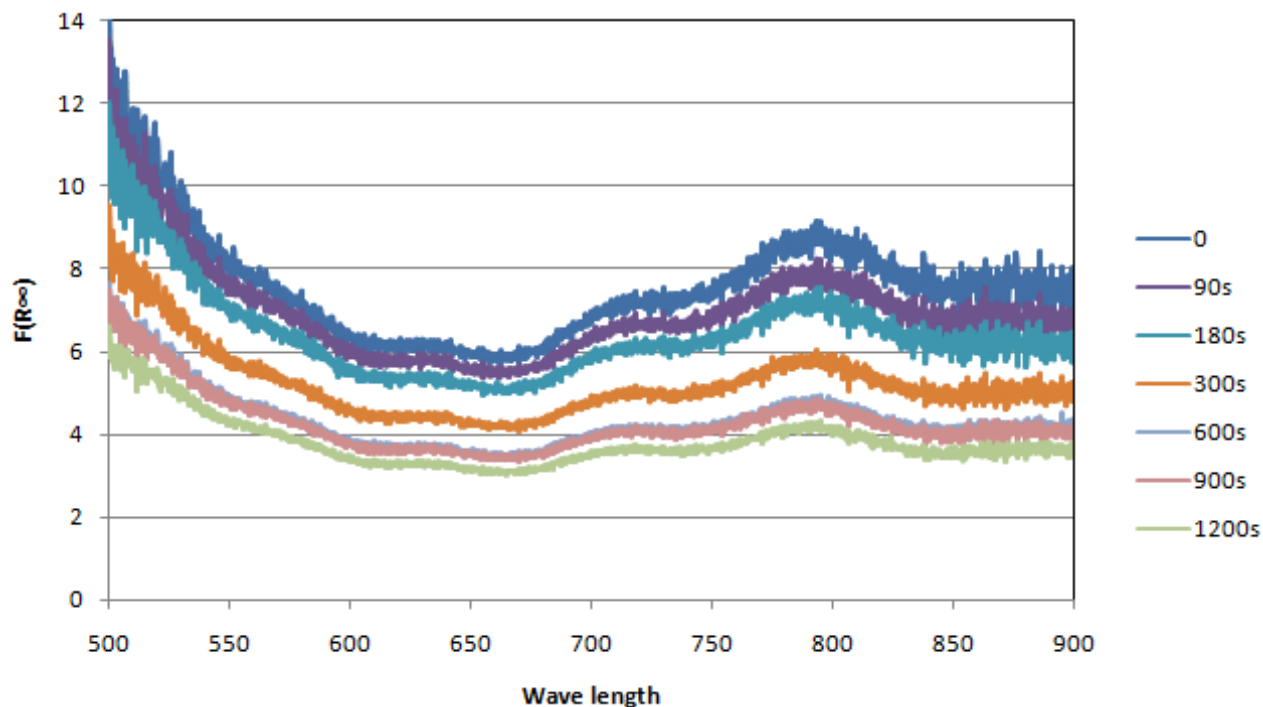


Figure 117: Kubelka-Munk function versus Wave length. Third cycle, Reaction conditions: T=503K PTotal=1 bar PETH=0.1 $CuCl_2.CeO_2/\gamma-Al_2O_3$ (5wt% Cu, 1wt% Ceria)

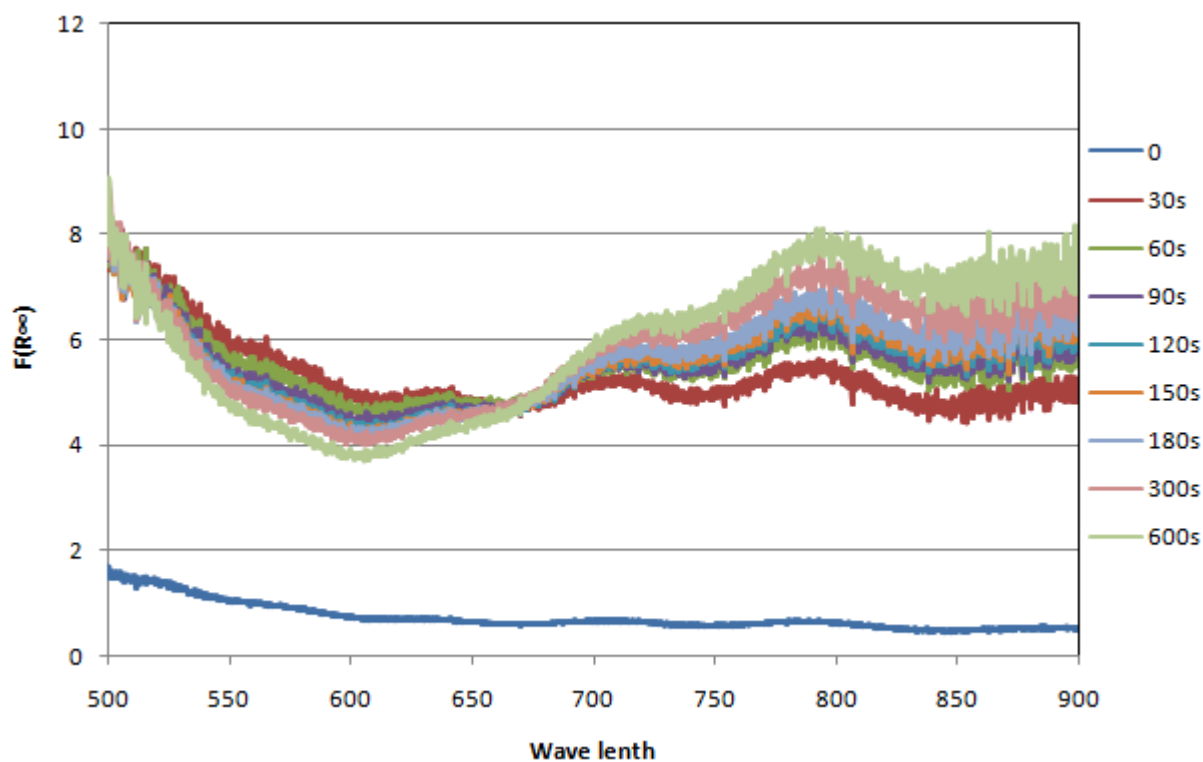


Figure 118: Kubelka-Munk function versus Wave length. First cycle, Reaction conditions: T=503K PTotal=1 bar $PO_2=0.1$ $CuCl_2.CeO_2/\gamma-Al_2O_3$ (5wt% Cu, 1wt% Ceria)

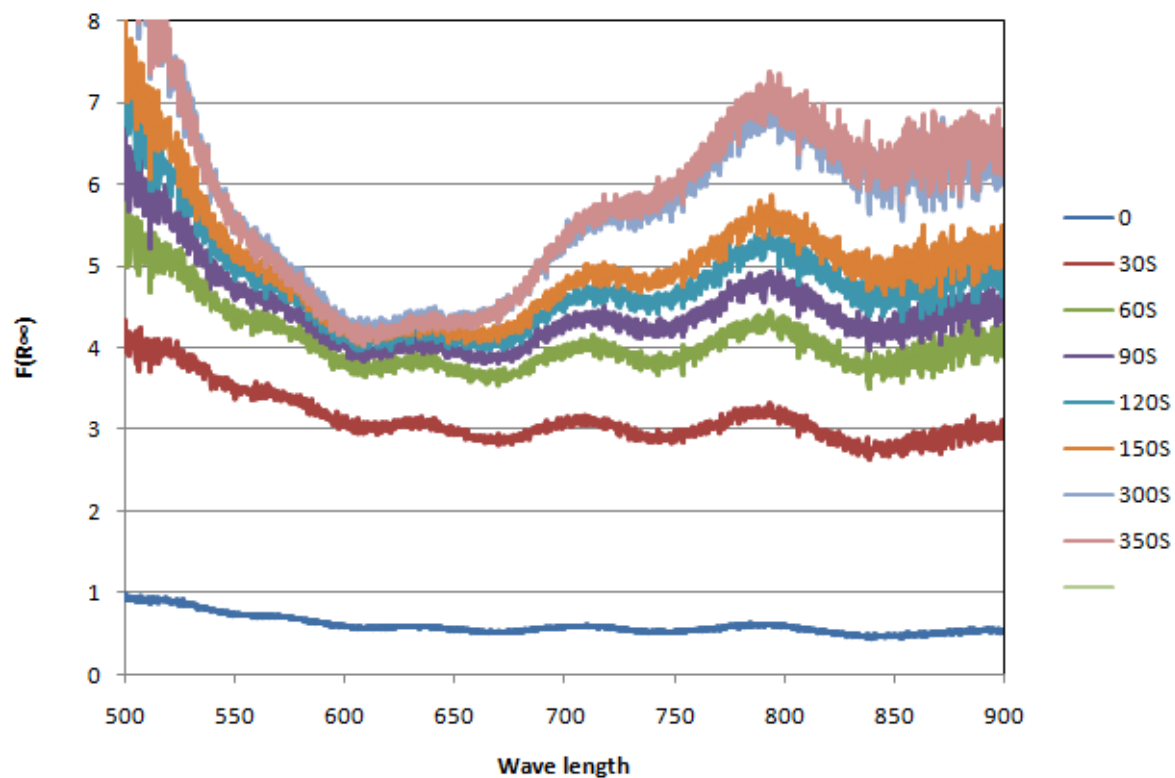


Figure 119: Kubelka-Munk function versus Wave length. Second cycle, Reaction conditions: T=503K PTotal=1 bar PO₂=0.1 CuCl₂.CeO₂/γ-Al₂O₃ (5wt% Cu, 1wt% Ceria)

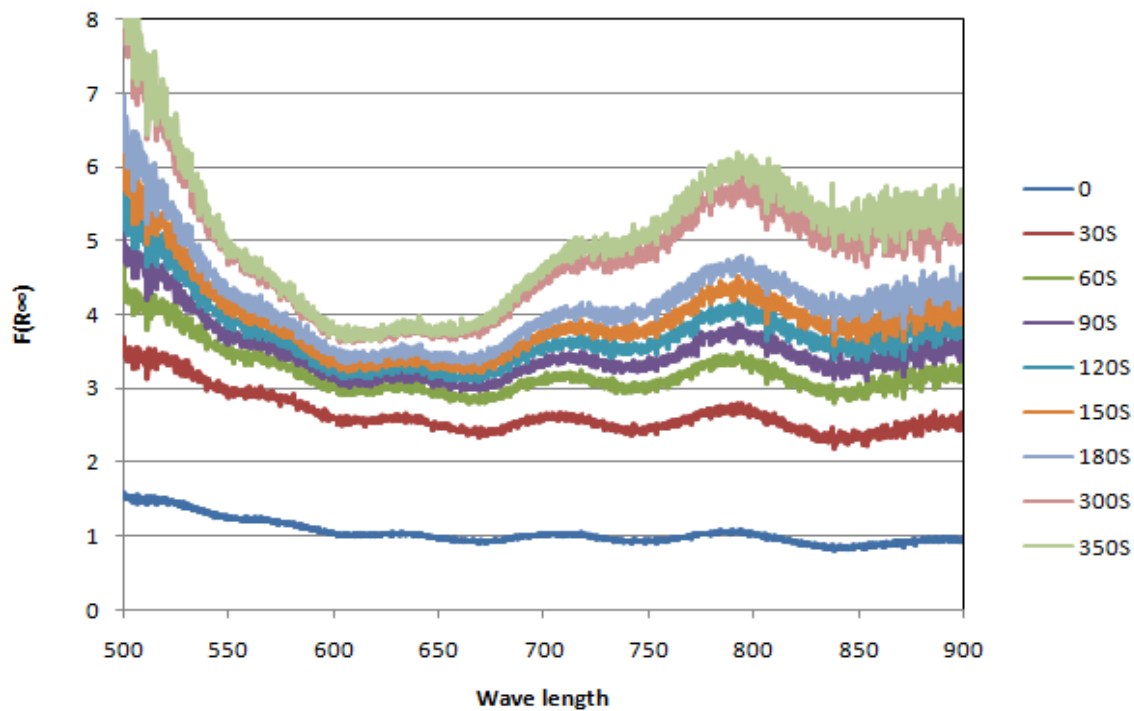


Figure 120: Kubelka-Munk function versus Wave length. Third cycle, Reaction conditions: T=503K PTotal=1 bar PO₂=0.1 CuCl₂.CeO₂/γ-Al₂O₃ (5wt% Cu, 1wt% Ceria)

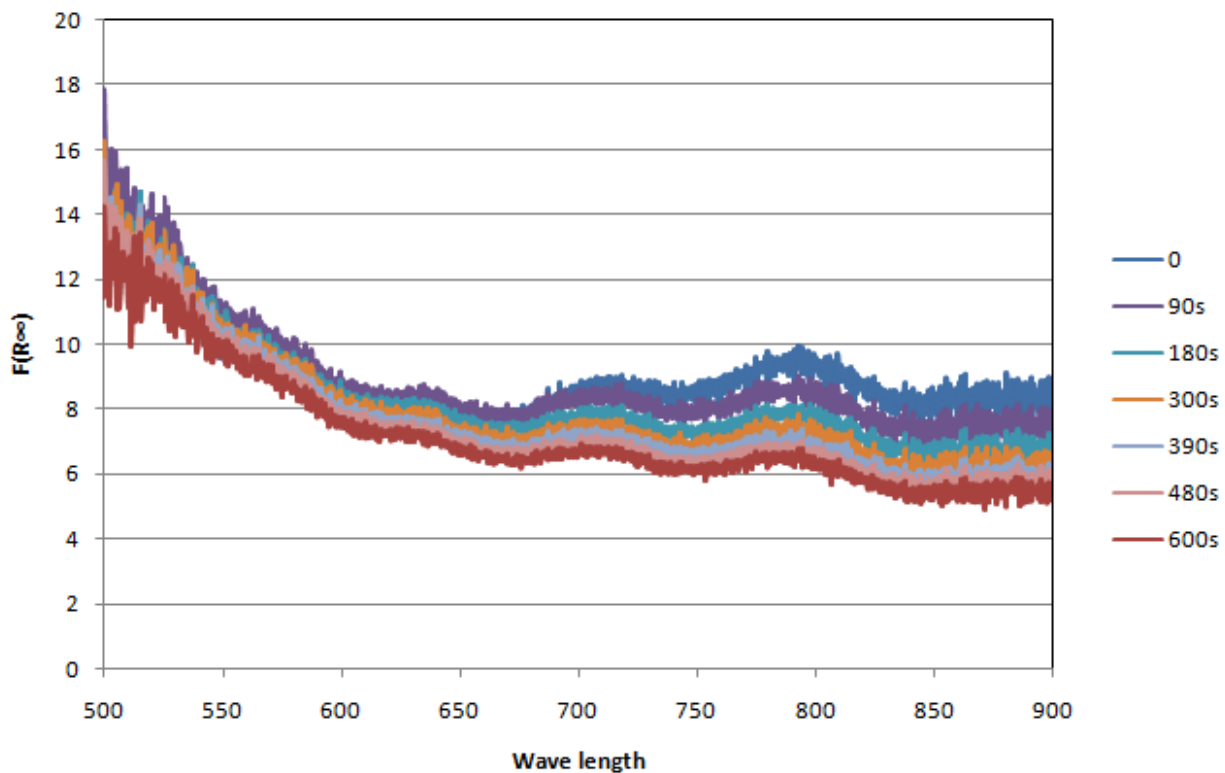


Figure 121: Kubelka-Munk function versus Wave length. First cycle, Reaction conditions: T=503K PTotal=1 bar PEth=0.1 $CuCl_2.CeO_2/\gamma-Al_2O_3$ (5wt% Cu, 3wt% Ceria)

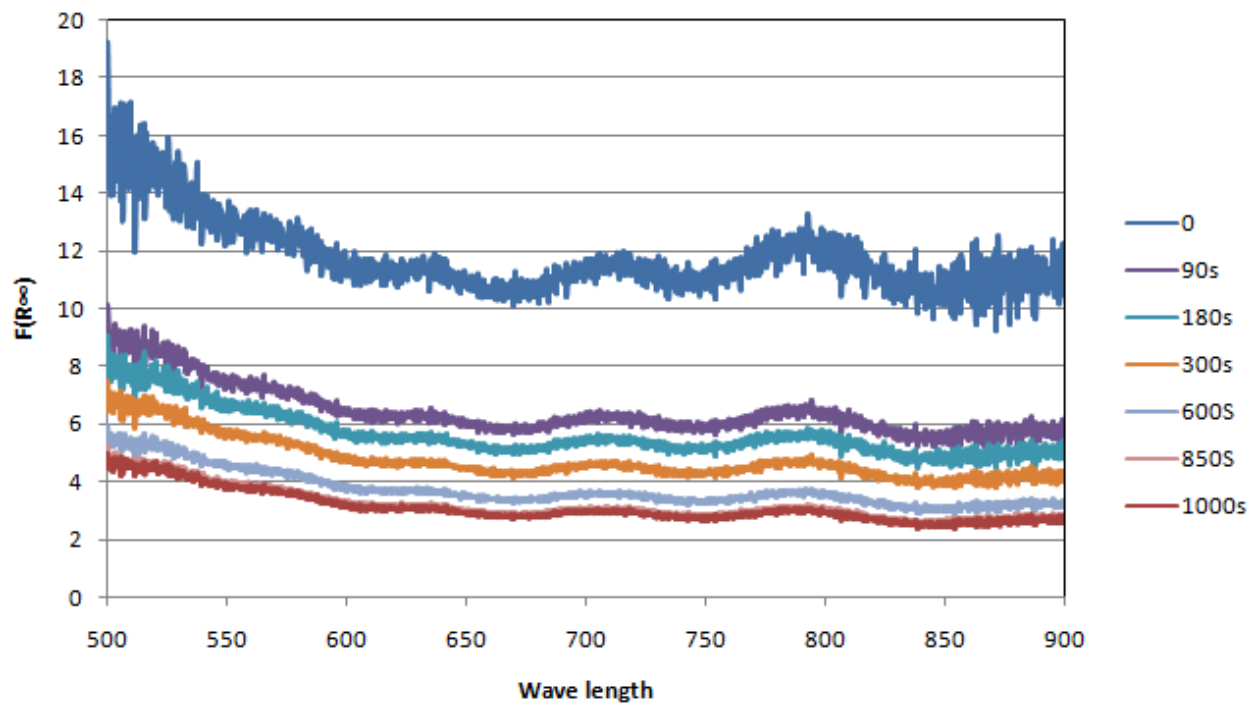


Figure 122: Kubelka-Munk function versus Wave length. Second cycle, Reaction conditions: T=503K PTotal=1 bar PEth=0.1 $CuCl_2.CeO_2/\gamma-Al_2O_3$ (5wt% Cu, 3wt% Ceria)

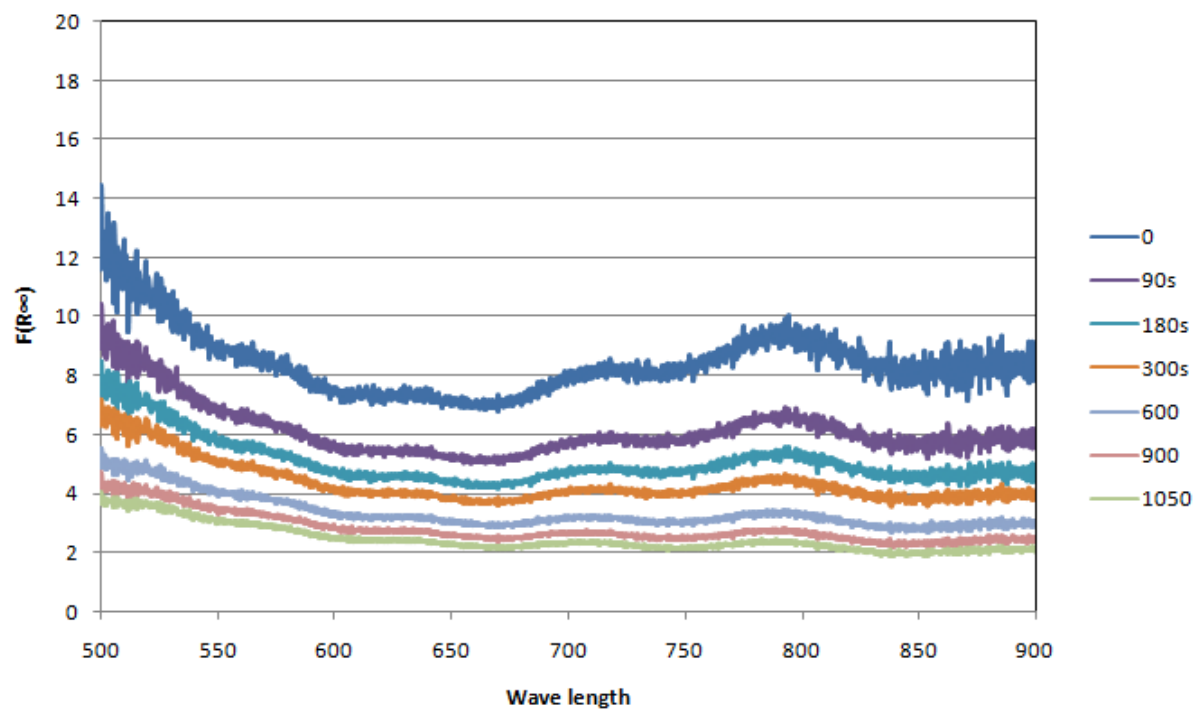


Figure 123: Kubelka-Munk function versus Wave length. Third cycle, Reaction conditions: $T=503K$ $P_{Total}=1$ bar $P_{Eth}=0.1$ $CuCl_2.CeO_2/\gamma-Al_2O_3$ (5wt% Cu, 3wt% Ceria)

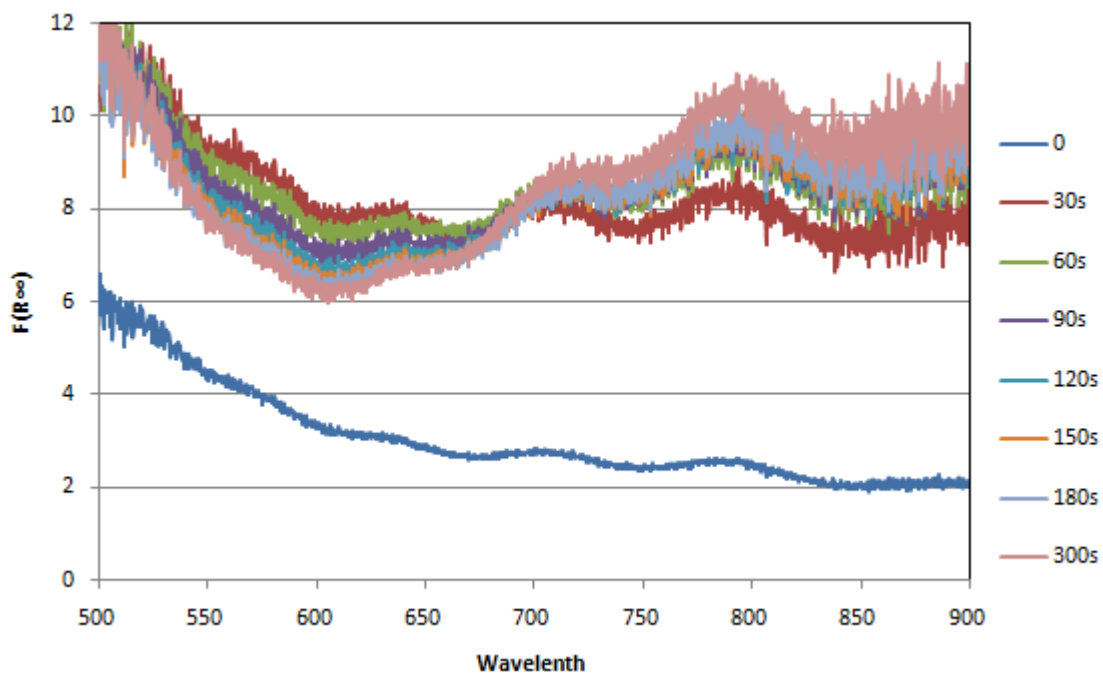


Figure 124: Kubelka-Munk function versus Wave length. First cycle, Reaction conditions: $T=503K$ $P_{Total}=1$ bar $P_{O_2}=0.1$ $CuCl_2.CeO_2/\gamma-Al_2O_3$ (5wt% Cu, 3wt% Ceria)

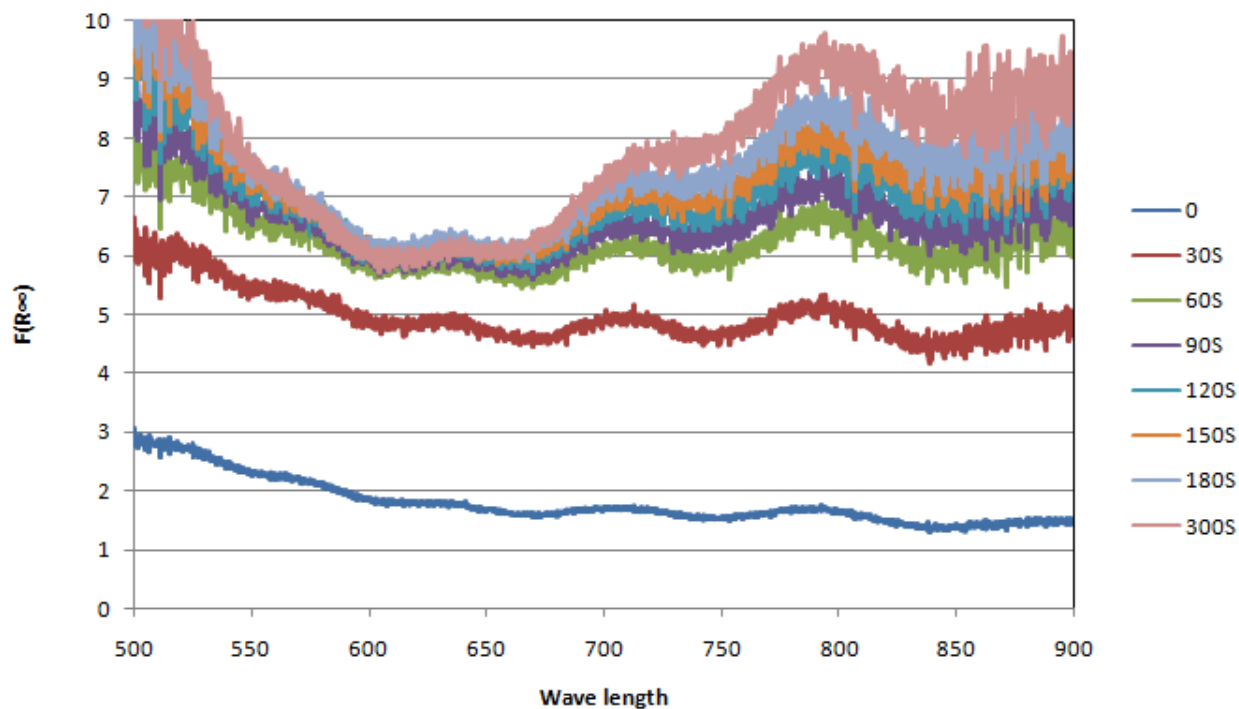


Figure 125: Kubelka-Munk function versus Wave length. Second cycle, Reaction conditions: T=503K PTotal=1 bar PO2=0.1 $CuCl_2.CeO_2/\gamma-Al_2O_3$ (5wt% Cu, 3wt% Ceria)

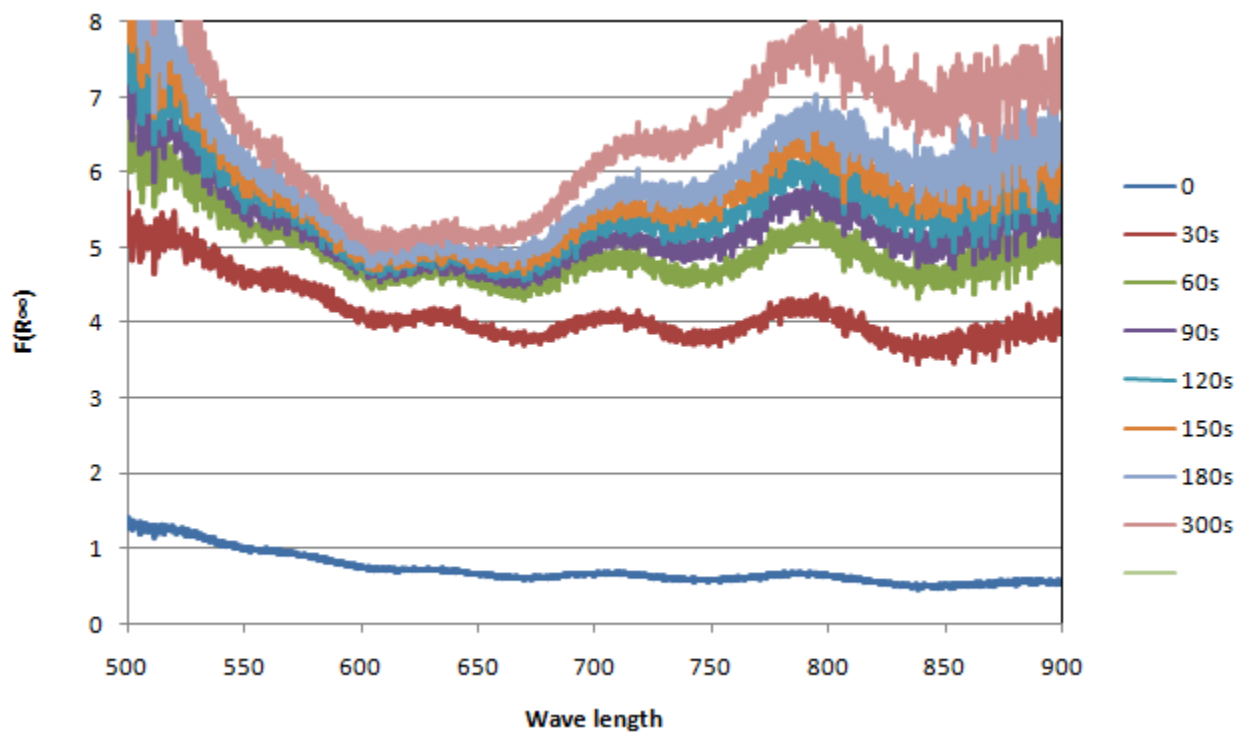


Figure 126: Kubelka-Munk function versus Wave length. Third cycle, Reaction conditions: T=503K PTotal=1 bar PO2=0.1 $CuCl_2.CeO_2/\gamma-Al_2O_3$ (5wt% Cu, 3wt% Ceria)

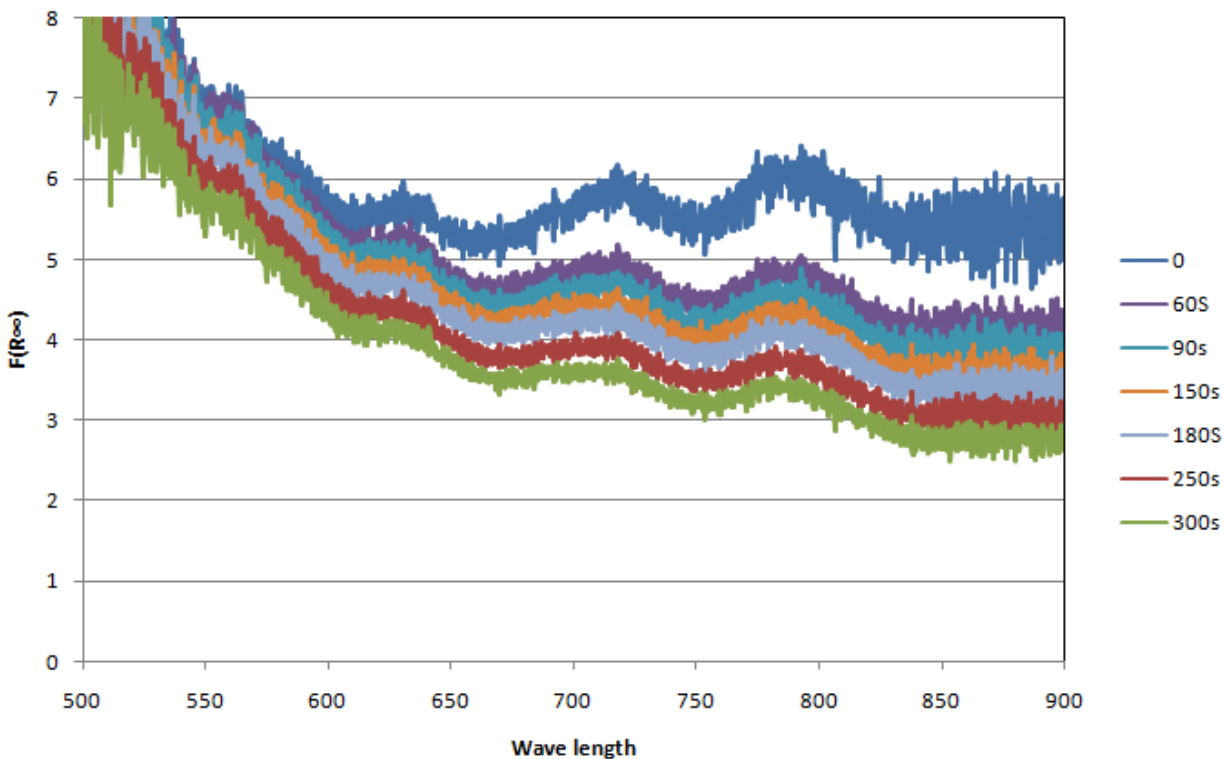


Figure 127: Kubelka-Munk function versus Wave length. First cycle, Reaction conditions: T=503K PTotal=1 bar PEth=0.1 $\text{CuCl}_2 \cdot \text{CeO}_2 / \gamma - \text{Al}_2\text{O}_3$ (4.73wt% Cu, 5wt% Ceria)

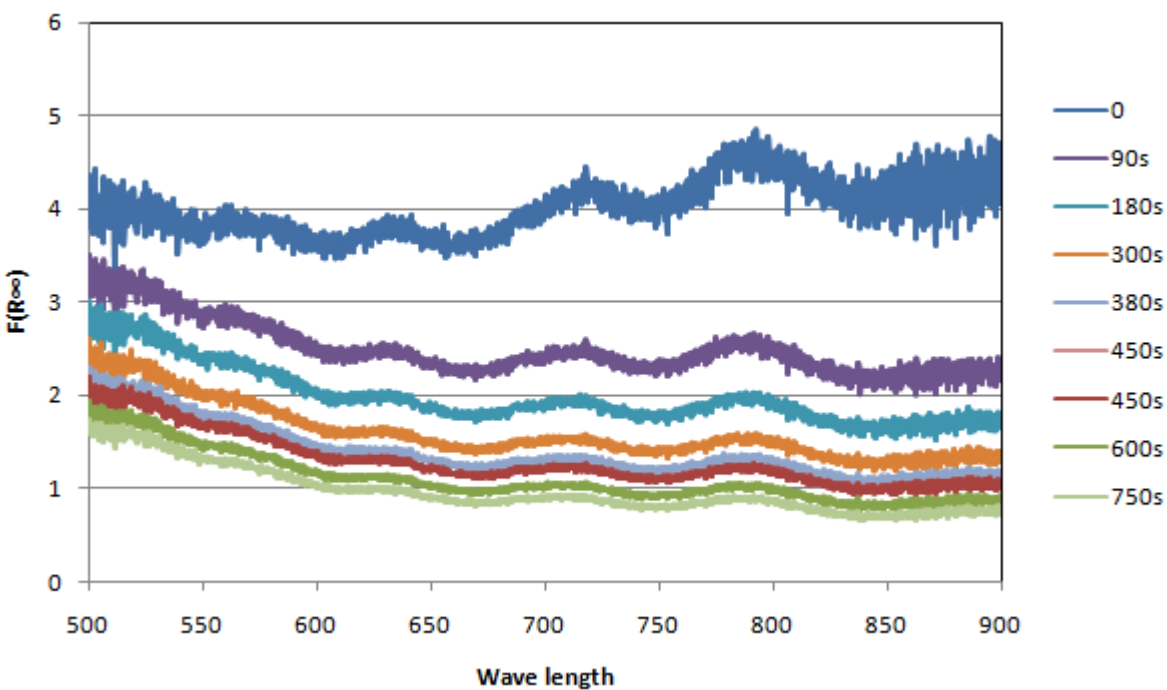


Figure 128: Kubelka-Munk function versus Wave length. Second cycle, Reaction conditions: T=503K PTotal=1 bar PEth=0.1 $\text{CuCl}_2 \cdot \text{CeO}_2 / \gamma - \text{Al}_2\text{O}_3$ (4.73wt% Cu, 5wt% Ceria)

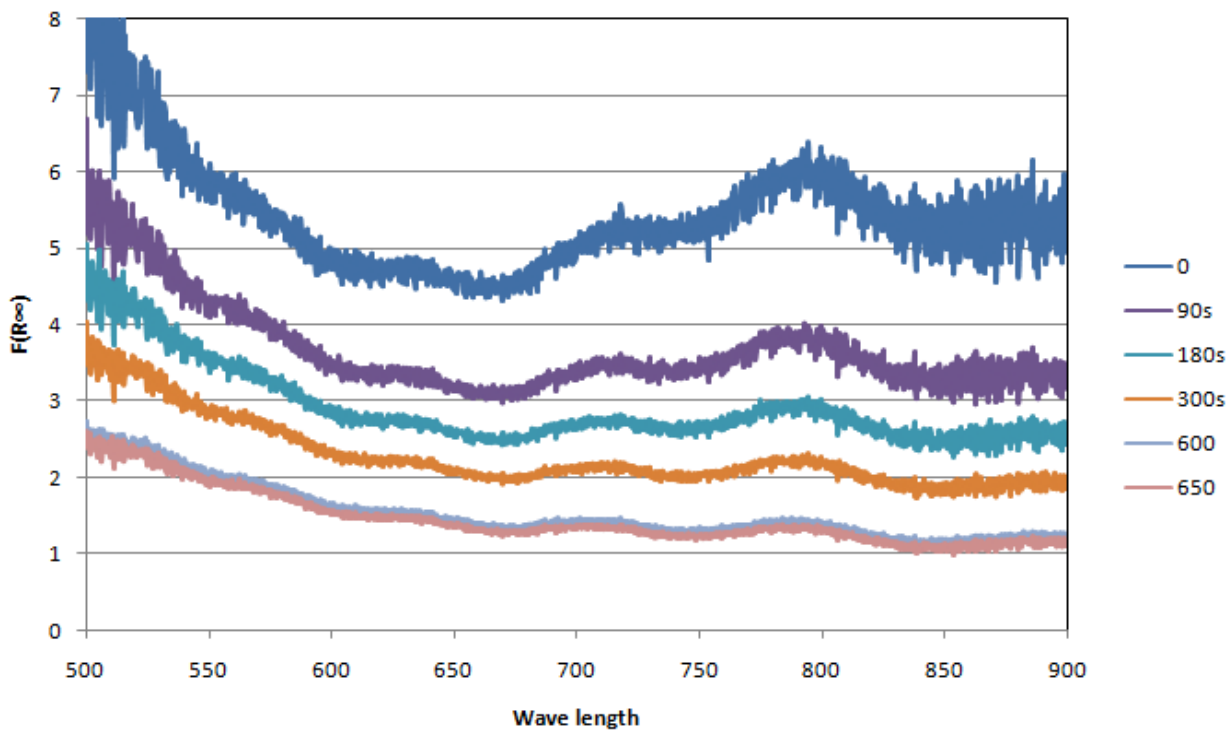


Figure 129: Kubelka-Munk function versus Wave length. Third cycle, Reaction conditions: T=503K PTotal=1 bar PEth=0.1 $CuCl_2.CeO_2/\gamma-Al_2O_3$ (4.73wt% Cu, 5wt% Ceria)

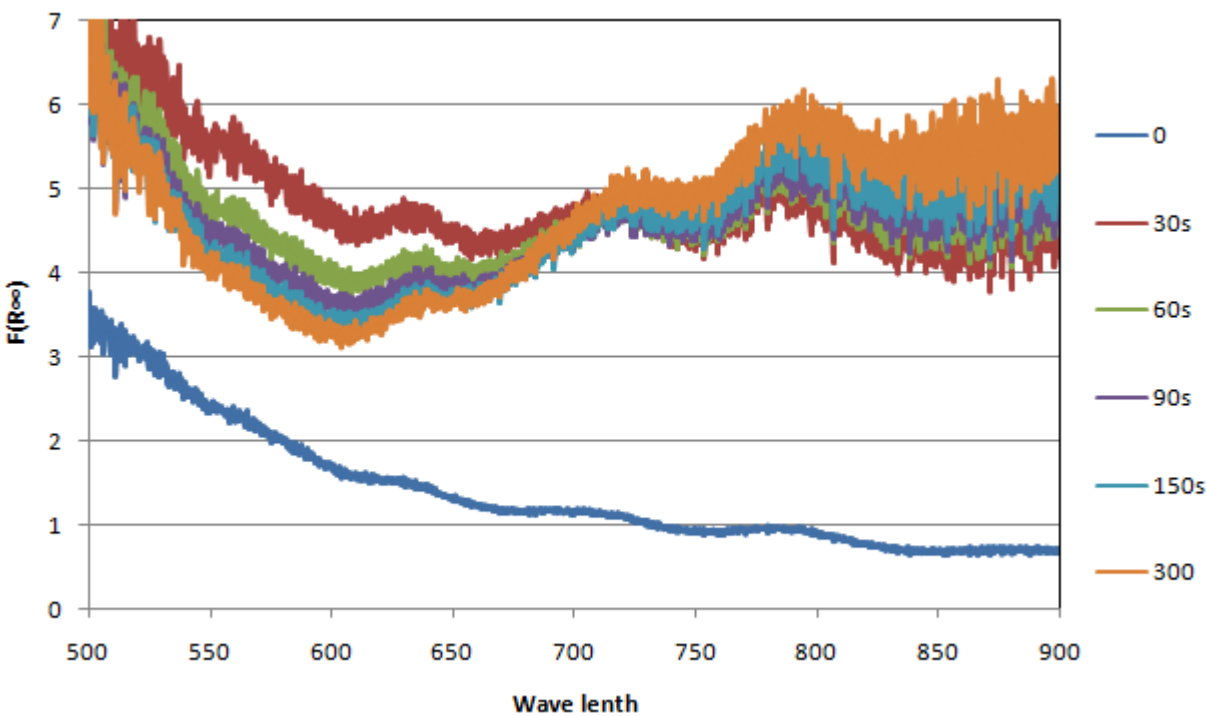


Figure 130: Kubelka-Munk function versus Wave length. First cycle, Reaction conditions: T=503K PTotal=1 bar $PO_2=0.1$ $CuCl_2.CeO_2/\gamma-Al_2O_3$ (4.73wt% Cu, 5wt% Ceria)

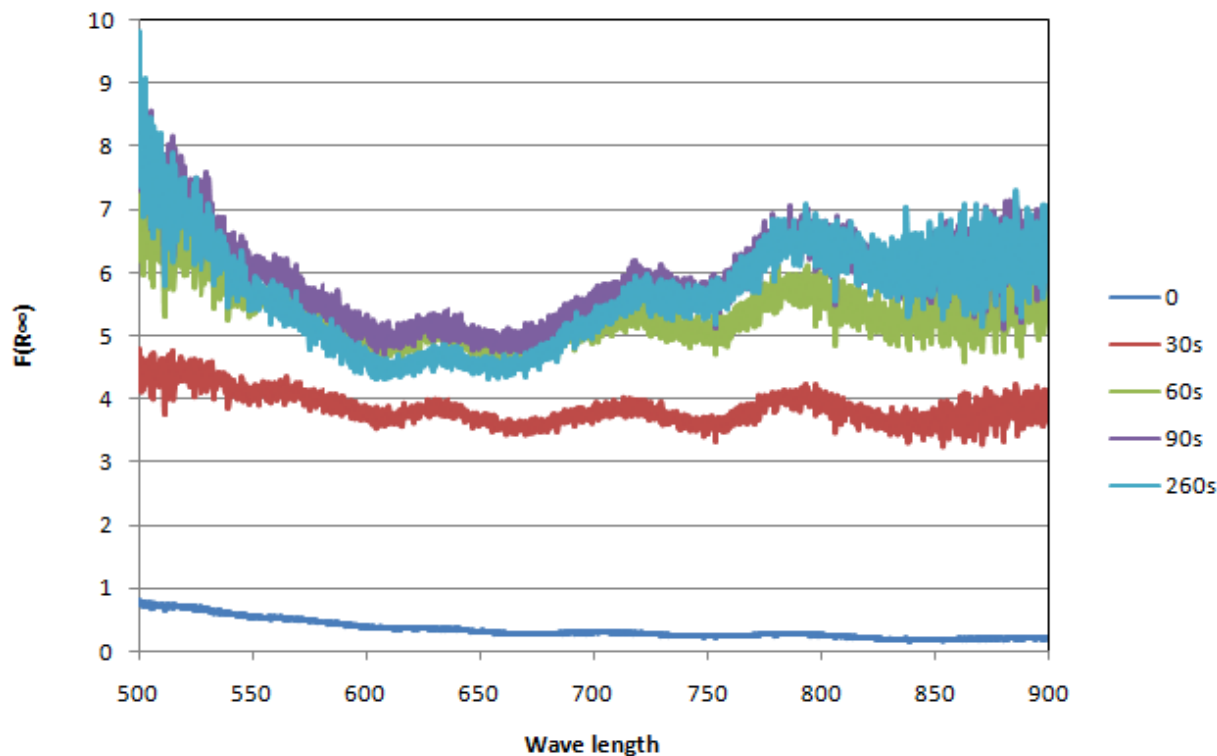


Figure 131: Kubelka-Munk function versus Wave length. Second cycle, Reaction conditions: T=503K PTotal=1 bar PO₂=0.1 CuCl₂.CeO₂/γ-Al₂O₃ (4.73wt% Cu, 5wt% Ceria)

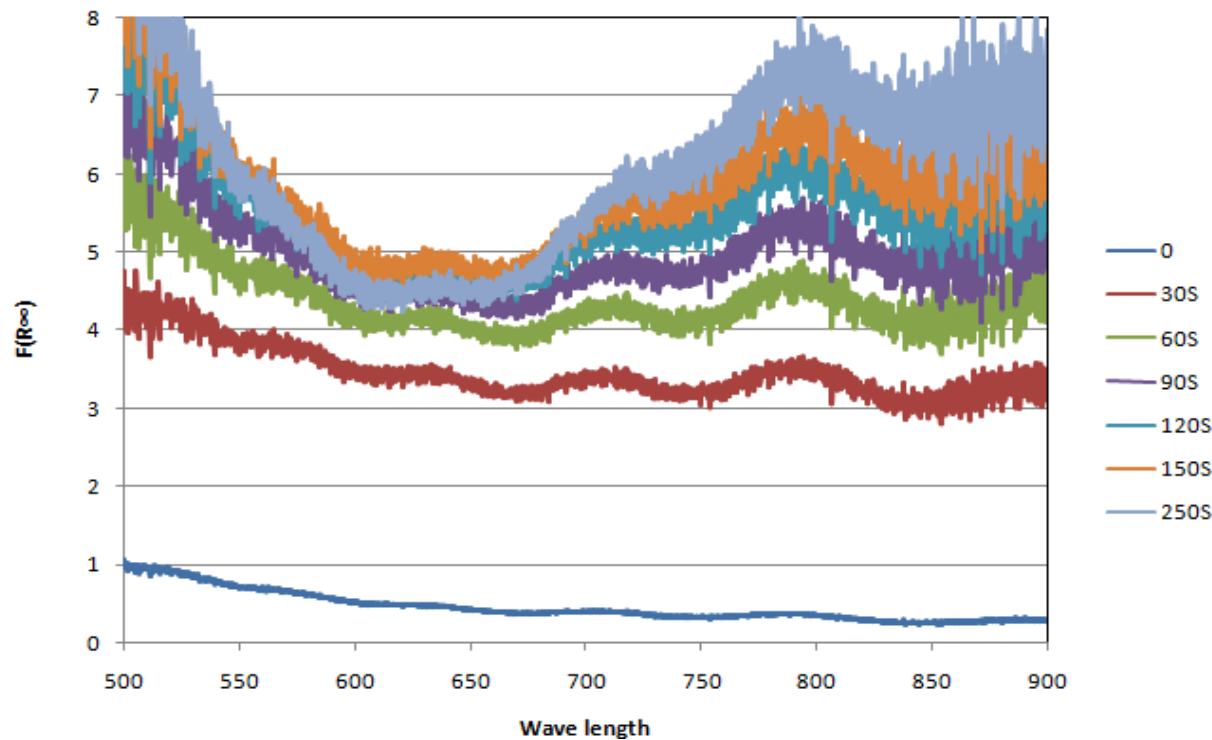


Figure 132: Kubelka-Munk function versus Wave length. Third cycle, Reaction conditions: T=503K PTotal=1 bar PO₂=0.1 CuCl₂.CeO₂/γ-Al₂O₃ (4.73wt% Cu, 5wt% Ceria)

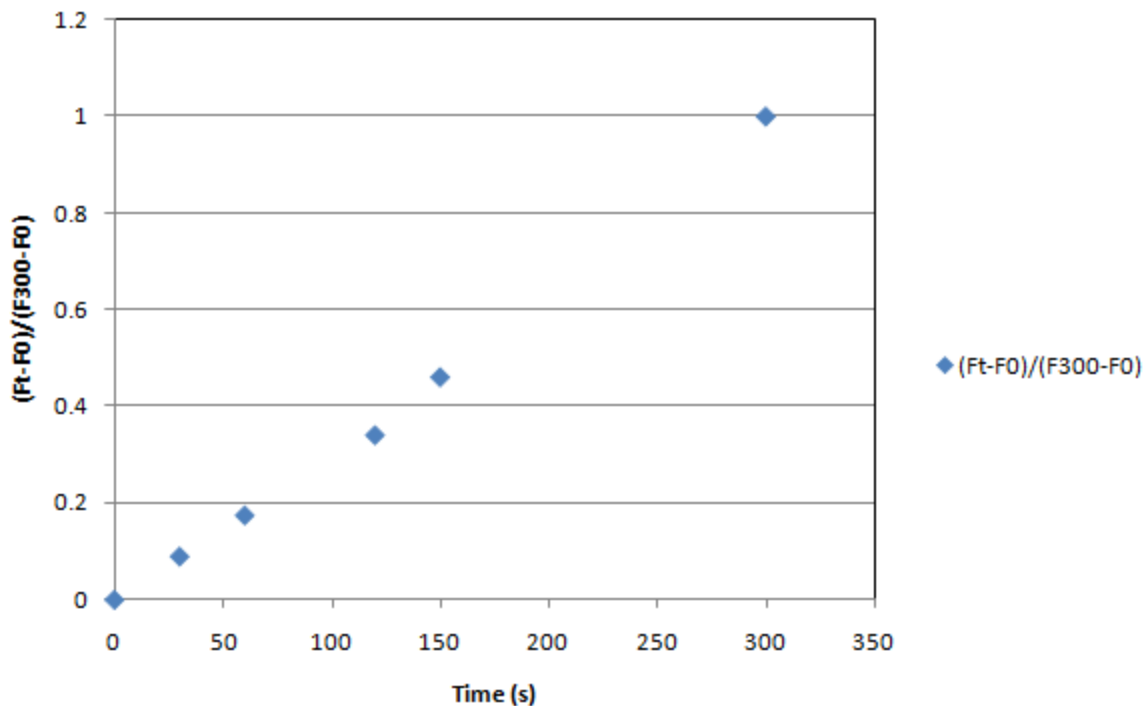


Figure 133: Relative Kubelka-Munk function versus Time. First cycle, Reaction conditions: T=503K P_{Total}=1 bar PO₂=0.1 CuCl₂/γ - Al₂O₃ (4.81wt% Cu, 0wt% Ceria)

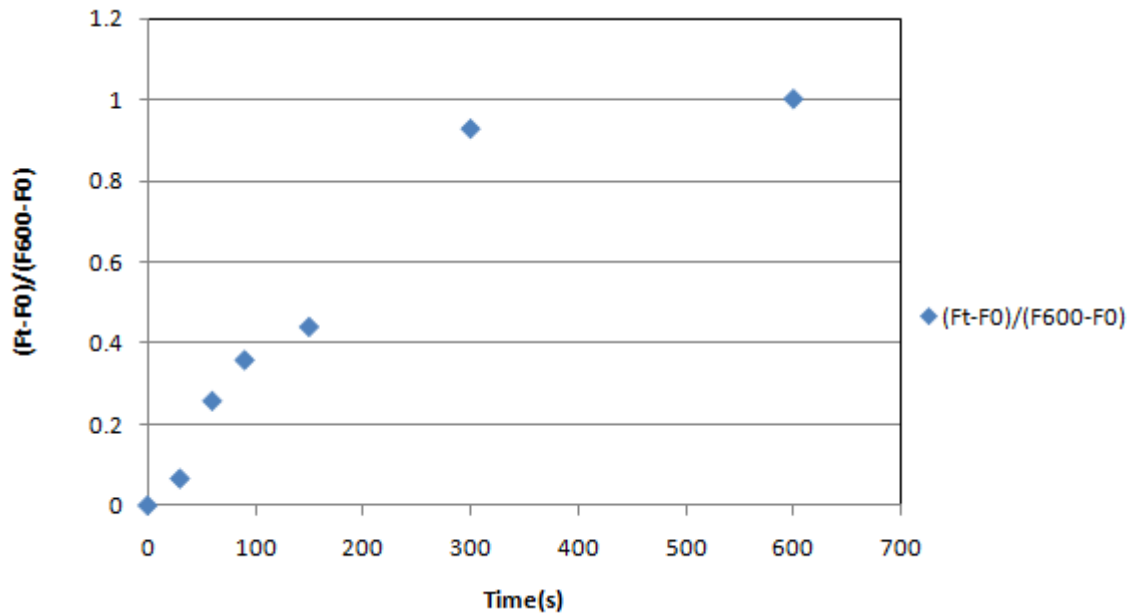


Figure 134: Relative Kubelka-Munk function versus Time. Second cycle, Reaction conditions: T=503K P_{Total}=1 bar PO₂=0.1 CuCl₂/γ - Al₂O₃ (4.81wt% Cu, 0wt% Ceria)

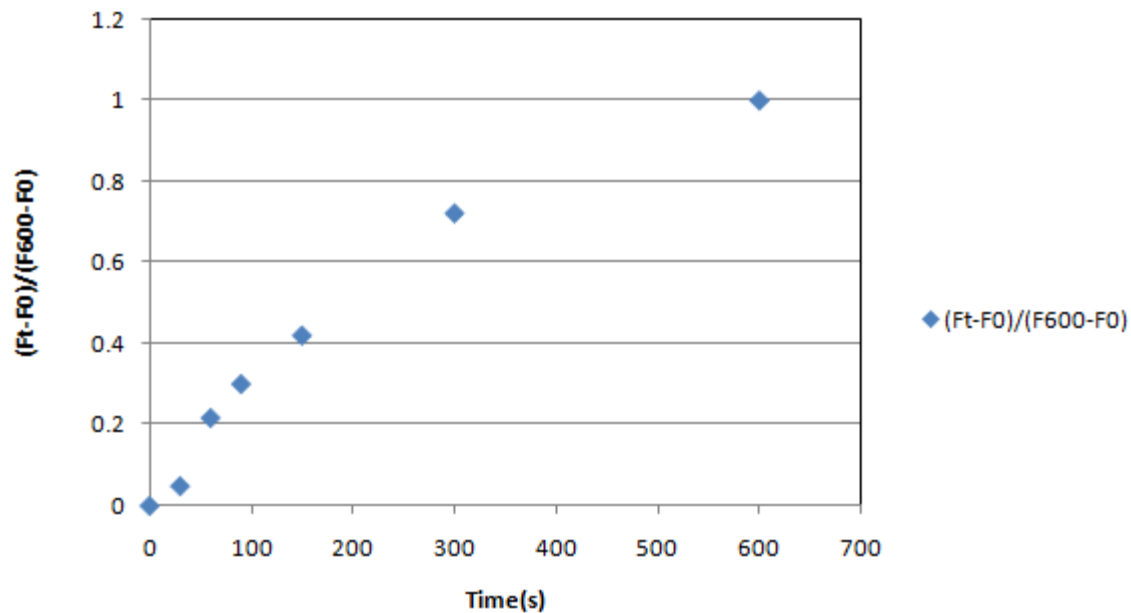


Figure 135: Relative Kubelka-Munk function versus Time. Third cycle, Reaction conditions: T=503K PTotal=1 bar PO₂=0.1 CuCl₂/γ-Al₂O₃ (4.81wt% Cu, 0wt% Ceria)

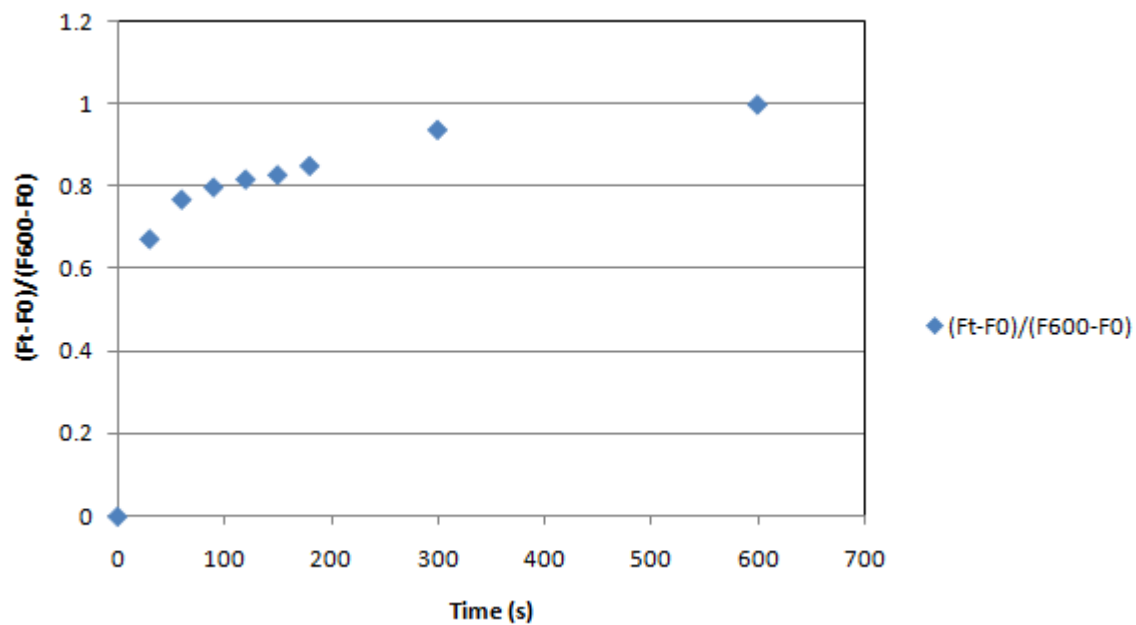


Figure 136: Relative Kubelka-Munk function versus Time. First cycle, Reaction conditions: T=503K PTotal=1 bar PO₂=0.1 CuCl₂.CeO₂/γ-Al₂O₃ (5wt% Cu, 1wt% Ceria)

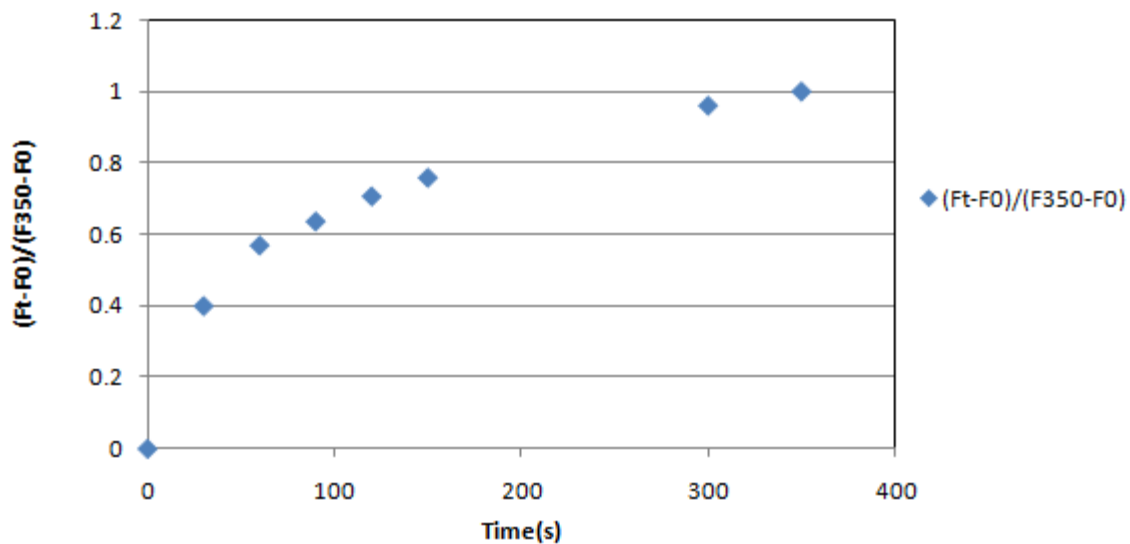


Figure 137: Relative Kubelka-Munk function versus Time. Second cycle, Reaction conditions: T=503K PTotal=1 bar PO2=0.1 $CuCl_2 \cdot CeO_2 / \gamma - Al_2O_3$ (5wt% Cu, 1wt% Ceria)

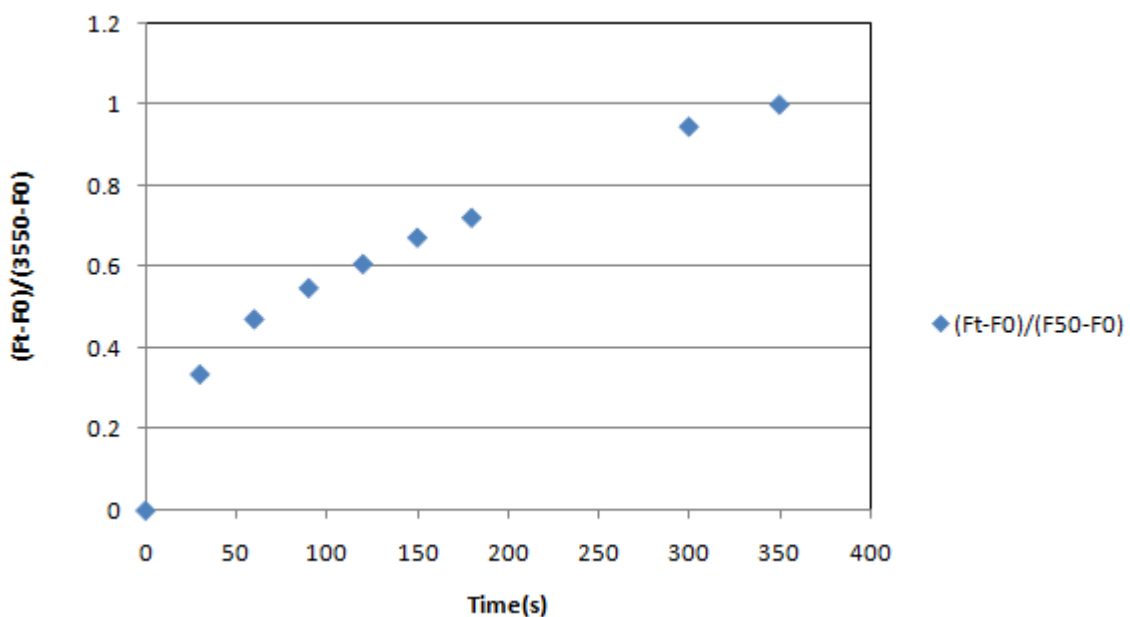


Figure 138: Relative Kubelka-Munk function versus Time. Third cycle, Reaction conditions: T=503K PTotal=1 bar PO2=0.1 $CuCl_2 \cdot CeO_2 / \gamma - Al_2O_3$ (5wt% Cu, 1wt% Ceria)

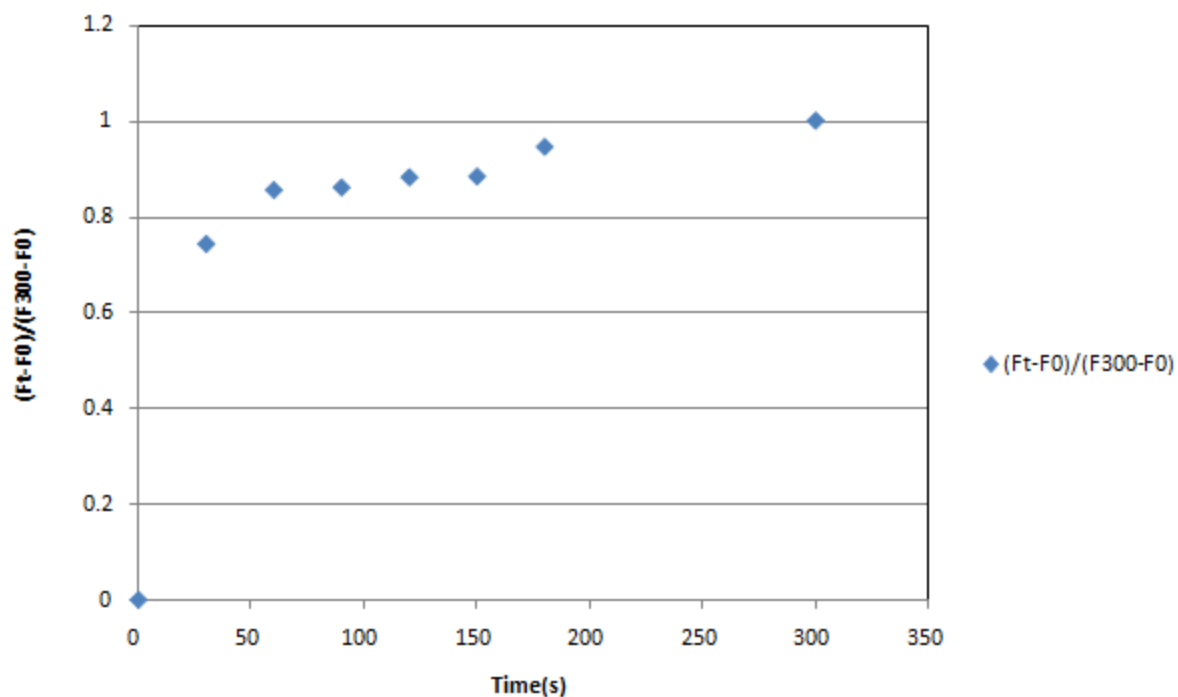


Figure 139: Relative Kubelka-Munk function versus Time. First cycle, Reaction conditions: T=503K PTotal=1 bar PO₂=0.1 CuCl₂.CeO₂/γ-Al₂O₃ (5wt% Cu, 3wt% Ceria)

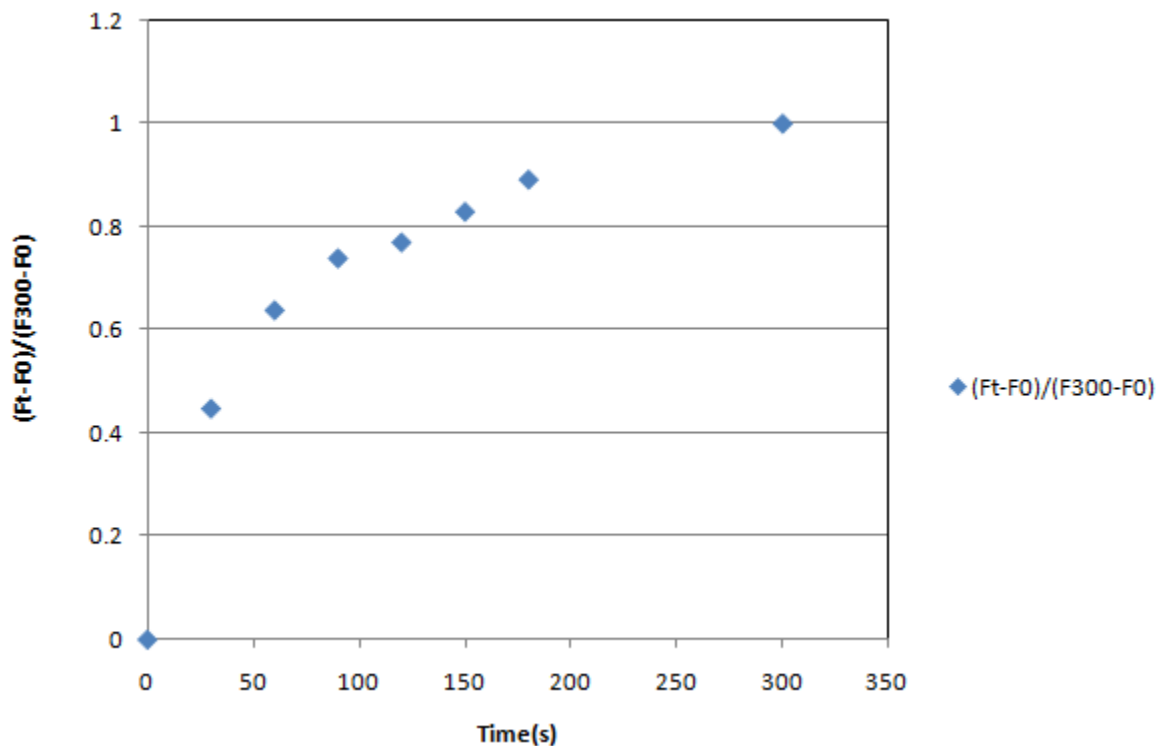


Figure 140: Relative Kubelka-Munk function versus Time. Second cycle, Reaction conditions: T=503K PTotal=1 bar PO₂=0.1 CuCl₂.CeO₂/γ-Al₂O₃ (5wt% Cu, 3wt% Ceria)

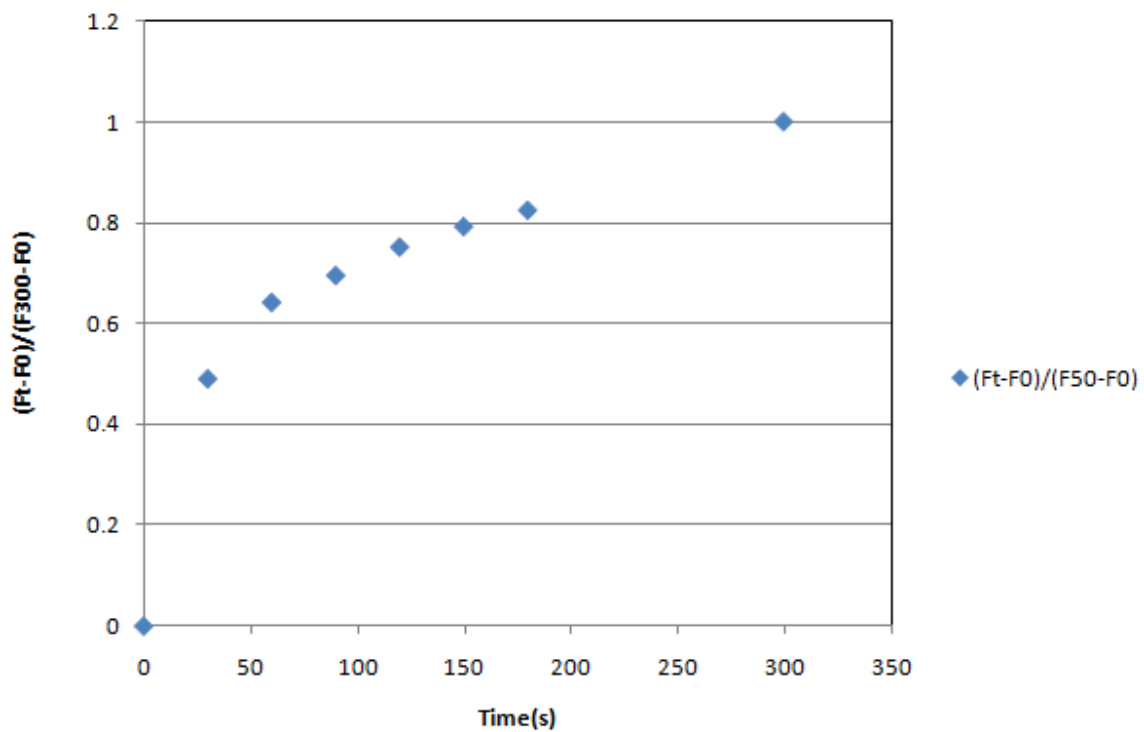


Figure 141: Relative Kubelka-Munk function versus Time. Third cycle, Reaction conditions: T=503K PTotal=1 bar PO₂=0.1 CuCl₂.CeO₂/γ-Al₂O₃ (5wt% Cu, 3wt% Ceria)

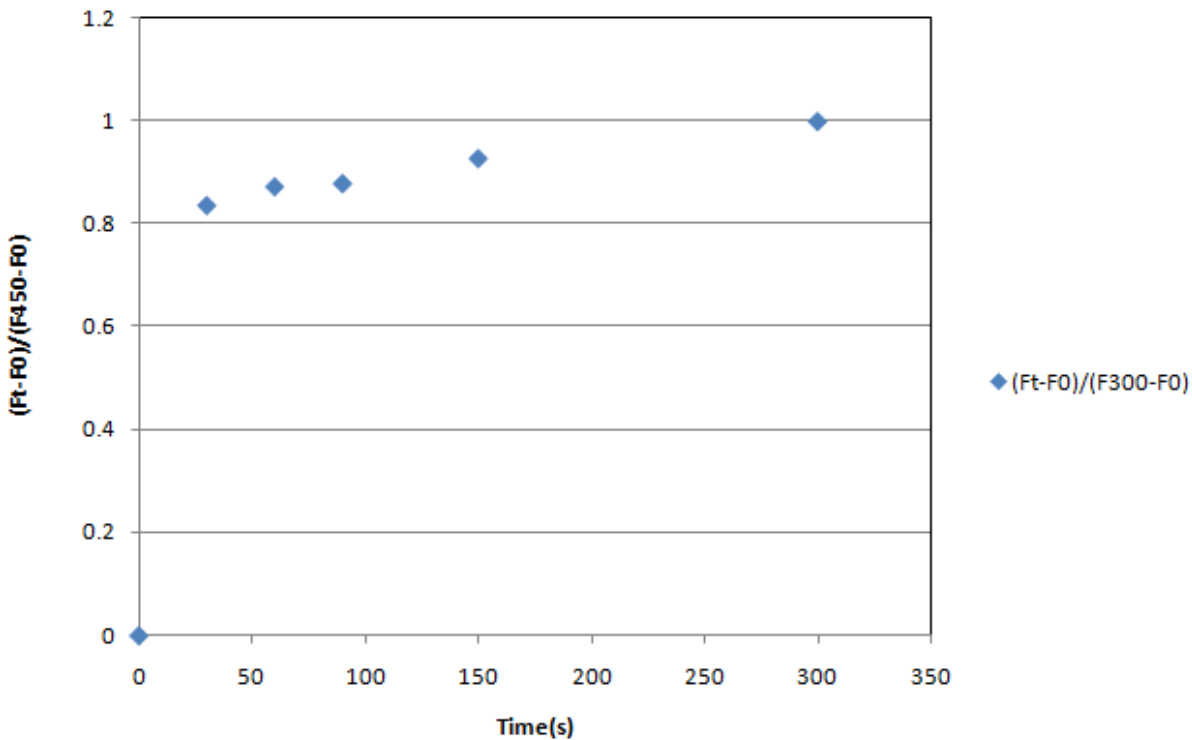


Figure 142: Relative Kubelka-Munk function versus Time. First cycle, Reaction conditions: T=503K PTotal=1 bar PO₂=0.1 CuCl₂.CeO₂/γ-Al₂O₃ (4.73wt% Cu, 5wt% Ceria)

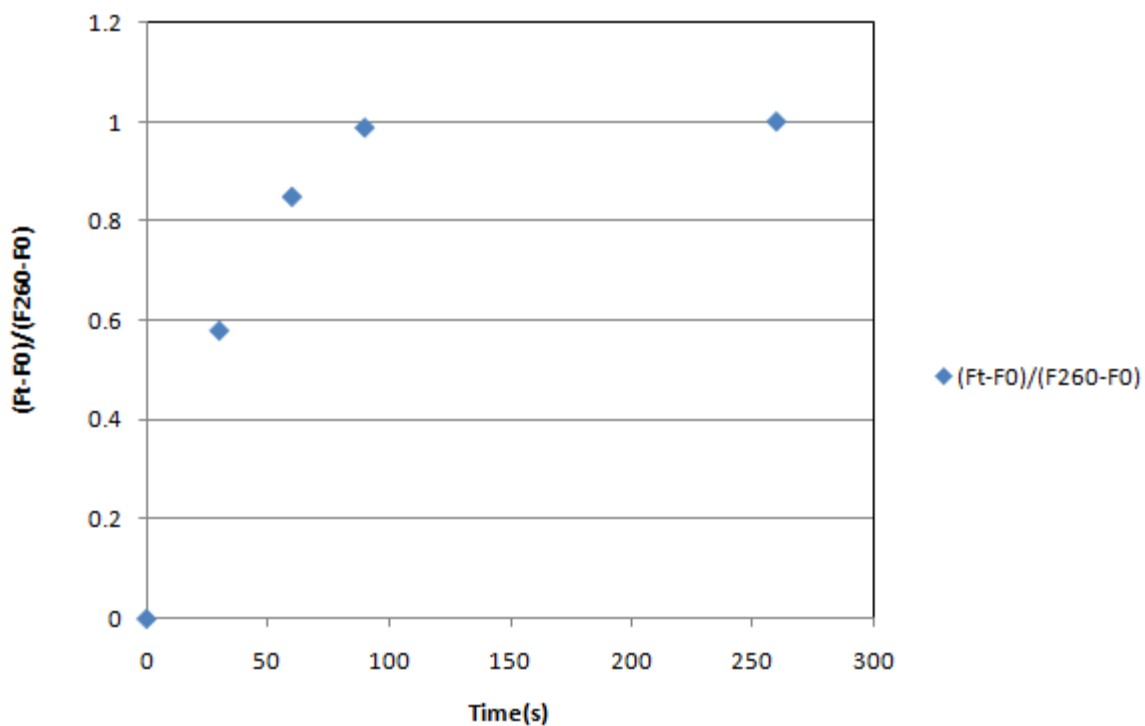


Figure 143: Relative Kubelka-Munk function versus Time. Second cycle, Reaction conditions: T=503K PTotal=1 bar PO₂=0.1 CuCl₂.CeO₂/γ-Al₂O₃ (4.73wt% Cu, 5wt% Ceria)

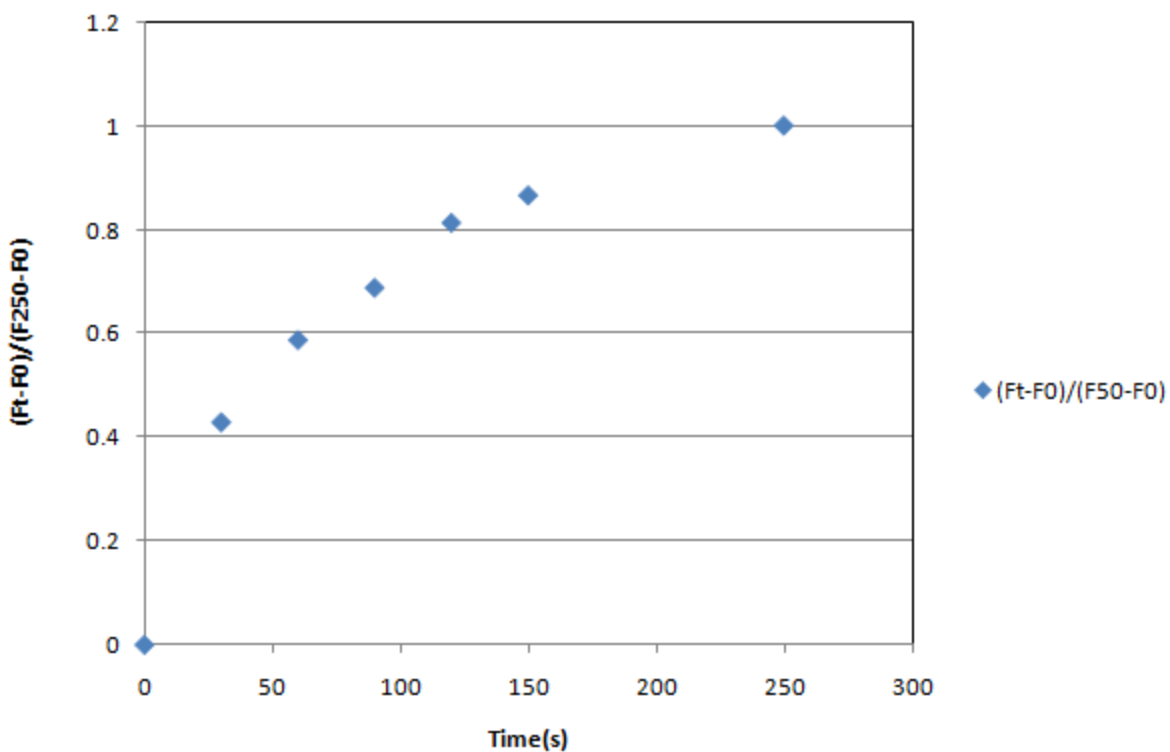


Figure 144: Relative Kubelka-Munk function versus Time. Third cycle, Reaction conditions: T=503K PTotal=1 bar PO₂=0.1 CuCl₂.CeO₂/γ-Al₂O₃ (4.73wt% Cu, 5wt% Ceria)

Appendix C: Correlation of MS and UV/VIS Data

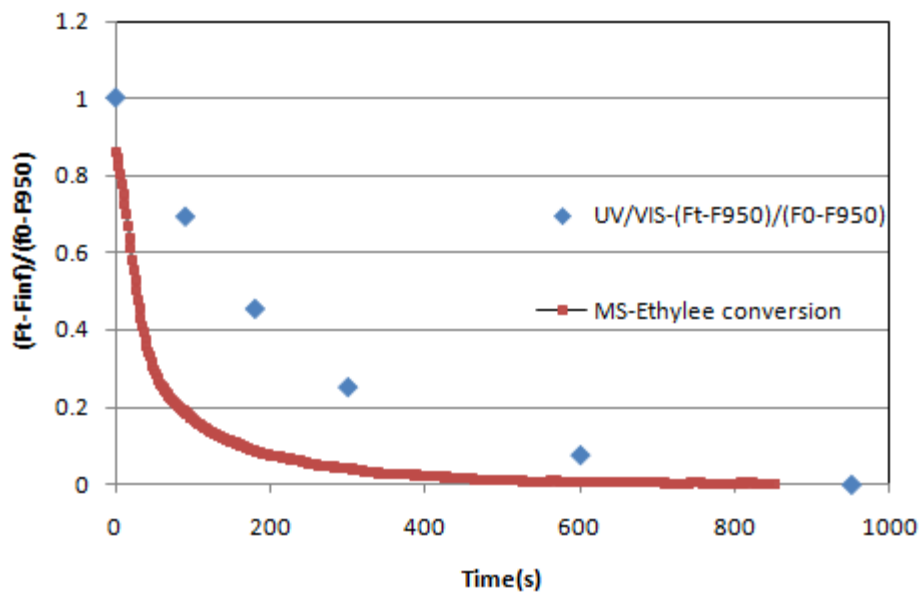


Figure 145: Correlation between Ethylene conversion and Relative Kubelka-Munk function. First cycle, Reaction conditions: $T=503K$ $P_{Total}=1$ bar $P_{Eth}=0.1$ $CuCl_2/\gamma-Al_2O_3$ (4.81wt% Cu, 0wt% Ceria)

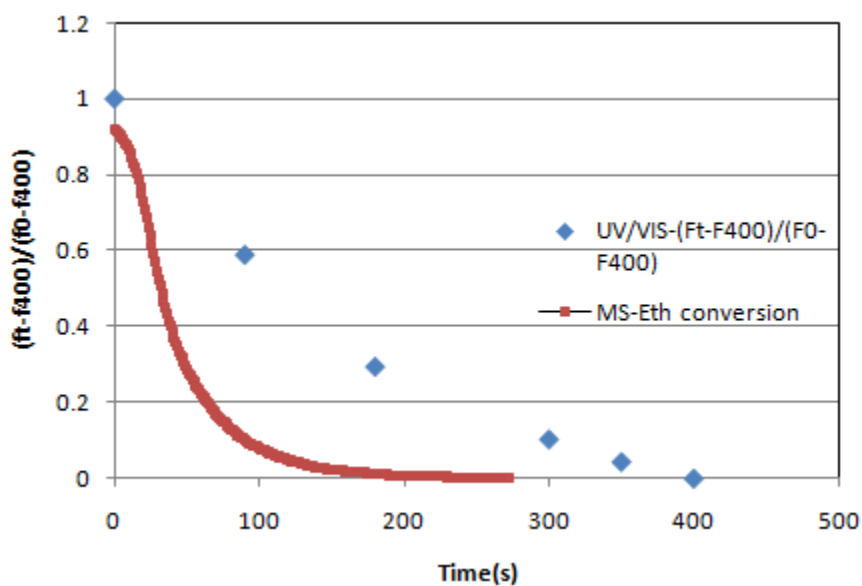


Figure 146: Correlation between Ethylene conversion and Relative Kubelka-Munk function. Second cycle, Reaction conditions: $T=503K$ $P_{Total}=1$ bar $P_{Eth}=0.1$ $CuCl_2/\gamma-Al_2O_3$ (4.81wt% Cu, 0wt% Ceria)

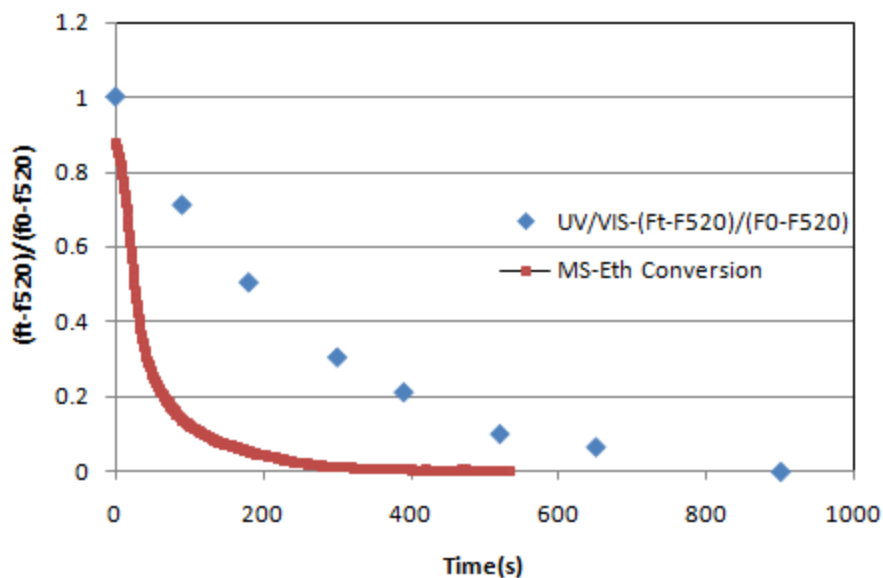


Figure 147: Correlation between Ethylene conversion and Relative Kubelka-Munk function. Third cycle, Reaction conditions: T=503K PTotal=1 bar PEth=0.1 $\text{CuCl}_2/\gamma - \text{Al}_2\text{O}_3$ (4.81wt% Cu, 0wt% Ceria)

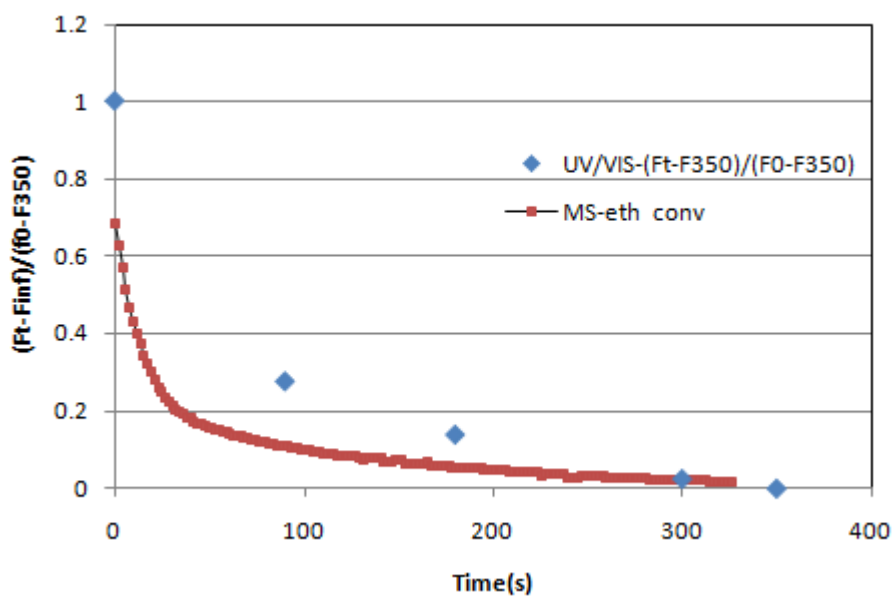


Figure 148: Correlation between Ethylene conversion and Relative Kubelka-Munk function. First cycle Reaction conditions: T=503K PTotal=1 bar PEth=0.1 $\text{CuCl}_2.\text{CeO}_2/\gamma - \text{Al}_2\text{O}_3$ (5wt% Cu, 1wt% Ceria)

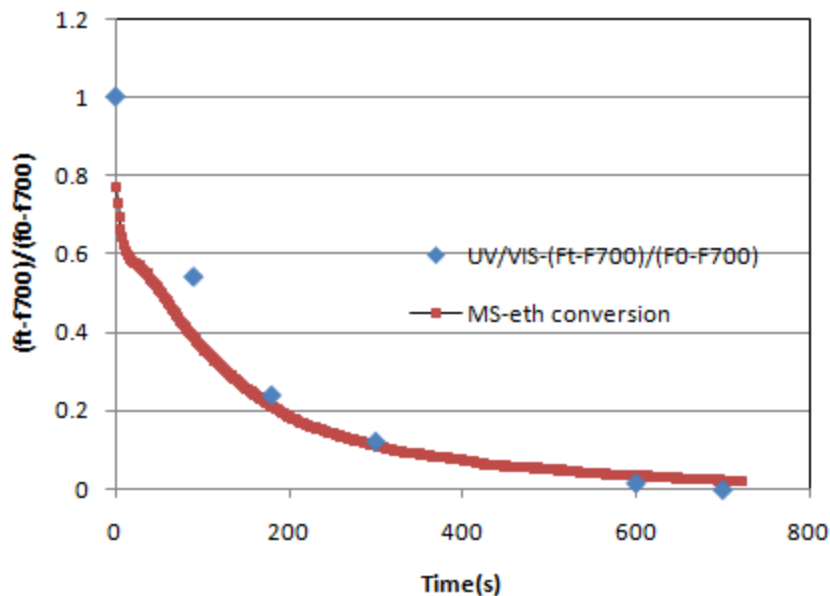


Figure 149: Correlation between Ethylene conversion and Relative Kubelka-Munk function. Second cycle, Reaction conditions: T=503K PTotal=1 bar PEth=0.1 $CuCl_2.CeO_2/\gamma-Al_2O_3$ (5wt% Cu, 1wt% Ceria)

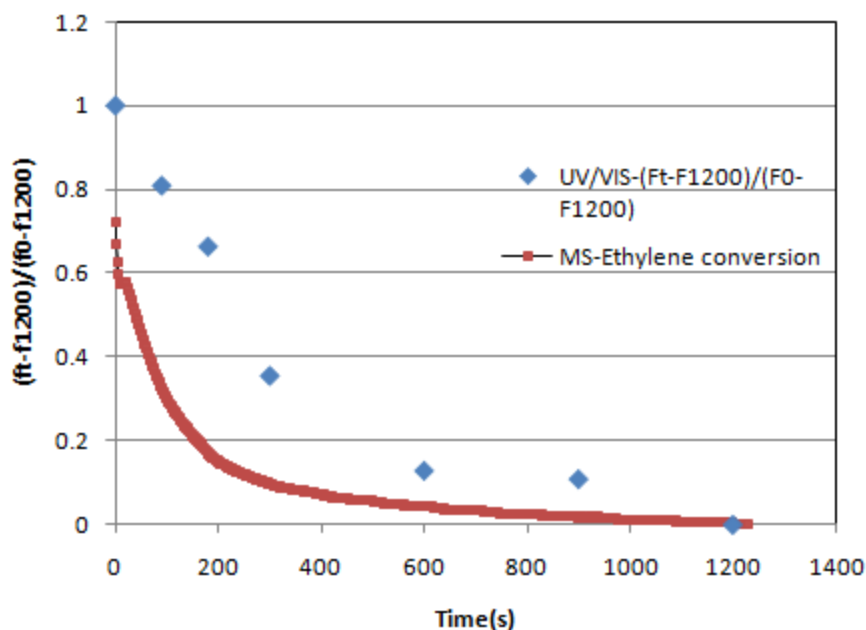


Figure 150: Correlation between Ethylene conversion and Relative Kubelka-Munk function. Third cycle, Reaction conditions: T=503K PTotal=1 bar PEth=0.1 $CuCl_2.CeO_2/\gamma-Al_2O_3$ (5wt% Cu, 1wt% Ceria)

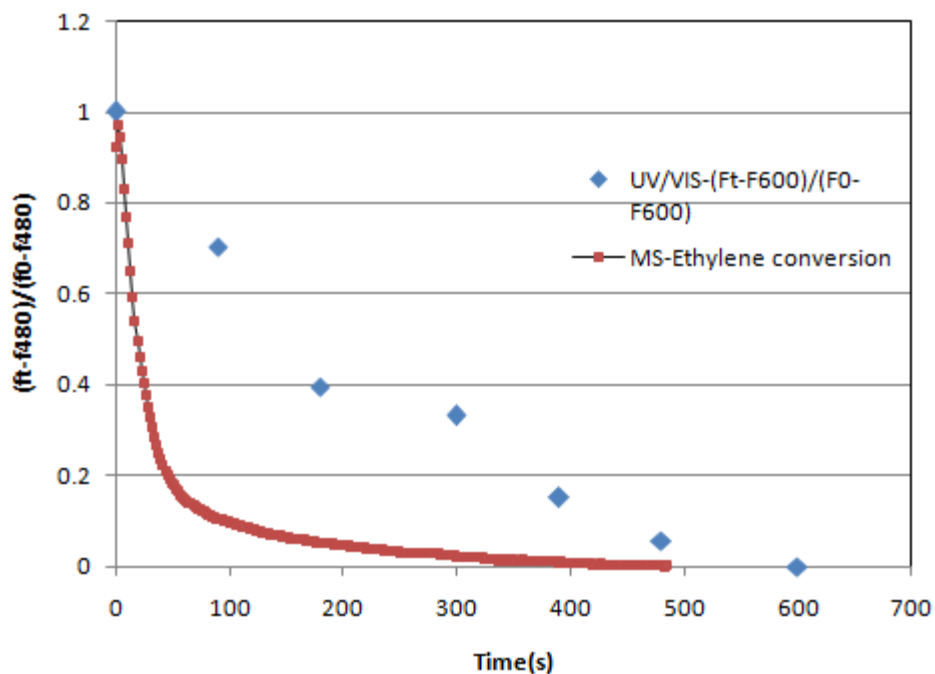


Figure 151: Correlation between Ethylene conversion and Relative Kubelka-Munk function. First cycle, Reaction conditions: $T=503K$ $P_{Total}=1$ bar $P_{Eth}=0.1$ $CuCl_2.CeO_2/\gamma-Al_2O_3$ (5wt% Cu, 3wt% Ceria)

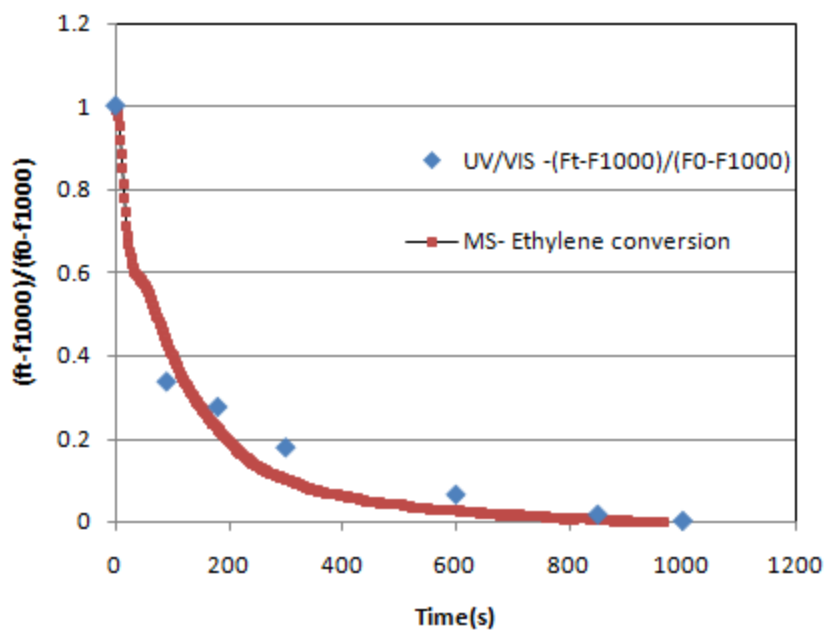


Figure 152: Correlation between Ethylene conversion and Relative Kubelka-Munk function. Second cycle, Reaction conditions: $T=503K$ $P_{Total}=1$ bar $P_{Eth}=0.1$ $CuCl_2.CeO_2/\gamma-Al_2O_3$ (5wt% Cu, 3wt% Ceria)

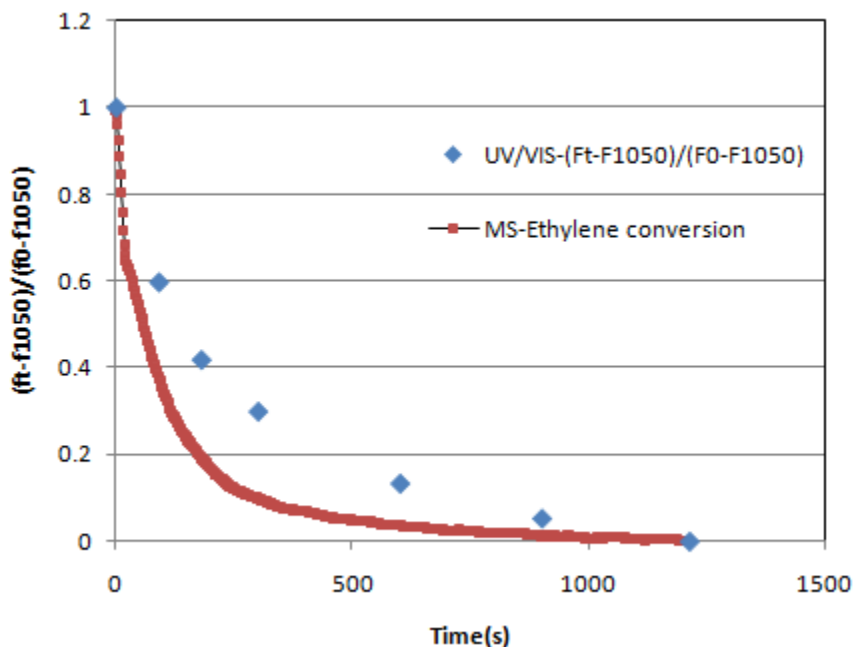


Figure 153: Correlation between Ethylene conversion and Relative Kubelka-Munk function. Third cycle, Reaction conditions: T=503K PTotal=1 bar PEth=0.1 $CuCl_2.CeO_2/\gamma-Al_2O_3$ (5wt% Cu, 3wt% Ceria)

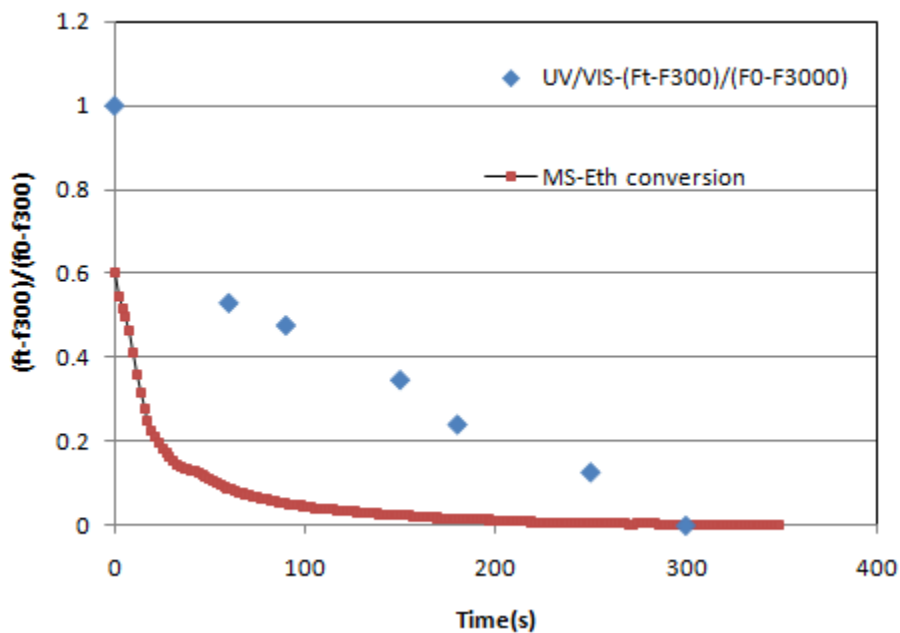


Figure 154: Correlation between Ethylene conversion and Relative Kubelka-Munk function. First cycle Reaction conditions: T=503K PTotal=1 bar PEth=0.1 $CuCl_2.CeO_2/\gamma-Al_2O_3$ (4.73wt% Cu, 5wt% Ceria)

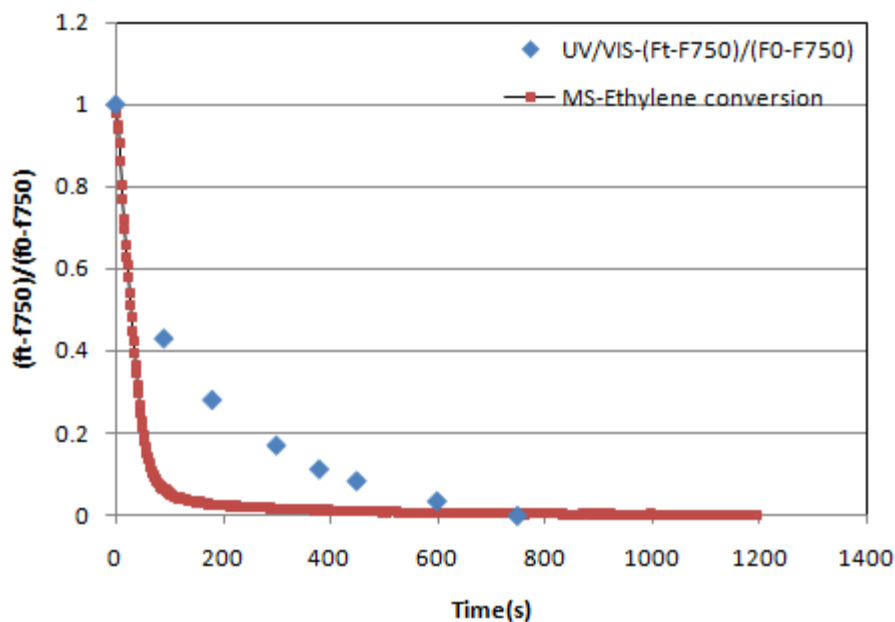


Figure 155: Correlation between Ethylene conversion and Relative Kubelka-Munk function. Second cycle, Reaction conditions: T=503K PTotal=1 bar PEth=0.1 $CuCl_2.CeO_2/\gamma-Al_2O_3$ (4.73wt% Cu, 5wt% Ceria)

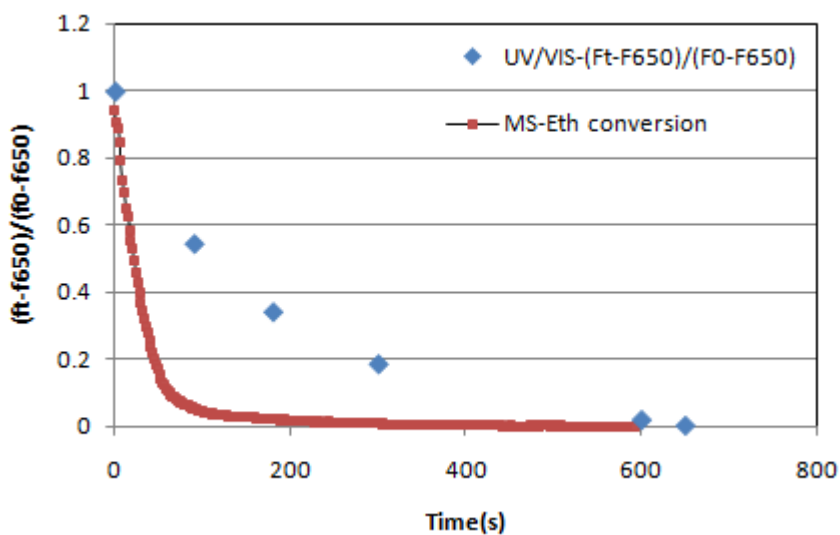


Figure 156: Correlation between Ethylene conversion and Relative Kubelka-Munk function. Third cycle, Reaction conditions: T=503K PTotal=1 bar PEth=0.1 $CuCl_2.CeO_2/\gamma-Al_2O_3$ (4.73wt% Cu, 5wt% Ceria)

Appendix D: Calibration of Mass Flow Controlers

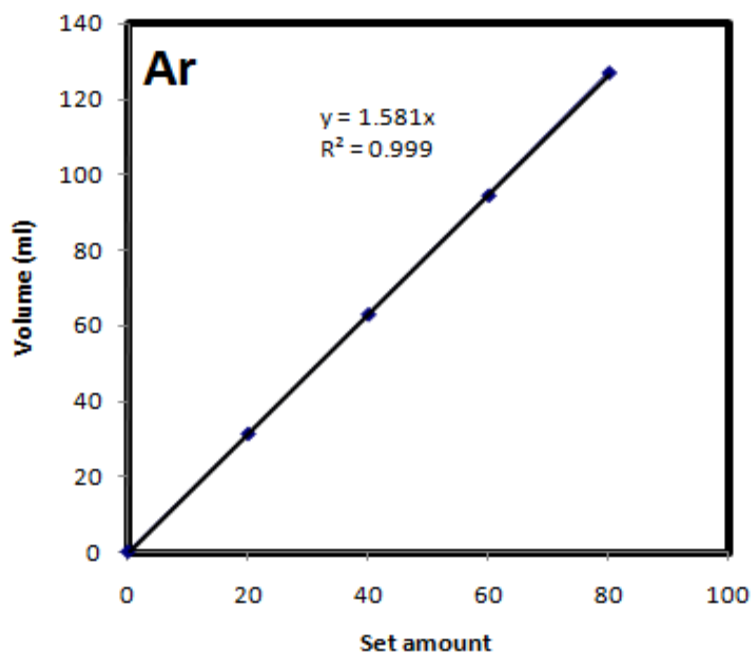


Figure 157: Calibration of Mass flow controller belong to bottle of Argon. Conditions: T: 298 K P: 1atm

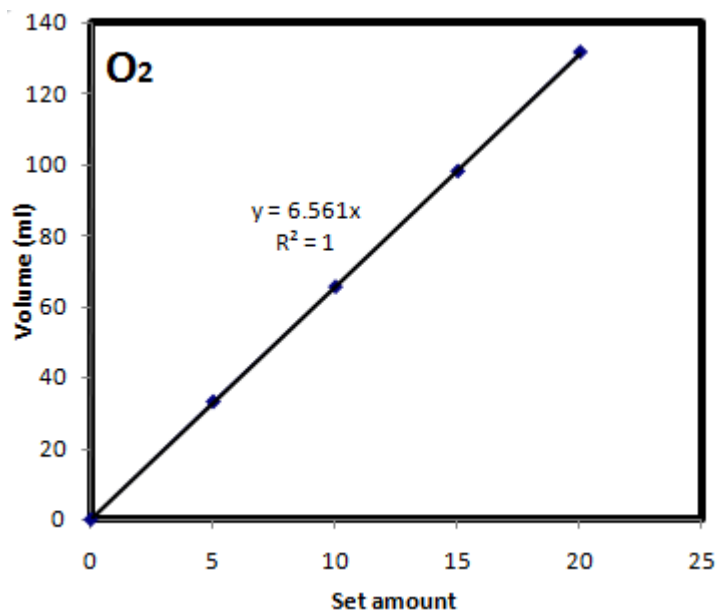


Figure 158 : Calibration of Mass flow controller belong to bottle of Oxygen. Conditions: T: 298 K P: 1atm

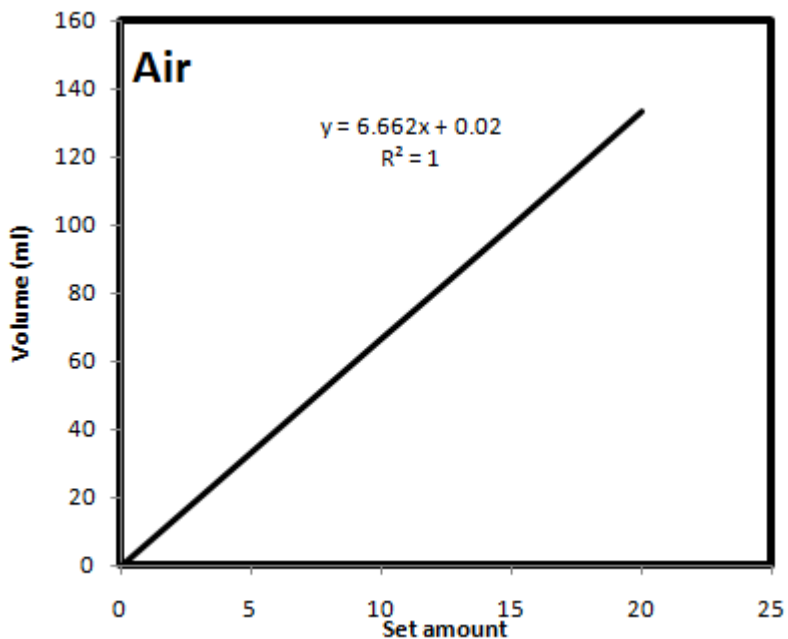


Figure 159: Calibration of Mass flow controller belong to bottle of Air. Conditions: T: 298 K P: 1atm

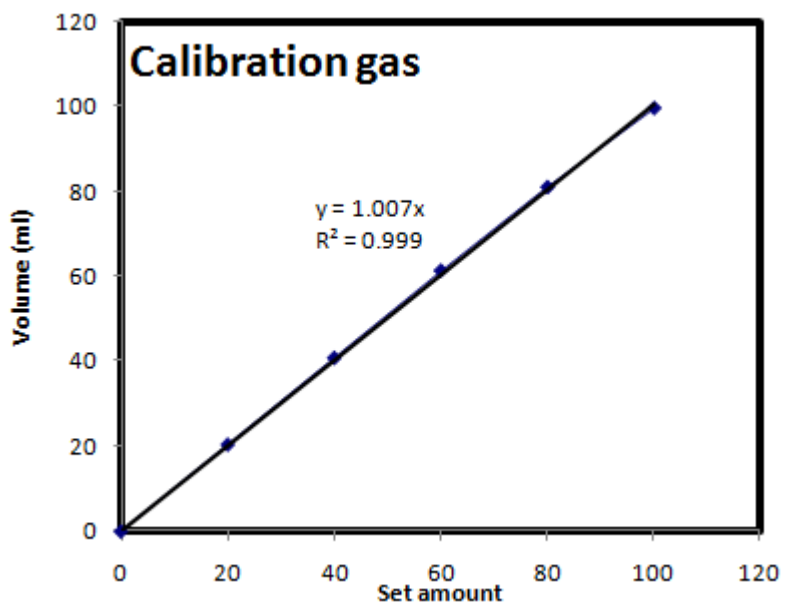


Figure 160: Calibration of Mass flow controller belong to bottle of calibration gas. Conditions: T: 298 K P: 1atm

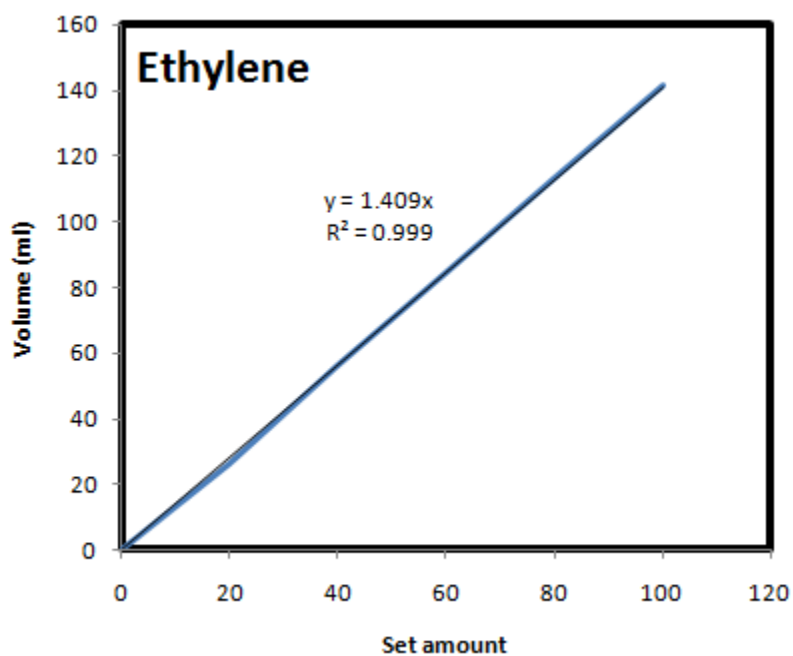


Figure 161: Calibration of Mass flow controller belong to bottle of Ethylene gas. Conditions: T: 298 K P: 1atm

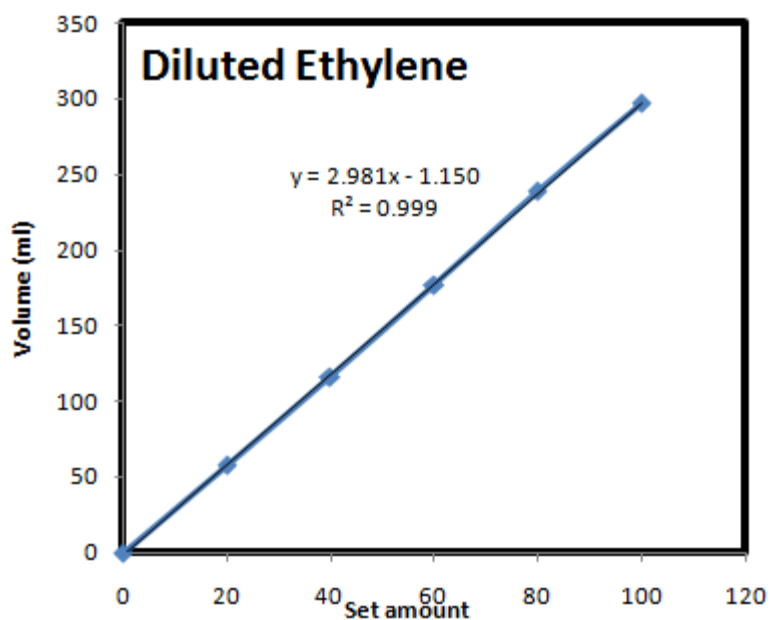


Figure 162: Calibration of Mass flow controller belong to bottle of Diluted Ethylene gas. Conditions: T: 298 K P: 1atm

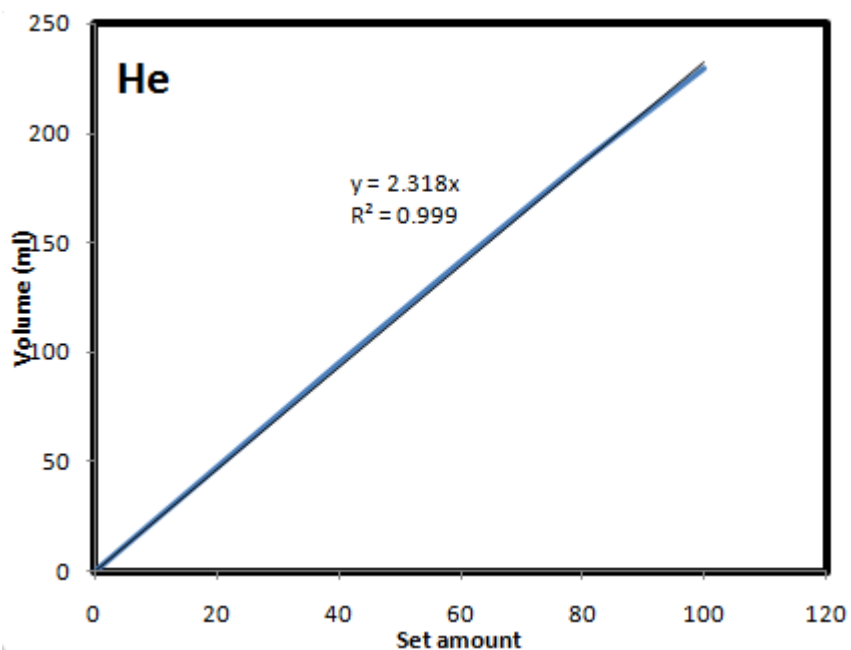


Figure 163: Calibration of Mass flow controller belong to bottle of Helium gas. Conditions: T: 298 K P: 1atm

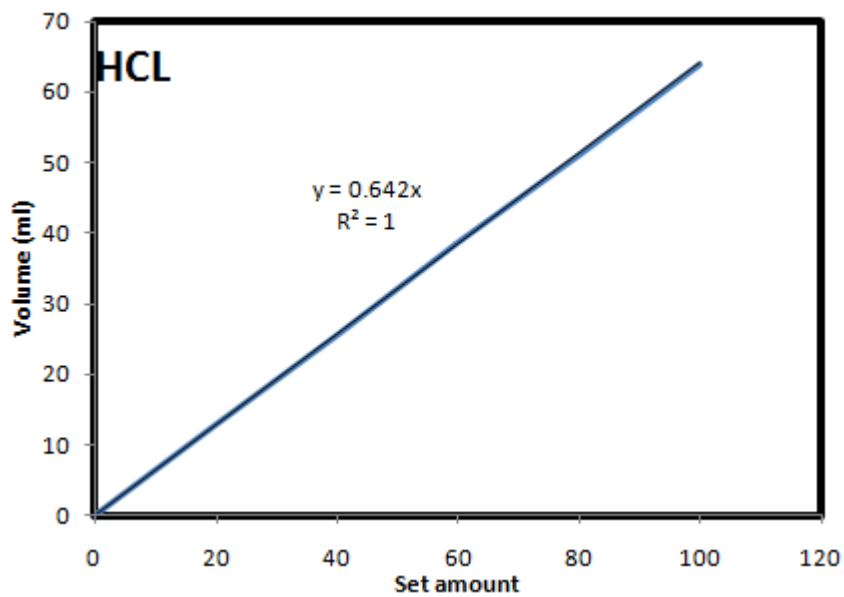


Figure 164: Calibration of Mass flow controller belong to bottle of Hydrogen chloride gas. Conditions: T: 298 K P: 1atm